The C_4-Dicarboxylate Carriers DcuB and DctA of *Escherichia coli*: Function as Cosensors and Topology

Dissertation

zur Erlangung des Grades

"Doktor der Naturwissenschaften"

Am Fachbereich Biologie

der Johannes Gutenberg-Universität Mainz

Julia Bauer

geb. am 26.02.1980 in Darmstadt

Mainz, 19.02.2010

Dekan:

1. Berichterstatter:
2. Berichterstatter:

Tag der mündlichen Prüfung: 13.04.2010

1. Abstract

The facultative anaerobic enteric bacterium *Escherichia coli* can use C_4-dicarboxylates as a carbon and energy source during aerobic and anaerobic growth. C_4-dicarboxylate uptake and energy conservation via fumarate respiration is regulated by the two-component system DcuSR. In response to C_4-dicarboxylates, the sensor kinase DcuS and the response regulator DcuR activate expression of the genes coding for the succinate carrier DctA, the anaerobic fumarate/succinate antiporter DcuB, the fumarase B and the fumarate reductase FrdABCD. The transporters DctA and DcuB show a severe regulatory effect on DcuSR dependent gene expression under aerobic and anaerobic conditions. Deletion of DctA or DcuB causes a strongly increased expression of *dctA´-´lacZ* or *dcuB´-´lacZ* in the absence of effector, implying a negative effect of the transporters on C_4-dicarboxylate-sensing. For DcuB, independent sites for transport and regulation were identified by random and site-directed mutagenesis, indicating that DcuB is a bifunctional protein which acts as a second sensor of the DcuSR system.

In this work, the topology of membrane-embedded DcuB and of the regulatory sites was determined by reporter gene fusions with the alkaline phosphatase and the ß-lactamase. In addition, labeling experiments with membrane-permeable and membrane-impermeable sulphydryl reagents were performed to identify accessible amino acid residues of DcuB. The data indicate the existence of a deep aqueous channel opened to the periplasmic side of the membrane. Based on the results of the topology mapping, on a hydropathy blot and predicted secondary structure, a topology model of DcuB was created. DcuB contains 12 transmembrane helices with short C- and N-termini ends located in the periplasm and two large hydrophilic loops between TM VII/VIII and TM XI/XII. The regulatory competent residues K353, T396 and D398 are located in TM XI and the adjacent cytoplasmic loop XI-XII. The data from structural and functional studies were applied to predict a model of C_4-dicarboxylate-dependent gene expression by combined action of the carrier DcuB and the sensor kinase DcuS.

The effect of DctA and DcuSR on the expression of *dctA´-´lacZ* and C_4-dicarboxylate uptake under aerobic conditions was investigated by ß-galactosidase assays and growth experiments. Interaction studies by using fusions of DctA and DcuS with derivatives of the green fluorescent protein for *in-vivo* FRET measurements showed a direct interaction between the carrier DctA and the sensor DcuS. This finding strongly supports the model of regulation of DcuS by C_4-dicarboxylates and DctA or DcuB as cosensor by direct interaction.

2. Introduction

2.1 Regulation of C_4-dicarboxylate metabolism in *E. coli*

The facultative anaerobic enteric bacterium *Escherichia coli* is able to grow on C_4-dicarboxylates under aerobic and anaerobic conditions (Unden & Kleefeld, 2004). In aerobic growth, C_4-dicarboxylates can be used as sole carbon and energy source. Succinate, fumarate, L-malate and also the amino acid aspartate are transported into the cell by the uptake carrier DctA (Dicarboxylate Transport). The substrates are oxidized to CO_2 by the use of the citric acid cycle and aerobic respiration (Fig. I2).

In the absence of oxygen, *E. coli* is able to grow on fumarate, L-malate or aspartate in combination with an additional carbon source. L-malate and aspartate are converted to fumarate by the enzymes fumarase and aspartase and fumarate is used as an electron acceptor in fumarate respiration. It is reduced to succinate at the active site of the membrane-bound fumarate reductase FrdABCD, generating a proton potential for ATP synthesis. The energy conservation is obtained by the dehydrogenases NADH dehydrogenase I (*nuoA-N*), anaerobic glycerol-3-phosphate dehydrogenase (*glpABC*) or hydrogenase 2 (*hybAB*) in the fumarate respiratory chain. Under anaerobic conditions succinate cannot be further catabolized and is excreted (Fig. I1). The main carrier for C_4-dicarboxylate uptake and succinate efflux during fumarate respiration is the antiporter DcuB (Dicarboylate Uptake).

2.1.1 The DcuSR two-component system

Histidine kinase/response regulator systems for adaption to environmental conditions are widely distributed among bacteria and represent the most common systems for signal transduction (West & Stock, 2001; Mascher *et al.*, 2006). Typically an external stimulus leads to a phosphorelay cascade resulting in the activation of a transcriptional regulator. The two-component system DcuSR consists of the membrane integrated C_4-dicarboxylate-sensing histidine kinase DcuS and the cytoplasmic response regulator DcuR. The *dcuS* gene and the *dcuR* gene are expressed in *E. coli* constitutively.

The sensory region of DcuS is located in a periplasmic loop between two transmembrane helices and has been characterized by NMR-spectroscopy and crystallography (Pappalardo *et al*., 2003; Cheung & Hendrickson, 2008) and site-directed mutagenesis (Janausch *et al*., 2004; Kneuper *et al.*, 2005; Krämer *et al.*, 2007). This N-terminal input-domain is followed by a

cytoplasmic PAS (Per-Arnt-Sim) domain and the kinase domain. The function of the cytoplasmic PAS domain is still unknown (Etzkorn *et al.*, 2008), but pro- and eukaryotic PAS domains in general are involved in sensing and signal transfer (Taylor & Zhulin, 1999; Kneuper *et al.*, 2010).

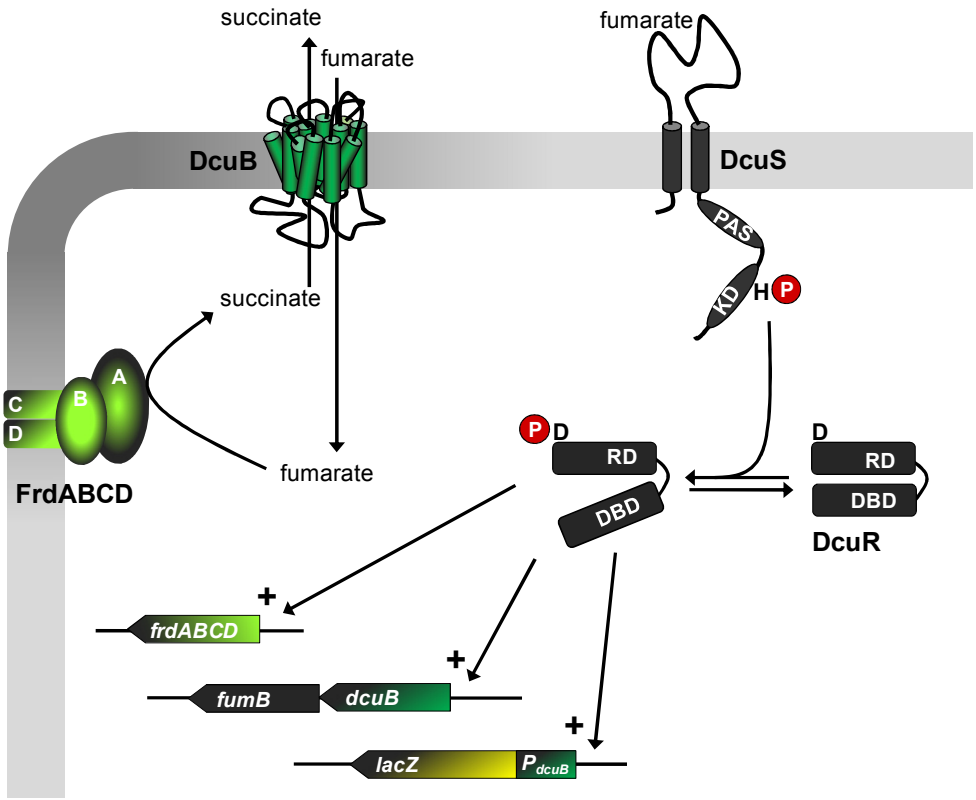

Figure I1: DcuSR dependant gene expression under anaerobic conditions/ Regulation of fumarate respiration in *E. coli*. External C_4-dicarboxylates like fumarate are recognised by the periplasmic sensing domain of the sensor kinase DcuS. Effector binding leads to signal transduction through the membrane and autophosphorylation of a conserved histidine residue within the kinase domain of DcuS. The phosphoryl group (P) is transferred to the response regulator DcuR. The phosphorylation of a conserved aspartate residue located in the receiver domain of DcuR results in an activation of the response regulator which finally binds to the DNA and induces the expression of the target genes. Under anaerobic conditions DcuSR regulates gene expression of the fumarate reductase (*frdABCD*), *dcuB* and the fumaraseB (*fumB*) co-transcribed with *dcuB*. Expression of a *dcuB´-´lacZ* reporter gene fusion therefore can be used as a marker for DcuSR-activity. PAS, Per-Arnt-Sim domain; KD, kinase domain RD, receiver domain; DBD, DNA-binding domain

Recognition of external C_4-dicarboxylates by DcuS results in signal transduction through the membrane and activation of the response regulator (Fig. I1, I2). Thereby, periplasmic effector binding causes a conformational change of DcuS followed by an ATP-dependant autophosphorylation of a conserved histidine residue in the cytopsolic kinase domain. The phosphoryl group is subsequently transmitted to a conserved aspartate residue within the

receiver domain of DcuR resulting in a conformational change of the response regulator. The helix-turn-helix motif of the DNA binding domain of actived DcuR binds to the promotor regions of the target genes. Under anaerobic conditions DcuSR stimulates the expression of the fumarate reductase (*frdABCD*) and the fumarate/succinate antiporter DcuB (*dcuB*). Expression of the anaerobic fumarase B (*fumB*) is indirectly controlled by DcuSR (Tseng, 1997), due to partial co-transcription with *dcuB*.

The importance of DcuSR is mainly based on gene expression during anaerobic fumarate respiration. However, expression of the aerobic succinate uptake carrier DctA also is activated by DcuSR in the presence C_4-dicarboxylates (Fig. I2).

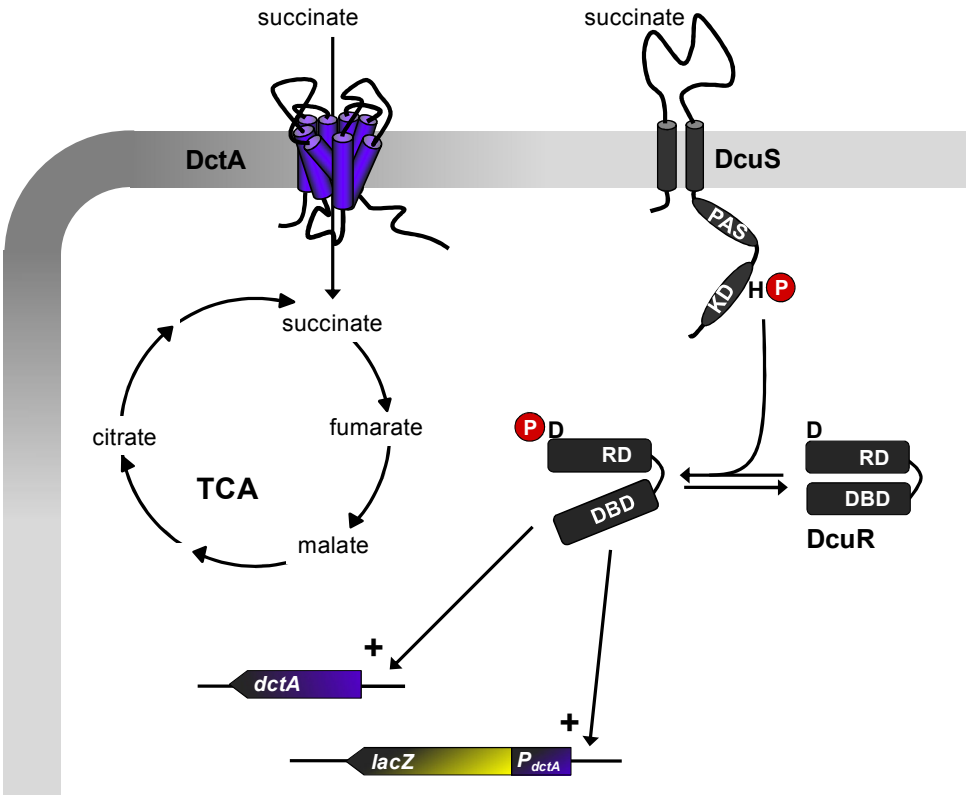

Figure I2: Aerobic growth on C_4-dicarboxylates controlled by DcuSR. In the presence of the terminal electron acceptor oxygen, expression of the C_4-dicarboxylate carrier DctA is induced by the two-component system DcuSR. The binding of C_4-dicarboxylates like succinate, fumarate, malate or aspartate to the periplasmic sensory domain of the senor kinase DcuS results in autophosphorylation of DcuS and phosphorylation of the DcuR receiver domain. As a consequence, the DNA-affinity of the response regulator DcuR increases, resulting in activation of *dctA* expression or expression of a *dctA´-´lacZ* reporter gene fusion. During aerobic respiration C_4-dicarboxylates are fully oxidized to carbon dioxide in the tricarboxylic acid cycle (TCA). PAS, Per-Arnt-Sim domain; KD, kinase domainRD, receiver domain; DBD, DNA-binding domain.

2.1.2 Global regulatory systems of E. coli

Expression of the genes for anaerobic fumarate respiration (*fumB, dcuB, frdABCD*) as well as *dctA* is regulated by the two-component system DcuSR in response to external C_4-dicarboxylates (Zientz *et al*., 1998; Golby et al. 1999). Expression of the DcuSR target genes also depends on the regulatory control systems ArcBC (*dctA*), FNR (*frdABCD, fumB, dcuB*) and NarXL (*dcuB*). To guarantee maximal energy conservation, the metabolism of bacteria is controlled in a hierarchic order which is based on the oxidation-reduction potential of available external electron acceptors. *E. coli* can use nitrate (E_0' = +0,42V), dimethylsulfoxide (E_0' = +0,16V), trimethylamine-N-oxide (E_0' = +0,13V) and fumarate (E_0' = +0,03V) as external electron acceptors in the anaerobic respiration pathways. Growth by aerobic respiration is favored since oxygen is the most electro-positive electron acceptor (E_0' = +0,82V) and provides the highest gain of energy. In the absence of oxygen, the global two-component system ArcBC (Aerobic Respiration Control) represses the genes of the aerobic metabolism (Iuchi & Lin, 1988; Iuchi *et al*., 1989). Simultaneously, synthesis of anaerobic enzymes is stimulated by the global cytoplasmic regulator FNR (Fumarate/Nitrate Regulator) which functions as a gene activator (Shaw & Guest, 1982). Gene expression of nitrate and nitrite respiration is induced by the homologeous two-component systems NarXL and NarQP (Stewart, 1993; Stewart & Rabin, 1995) while genes of less preferred anaerobic respirations or fermentation are repressed.

2.2 Transport of C_4-dicarboxylates in *E. coli*

Uptake of C_4-dicarboxylates is catalized by various transport proteins, depending on the growth conditions. Under anaerobic conditions transport of fumarate, malate and aspartate is accomplished by the secondary carriers DcuA, DcuB and DcuC (Engel *et al*., 1992, 1994; Golby *et al*., 1998; Six *et al*., 1994; Zientz *et al*., 1996). DcuA and DcuB belong to the DcuAB family of carriers which is only present in anaerobic and facultative anaerobic bacteria capable of fumarate respiration (Janausch *et al.*, 2002). The efflux carrier DcuC belongs to the distinct family of DcuC carriers and seems to play an important role in electrogenic succinate-efflux during hexose fermentation and succinate production (Zientz *et al.,* 1996).

DcuA is a general uptake carrier for electroneutral transport of C_4-dicarboxylates in symport with protons. The *dcuA* gene and the adjoining *aspA* gene (L-aspartase) are constitutively expressed (Golby *et al.*, 1998; Zientz *et al.*, 1999), but DcuA does not support aerobic growth

on C_4-dicarboxylates (Davies *et al.*, 1999; Janausch *et al.*, 2001). This indicates a posttranslational inactivation of the carrier. The closely related DcuB carrier (35% sequence identity; 67% similarity) catalyzes fumarate/succinate antiport. In contrast to *dcuA* and *dcuC*, expression of *dcuB* is highly regulated by the two-component system DcuSR, demonstrating the importance of DcuB during fumarate respiration.

Basically, all Dcu carriers show uptake, efflux or exchange activity, but each carrier is specialized for a specific transport modus. A posttranscriptional, reversible inactivation of the anaerobic transport system which is caused by oxygen was postulated (Engel *et al.*, 1992).

Further carriers for anaerobic C_4-dicarboxylate transport in *E. coli* are the citrate/succinate antiporter CitT (Pos *et al*., 1998) and the putative tartrate/succinate antiporter TtdT (Kim, 2006) which belong to the carboxylate-C_4-dicarboxylate antiporter family. The antiporters are required in citrate fermentation and L-tartrate fermentation, respectively, and cannot be replaced by the Dcu carriers.

2.2.1 The anaerobic fumarate/succinate antiporter DcuB

Expression of DcuB is activated by the oxygen sensing regulator FNR under anaerobic conditions. According to the redox potential based hierarchic order of gene expression, nitrate causes *dcuB* repression by the two-component system NarXL. The availability of glucose also results in a strong inhibition of *dcuB* expression since, *dcuB* is subjected to cyclic AMP receptor protein (CRP) mediated catabolite repression. Since DcuB is the most important carrier in *E. coli* during fumarate respiration it is strongly regulated by DcuSR. Under anaerobic conditions in the absence of nitrate and glucose, expression of *dcuB* is induced by DcuSR in response to external C_4-dicarboxylates. DcuB shows the highest transport activities relative to the other Dcu carriers and the apparent K_m value of DcuB for C_4-dicarboxylates is about 100 µM (Engel *et al.*, 1994). Hence, the affinity to C_4-dicarboxylates of DcuB is 30-100 times higher than that of the sensor DcuS.

Current results show that DcuB is required for DcuSR dependent response to C_4-dicarboxylates. Since expression of the *dcuB* gene under anaerobioses strongly depends on DcuSR, a chromosomal *dcuB´-´lacZ* reporter gene fusion (Fig. I1) was used as an indicator for the functional state of DcuSR. Deletion or inactivation of *dcuB* results in constitutive and effector-independent expression of *dcuB´-´lacZ*. The derepression in the absence of effector depends on a functional DcuSR system, indicating an influence of DcuB on DcuSR-induced gene expression (Kleefeld, 2002; Kleefeld *et al.*, 2009).

Mutation studies demonstrate that the DcuB carrier is a bifunctional protein and acts as a co-sensor of the DcuSR two-component system (Kleefeld *et al.*, 2009). Point mutants of DcuB which are deficient either in transport or in regulatory function were identified, confirming independent sites for transport and regulation within the protein. The mechanism of how the regulatory domain of DcuB controls DcuSR function is not known yet, but a direct interaction of DcuS with DcuB is suggested.

2.2.2 The aerobic C_4-dicarboxylate carrier DctA

In contrast to the high number of anaerobic C_4-dicarboxylate transport systems, only one carrier for aerobic uptake of C_4-dicarboxylate in *E. coli* is identified. DctA of *E. coli* belongs to the subfamily of DctA carriers which is found in aerobic gram-negative and aerobic gram-positive bacteria with low G+C contents (Janausch *et al.*, 2002). The monocystronic *dctA* gene possesses a single transcription start site and expression of *dctA* is strongly subjected to catabolite repression (Kay & Kornberg, 1971) and anaerobic repression by ArcA. As observed for other CRP-regulated genes, expression of *dctA* varies in a growth-phase-dependent manner and increase up to 19-fold in the stationary phase relative to the early-log-phase (Davies *et al.*, 1999).

Expression of *dctA* in response to C_4-dicarboxylates is about 2-fold induced by the DcuSR two-component system (Zientz *et al.*, 1998; Golby *et al.*, 1999; Davies *et al.*, 1999). In contrast to the anaerobic Dcu carriers, DctA catalyses only the uptake of C_4-dicarboxylates. The uptake is driven by the electrochemical proton gradient. With each C_4-dicarboxylate 2-3 H^+ are transferred through the membrane (Gutowski *et al*., 1975). The DctA carrier of *E. coli* shows a broad substrate specifity including C_4-dicarboxylate like succinate, fumarate, malate, asparte and tartrate and also the cyclic monocarboxylate orotate (Baker *et al.*, 1996; Kay and Kornberg, 1971). The apparent K_m value for these substrates is about 10-30µM.

DctA is the most active carrier under aerobic conditions and *dctA* mutants show poor growth on fumarate, malate and aspartate (Golby *et al.*, 1999). Apart from DctA *E. coli* possesses a glutamate carrier, GltP, catalysing Δp-dependent uptake of aspartate (Deguchi *et al.*, 1989; Kay & Kornberg 1971). But for some reason this carrier is only of minor significance for aspartate catabolism. The *dctA* mutant is still able to grow on succinate indicating the presence of a so far unknown succinate-uptake carrier. In its mono-protonated form succinate can pass the membrane by diffusion, but low pH is required and the rates are not sufficient for growth (Janausch *et al*., 2001).

Similar to DcuB, expression of *dctA* becomes independent of C_4-dicarboxylates in a *dctA* mutant (Davies *et al*., 1999), indicating that DctA affects DcuSR-dependent expression under aerobic conditions.

2.3 Transport proteins with co-sensoric properties

Besides the C_4-dicarboxylate carrier DcuB and DctA further membrane-integrated transport proteins of *E. coli* are found to be involved in regulatory processes. The secondary carriers LysP (lysine-specific permease) and UhpC (hexose phosphate transporter) as well the ABC transporters $PstSCAB_2$ (high-affinity phosphate transporter) and MalEFGK (maltose translocation system) were shown to act as co-sensors of membrane-bound transcriptional activators and histidine kinases.

The membrane-integrated transcription factor CadC of *E. coli* induces synthesis of the lysine decarboxylase CadA and the lysine/cadaverine antiporter CadB in response to low external pH in common with the presence of lysine. Deletion of the lysine-specific permease LysP causes a lysine-independent expression of *cadBA* indicating that LysP acts as co-sensor of CadC by repressing gene expression in the absence of lysine (Popkin & Maas, 1980). Cross-linking studies confirmed a direct interaction between the membrane-domains of LysP and CadC (Tetsch *et al.*, 2008).

Expression of the inducible hexose phosphate transporter UhpT depends on the UhpBA two-component system and is induced by glucose-6-phosphate. For signal transduction the UhpT-homologous, transport-inefficient carrier UhpC is required. Only binding of glucose-6-phosphate to UhpC allows autophosphorylation of the sensor kinase UhpB and activation of the response-regulator (Island & Kadner, 1993; Schwöppe *et al*., 2003).

The ABC-transporter $PstSCAB_2$ of *E. coli* is the main phosphate transporter during growth under phosphate-limiting conditions. Via the peripheral membrane protein PhoU, $PstSCAB_2$ causes activation of the two-component system PhoRB by an unknown mechanism (Wanner, 1996). As shown for DcuB of *E. coli*, the regulatory process is independent of transport (Cox *et al*., 1989). PhoRB stimulates the expression of the Pho regulon including the genes *pstSCAB*$_2$, *phoA* (alkaline phosphatase), *phoR* (sensor histidine kinase), *phoB* (response regulator) and *phoU*. An excess of inorganic phosphate leads to a $PstSCAB_2$-transmitted repression of the Pho regulon based on a stimulation of the PhoR phosphatase activity.

The maltose translocation system MalEFGK of *E. coli* (Hazelbauer, 1975) and the citrate-uptake tripartite tricarboxylate transporter system BctCBA of *Bordetella pertussis* (Antoine *et al.*, 2005) are examples for the periplasmic-mediated interaction of a transporter with a sensor kinase. In the presence of maltose, the periplasmic maltose-binding protein MalE interacts with the chemoreceptor Tar finally resulting in maltose taxis. Expression of the *bctCBA* operon of *Bordetella pertussis* is induced in the presence of external citrate by the signal transduction two-component system BctDE. Deletion of the periplasmic citrate-binding protein BctC (BctA and BctB are membrane integratal proteins) causes strongly reduced expression of *bctCBA* indicating that BctC is part of the signalling cascade. Interaction studies demonstrated that BctC interacts with the periplasmic domain of the sensor protein BctE.

In *Rhizobium meliloti*, C_4-dicarboxylate dependent gene expression is regulated by the DctBD two-component system. As a consequence of C_4-dicarboxylate binding, the sensor-regulator pair activates the expression of *dctA* encoding the succinate uptake carrier DctA. Genetic deletion of DctA leads to constitutive expression of the *dctA* gene, indicating an important role of the Carrier in DctBD-dependent sensing. Due to different substrate-recognition it is supposed that interaction with DctA leads to an an improved substrate specific of DctB (Reid & Poole, 1998; Yurgel *et al.*, 2000).

2.4 Experiments of this study

The topology of an integral membrane protein is defined as the orientation of membrane-spanning and soluble segments of the polypeptide chain within and relative to the membrane. In this study, the topology of the succinate/fumarate antiporter DcuB was experimentally determined by combined reporter fusions with alkaline phosphatase and ß-lactamase. Topology mapping was followed by Cys-labeling based accessibility studies providing new information on DcuB arrangement and function. In addition, the regulatory properties of DcuB were specified by means of alternative DcuB proteins of various bacteria and modification of the related DcuA carrier. The experimental data obtained by structural and functional studies of DcuB are significant for subsequent approaches, for example to establish a suitable method for detection of DcuB-DcuS interaction.

The function of DctA as a cosensor of the DcuSR system during aerobic growth was investigated by mutation analysis of DctA and by interaction studies of DctA with DcuS using in vivo FRET.

Interaction studies by *in vivo* FRET measurements were conducted in cooperation with Dr. Wolfgang Erker from the group of Prof. Dr. T. Basché at the Institut für Physikalische Chemie, Johannes Gutenberg-Universität Mainz.

Sulphydryl labeling experiments were performed in cooperation with the groups of Prof. Tracy Palmer and Prof. Frank Sargent at the College of Life Science, University of Dundee, Scotland.

3. Materials and methods

3.1 Bacterial strains and plasmids

Table M1: bacterial strains

Strain	Genotype / Characteristics	Reference
***E.coli* K12 strains**		
AN387	wild type	Wallace & Young, 1977
JM109	*recA1 supE44 endA1 hsdR17 gyrA96 relA1 thi* Δ*(lac-proAB) F´[traD36 proAB*$^{+}$*, lacIq lacZΔM15]*	Yanisch-Perron *et al.*, 1985
MC4100	F^{-} *araD139* Δ(*argF-lac*)*U169*, *rpsL150, (ΔlacZ), relA1 flbB530 deoC1 ptsF25 rbsR*	Silhavy *et al.*, 1984
BL21DE3	*E. coli* B,*F' hsdS gal1* DE3, with IPTG-inducable chromosomal T7 RNA polymerase, strain for protein overexpression	Studier & Moffat, 1986
C43DE3	spontaneous mutation of BL21DE3 for overexpression of membrane proteins	Miroux & Walker, 1996
CC181	*F128lacIq* Δ*(ara,leu)7679* Δ*lacX74* Δ*phoA20 galE galK thi rpsE rpoB argEam lacY328am recA1*	Calamia & Manoil, 1986
MDO800	AN387 *dctA*::*Spec*^{r}	Six *et al.*, 1994
IMW237	MC4100, λ (Φ *dcuB' - 'lacZ)* hyb, *bla*	Zientz, 1998
IMW385	MC4100, λ (Φ *dctA' - 'lacZ*) hyb, *bla*	Kleefeld, 2002
IMW386	P1 (MDO800) x IMW385 *dctA:: Spec*^{r}*,* λ (Φ *dctA' - 'lacZ*) hyb, *bla*	Kleefeld, 2002
IMW389	P1 (IMW260) x IMW385 *dcuS::Cam*^{r}, λ (Φ *dctA' - 'lacZ*) hyb, *bla*	Kleefeld, 2002
IMW503	MC4100 but Δ*dcuB*, λ (Φ *dcuB´-´lacZ*)	Kleefeld, 2006
IMW504	P1 (JRG2821) x IMW503 MC4100 but λ (Φ *dcuB´-´lacZ*) *dcuA::Spec*^{r} Δ*dcuB*	Kleefeld, 2006
IMW538	P1 (MDO800) x IMW389 *dctA::Spec*^{r} *dcuS::Cam*^{r}*, λ (* Φ *dctA´-´lacZ)*	Kleefeld, 2006
IMW505	P1 (IMW157) x IMW504 MC4100 but λ (Φ *dcuB´-´lacZ*) *dcuA::Spec*^{r} Δ*dcuB dcuC::Cam*^{r}	Kleefeld, 2006
others		
Salmonella typhimurium	DSM 8274, *Salmonella enterica subsp. enterica* (Loeffler, 1892), strain TA 1535	DSMZ, Braunschweig
Pectobacterium atrosepticum	DSM 30184, syn. *Erwinia carotovora subsp. atroseptica* (van Hall, 1902)	DSMZ, Braunschweig
Campylobacter jejunii	Strain NCTC 11168	Provided by D. Kelly
Corynebacterium diphtheriae	Wild type strain ATCC 13032	Provided by A. Burkovski

Table M2: Plasmids I; expression vectors, plasmids for functional studies and FRET experiments

Plasmid	Genotype / Characteristics	Reference
pASK-IBA3$^+$	vector for protein expression with C-terminal streptagII, AHT-inducible; *Amp^r*	IBA, Göttingen
pASK-IBA33$^+$	vector for protein expression with C-terminal histag, AHT-inducible; *Amp^r*	IBA, Göttingen
pBAD18-Kan	expression vector; pBR322 *ori*, arabinose-inducible P_{BAD} promoter, *Kan^r*	Guzman *et al.*, 1995
pBAD30	expression vector; pACYC *ori*, arabinose-inducible P_{BAD} promoter, *Amp^r*	Guzman *et al.*, 1995
pBAD18-Kan*	pBAD18-Kan, with just one *Hind*III-restriction site left (within the MCS); amino acid sequence remained intact	Scheu, 2009
pME6010	low-copy plasmid, *Tet^r*	Heeb *et al*., 1999
pET-28a	expression vector; pBR322 *ori*, IPTG-inducible T7 promoter, C- and N-terminal histag, *Kan^r*	Novagen, Madison, USA
pT7-5-putP-lacZ	plasmid for expression of *putP-lacZ*; source for *lacZ* (AA10), *Amp^r*	Jung *et. al*., 1998
pT7-5-putP-phoA	plasmid for expression of *putP-phoA*; source for *phoA* without export signal (AA27), *Amp^r*	Jung *et. al*., 1998
pHASoxYZ	plasmid for constitutive expression of *soxY*-HA and *soxZ* from *Paracoccus pantotrophus*, *Cam^r*	Fritsch, group of T. Palmer, unpublished
pW2E6	pBR322 with *dcuB* of *Wolinella succinogenes*	Ullmann *et al*., 2000
***dcuB*-containing plasmids**		
pMW228	*dcuB Eco*RI-*Xho*I with own promotor in pME6010, *Tet^r*	Kleefeld, 2002
pMW755	pMW228 but *dcuB* with C-terminal histag	This study
pMW789	pMW228 but *dcuB* with C-terminal streptagII	This study
pMW808	pMW228 but *dcuB*S420C	This study
pMW280	*dcuB Bam*HI-*Xho*I with N-terminal histag in pET28a, *Kan^r*	Kleefeld, 2006
pMW281	*dcuB Eco*RI-*Xho*I with own promotor in pET28a, *Kan^r*	Kleefeld, 2006
pMW406	*dcuB Eco*RI-*Xho*I in pASK-IBA3$^+$, *Amp^r*	Bauer, 2006
pMW445	*dcuB Xba*I-*Hind*III with C-terminal Streptag in pBAD18-Kan*, 6871 bps, *Kan^r*	This study
***dcuB* genes of alternative bacteria**		
pMW412	$dcuB_{Salty}$ *Bam*HI -*Xho*I in pASK-IBA3$^+$, 4588 bps, *Amp^r*	Bauer, 2006
pMW415	$dcuB_{Salty}$ *Xba*I-*Hind*III in pBAD18-Kan*, 6910 bps, *Kan^r*	Bauer, 2006
pMW416	$dcuB_{Wolsu}$ *Eco*RI-*Xho*I in pASK-IBA3$^+$, 4570 bps, *Amp^r*	Bauer, 2006
pMW417	$dcuB_{Erwca}$ *Eco*RI-*Xho*I in pASK-IBA3$^+$, 4573 bps, *Amp^r*	Bauer, 2006
pMW443	$dcuB_{Erwca}$ *Xba*I-*Hind*III in pBAD18-Kan*, 6895 bps, *Kan^r*	This study
pMW447	$dcuB_{Wolsu}$ *Xba*I-*Hind*III in pBAD18-Kan*, 6892 bps, *Kan^r*	This study
pMW467	$dcuB_{Camje}$ *Sal*I-*Pst*I in pASK-IBA3$^+$, 4663 bps, *Amp^r*	This study
pMW470	$dcuB_{Camje}$ *Xba*I-*Hind*III in pBAD18-Kan*, *Kan^r*	This study
pMW503	$dcuB_{Cordi}$ *Xba*I-*Hind*III in pBAD18-Kan*, subcloned from pASK-IBA3$^+$- *dcuBCordi*	This study

Plasmid	Genotype / Characteristics	Reference
***dcuA*-containing plasmids**		
pMW449	*dcuA Eco*RI-*Xba*I with own promotor in pBAD18-Kan*, 7.051bps, *Kan*^{r}	This study
pMW450	pMW449 but *dcuA*L387D	This study
pMW451	pMW449 but *dcuA*T386S, L387D and V388L	This study
pMW629	pMW449 but *dcuA -dcuB* hybrid *dcuA*(A374)-G-(Y387)*dcuB*	This study
pMW630	pMW449 but *dcuA -dcuB* hybrid *dcuA*(K352)-GL-(V366)*dcuB*	This study
***dctA*-containing plasmids**		
pMW457	*dctA Bam*HI-*Xho*I with own promotor in pET28a, *Kan*^{r}	Kleefeld, 2006
pMW458	pMW457 but *dctA* S380I	Kleefeld, 2006
pMW468	pMW457 but *dctA* S380A	Kleefeld, 2006
pMW782	pMW457 but *dctA* K341A	This study
pMW783	pMW457 but *dctA* T296A	This study
pMW784	pMW457 but *dctA* D303A	This study
pMW785	pMW457 but *dctA* S340A	This study
pMW505	*dctA Bam*HI-*Xho*I with N- and C-terminal histag in pET28a, *Kan*^{r}	This study
plasmids for FRET		
dcuS		
pMW389	*cfp-dcuS* in pBAD18-Kan, *Kan*^{r}	Scheu, 2005
pMW407	*dcuS-yfp* in pBAD30, *Amp*^{r}	Scheu *et al.*, 2008
pMW408	*dcuS-cfp* in pBAD18-Kan, *Kan*^{r}	Scheu, 2009
dcuB		
pMW466	*cfp Pst*I-*Hind*III in pMW445 for expression of *dcuB-cfp*, *Kan*^{r}	This study
pMW493	*cfp Sac*II-*Eco*RI in pMW445 for expression of *cfp-dcuB*, 7603 bps, *Kan*^{r}	This study
pMW494	*yfp Sac*II-*Eco*RI in pMW445 for expression of *yfp-dcuB*, 7603 bps, *Kan*^{r}	This study
dctA		
pMW517	*cfp Nco*I-*Bam*HI in pMW505 (-*Hind*III) for expression of *cfp-dctA*, 7252 bps, *Kan*^{r}	This study
pMW518	*yfp Nco*I-*Bam*HI in pMW505 (-*Hind*III) for expression of *yfp-dctA*, 7252 bps, *Kan*^{r}	This study
pMW519	*cfp Xho*I-*Hind*III in pMW505 (-*Hind*III) for expression of *dctA-cfp*, 7369 bps, *Kan*^{r}	This study
pMW520	*cfp Xho*I-*Hind*III in pMW505 (-*Hind*III) for expression of *dctA-cfp*, 7369 bps, *Kan*^{r}	This study
pMW523	*cfp-dctA* in pBAD18-Kan*, subcloned from pMW517 via *Xba*I and *Hind*III, *Kan*^{r}	This study

Plasmid	Genotype / Characteristics	Reference
pMW524	*dctA-cfp* in pBAD18-Kan*, subcloned from pMW518 via *Xba*I and *Hind*III, *Kan*^{r}	This study
pMW525	*yfp-dctA* in pBAD30, subcloned from pMW519 via *Xba*I and *Hind*III, *Amp*^{r}	This study
pMW526	*dctA-yfp* in pBAD30, subcloned from pMW520 via *Xba*I and *Hind*III, *Amp*^{r}	This study
pMW741	pMW526 but *dctA* D376A	This study
pMW742	pMW526 but *dctA* S380A	This study
pMW743	pMW526 but *dctA* S380I	This study
pMW744	pMW526 but *dctA* E381A	This study
pMW745	pMW526 but *dctA* R383A	This study
pMW756	pMW526 but *dctA* T296A	This study
pMW757	pMW526 but *dctA* D303A	This study
pMW758	pMW526 but *dctA* S340A	This study
pMW759	pMW526 but *dctA* K341A	This study
tar		
pMW801	pMW762 with $tar_{1\text{-}331}$ *Nco*I-*Nco*I for expression of $tar_{1\text{-}331}$-*cfp*	This study
pDK108	pTrc99a derivative for IPTG-inducible expression of $tar_{1\text{-}331}$-*yfp*, pBR ori, pTrc promoter, A*mp*^{r}	Kentner *et al.*, 2006
cfp/yfp controls		
pECFP	Vector containing enhanced GFP-variant CFP, *Amp*^{r}	Clontech
pEYFP	Vector containing enhanced GFP-variant YFP, *Amp*^{r}	Clontech
pMW762	*cfp Nco*I-*Hind*III in pBAD18-Kan*, subcloned from pET28a by using *Xba*I and *Hind*III, *Kan*^{r}	Scheu 2009
pMW763	*yfp Nco*I-*Hind*III in pBAD18-Kan*, subcloned from pET28a by using *Xba*I and *Hind*III, *Kan*^{r}	This study
pMW764	*cfp Nco*I-*Hind*III in pBAD30, subcloned from pET28a by using *Xba*I and *Hind*III, *Amp*^{r}	This study
pMW765	*yfp Nco*I-*Hind*III in pBAD30, subcloned from pET28a by using *Xba*I and *Hind*III, *Amp*^{r}	Scheu 2009
pMW766	*cfp-yfp Xba*I-*Hind*III in pBAD18-Kan*, *Kan*^{r}	Scheu 2009
pMW767	*yfp-cfp Xba*I-*Hind*III in pBAD18-Kan*, *Kan*^{r}	This study
pMW768	*cfp-yfp Xba*I-*Hind*III in pBAD30, *Amp*^{r}	This study
pMW769	*yfp-cfp Xba*I-*Hind*III in pBAD30, *Amp*^{r}	This study

Table M3: Plasmids II; plasmids for topology studies

Plasmid	Synonyme	Genotype / Characteristics	Reference
plasmids coding for DcuB fusion proteins			
bla			
pMW516		*bla Pst*I-*Hind*III in pMW445 for expression of *dcuB-bla*; 7252 bps, *Kan*^{r}	This study
pMW527		*blaM* (without export signal) *Pst*I-*Hind*III in pMW445 for expression of *dcuB-blaM*, *Kan*^{r}	This study
pMW547	H411	pMW527 but C-terminal truncated *dcuB*-H411	This study
pMW548	G373	pMW527 but C-terminal truncated *dcuB*-G373	This study
pMW549	L333	pMW527 but C-terminal truncated *dcuB*-L333	This study
pMW550	H168	pMW527 but C-terminal truncated *dcuB*-H168	This study
pMW551	R127	pMW527 but C-terminal truncated *dcuB*-R127	This study
lacZ			
pMW560		*lacZ Pst*I-*Hind*III in pMW445 for expression of *dcuB-lacZ*; 9886 bps, *Kan*^{r}	This study
pMW576	**F435**	pMW560 but C-terminal truncated *dcuB*-F435	This study
pMW566	**H411**	pMW560 but C-terminal truncated *dcuB*-H411	This study
pMW594	**L399**	pMW560 but C-terminal truncated *dcuB*-L399	This study
pMW575	**L392**	pMW560 but C-terminal truncated *dcuB*-L392	This study
pMW567	**G373**	pMW560 but C-terminal truncated *dcuB*-G373	This study
pMW574	**Y340**	pMW560 but C-terminal truncated *dcuB*-Y340	This study
pMW568	**L333**	pMW560 but C-terminal truncated *dcuB*-L333	This study
pMW573	**S296**	pMW560 but C-terminal truncated *dcuB*-S296	This study
pMW572	**L258**	pMW560 but C-terminal truncated *dcuB*-L258	This study
pMW595	**L237**	pMW560 but C-terminal truncated *dcuB*-L237	This study
pMW571	**L200**	pMW560 but C-terminal truncated *dcuB*-L200	This study
pMW596	**L174**	pMW560 but C-terminal truncated *dcuB*-L174	This study
pMW569	**H168**	pMW560 but C-terminal truncated *dcuB*-H168	This study
pMW652	**L159**	pMW560 but C-terminal truncated *dcuB*-L159	This study
pMW597	**A139**	pMW560 but C-terminal truncated *dcuB*-A139	This study
pMW651	**P131**	pMW560 but C-terminal truncated *dcuB*-P131	This study
pMW570	**R127**	pMW560 but C-terminal truncated *dcuB*-R127	This study
pMW650	**A121**	pMW560 but C-terminal truncated *dcuB*-A121	This study
pMW598	**L114**	pMW560 but C-terminal truncated *dcu*B-L114	This study
pMW649	**G107**	pMW560 but C-terminal truncated *dcuB*-G107	This study
pMW648	**V92**	pMW560 but C-terminal truncated *dcuB*-V92	This study
pMW599	**N85**	pMW560 but C-terminal truncated *dcuB*-N85	This study
pMW647	**L81**	pMW560 but C-terminal truncated *dcuB*-L81	This study
pMW646	**L71**	pMW560 but C-terminal truncated *dcuB*-L71	This study
pMW645	**L53**	pMW560 but C-terminal truncated *dcuB*-L53	This study
phoA			
pMW561		*phoA* (without export signal) *Pst*I-*Hind*III in pMW445 for expression of *dcuB-phoA*; 8275 bps, *Kan*^{r}	This study

Plasmid	Synonyme	Genotype / Characteristics	Reference
pMW627		pMW561 but *dcuB* R414A	This study
pMW578	**F435**	pMW561 but C-terminal truncated *dcuB*-F435	This study
pMW579	**H411**	pMW561 but C-terminal truncated *dcuB*-H411	This study
pMW600	**L399**	pMW561 but C-terminal truncated *dcuB*-L399	This study
pMW580	**L392**	pMW561 but C-terminal truncated *dcuB*-L392	This study
pMW581	**G373**	pMW561 but C-terminal truncated *dcuB*-G373	This study
pMW582	**Y340**	pMW561 but C-terminal truncated *dcuB*-Y340	This study
pMW583	**L333**	pMW561 but C-terminal truncated *dcuB*-L333	This study
pMW584	**S296**	pMW561 but C-terminal truncated *dcuB*-S296	This study
pMW585	**L258**	pMW561 but C-terminal truncated *dcuB*-L258	This study
pMW601	**L237**	pMW561 but C-terminal truncated *dcuB*-L237	This study
pMW586	**L200**	pMW561 but C-terminal truncated *dcuB*-L200	This study
pMW602	**L174**	pMW561 but C-terminal truncated *dcuB*-L174	This study
pMW587	**H168**	pMW561 but C-terminal truncated *dcuB*-H168	This study
pMW661	**L159**	pMW561 but C-terminal truncated *dcuB*-L159	This study
pMW603	**A139**	pMW561 but C-terminal truncated *dcuB*-A139	This study
pMW660	**P131**	pMW561 but C-terminal truncated *dcuB*-P131	This study
pMW588	**L127**	pMW561 but C-terminal truncated *dcuB*-R127	This study
pMW659	**A121**	pMW561 but C-terminal truncated *dcuB*-A121	This study
pMW604	**L114**	pMW561 but C-terminal truncated *dcuB*-L114	This study
pMW658	**G107**	pMW561 but C-terminal truncated *dcuB*-G107	This study
pMW657	**V92**	pMW561 but C-terminal truncated *dcuB*-V92	This study
pMW605	**N85**	pMW561 but C-terminal truncated *dcuB*-N85	This study
pMW656	**L81**	pMW561 but C-terminal truncated *dcuB*-L81	This study
pMW655	**L75**	pMW561 but C-terminal truncated *dcuB*-L75	This study
pMW654	**L71**	pMW561 but C-terminal truncated *dcuB*-L71	This study
pMW653	**L53**	pMW561 but C-terminal truncated *dcuB*-L53	This study
plasmids coding for DcuA fusion proteins			
bla			
pMW553		pMW527 but *dcuA Eco*RI-*Xho*I instead of *dcuB*	This study
lacZ			
pMW565		pMW560 but *dcuA Xba*I-*Xho*I instead of *dcuB*	This study
pMW606	**R400**	pMW565 but C-terminal truncated *dcuA*-R400	This study
pMW681	**L416**	pMW565 but C-terminal truncated *dcuA*-L416	This study
pMW680	**L387**	pMW565 but C-terminal truncated *dcuA*-L387	This study
pMW679	**S364**	pMW565 but C-terminal truncated *dcuA*-S364	This study
pMW607	**A353**	pMW565 but C-terminal truncated *dcuA*-A353	This study
pMW608	**V325**	pMW565 but C-terminal truncated *dcuA*-V325	This study
pMW678	**T289**	pMW565 but C-terminal truncated *dcuA*-T289	This study
pMW677	**A261**	pMW565 but C-terminal truncated *dcuA*-A261	This study
pMW676	**L229**	pMW565 but C-terminal truncated *dcuA*-L229	This study
pMW609	**L194**	pMW565 but C-terminal truncated *dcuA*-L194	This study
pMW675	**V171**	pMW565 but C-terminal truncated *dcuA*-V171	This study

Plasmid	Synonyme	Genotype / Characteristics	Reference
pMW610	**V156**	pMW565 but C-terminal truncated *dcuA*-V156	This study
pMW611	**G122**	pMW565 but C-terminal truncated *dcuA*-G122	This study
pMW674	**S107**	pMW565 but C-terminal truncated *dcuA*-S107	This study
pMW673	**R82**	pMW565 but C-terminal truncated *dcuA*-R82	This study
pMW672	**V49**	pMW565 but C-terminal truncated *dcuA*-V49	This study
phoA			
pMW577		pMW561 but *dcuA Xba*I-*Xho*I instead of *dcuB*	This study
pMW612	**R400**	pMW577 but C-terminal truncated *dcuA*-R400	This study
pMW691	**L416**	pMW577 but C-terminal truncated *dcuA*-L416	This study
pMW690	**L387**	pMW577 but C-terminal truncated *dcuA*-L387	This study
pMW689	**S364**	pMW577 but C-terminal truncated *dcuA*-S364	This study
pMW613	**A353**	pMW577 but C-terminal truncated *dcuA*-A353	This study
pMW614	**V325**	pMW577 but C-terminal truncated *dcuA*-V325	This study
pMW688	**T289**	pMW577 but C-terminal truncated *dcuA*-T289	This study
pMW687	**A261**	pMW577 but C-terminal truncated *dcuA*-A261	This study
pMW686	**L229**	pMW577 but C-terminal truncated *dcuA*-L229	This study
pMW615	**L194**	pMW577 but C-terminal truncated *dcuA*-L194	This study
pMW685	**V171**	pMW577 but C-terminal truncated *dcuA*-V171	This study
pMW616	**V156**	pMW577 but C-terminal truncated *dcuA*-V156	This study
pMW684	**S107**	pMW577 but C-terminal truncated *dcuA*-S107	This study
pMW683	**R82**	pMW577 but C-terminal truncated *dcuA*-R82	This study
pMW682	**V49**	pMW577 but C-terminal truncated *dcuA*-V49	This study
plasmids coding for DctA fusion proteins			
bla			
pMW554		*blaM Xho*I-*Hind*III in pMW505(-*Hind*III) for expression of *dctA-blaM*, *Kan*^{r}	This study
pMW555		*bla Nco*I-*Bam*HI in pMW505(-*Hind*III) for expression of *bla-dctA*, *Kan*^{r}	This study
pMW556		*blaM* (without export signal)*Nco*I-*Bam*HI in pMW505(-*Hind*III) for expression of *blaM-dctA*, *Kan*^{r}	This study
plasmids coding for Cys-mutants of DcuB			
pMW738		pMW281 but *dcuB* C13S, C98S, C104S, C387S and C433S, *Kan*^{R}	This study
pMW228		*dcuB Eco*RI-*Xho*I with own promotor in pME6010, *Tet*^{r}	Kleefeld, 2002
pMW462	**C1mut**	pMW228 but *dcuB* C13S	This study
pMW463	**C23mut**	pMW228 but *dcuB* C98S and C104S	This study
pMW464	**C4mut**	pMW228 but *dcuB* C387S	This study
pMW465	**C5mut**	pMW228 but *dcuB* C433S	This study
pMW735	**C45mut**	pMW228 but *dcuB* C387S and C433S	This study
pMW736	**C2345mut**	pMW228 but *dcuB* C98S, C104S, C387S and C433S	This study
pMW788	**C1235mut**	pMW228 but *dcuB* C13S, C98S, C104S and C433S	This study

Plasmid	Synonyme	Genotype / Characteristics	Reference
pMW737	**C12345mut**	pMW228 but *dcuB* C13S, C98S, C104S, C387S and C433S, *Tet*^{r}	This study
pMW746	**L446C**	pMW737 but *dcuB* L446C	This study
pMW751	**S420C**	pMW737 but *dcuB* S420C	This study
pMW750	**S261C**	pMW737 but *dcuB* S261C	This study
pMW749	**S211C**	pMW737 but *dcuB* S211C	This study
pMW747	**S90C**	pMW737 but *dcuB* S90C	This study
pMW786	**V49C**	pMW737 but *dcuB* V49C	This study
pMW754	**G21C**	pMW737 but *dcuB* G21C	This study
pMW753	**L2C**	pMW737 but *dcuB* L2C	This study
pMW635		pMW445 but *dcuB* C13S, C98S, C104S, C387S and C433S, *Kan*^{r}	This study
pMW561		*phoA* (without export signal) *Pst*I-*Hind*III in pMW445 for expression of *dcuB-phoA*; 8275 bps, *Kan*^{r}	This study
pMW821		pMW651 but *dcuB* C13S, C98S, C104S, C387S	This study
pMW822		pMW651 but *dcuB* C98S, C104S, C387S and C433S	This study
pMW823		pMW651 but *dcuB* C13S, C98S, C104S, C387S and C(linker)S	This study
pMW824		pMW651,but *dcuB* C13S, C98S, C104S, C433S and C(linker)S	This study
pMW825		pMW651 but *dcuB* C98S, C104S, C387S, C433S and C(linker)S	This study
pMW826		pMW651 but *dcuB* fivefold-mutant: C13S, C98S, C104S, C387S, C433S plus C(linker)S	This study
pMW832		pMW826 but *dcuB* S211C	This study
pMW833		pMW826 but *dcuB* L446C	This study
pMW834		pMW826 but *dcuB* S90C	This study
pMW835		pMW826 but *dcuB* M1C	This study
pMW836		pMW826 but *dcuB* G21C	This study
pMW837		pMW826 but *dcuB* V49C	This study
pMW838		pMW826 but *dcuB* S261C	This study
pMW829		pMW826 but *phoA* C168S and C286S	This study
pMW830		pMW826 but *phoA* C178S and C336S	This study
pMW831		pMW826 but *phoA* C178S and C286S	This study
pMW911		pMW826 but *phoA* C168S, C286S and C336S	This study
pMW912		pMW826 but *phoA* C168S, C178S and C336S	This study
pMW828		pMW826 but *phoA* C168S, C178S; C286S and C336S	This study
pMW879	**M1C**	pMW828 but *dcuB* M1C	This study
pMW845	**C13**	pMW828 but *dcuB* S13C (C1 removed)	This study
pMW880	**R19C**	pMW828 but *dcuB* R19C	This study
pMW839	**G21C**	pMW828 but *dcuB* G21C	This study
pMW881	**K46C**	pMW828 but *dcuB* K46C	This study
pMW882	**E79C**	pMW828 but *dcuB* E79C	This study

Plasmid	Synonyme	Genotype / Characteristics	Reference
pMW883	**K87C**	pMW828 but *dcuB* K87C	This study
pMW840	**S90C**	pMW828 but *dcuB* S90C	This study
pMW884	**C89**	pMW828 but *dcuB* S89C (C2 removed)	This study
pMW846	**C104**	pMW828 but *dcuB* S104C (C3 removed)	This study
pMW885	**T112C**	pMW828 but *dcuB* T112C	This study
pMW886	**Y118C**	pMW828 but *dcuB* Y118C	This study
pMW887	**N125C**	pMW828 but *dcuB* N125C	This study
pMW888	**S135C**	pMW828 but *dcuB* S135C	This study
pMW889	**G138C**	pMW828 but *dcuB* G138C	This study
pMW890	**S146C**	pMW828 but *dcuB* S146C	This study
pMW891	**S154C**	pMW828 but *dcuB* S154C	This study
pMW892	**T163C**	pMW828 but *dcuB* T163C	This study
pMW893	**R167C**	pMW828 but *dcuB* R167C	This study
pMW894	**L172C**	pMW828 but *dcuB* L172C	This study
pMW895	**D173C**	pMW828 but *dcuB* D173C	This study
pMW896	**E204C**	pMW828 but *dcuB* E204C	This study
pMW897	**E217C**	pMW828 but *dcuB* E217C	This study
pMW844	**S211C**	pMW828 but *dcuB* S211C	This study
pMW898	**D222C**	pMW828 but *dcuB* D222C	This study
pMW899	**K230C**	pMW828 but *dcuB* K230C	This study
pMW900	**R259C**	pMW828 but *dcuB* R259C	This study
pMW901	**S261C**	pMW828 but *dcuB* S261C	This study
pMW902	**E299C**	pMW828 but *dcuB* E299C	This study
pMW903	**E328C**	pMW828 but *dcuB* E328C	This study
pMW904	**K338C**	pMW828 but *dcuB* K338C	This study
pMW905	**S352C**	pMW828 but *dcuB* S352C	This study
pMW906	**S357C**	pMW828 but *dcuB* S357C	This study
pMW907	**D375C**	pMW828 but *dcuB* D375C	This study
pMW847	**C387**	pMW828 but *dcuB* S387C (C4 removed)	This study
pMW908	**R406C**	pMW828 but *dcuB* R406C	This study
pMW909	**R414C**	pMW828 but *dcuB* B R414C	This study
pMW848	**C433**	pMW828 but *dcuB* S433C (C5 removed)	This study
pMW910	**L446C**	pMW828 but *dcuB* L446C	This study

3.2 Growth and media

Growth of *Escherichia coli*

For **genetic methods** bacteria were grown aerobically in LB broth at 37°C.

Cultivation of *E. coli* for **growth experiments** was performed in enriched M9 medium supplemented with the carbon source, electron acceptor and effector as indicated. Cells were grown under aerobic or anaerobic conditions for testing the effects of DctA or DcuB, respectively, at 37°C. Aerobic growth was performed in Erlenmeyer flasks or test tubes on a rotary shaker. Precultures for anaerobic growth were cultivated semi-anaerobically in test tubes without shaking, whereas the main cultures were incubated in degassed infusion bottles (Müller-Krempel) or rubber stoppered tubes (Sovirell) under nitrogen atmosphere (N_2 5.0, purity >99.999 %, Linde).

For determination of **chromosomal encoded β-galactosidase activity**, *E. coli* IMW505 (*dcuB´-´lacZ*) was grown anaerobically in rubber stoppered tubes at 37°C in 5 ml enriched M9 medium supplemented with glycerol, DMSO, with or without fumarate. The medium was inoculated with 5 % (v/v) of a 5 ml preculture grown semi-anaerobically overnight. The ß-galactosidase assays were performed with cells harvested in the mid-exponential phase of growth (optical density (OD_{578nm}) of 0.5 - 0.8). Cells with chromosomal encoded *dctA´-´lacZ* reporter gene fusion (*E. coli* IMW385, IMW386, IMW389 and IMW538) were cultivated in shaking test tubes since no difference in ß-galactosidase activity was found to cells grown aerobically in shaking flasks. Cells were grown in enriched M9 medium with different carbon sources and effectors for 14 h, corresponding to the early log phase.

Growth for ***lacZ-* or *phoA-* expression studies** (plasmid-encoded *lacZ* or *phoA* fusions) was performed in LB broth under aerobic conditions at 37°C. After 4 h cells were induced by adding 0.2% (13.3mM) arabinose in the mid-exponential phase and harvested after further 3 hours of incubation at 30°C.

Uptake of ^{14}C-succinate was measured in anaerobically cultivated cells during the late exponential growth phase. Growth was performed in 50 ml enriched M9 medium plus glycerol, DMSO and fumarate in degassed infusion bottles at 37°C.

For ***in vivo* FRET measurements** cells were grown aerobically in 5 ml LB broth with 300µM L-arabinose at 30°C for 3-5 h. The medium was inoculated with 2 % (v/v) of a preculture

grown overnight in LB broth on a rotary shaker. Aerobic growth was performed in shaking tubes containing a culture volume of 5 ml.

Labeling by AMS, NEM and PEGmal was performed with cells cultivated on a rotary shaker in 25 ml LB broth with 50mM Na-fumarate. At an OD of about 0.6 to 1.0, 20 mM potassium phosphate pH 6.8 was added and protein expression was induced by 0.2% arabinose. Cells were incubated aerobically for further 4 hours at 30°C. The cultures were stored at 4°C over night until use.

Precultures were grown under comparable conditions and in the same medium (except for inducers) as the corresponding main cultures.

If appropriated, antibiotics were added to the media. When two or more antibiotics were supplied simultaneously, half of the concentrations were added.

Media and buffers

All media were autoclaved or filter-sterilised prior to use.

Complex medium, LB (Luria Bertani) broth (Sambrook and Russell, 2001)

10 g/l Casein (Select peptone Nr. 140, Gibco)
5 g/l Yeast extract (Servabacter 24540, Serva)
5 g/l NaCl (Roth)

LB agar LB broth with 15 g/l Agar-Agar, Kobe I pulv. (Roth)

Minimal medium, M9 medium (10x), pH 7 (Miller, 1992)

75 g/l Na_2HPO_4 x 2 H_2O (Roth)
30 g/l KH_2PO_4 (Roth)
5 g/l NaCl
10 g/l NH_4Cl (Fluka)

Enrichments (autoclaved separately)

10 ml/l $CaCl_2$ x 2 H_2O (Roth), 10 mM
10 ml/l Acid-hydrolysed caseine (AHC, peptone Nr. 5, Gibco), 10 %
5 ml/l L-tryptophan (Serva), 1 %
1 ml/l $MgSO_4$ x 7 H_2O (Roth), 1 M

Carbon sources, electron acceptors and effectors (final concentration)

50 mM Glycerol (Fluka)

50 mM Na-gluconate, filter-sterilised (Sigma)

50 mM Na-pyruvate

50 mM Na-acetate (Roth)

50 mM Dimethylsulfoxide (DMSO, Fluka)

50 mM Na_2-fumarate (Fluka)

50 mM Na-malate

50 mM Na-aspartate

Transformation SOC medium (Sambrook and Russell, 2001)

20 g/l Casein (Select peptone Nr. 140, Gibco)

5 g/l Yeast extract (Servabacter 24540, Serva)

0.584 g/l NaCl

0.19 g/l KCl (Roth)

2.46 g/l $MgSO_4$ x 7 H_2O

2.03 g/l $MgCl_2$ x 6 H_2O (Fluka)

3.96 g/l Glucose x H_2O (Roth)

TSB medium

20 g PEG 6000 (Duchefa Biochemie, Haarlem, NL)

2 ml 1M $MgSO_4$

2 ml 1M $MgCl_2$

ad LB broth to 200 ml

Inducers (stock solution)

1 M Isopropyl-β-D-thiogalactopyranoside (IPTG, Roth)

1 M L(+)-arabinose (Roth)

Antibiotics	stock solution	final concentration
Ampicillin (Roth)	50 mg/ml in H_2O	100 µg/ml
Kanamycinsulfat (Roth)	50 mg/ml in H_2O	50 µg/ml
Spectinomycin (Sigma)	50 mg/ml in H_2O	50 µg/ml
Chloramphenicol (Fluka)	20 mg/ml in EtOH	20 µg/ml
Tetracycline (Fluka)	50 mg/ml in H_2O /EtOH (1:1)	15 µg/ml

Buffer for FRET

PBS buffer (1x) (Sambrook and Russell, 2001)

137 mM NaCl

2.7 mM KCl

10 mM Na_2HPO_4

2 mM KH_2PO_4

adjusted with HCl to pH 7.5

Buffer and reagents for transport measurements

Puffer A 100 mM Na/KPi buffer (1 M Na_2HPO_4, 1 M KH_2PO_4, pH 7)

1 mM MgSO4

ad dH_2O to final volume, degasse

Reagents for transport measurements 1 M Glucose, degassed

2,3-[^{14}C]-Succinate (Hartmann Analytic, 9.25 MBq, 44.8 mCi/mmol)

0.1 LiCl

Scintillation solution (Rotiszint® ecoplus, Roth)

Buffer and reagents for β-galactosidase assays (Miller, 1992)

β-Galactosidase reaction buffer (pH 7)

0.1 M KP_i buffer (1 M KH_2PO_4, 1 M K_2HPO_4, pH 7)

10 mM KCl

1 mM $MgCl_2$ (Fluka)

ad 2.7 ml/l 2-Mercaptoethanol prior to use.

Reagents for the β-galactosidase assays

4 mg/ml o-Nitrophenyl-ß-D-galactopyranoside (ONPG, Fluka)

1 M Na_2CO_3 (Fluka)

0.1 % (w/v) Sodiumdodecylsulfate (SDS, Roth)

Buffer and reagents for alkaline phosphatase assays (Calamia & Manoil, 1990)

Puffer A 10 mM Tris/HCI, pH 8.0
150mM NaCI

Puffer B 1 M TrislHCl, pH 8.0
1 mM $ZnCl_2$

pNPP-solution (p-nitrophenyl phosphate) 0,4 % pNPP (w/v) in 1 M Tris/HCl, pH 8.0

Buffers and reagents for sulphydryl-labeling

HEPES buffer; pH 6.8
50 mM HEPES (Melford Laboratries Ltd, Ipswich, UK)
50 mM NaCl
ad dH_2O to final volume

HEPES/ NaCl buffer; pH 6.8
50 mM HEPES
250 mM NaCl
ad dH_2O to final volume

NEM stock solution (50mM)

0.0062 g N-Ethylmaleimide (NEM; Sigma)
dissolve in 1 ml HEPES buffer; pH 6.8
prepare freshly prior to use

AMS stock solution (20mM)

25 mg 4-Acetamido-4´-maleimidylstilbene-2,2´-disulfonic acid, disodium salt (AMS; Invitrogen)
dissolve in 2.33 ml HEPES buffer; pH 6.8
store at -80°C in aliquots à 100 µl and protect from light

PEGmal stock solution (50mM)

0.025 g alpha-Methoxy-omega-ethyl-maleimide polyethylene glycol, 5000 Da (PEGmal; NOF Corporation, Tokyo, Japan, Sunbright MA series)
dissolve in 0.1 ml HEPES buffer; pH 6.8
prepare freshly prior to use

SDS-PAGE

Resolving Gel (10%)
- 3.33 ml 30% Acrylamid (Flowgen Biosciences)
- 3.75 ml 1M Tris-HCl; pH 8.8
- 0.1 ml 10% (w/v) SDS
- 0.01 ml TEMED (BDH Electran)
- 0.1 ml 10% APS (Melford Laboratries Ltd, Ipswich, UK)
- 2.7 ml H_2O

Stacking Gel (4%)
- 0.67 ml 30% Acrylamid
- 1.25 ml 1M Tris-HCl; pH 6.8
- 0.05 ml 10% SDS
- 0.005 ml TEMED
- 0.05 ml 10% APS
- 2.98 ml H_2O

SDS Sample buffer (2x) (Laemmli, 1970)
- 100 mM Tris/HCl, pH 6.8
- 200 mM Dithiothreitol (DTT, Sigma)
- 4 % (w/v) SDS (Roth)
- 0.2 % Bromphenol blue (Janssen Chimica)
- 20 % Glycerol
- or Laemmli sample buffer (Bio-Rad)

SDS Running buffer (10x)
- 250 mM Tris base (Formedium Ltd, Hunstanton, UK)
- 1.92 M Glycine
- 1 % (w/v) SDS
- ad dH_2O to final volume

Buffers and solutions for semi-dry Western blotting (Towbin *et al.*, 1979)

Tris-Glycine Transfer Buffer
- 25 mM Tris base
- 192 mM Glycine
- 20 % Methanol (v/v) (Roth)
- ad dH_2O to final volume

Carbonate Transfer Buffer	0.07g Na_2CO_3 (anhydrous) 0.17g $NaHCO_3$ dissolve in 160 ml H_2O ad 40 ml MeOH
Blocking buffer	PBS buffer (1x) 5 % skimmed milk powder (Marvel Original, Premier International Foods (UK) Ltd) 0.1 % Tween 20 (w/v) (Serva)
Washing buffer	0.1 % Tween 20 in 1x PBS buffer
Antibody solution	1x PBS buffer 5 % skimmed milk powder 0.1 % Tween 20 Antibody dilution
Antibodies	
Primary antibodies:	Monoclonal Anti-PhoA produced in mouse (Sigma), dilution 1:20000 Monoclonal Anti-HA, coupled to horse-radish peroxidase HRP (Sigma), dilution 1:20000
Secondary antibodies:	Anti-IgG-rabbit, coupled to HRP (Bio-RAD), dilution 1:10000 Anti-IgG-mouse, coupled to HRP (Qiagen), dilution 1:10000
Developer solution	Millipore Immobilon Western Chemiluminescent HRP Substrate (Millipore)

3.3 Molecular genetic methods

Molecular genetic methods such as gene amplification via PCR, restriction and ligation of DNA fragments were performed by using standard procedures (Sambrook and Russell, 2001). Plasmids were isolated by using the QIAprep Spin Miniprep kit (Qiagen, Hilden); for isolation of genomic DNA the Nucleospin C+T kit (Macherey & Nagel) was used.

PCR products and restriction fragments were purified with the QIAquick PCR Purification kit (Qiagen, Hilden). Restriction endonucleases and T4 DNA ligase were applied from MBI Fermentas. Prior to ligation, dephosphorylation of the restricted vector was accomplished by incubation with CIAP-phosphatase (Fermentas). DNA concentrations were determined with the Biophotometer (Eppendorf) or by using the NanoDrop ND-1000 Spectrophotometer (Labtech). For Ligation the insert was added at a 5-fold molecular excess in respect to the vector. Ligations were incubated for 3 h at 37°C or overnight at 16°C and precipitated with butanol prior to transformation. *E. coli* strains were transformed by electroporation (Dower *et al*., 1988) or heatshock. Preparation of electro-competent cells was performed according to Farinha *et al.* (1990). The sequences of resulting constructs were verified by DNA sequencing self-designed primers (Agowa LGC group, Berlin; Genterprise, Mainz).

For generation of plasmid-encoded point mutants the QuikChange Site-Directed Mutagenesis kit (Stratagene, La Jolla, USA) was used or alternatively *Pfu*Ultra (Stratagene) in combination with *Dpn*I endonuclease (Fermentas) and heatshock-competent JM109 cells. The complementary primer pairs were applied from MWG Biotech and Sigma Aldrich.

When required (as for FRET measurements and labeling experiments), two plasmids with different antibiotic resistance genes and different origins of replication (Novick, 1987) were transformed into one cell.

Heatshock

Heatshock-competent cells were prepared as followed. Cells were grown in 5 ml LB with appropriate antibiotics with vigorous shaking to the early log phase (OD_{578nm} = 0.5). The culture was chilled on ice for at least 10 min and cells were harvested by centrifugation. The cell pellet was resuspended in 500 µl ice-cold TSB and chilled again for at least 20 min. When not used immediately, cells were freezed in liquid nitrogen and stored at -80°C.

For transformation plasmid DNA (plasmids, 1-10 ng of DNA; mutagenesis, 2 µl *Dpn*I-digest) was added to 100 µl competent cells, mixed by vortexing and incubated for 30 minutes on ice. The mixture was heated for 90 sec at 42°C immediately followed by chilling on ice for 2 minutes. After adding 1 ml LB broth cells were incubated with shaking at 37°C for one hour until spread on LB agar plates containing appropriate antibiotics.

3.3.1 Polymerase chain reaction (PCR)

In vitro gene amplification was carried out by the polymerase chain reaction (Mullis *et al.*, 1986). For all reactions with plasmid DNA as a template (including site-directed mutagenesis) the proof-reading polymerases *Pfu*Ultra or *Pfu*Turbo (Stratagene) were used. When required (since there was no product obtained by *Pfu*Ultra), amplifications of chromosomal DNA was performed with the *Taq* polymerase (Abgene). The components of a 50 µl PCR reaction mixture are listed in Tab. M4; the PCR protocols in Tab. M5.

Table M4: Final concentration of the components added to a 50 µl PCR reaction mixture.

Components	*Pfu*Ultra (Stratagene)	*Taq* (Abgene)
PCR buffer	1x	1x
10 mM dNTP mix	250 µM each	200 µM each
$MgCl_2$	included in the buffer	1.5 - 3 mM
Primer	0.5 µM each (10 pmol)	0.5 µM each (10 pmol)
Template DNA	50-100 ng	100 ng
Polymerase	2.5 U	2.5 U
DMSO	1 - 10 %	1 - 10 %
bdH_2O	Ad to a final volume of 50µl	Ad to a final volume of 50µl

Table M5: PCR protocols for the DNA polymerases used.

Step	*Pfu*Ultra (Stratagene)	*Taq* (Abgene)	Site-directed mutagenesis (*Pfu*Turbo, Stratagene)
1. Initial denaturation	95°C, 3 min	94°C, 4 min	95°C, 30 sec
2. Denaturation*	95°C, 30 sec	94°C, 20 sec	95°C, 30 sec
3. Annealing*	T_m - 5°C, 30 sec	T_m - 5°C, 30 sec	58°C, 1 min
4. Elongation*	72°C, 1 min/kb	72°C, 1 min/kb	72°C, 1 min/kb
5. Final elongation	72°C, 10 min	72°C, 10 min	72°C, 10 min

*The cycle (steps 2 - 4) was repeated 30-35 times.

The annealing temperature for the amplification of DNA fragments was chosen 5°C below the melting temperature T_m of the primer pair and, if required ascertained by step gradient PCR. For elongation, time depended on the size of the amplified DNA fragment. The primers used for cloning and for site-directed mutagenesis are listed in the appendix. PCR was performed in the iCycler (Bio-Rad), MyCycler (Bio-Rad) or Progene Thermocycler (Techne).

3.3.2 Construction of expression vectors

Systems for plasmid-encoded gene expression were created as described on the following pages. The constructs were verified by restriction assays and the encoded gene or gene fusion finally controlled by sequencing.

Plasmids for inducible gene expression

Genes were expressed under the control of the arabinose-inducible pBAD promoter in pBAD18-Kan* and pBAD30 (Guzman *et al.*, 1995) or the IPTG-inducable T7 promotor in pET28a. Due to the lack of a ribosome binding site (RBS) in the pBAD vectors, genes for expression in pBAD18-Kan* and pBAD30 were first cloned into the AHT-inducible expression vector pASK-IBA3$^+$ or pET28a. By using the restriction sites *Xba*I and *Hind*III the genes including the RBS sequence of pASK-IBA3$^+$ or pET28a were inserted into the respective pBAD vectors.

Plasmids for study of protein function

***dcuB*$_{E.coli}$ and alternative *dcuB* genes**

For complementation studies of alternative DcuB carriers in *E. coli* the arabinose-inducible expression vector pBAD18-Kan* was used. The *dcuB* genes without corresponding promoter regions of *Escherichia coli, Salmonella typhimurium, Erwinia carotovora, Wolinella succinogenes, Campylobacter diphtheria* and *Corynebacterium jejunii* were amplified from genomic DNA or plasmids by PCR and cloned into the AHT-inducible expression vector pASK-IBA3$^+$ obtaining the plasmids pMW406$_{Ecoli}$, pMW412$_{Salty}$, pMW416$_{Wolsu}$, pMW417$_{Erwca}$, pMW467$_{Camje}$ and pASK-IBA3$^+$_dcuB$_{Cordi}$.

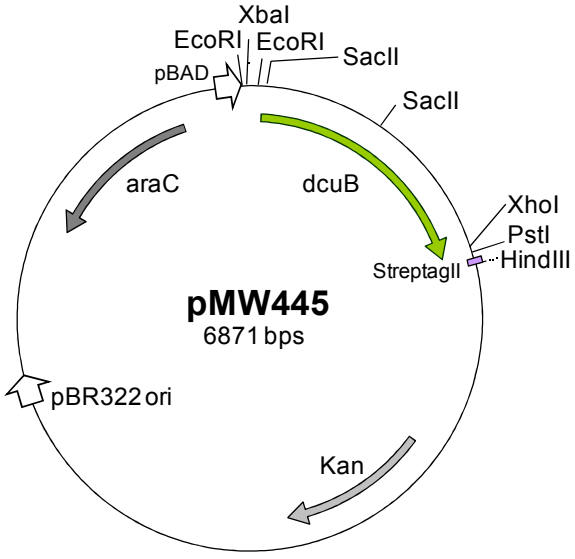

Figure M1: Plasmid pMW445 for arabinose-induced expression of DcuB-Strep. A DNA fragment including RBS and *dcuB* gene with C-terminal StreptagII from pMW406 was cloned into the pBAD18-Kan* vector.

For adjustable expression of *dcuB*, the genes were subsequently cloned into the pBAD18-Kan* vector via *Xba*I and *Hind*III. The resulting constructs pMW445$_{Ecoli}$, pMW415$_{Salty}$, pMW443$_{Erwca}$, pMW447$_{Wolsu}$, pMW470$_{Camje}$ and pMW503$_{Cordi}$ encode for the different DcuB proteins with C-terminal linked StreptagII. The *E. coli dcuB*-containing plasmid pMW445 (MGDRGPE-DcuB(3-444)-LEVDLGGDHGISAWSHPQFEK, Fig. M1) served as an origin for construction of all *dcuB* fusion plasmids.

Gene fusions for FRET measurements

***dcuB-gfp* fusions**

For FRET measurements in-frame fusions of *dcuB* with derivatives of the green fluorescent protein were constructed. The *ecfp* gene was amplified from plasmid pECFP by PCR using the primers PstI-CFP and CFP-HindIII. A *Pst*I restriction site within the *gfp* sequence was removed by site-directed mutagenesis with the primer pair cfp-PstImut-for/ -rev. The PCR fragment was cloned into the plasmid pMW445. The resulting plasmid pMW466 encodes for DcuB with C-terminal CFP. For N-terminal GFP fusions *ecfp* and *eyfp* were amplified from pECFP and pEYFP with the oligonucleotides SacII-gfp and gfp-EcoRI. In pMW445, second restriction sites for *Sac*II (within *dcuB*) and *Eco*RI (pBAD promoter region) were removed by site directed mutagenesis. The amino acid sequence of pMW445 remained unaltered by the mutagenesis. The PCR fragments were cloned via the flanking *Sac*II and *EcoR*I restriction sites into the mutated pMW445 receiving the plasmids pMW493 and pMW494.

***dctA-gfp* fusions**

The *dctA* gene encoded on plasmid pMW457 was amplified using the primers dctA-BamHI-for and dctA-XhoI-rev and cloned into the vector pET28a. The resulting plasmid pMW505 (Fig. M2) codes for DctA with N- and C-terminal Histag under the control of the IPTG-inducible T7 promotor. By site-directed mutagenesis a *Hind*III restriction site was inserted behind the histag using the **c**omplementary primers pMWHindIIIfor and pMW505HindIIIrev. For N-terminal *gfp-dctA* fusions *ecfp* and *eyfp* were amplified by PCR from pECFP and pEYFP with for-gfp-NcoI and rev-BamHI-gfp and cloned in front of the *dctA* gene (plasmids pMW517 and pMW518). C-terminal fusion proteins were obtained by amplifying the *egfp* genes with the primer pair for-gfp-XhoI and HindIII-gfp-rev. After cloning of the PCR product into pMW505, the additional inserted *Xba*I site was removed by mutagenesis with the primers pEGFP-XbaImutfor and -XbaImutrev.

CFP fusions encoding constructs were finally subcloned into the pBAD18-Kan* vector, whereas *yfp* fusions were inserted into the pBAD30 vector via the restriction sites *Xba*I and *Hind*III. The resulting plasmids pMW523, pMW524, pMW525 and pMW526 (Fig. M2) contain an arabinose-inducable fusion protein of DctA and GFP with either C- or N-terminal Histag.

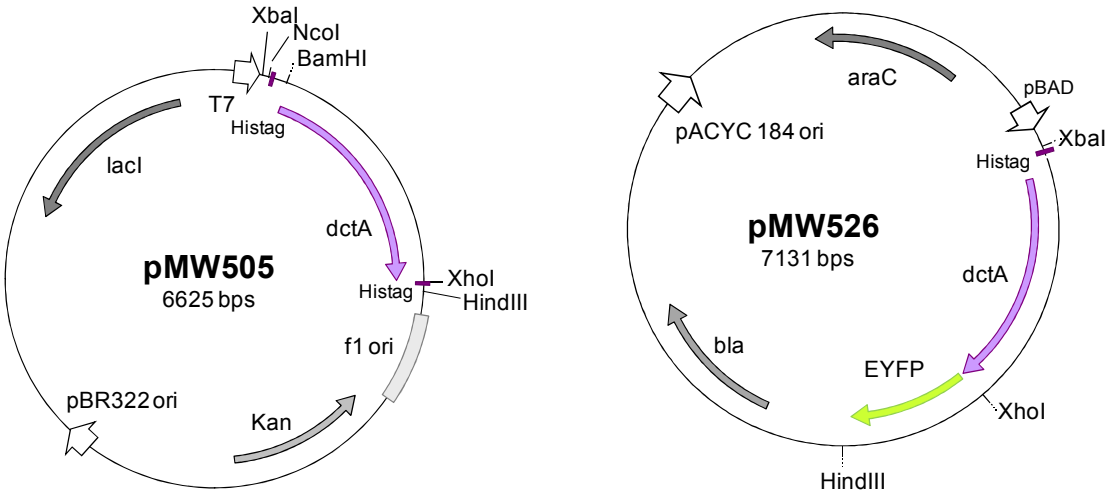

Figure M2: Plasmids pMW505 and pMW526 for expression of DctA-His and DctA-YFP. The pET28a derivative pMW505 was used for construction of an in-frame *dctA-yfp* gene fusion. The *yfp* gene was cloned into pMW505 via *Xho*I and *Hind*III restriction sites and the *dctA-yfp* gene fusion was subcloned in pBAD18-Kan* by using the *Xba*I and *Hind*III restriction sites.

cfp-yfp fusions

For expression of fusions of CFP and YFP with each other, the genes *ecfp* and *eyfp* were amplified from pECFP and pEYFP with BamHI-gfp-for and HindIII-gfp-rev. The *dctA* gene of pMW516 and pMW517 was substituted by the PCR fragment via restriction with *Bam*HI and *Hind*III. As described for *dctA-gfp* constructs, the additional *Xba*I site between the freshly inserted *egfp* gene and the *Hind*III restriction site was removed by mutagenesis. Finally both gene fusions *cfp-yfp* and *yfp-cfp* were transferred into the pBAD18-Kan* and the pBAD30 vector via *Xba*I and *Hind*III resulting in the plasmids pMW766, pMW767, pMW768 and pMW769. The mainly used plasmid pMW766 (Fig. M3) encodes for ECFP(1-239)-YSSRVPVAT-EYFP(1-239).

cfp/ yfp

Derivatives of pBAD18-Kan* and pBAD30 with single *cfp* or *yfp* were constructed as follows. The genes *ecfp* and *eyfp* were amplified from pECFP or pEYFP, respectively, by PCR with oligonucleotide primers for-gfp-NcoI and HindIII-gfp-rev. The amplification

products were integrated into pET28a using the flanking restriction sites *Nco*I and *Hind*III. For expression of both proteins in one cell, *ecfp* and *eyfp* were cloned into pBAD18-Kan* and pBAD30 via restriction endonucleases *Xba*I and *Hind*III. Thus two plasmid pairs for *cfp/ yfp* co-expression were obtained; pMW762/ pMW765 (Fig. M3) and pMW763/ pMW764.

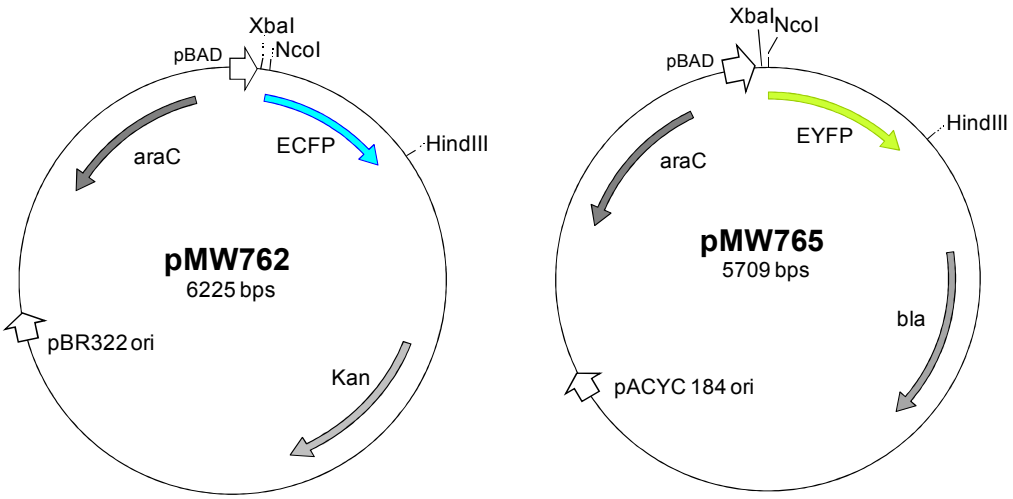

Figure M3: Control plasmids for FRET measurements. Plasmids pMW762 and pMW765 for co-expression of the GFP derivatives CFP and YFP were obtained by cloning *yfp* or *cfp* fragments into plasmids pBAD30 and pBAD18-Kan*, respectively. The required ribosome binding site was derived from plasmid pET28a. Both genes are expressed under the control of the arabinose-inducible P_{BAD} promoter, but the plasmids contain different antibiotic resistance genes and different origins of replication.
The pBAD18-Kan* derivative pMW766 harbours a *cfp-yfp* gene fusion for arabinose-inducible expression of CFP-YFP.

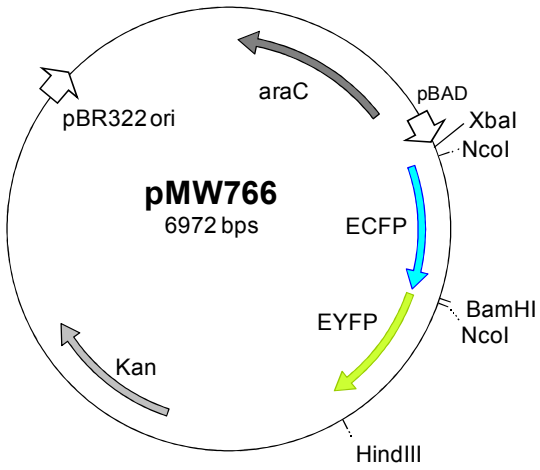

Tar$_{1-331}$*-cfp* fusion

The *tar* gene was amplified from pDK108 (Kentner *et al.,* 2006) by PCR by the use of the oligonucleotides Tar_NcoI-for and Tar_NcoI-rev and cloned into pMW762. The plasmid carrying the right gene orientation was identified by sequencing and termed as pMW801.

dcuS-yfp fusion

The pBAD30 derivative pMW407 encoding for His-DcuS(1-539)-(Lys)-EYFP(4-240) was obtained from P. Scheu (Scheu *et al*., 2009)

Gene fusions of *dcuB* for topology studies

***dcuB-blaM* fusion**

The ß-lactamase gene *bla* of *E. coli* was amplified from vector pASK-IBA3$^+$ by PCR with for-PstI-bla and HindIII-bla-rev and cloned into the *dcuB* containing pBAD18 derivative pMW445. The resulting plasmid pMW516, carrying an in-frame fusion of *dcuB-bla* including the ß-lactamase leader peptide, was modified by site-directed mutagenesis. By using the oligonucleotides blalead-PstI-for and blalead-PstI-rev a second *Pst*I site was inserted between the export signal and the mature ß-lactamase *blaM* gene. After digestion of pMW516 with *Pst*I and relegation, the leader-free construct pMW527 was identified by sequencing. Plasmid pMW527 codes for MGDRGPE-DcuB(3-444)-LEVDLQ-Bla(25-286), hereafter referred to as DcuB-BlaM. Figure M4 shows the map of pMW527 after removing of the additional *Eco*RI and *Xho*I restriction sites. For *dcuB-blaM* fusions with C-terminal truncated *dcuB* part, *dcuB* fragments were amplified from pMW445 with pBAD-dcuBXbaIfor and dcuB-PstI-re primers. The gene fragments were cloned in plasmid pMW527 replacing full-length *dcuB*.

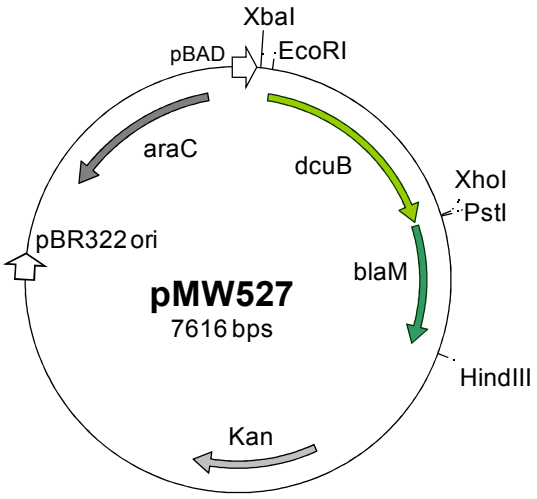

Figure M4: Plasmid pMW526 for arabinose-inducible expression of DcuB-BlaM. The *blaM* gene was cloned into pMW445 (Fig. M1) in frame with the *dcuB* gene by using *Pst*I and *Hind*III restriction sites.

***dcuB-lacZ* fusions**

For expression studies of *dcuB-lacZ,* the *lacZ* gene was amplified from plasmid pT7-5-putP-lacZ (Jung *et al.,* 1998) by PCR by with the primers lacpho2-PstI-for and lacZ2-rev. The *Pst*I and *Hind*III digested PCR product was cloned into pMW445 to obtain pMW560 (Fig. M5) coding for MGDRGPE-DcuB(3-444)-LEVDLQESAS-LacZ(10-1024), hereafter reffered to as DcuB-LacZ. For *dcuB-lacZ* fusions with C-terminal truncated *dcuB* part, *dcuB* fragments were amplified from pMW445 with pBAD-dcuBXbaIfor in combination with a series of dcuB-PstI-re primers and cloned into pMW560 (in exchange with full-length *dcuB*).

dcuB-phoA fusions

The *phoA* gene encoding for the bacterial alkaline phosphatase was obtained from plasmid pT7-5-putP-phoA (Jung *et al.,* 1998). For amplification of *phoA* via PCR the primers lacpho2-PstI-for and phoA2-HindIII-re were used. The PCR fragment was inserted into pMW445 with its flanking *Pst*I and *Hind*III restriction sites. The resulting plasmid pMW561 codes for MGDRGPE-DcuB(3-444)-LEVDLQESASDSYTQVASWTEPFPFC-PhoA(27-471), hereafter referred to as DcuB-PhoA. DcuB-abbreviated forms of DcuB-PhoA were received by amplification of the *dcuB* gene from pMW445 with pBAD-dcuBXbaIfor and a series of dcuB-PstI-re primers as already described for the DcuB-LacZ fusions.

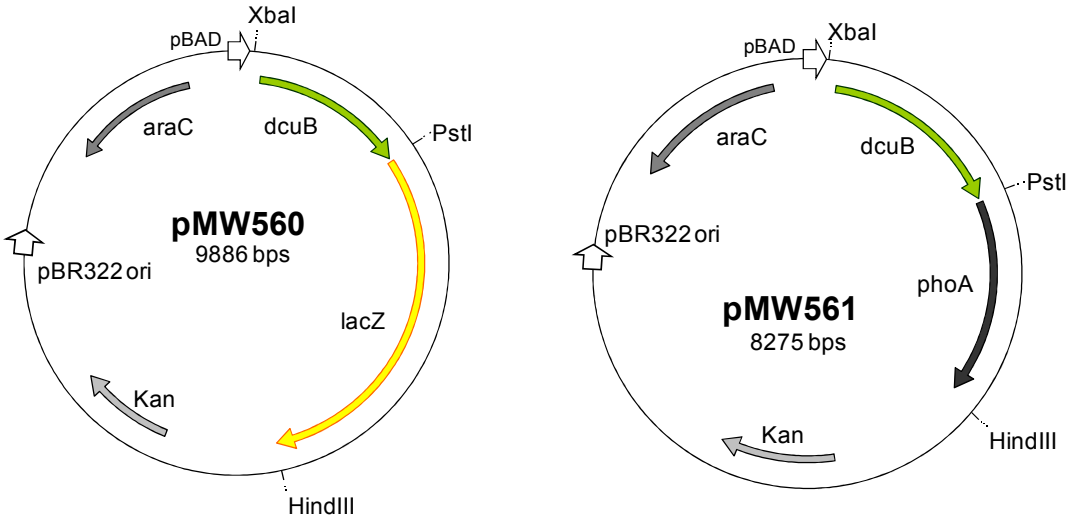

Figure M5: Vector maps of pMW560 and pMW561, coding for DcuB-LacZ and DcuB-PhoA fusion proteins, respectively. Gene expression is induced by arabinose. The C-terminal fused reporter genes *lacZ* and *phoA* were cloned into the *dcuB*-containing pBAD18-Kan* derivative pMW445 (Fig. M1) via *Pst*I and *Hind*III restriction sites.

dcuA-blaM fusion

To construct a plasmid for inducible expression of a DcuA-BlaM fusion the DcuB-BlaM encoding plasmid pMW527 (Fig. M4) was used. Amplification of the *dcuA* gene with simultaneously eliminating of the stop-codon was done from pMW449 with the oligonucleotides EcoRI-dcuA-for and XhoI-dcuA-rev. After removing of the additional *EcoR*I and *Xho*I sites by site-directed mutagenesis with pMW527-EcoRI-for/ -rev and pMW527-XhoI-for/ -rev the *dcuB* gene was replaced by *dcuA* via the remaining *EcoR*I and *Xho*I restriction sites. The resulting plasmid pMW553 contains an in-frame fusion of full-length *dcuA* with the *blaM* gene lacking its leader peptide (MGDRGPEF-DcuA(2-433)-EVDLQ-BlaM(25-286)).

dcuA-lacZ and *dcuA-phoA* fusions

The *dcuA* gene was amplified from pMW553 by PCR with the primers pBAD-dcuBXbaI-for and XhoI-dcuA-rev. The *dcuB* genes of pMW560 and pMW561 were replaced by the PCR fragment via *Xba*I and *Xho*I resulting in the plasmid pMW565 encoding MGDRGPEF-DcuA-(2-433)-EVDLQESASDSYTQVASWTEPFPFC-PhoA(27-471) and pMW577 (MGDRGPEF-DcuA(2-433)-EVDLQESAS-LacZ(10-1024)). C-terminal truncated *dcuA* fragments were amplified from pMW553 with pBAD-dcuBXbaIfor and different dcuA-XhoI-re primers and cloned into pMW560 and pMW561 as described.

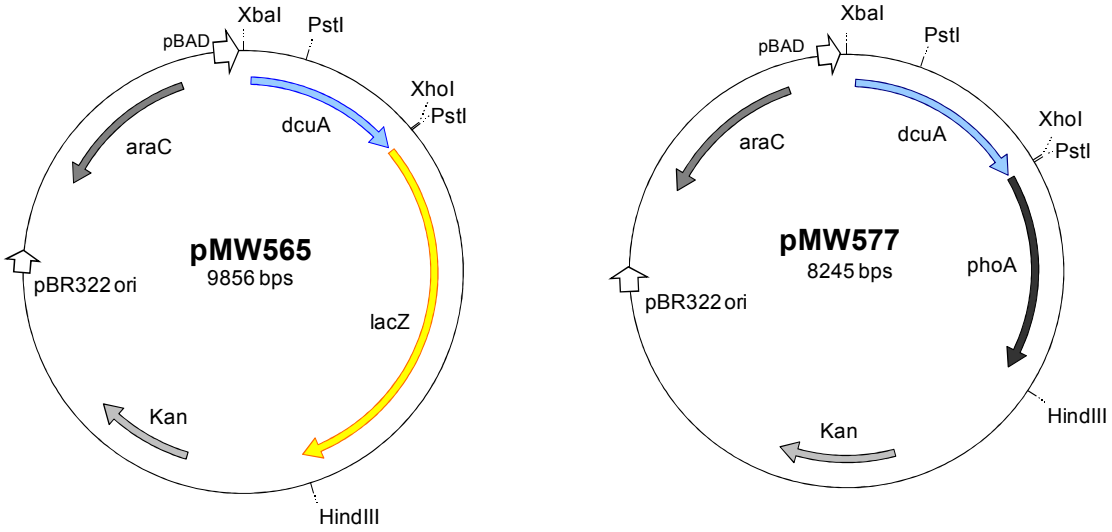

Figure M6: Plasmids pMW565 and pMW577 for expression of DcuA-LacZ and DcuA-PhoA fusion proteins, respectively. The *dcuA* gene was cloned into pMW560 and pMW561 (Fig. M5) via *Xba*I and *Xho*I, replacing the *dcuB* gene. Expression of the resulting *dcuA-lacZ* and *dcuA-phoA* fusions is induced by arabinose.

dctA-blaM fusions

The gene of the mature ß-lactamase was amplified from pASK-IBA3^{+} using the oligonucleotide primers XhoI-blaM-for and HindIII-bla-rev and cloned into the *dctA*-containing pET28a derivative pMW505 (Fig. M2). The resulting plasmid pMW554 (Fig. M7) codes for an IPTG-inducible DctA-BlaM fusion protein.

For N-terminal fused ß-lactamase-DctA constructs, *bla* and *blaM* were amplified with NcoI-blalead-for or NcoI-blaM-for and BamHI-bla-rev. The PCR fragments were cloned into plasmid pMW505 resulting in the expression plasmids pMW555 (*bla-dctA*) and pMW556 (*blaM-dctA*).

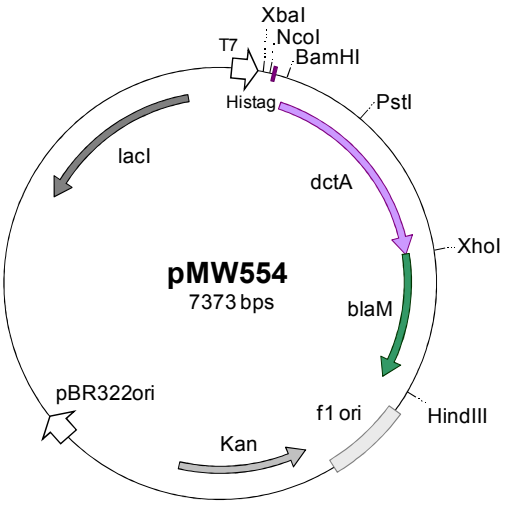

Figure M7: Plasmid pMW554 for IPTG-induced expression of DctA-BlaM. The gene of the maturated ß-lactamase, *blaM*, was cloned into pMW505 (Fig. M2) via *Xho*I and *Hind*III restriction sites.

Plasmids for gene expression with own promoter

dcuA

For studies of DcuA function the *dcuA* gene was amplified with its own promoter from genomic DNA of *E. coli* AN387 by PCR. Due to the *dcuA* promoter region is not known so far, the *dcuA* gene was amplified including the C-terminal part of the previously located *aspA* gene with the primer pair dcuA_for and dcuA_rev. The PCR fragment was inserted into pBAD18-Kan* using restriction endonucleases *EcoR*I and *Xba*I.

By site-directed mutagenesis with dcuAmut-for/ -rev and pMW450-mutfor/ -mutrev single amino acid residues of DcuA were substituted, resulting in the plasmids pMW450 and pMW451.

***dcuA-dcuB* hybrid**

For the expression of a DcuA-DcuB hybrid protein a *Pvu*II restriction site was inserted by mutation of pMW449 with the complementary mutagenesis primers dcuA-PvuIImut-fo/-re and dcuAPvuIImut2-fo/-re. The respective end of *dcuA* was then replaced by the corresponding part of *dcuB* via *Pvu*II and *Xba*I restriction sites. For the *dcuB* part, the pET28a derivative pMW280 was modified by site-directed mutagenesis with the primers pMW280mut-for and pMW280mut-rev. The stop-codon and the flanking *Xho*I site were removed by mutagenesis. Simultaneously, a frame-shift is caused, resulting in *dcuB* coming in-frame with the histag sequence. From this construct *dcuB-his* was amplified by PCR with the forward primers cterm-dcuB-PvuII or ctermdcuBPvuII2 and the reverse primer cterm-dcuB-XbaI (binds within the f1-ori) and cloned behind the C-terminal restricted *dcuA* gene in pMW449.

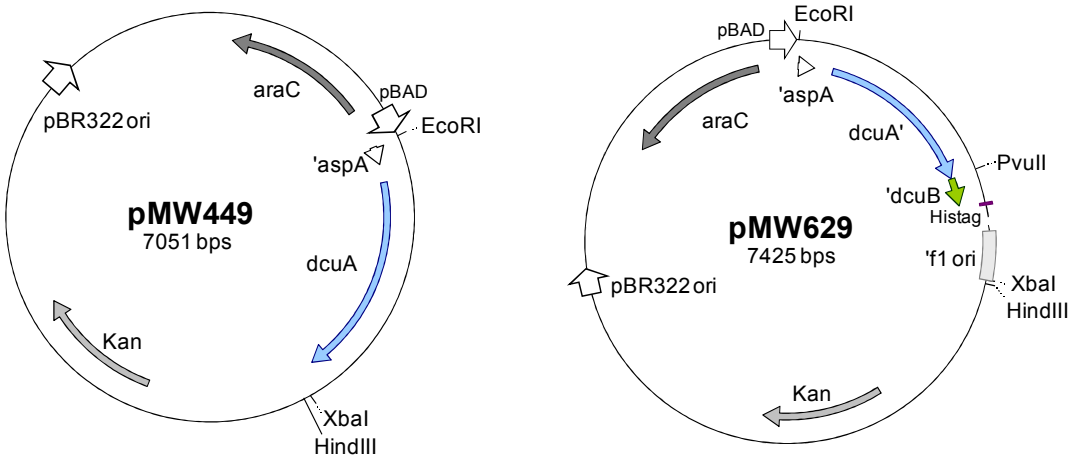

Figure M8: Plasmids pMW449 and pMW629 for physiological expression of DcuA. The *dctA* gene including the according promoter region was cloned into pBAD18-Kan* by using endonucleases *Eco*RI and *Xba*I. The resulting plasmid pMW449 was modified by site directed mutagenesis to insert a *Pvu*II restriction site within the 3´-part of *dcuA*. The 3´-part of *dcuB-his* (amplified from a pMW280 derivative) was cloned into pMW466 via *Hind*III and the new *Pvu*II restriction site, resulting in pMW629 for expression of a DcuA-DcuB hybrid protein under the control of the *dcuA* promoter, in which the C-terminal part of DcuA is replaced by the corresponding C-terminal part.

dcuB

For physiological expression of *dcuB*, required for transport measurements and complementation experiments, pMW228 (Kleefeld, 2002) and pMW228 derivatives were used. The pMW6010 derivative contains the full-length *dcuB* gene plus the according *dcuB* promoter. Due to the size and selection (tetracycline resistence cassette) of pMW228, site-directed mutagenesis of *dcuB* was performed in the pET28a plasmid pMW281. The mutated *dcuB* construct was transferred into pME6010 via its flanking *EcoR*I and *Xho*I restriction sites, resulting in a mutated pMW228 variant.

A pMW228 variant encoding for DcuB with C-terminal Streptag was constructed as follows. The *Xho*I restriction site of pMW445 was removed ander simultaneous addition of DcuB F443 by mutagenesis with the primer pair pMW445-stopF-for/ -rev. The C-terminal part of *dcuB* including *streptagII* was amplified via dcuB-BglII-for and Strep-XhoI-rev and cloned into pMW228. The resulting pMW787 encodes for DcuB(1-446)-EVDLQGDHGLSA-StreptagII ander the control of the *dcuB* promoter.

The pMW228-Histag variant was obtained by amplifying the C-terminal *dcuB* fragment with dcuB-BglII-for and dcuBhis-XhoI-rev from pMW280 lacking its *Xho*I restriction site as well as the *dcuB* stop-codon (compare with construction of *dcuA-dcuB* hybrid). The PCR product was cloned into pMW228 resulting in the plasmid pMW755 (DcuB(1-446)-YMHYE-His_6).

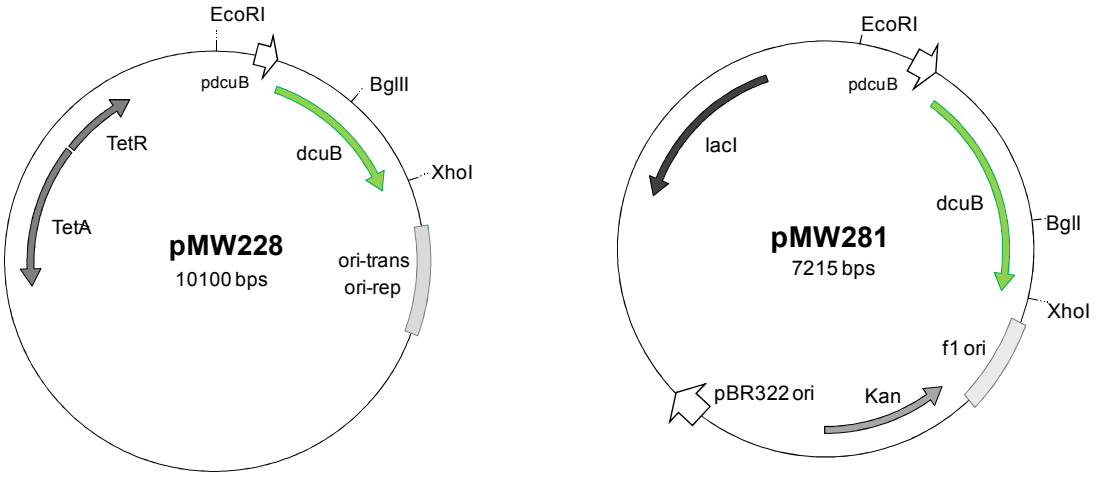

Figure M9: Plasmids pMW228 and pMW281 (Kleefeld et al., 2009) for P_{dcuB} controlled expression of *dcuB*. Low-copy pMW228 is suitable for physiological expression of *dcuB* induced by fumarate under anaerobic conditions. For site-directed mutagenesis of *dcuB*, the pET28a pMW281 derivative was used as a template. The *dcuB* gene including its promoter region can be transferred between pMW281 and pMW228 by using the flanking *Eco*RI and *Xho*I restrict sites.

Construction of *dcuB* cysteine mutants

For transport measurements and sulphydryl-labeling, single and multiple cysteine mutants of DcuB and DcuB-PhoA were generated by site-directed mutagenesis. Step by step all 5 cysteine residues of DcuB were replaced by serine residues using complementary mutagenesis primer pairs dcuB-Cys1mut-for/ -rev, dcuB-Cys2mut-for/ -rev (for simultaneously exchange of C2S and C3S), dcuB-Cys4mut-for/ -rev and dcuB-Cys5mut-for/ -rev. As a template the *dcuB* containing plasmids pMW281, pMW445 and pMW561 were used. Removing of the 4 cysteine residues of PhoA as well as the cysteine within the linker of DcuB-PhoA was performed with PhoA-C1S-for/ -rev, PhoA-C2S-for/ -rev PhoA-C3S-for/ -rev PhoA-C4S-for/ -rev and C-linker-PhoA-for/ -rev.

For growth experiments, ß-galactosidase assays and transport measurements the mutated *dcuB* gene from pMW281 was cloned into pME6010 via restriction endonucleases *EcoR*I and *Xho*I as described. The plasmids for expression of completely cysteine-free DcuB are termed as follows. pMW737 (pMW228 derivative), pMW635 (pMW445 derivative) and pMW828 (pMW561 derivative; all cysteines of the DcuB-PhoA fusion protein were substituted by serine). Plasmids pMW737 and pMW828 were used as templates for single cysteine-replacements on positions of interest.

3.4 Biochemical methods

3.4.1 Sulphydryl-labeling

Sample preparation

Accessibility studies of DcuB were performed with *E. coli* C43DE3 carrying a pMW828 derivative in combination with pHASoxYZ. Plasmid pHASoxYZ codes for constitutively expressed HA(hemeagglutinine)-tagged SoxY of *Paracoccus pantotrophus,* which was used as a cytoplasmic control for the current state of the cells. Cells expressing a single-cysteine variant of the DcuB-PhoA fusion protein and SoxY were cultivated aerobically in LB broth supplemented with 50mM fumarate and 20mM K-phosphate for 4 hours at 30°C.

After cultivation, cells were continuously hold on ice and treated exclusively with pre-cooled buffers. Cells were harvested by centrifugation (5000 x g, 10 min, 4°C), washed with 10 ml HEPES/NaCl pH 6.8 buffer and resuspended in 1 ml HEPES/NaCl buffer. The cell suspension was transferred into 1.5 ml microtubes and spun down again (12000 x g, 5 min, 4°C). Samples that were not labeled at the same day were snap freezed in liquid nitrogen and stored at -20°C until use. For labeling, the cell pellets were resuspended in HEPES buffer pH 6.8. To obtain a total cell protein concentration of 10 µg/µl, the buffer volume was calculated (equation 1), with OD_{harv}, optical density at the harvest and Vol_C, culture volume (20-25ml). Vol_B (equation 2) gives the buffer volume required for a total cell protein concentration of 10 µg/µl.

1. $(OD_{harv} \times 280\ mg \times Vol_C\ [ml])/1000\ ml = mg\ protein/pellet$
2. $Vol_B\ [\mu l] = mg\ protein \times 100$

Labeling procedure

Each cell sample was splitted into four or five labeling fractions: sample (A), sample (N), sample (-), sample (=) and, if required, sample (AS). The different labeling procedures applied on whole cells and denaturated protein solutions are shown in Table M6 and M7. 10 µl cell suspension (100 µg total cell protein) were supplied with HEPES buffer and label reagent as indicated to a reaction mixture with a total volume of 50 µl. Sample (A) was incubated with AMS (Fig. M10), sample (N) with NEM and sample (-) without any labeling reagent in the absence of SDS. Sample (=) and sample (AS) contain 1% SDS for cell disruption and protein denaturation. Additional, sample (AS) is incubated with AMS. All mixtures were vortexed vigorously. The

labeling reactions were conducted at room temperature with occasional vortexing. Light exposure was avoided.

Table M6: Pre-labeling of whole cells. Volumes and concentrations of the labelling components in 50 µl reaction mixture (final volume)

sample	A	N	-	=	AS
Cell sample (10 µg/µl prot.)	10 µl	10 µl	10 µl	10 µl	10 µl
HEPES pH 6.8	35 µl	38 µl	40 µl	-	-
HEPES pH 6.8 + 1.3% SDS	-	-	-	40 µl	30 µl
Labeling reagent 20mM AMS, 50mM NEM	5 µl AMS	2 µl NEM	-	-	5 µl AMS

The reactions in sample (A), (N) and (-) were stopped by 20-fold dilution with HEPES buffer followed immediately by centrifugation. The cell pellets were washed with 1.2 ml HEPES buffer and the supernatants were carefully removed with a pipet. The pellets were resuspended in HEPES buffer containing 1.3 % SDS and PEGmal (Fig. M10) was added to the denatured protein solutions (Tab. M7). Sample (AS), was directly mixed with PEGmal.

Table M7: PEGmal labeling of denaturated proteins. Volumes and concentrations of the labelling components added to a 50 µl reaction mixture.

sample	A	N	-	=	AS
Cell sample/ pellet	pellet	pellet	pellet	10 µl	10 µl
HEPES pH 6.8 + 1.3% SDS	40 µl	40 µl	40 µl	40 µl	35 µl
Labeling reagent 50mM PEGmal	5 µl PEGmal	5 µl PEGmal	5 µl PEGmal	-	5 µl PEGmal

The finale reaction of denaturated proteins with or without PEGmal was terminated by adding 5 µl 0.5 M dithiothreitol. The protein samples were immediately mixed with SDS loading buffer, boiled in a water bath for 10 min and subjected to SDS-PAGE. The experiments were analysed by immunoblotting with anti-HA (detection of SoxY) and anti-PhoA (detection of DcuB-PhoA).

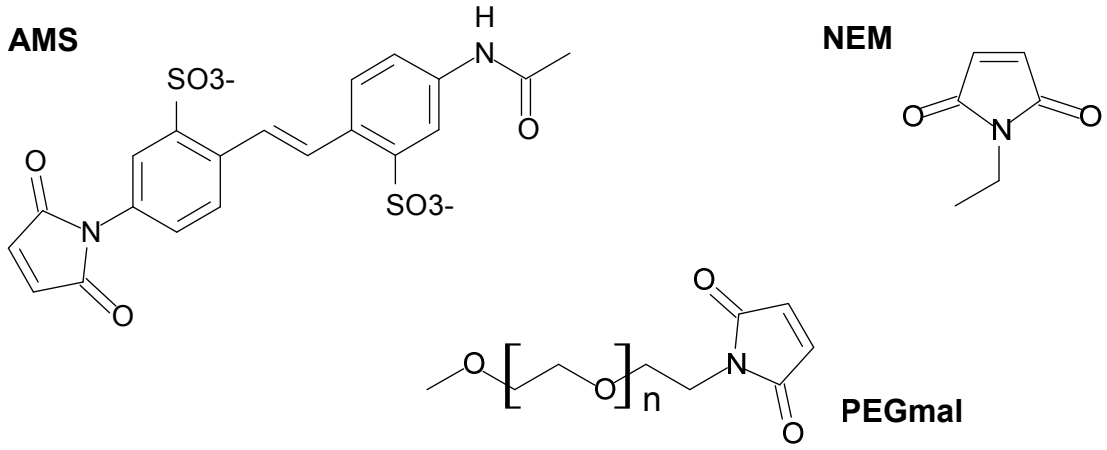

Figure M10: Chemical structure of the maleimide derivatives NEM, AMS and PEGmal. Maleimide derivatives are suitable reagents for specific protein modification. The favored reaction is the addition of a cysteinyl thiolate anion to the maleimide double bound. The reaction requires a molecule of water for deprotonation of the sulphydryl group. Since the thiol pKa for most water exposed cysteine residues lies in a range of 8-9 the pH optimum for this reaction is about 8.5. For a higher specificity (maleimides are known to react with primary amines (lysine residues) at pH values above 7.5 (Culham *et al*., 2003)), a lower pH of 6.8 was chosen for the labeling reaction.

Western blotting (semi-dry)

For detection of DcuB-PhoA, and SoxY protein samples were subject to SDS-PAGE and subsequently transferred to a nitrocellulose membrane (Protran, Schleicher & Schuell or Amersham Hybond-ECL) (Towbin *et al.*, 1979). Four filter layers of Whatman paper and the nitrocellulose membrane were soaked in methanol-containing transfer buffer. SDS gel, membrane and Whatman paper were piled to a sandwich with gel and membrane in the middle. The membrane-containing side was located on the anode of the blotting device and bubbles between the layers were removed carefully. The proteins were transferred to the membrane at a constant voltage of 10 V for 30 min (1 gel) to 1 h (2 or 3 gels).

For BSA-saturation, the blotted membrane was incubated in blocking buffer for at least 1 h at room temperature on a tumble shaker. If required, the blotted SDS gel was checked by Coomassie Brilliant Blue (Serva) staining. The protein-saturated membrane was incubated with the primary antibody (1:2000 in 10 ml antibody solution) for 1-2 h. The membrane was washed for 2 x 5 min in 20 ml washing buffer and then incubated for 2 h with the secondary antibody (1:1000 in 10 ml antibody solution). After removing of the secondary antibody and additional washing steps, protein bands were visualized by membrane-incubation with Millipore Immobilon Western Chemiluminescent HR Substrate (Millipore). The developer solution is prepared by combining equal volumes of Luminol Reagent and Peroxide Solution.

Antibody-coupled HRP in combination with H_2O_2 is used to oxidize the agent luminol, resulting in chemiluminescence proportional to the amount of protein. A sensitive sheet of photographic film is placed against the membrane, and exposure to the emitted light from the reaction creates an image of the antibodies bound to the blot. The produced chemiluminescence provides a highly sensitive detection of low amounts of protein.

3.4.2 Determination of ß-lactamase activity

The bacterial ß-lactamase (Bla) provides resistance to ß-lactam antibiotics and is synthesized as a pre-protein with an N-terminal signal peptide for export to the periplasmic space. In the maturated form, ß-lactamase can be used as a reporter for membrane protein topology. The ability to protect individual cells against ampicillin correlates with the cellular orientation of the ß-lactamase part of plasmid-encoded ß-lactamase fusion proteins (Broome-Smith & Spratt, 1986). Only translocated forms of maturated, leader-less Bla (BlaM) allow single cells to survive on ampicillin-containing plates. To identify the MIC (Maximum Inhibitor Concentration) of single cells, 10^{-3}, 10^{-4}, 2 x 10^{-5} and 10^{-5} dilutions of an overnight culture expressing aprotein-BlaM fusions were made. For an optimal comparison of all transformants, prior to the dilution an optical density of 3 was adjusted. A volume of 4 µl was spottet on LB agar plates containing different concentration of ampicillin (1 to 80µg/ml) and of the inducers arabinose or IPTG. The final cell density was checked on LB agar without inhibitor identifying a number of about 20 cells in 4 µl of the 10^{-5} dilution.

3.4.3 Determination of alkaline phosphatase and β-galactosidase activity

Alkaline phosphatase assays (Michaelis *et al.*, 1983; Calamia & Manoil, 1990)

Cells expressing PhoA fusion proteins were harvested by centrifugation (8000 x g, 4 min) and resuspended in Buffer A (10 mM Tris/HCI, pH 8.0; 150 mM NaCI). An OD_{578nm} of about 2.5 was equilibrated and 0.2 ml of each cell solution was added to 0.8 ml Buffer B (1 M TrislHCl, pH 8.0; 1 mM $ZnCl_2$). Cells were permeabilisized by vortexing and 10-minute incubation with 50 µl chloroform and 25 µl 0.1% (w/v) SDS at 30°C. Time was immediately started after adding 0.2 ml p-nitrophenyl phosphate solution (0.1 g pNPP/ 25 ml 1 M Tris/HCl, pH 8.0). The reaction mixtures were incubated at 30°C until changing to a yellow color, but maximal for 30 min. The reaction was stopped with 0.5 ml 2.5 M K_2HPO_4 and cells were spun down (13200 x g; 10 min). Extinktion of the supernatant was determined at 420 nm.

Of each strain at least two independent cultures were grown and PhoA activities of each culture were determined in quadruplicate.

β-Galactosidase assays (Miller, 1992)

Measurements were performed with permeabilised bacteria as described by Miller, 1992. For expression studies of chromosomal encoded *dcuB´-´lacZ*, cultures were grown to the exponential growth phase at an optical density (OD_{578nm}) of 0.5 - 0.8. A volume of 0.2 ml of each culture was introduced to the ß-galactosidase assay. The activities reported for each strain are the average of at least four independent cultures measured in quadruple.

Strains expressing a *dctA´-´lacZ* reporter gene fusion were grown for about 14 h, corresponding to the postexponential or early stationary phase. The final OD_{578nm} values were in a range of about 0.5 to 7.7. Since a dilution of higher grown cultures prior to ß-galactosidase measurements did not affect the calculated ß-galactosidase activities, cells (0.2 ml culture) were directly applied from postexponentially growing cultures. Under each growth condition, at three independent cultures of each strain were grown. ß-galactosidase activities were determined in quadruplicate.

For topology studies, cells expressing LacZ fusion proteins were harvested by centrifugation and resuspended in ß-galactosidase buffer, adjusting an OD_{578nm} of about 0.6.

Calculation of PhoA and LacZ activity (Miller, 1972; Brickmann & Beckwith, 1975)

Reporter protein activities were calculated in Miller Units [MU] as described in the following equation, with ΔE_{420nm}, extinction of the sample at 420 nm (blank value subtracted); t, time; V, sample volume (0.2 ml); ΔOD_{578nm} optical density of the sample at 578 nm (blank value subtracted).

$$MU = 1000 \times \Delta E_{420nm} / (t\,[min] \times V\,[ml] \times \Delta OD_{578nm})$$

3.4.4 *In vivo* FRET measurements

E. coli expressing fluorescent proteins were harvested and washed twice by centrifugation in PBS buffer and finally resuspended in 1 ml PBS buffer. Absorption spectra were recorded before fluorescence measurements. Cells were diluted to an absorbance of 0.1 at 400 nm to avoid the inner filter effect and signal saturation.

FRET measurements and FRET calculations were performed by Dr. Yun-Feng Liao and Dr. Wolfgang Erker, group of Prof. Dr. Basché, Institut für Physikalische Chemie, Johannes Gutenberg-Universität, Mainz. Absorption and fluorescence spectra were measured in 1 ml quartz semi-microcuvettes at room temperature with a dual-beam UV-VIS spectrophotometer (OMEGA 20, Bruins Instruments, Germany) and a FluoroMax-2 spectrofluorometer (Jobin Yvon-Spex, NJ, USA). Fluorescence spectra were corrected for the wavelength dependence of the fluorometer and the inner filter effect (Lakowicz, 2006). Background-free spectra of donor, acceptor and mixtures of both were used to calculate fluorophore concentrations, donor fraction (f_D) and FRET efficiency (E) according to Gordon *et al.* (1998) (Liao, 2008). For more details see Scheu *et al*., (2009).

3.4.5 Transport measurements (Uptake of ^{14}C-succinate)

Preparation of cell suspensions

At an optical density of about 0.8 (exponential growth phase), cells were harvested by centrifugation (10000 x g, 20 min, 4°C) and washed twice in ice-cooled and degassed Buffer A (100 mM Na/K-phosphate pH 7.0, 1 mM $MgSO_4$). Henceforth, cells were continuosly hold on ice up to transport measurements. The cell pellet was resuspended in Buffer A, adjusting an OD_{578nm} of about 4.0 and transferred into a Sovirell tube. If required, the cell suspension was aliquoted. The cell suspension was degassed and incubated for at least one hour under nitrogen atmosphere on ice. The additional aliquots were supplemented with 100 mM sodium nitrate, 100 mM sodium chloride, 100 mM magnesium chloride or 100 mM magnesium sulfate prior to degassing and nitrogen flooding. To investigate the O_2-effect, one aliquot was stirred on ice in a beaker without salt addition. The exact OD values of each sample were determined again after the uptake measurements and used for calculation of transport activity.

Prior to the transport measurements, 20 mM degassed glucose solution was added to a preheated cell aliqot and incubated for 5 min at 37°C. The energized cells were used immediately, whereas the remaining sample was still hold on ice. For kinetic studie, 490 µl

cell suspension was mixed with 10 µl 1 M glucose in an 1.5 ml eppendorf tube; to determine the initial uptake rate, 198 µl cell suspension was added to 2 µl 1 M glucose.

Transport measurements

A 1.5 ml reaction tube containing 1 ml 200 µM [^{14}C]-succinate solution with a specific activity of 2004 dpm/nmol was pre-heated to 37°C. Reaction was started by mixing equal volumes of energized cells and ^{14}C-succinate solution, resulting in a final concentration of 100 µM ^{14}C-succinate. In periods of twenty seconds (for the first minute) and for kinetics additional after 2, 4 and 8 minutes, 100 µl of the radioactive suspension was pipetted into 0.9 ml ice-cooled 0.1 M LiCl solution to stop the uptake reaction. Cells were sectionated by a vacuum filtration device (FH 225V Ten-Place Filter Manifold, Hoefer Pharmacia Biotech, San Francisco, USA) using cellulose mixed ester filter papers (Ø 25 mm, 0,2 µm Porengröße, Schleicher & Schuell) soaked in 0,1 M LiCl solution. During filtration, cells were washed twice with 1 ml 0.1 M LiCl solution. The filter papers were dissolved in tubes containing 4 ml of Scintillation solution (Rotiszint® ecoplus, Roth) and radioactivity of each filter was determined in a Scintillation counter (Liquid Scintillation System, LS 6000SC, Beckman).

To make sure that no non-specific uptake or adhesion of radioactive substrate distorts the calculation, a blank value was determined for each run. Therefore, 50 µl of the energized cell solution was added to a reaction tube containing 0.9 ml 0.1 M LiCl-solution and 50 µl ^{14}C-succinate.

Calculation of transport activity

Transport activity for each incubation time was determined by the following equation, with DW, dry weight; Δdpm, radioactivity determined for the sample (blank value substracted); OD_{578nm}, optical cell density in the reaction mixture; 2004 dpm/nmol, specific activity of ^{14}C-succinate solution and 281 mg, cell dry weight at an OD of 1 per liter.

$$\mu mol/g\ DW = (\Delta dpm \times 10000) / (2004\ [dpm/nmol] \times OD_{578nm} \times 281mg\ DW)$$

The initial uptake rate was calculated in Units per gram DW [nmol mg^{-1} min^{-1}], with t, incubating time in minutes (time before uptake reaction was stopped by adding LiCl-solution) and Δdpm (t_0), radioactivity of sample with shortest incubation time (20 sec).

$$U/g\ DW = (\Delta dpm\ (t_0) \times 10000) / (2004\ [dpm/nmol] \times OD_{578nm} \times 281mg\ DW \times t\ [min])$$

3.5 Databases

Literature search

NCBI, PubMed: http://www.ncbi.nlm.nih.gov/pubmed/

Protein information

Swiss-Prot and associated links: http://www.expasy.org/sprot/

Predicted domain organisation of proteins

PSIPRED: http://bioinf.cs.ucl.ac.uk/psipred/

Putative transmembrane helices of proteins

TMHMM: http://www.cbs.dtu.dk/services/TMHMM/

SCAMPI, TopCons, OCTOPUS: http://www.cbr.su.se/Servers

TMHMMfix: http://www.sbc.su.se/~melen/TMHMMfix/

4. Results

4.1 Topology of the anaerobic fumarate/ succinate antiporter DcuB

DcuB acts as a cosensor of the two component system DcuSR (Kleefeld *et al.*, 2009). The carrier contains a regulatory domain and it was suggested that the carrier controls DcuS function by direct interaction of DcuS with the regulatory domain of DcuB (Kleefeld *et al*., 2009). To get a clue to potentially interacting sites, the topology of DcuB was determined, in particular the orientation of the C-terminus and the localization of the regulatory amino acid residues T394, D398 and K353.

4.1.1 Topology studies using DcuB-LacZ/ DcuB-PhoA reporter fusions

Analysis of protein fusions with the ß-galactosidase (*lacZ* gene) and the mature alkaline phosphatase (*phoA* gene) is a common method for predicting membrane protein topology (Manoil *et al*., 1988). The ß-galactosidase of *E. coli* is a cytoplasmic enzyme that catalizes hydrolysis of ß-galactosides into monosaccharides. Protein fusions with the ß-galactosidase result in LacZ activity only, when the LacZ remains in the cytoplasm. In contrast, the alkaline phosphatase is expressed as a preprotein with N-terminal signal peptide for excretion and is only active when translocated into the periplasm. Hence, LacZ and mature PhoA without signal peptide function as complementary sensors in topology studies leading to a reciprocal pattern of enzyme activities. The level of enzymatic activities therefore reveals the topology of the junction site of the hybrid protein.

Fusions of DcuB with the reporter proteins were generated genetically in the arabinose-inducible expression vector pBAD18-Kan*. The genes of the ß-galactosidase and the alkaline phosphatase were amplified from plasmids pT7-5-putP-lacZ and pT7-5-putP-phoA (Jung *et al.,* 1998) by PCR and cloned behind the *dcuB* gene of pMW445. The resulting plasmids pMW560 and pMW561 encodes full-length DcuB with C-terminal LacZ or mature PhoA reporter protein. For fusions with 3´-truncated *dcuB*, *dcuB* fragments were amplified from pMW445 and cloned into pMW560 and pMW561 plasmids by replacing the full-length *dcuB*. Positions of DcuB that form the new C-terminus of truncated constructs were selected on the basis of the hydropathy plot of the protein. Mainly amino acid residues that are clearly situated within a hydrophilic segment of the carrier were used as junction sites.

In addition, reporter fusions of the anaerobic uptake carrier DcuA were analysed. The topology of DcuA was already determined experimentally (Golby *et al.*, 1998) and the DcuA

fusions were used as a control. For reporter gene fusions *dcuA* was cloned into pMW560 and pMW561 to substituted *dcuB* resulting in pMW565 (*dcuA-phoA*) and pMW577 (*dcuA-lacZ*). Fusions containing 3´-truncated fragments of *dcuA* were created as described for *dcuB*. In Figure R1 the alignment of DcuA and DcuB is presented with the position of the junction site.

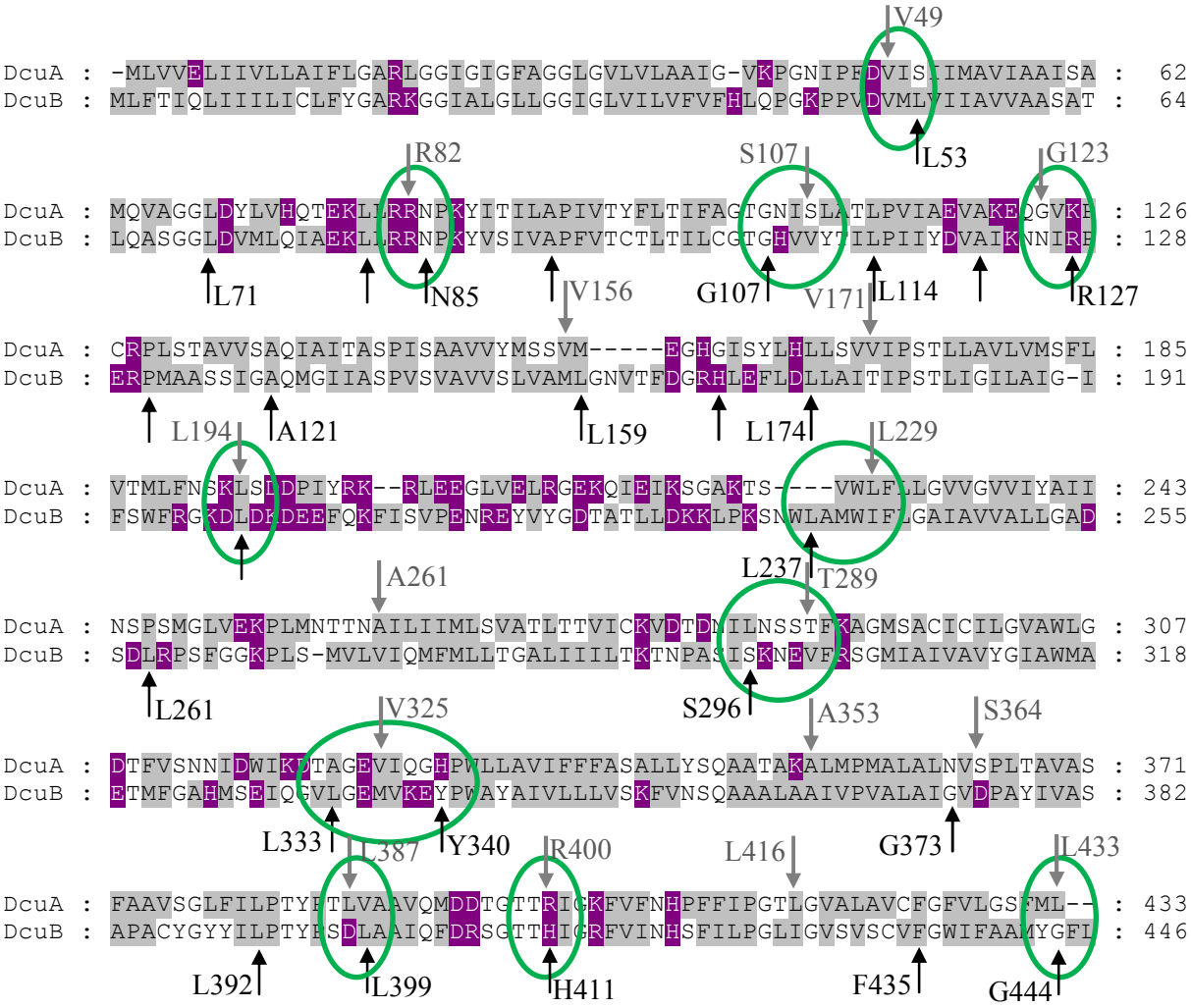

Figure R1: Sequence alignment of transporters DcuA and DcuB of *E. coli*. Hydrophobic parts are highlighted in grey, charged amino acid residues in purple. Black arrows label the C-terminal DcuB junction sites in DcuB´-´PhoA and -´LacZ fusions, grey arrows highlight the corresponding sites of DcuA. The junction sites were numbered according to their positions in DcuB and DcuA. Comparable positions within both carriers are surrounded with green circles.

The full-length DcuB-PhoA and DcuB-LacZ fusions were tested for DcuB activity by anaerobic growth on fumarate and for chromosomal *dcuB´-´lacZ* activity in the *dcuA dcuB dcuC*-minus strain IMW505 (Fig. R2). For growth experiments cells were cultivated in enriched M9 with glycerol, the effector fumarate and 100µM of the inducer arabinose. Cells of IMW505 complemented with pMW445 (wildtype DcuB) and pMW561 (DcuB-PhoA)

grew very well and achieved an OD of about 1.2 after 40 hours. In IMW505 expressing DcuB-LacZ growth reached at least a cell density of 0.8.

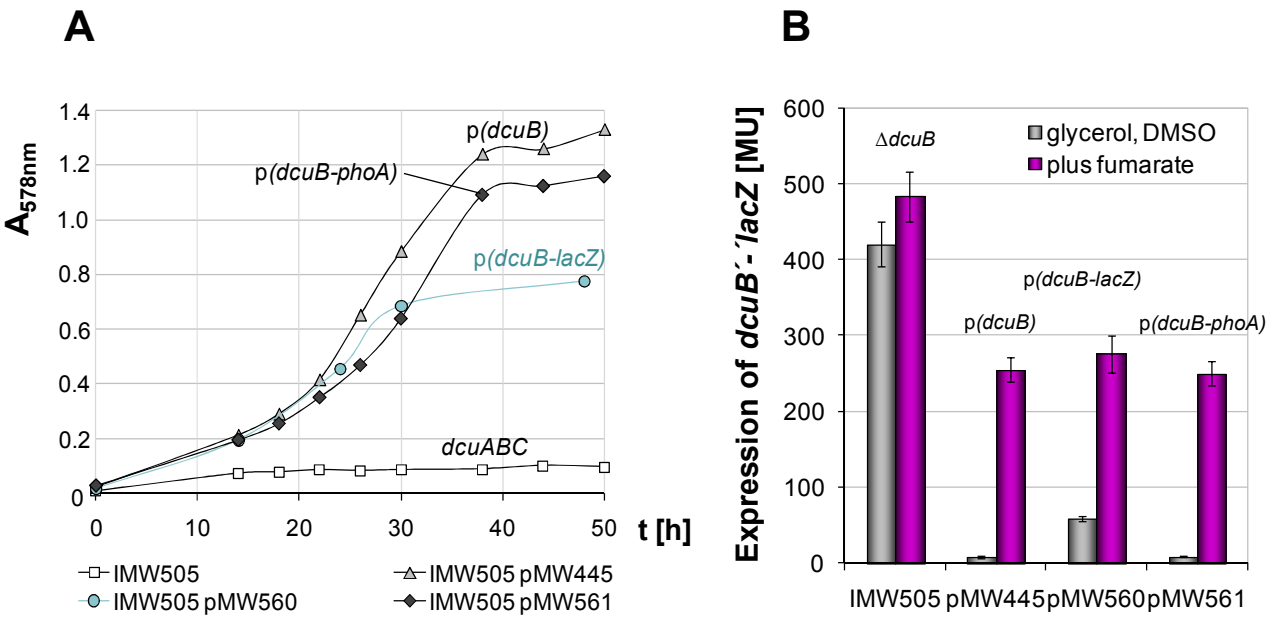

Figure R2: Complementation of DcuB function in *E. coli* IMW505 (*dcuA dcuB dcuC*) by DcuB-PhoA and DcuB-LacZ fusion proteins. (**A**) **Anaerobic growth of *dcuB*-complemented IMW505 cultivated in eM9 with glycerol and fumarate under anaerobic conditions.** The growth curves of strain IMW505 harbouring plasmids encoding DcuB (pMW445), DcuB-LacZ (pMW560) and DcuB-PhoA (pMW561) are shown. **(B) Regulatory effect on *dcuB* expression mediated by plasmid-encoded DcuB-PhoA and -LacZ fusions.** The ß-galactosidase activity of chromosomal encoded *dcuB´-´lacZ* was determined in *E. coli* IMW505 transformants carrying plasmid-encoded DcuB (pMW445), DcuB-LacZ (pMW560) or DcuB-PhoA (pMW561). The ß-galactosidase activities are shown in Miller Units with standard deviations. Cells were grown anaerobically in eM9 with glycerol, DMSO with or without fumarate in the absence of the inducer arabinose.

The regulatory activity of the hybrid proteins was tested in IMW505 by using a chromosomal *dcuB´-´lacZ* reporter gene fusion as a marker for DcuSR-induced expression. Cells harbouring pMW445 (DcuB), pMW560 (DcuB-LacZ) or pMW561 (DcuB-PhoA) were cultivated under anaerobic conditions in eM9 supplemented with glycerol, DMSO with or without fumarate. Due to the plasmid-encoded *dcuB-lacZ* fusion, in contrast to the growth experiments, no inducer arabinose was added. The P_{BAD} promoter allows weak expression of the genes in the absence of inducer which is sufficient to complement the regulatory effect of DcuB, and, by adding arabinose, the additional induction of pMW560-encoded *dcuB-lacZ* would cause an increased LacZ-activity. *E. coli* IMW505 producing DcuB, DcuB-LacZ or DcuB-PhoA showed an effector-dependent gene expression: *dcuB´-´lacZ* expression was observed only in

the presence of fumarate. In contrast, the *dcuB*-deficient strain IMW505 showed maximal expression of *dcuB* already in the absence effector. Therefore the DcuB fusion proteins both could restore DcuB function in IMW505 by allowing anaerobic growth by fumarate respiration and fumarate-dependent expression of the DcuSR target genes.

For determination of DcuB topology, gene fusions of DcuB were expressed in the *lacZ phoA*-negative strain CC181 (Calamia & Manoil 1990). Transformants of CC181 were cultivated in LB broth supplemented with 50 mM sodium fumarate under aerobic condition. At an optical density of about 0.8, expression of the fusion proteins was induced with 0.2% arabinose for further 3 hours. Cells were harvested by centrifugation and tested for alkaline phosphatase or ß-galactosidase activity.

Correct interpretation of the results is hindered by differences in the levels of PhoA and LacZ activity and expression of the truncated fusion proteins. Therefore the activity-ratio for the dual reporter system was calculated. It is assumed that the expression level of a certain fusion site affects the absolute activity of PhoA and LacZ but not the ratio of activities (Bogdanov *et al.*, 2005). The calculated PhoA/LacZ activity ratios of DcuB-reporter protein fusions are presented in Table R1 whereas Figure R3 shows the pattern of absolute enzyme activities.

Based on the results several soluble loops of DcuB could be identified that show either a relatively high PhoA/LacZ activity of > 1.0 (periplasmic localization of the residues) or a very low ratio of relative PhoA/LacZ activities of < 0.1(cytoplasmic localization). Amino acid residue L53 is located in the periplasm leading to a high activity ratio of 6.32 (Tab. R1). The residues L71 to V92 on the other hand showed a normalized PhoA/LacZ activity ratio of only 0.01-0.05 indicating a cytoplasmic localisation. Although the large hydrophilic segment harbouring amino acid residues L200 and L237 is definitely located in the cytoplasm. The respective fusion proteins showed a minimal PhoA/LacZ activity ratio of 0.01 and less. Due to a large number of positively charged residues present in this segment, this loop was predicted to be cytoplasmic by all servers that consider the positive-inside rule (von Heijne, 1986) as well.

Table R1: Data obtained from DcuB-PhoA and DcuB-LacZ activity studies. The absolute enzyme activity of each DcuB junction site and reporter fusion is shown in Miller Units. The ratio of PhoA/LacZ activities is calculated from absolute (fourth column) and normalized enzyme activities (last column). The orientation of the junction site is given: P, periplasmic; C, cytoplasmic, M, membrane-integrated. Orientations predicted with high confidence are highlighted in bold.

DcuB junction site	**LacZ activity** [MU]	**PhoA activity** [MU]	**PhoA/LacZ** ratio	**orientation**	**normalized PhoA/LacZ**
L53	316 ± 25	1478 ± 72	4.68	**P**	6.32
L71	1330 ± 103	51 ± 2	0.04	**C**	0.05
L81	1191 ± 103	21 ± 2	0.02	**C**	0.02
N85	1996 ± 170	19 ± 3	0.01	**C**	0.01
V92	1531 ± 112	11 ± 1	0.01	**C**	0.01
G107	407 ± 37	163 ± 8	0.40	**M**	0.54
L114	402 ± 125	350 ± 17	0.87	P	1.18
A121	255 ± 19	172 ± 5	0.67	P	0.91
R127	655 ± 39	197 ± 6	0.30	M	0.41
P131	379 ± 22	217 ± 14	0.57	M	0.77
A139	489 ± 123	213 ± 20	0.44	M	0.59
L159	186 ± 9	62 ± 4	0.33	**M**	0.45
H168	216 ± 33	200 ± 5	0.93	P	1.25
L174	82 ± 13	198 ± 18	2.41	**P**	3.26
L200	1100 ± 57	4 ± 3	0.00	**C**	0.00
L237	1466 ± 211	8 ± 2	0.01	**C**	0.01
L258	97 ± 4	475 ± 26	4.90	**P**	6.61
S296	1398 ± 94	13 ± 3	0.01	**C**	0.01
L333	297 ± 29	307 ± 10	1.03	**P**	1.40
Y340	127 ± 13	126 ± 4	0.99	**P**	1.34
G373	620 ± 707	23 ± 2	0.04	**C**	0.05
L392	316 ± 17	17 ± 2	0.05	**C**	0.07
L399	478 ± 74	19 ± 3	0.04	**C**	0.05
H411	701 ± 67	10 ± 1	0.01	**C**	0.02
F435	71 ± 5	24 ± 2	0.34	**M**	0.46
G444	102 ± 12	64 ± 5	0.63	**P**	0.85

The activities of the DcuBH168, DcuBL174 and DcuBL258 fusion proteins, on the other hand, refer to a periplasmic orientation of the junction sites. All constructs presented a high PhoA/LacZ ratio which was in clear contrast to the activity ratio of the fusions to DcuBL200 and DcuBL237. The next cytoplasmic loop contains the amino acid residue S296. Fusions of DcuBS296 with the reporters again led to a very low PhoA/LacZ ratio of 0.01. Also expression of hybrid proteins with the DcuB junction sites G373, L392, L399 and H411 resulted in PhoA/LacZ activities below 0.1 clearly indicating a large cytoplasmic loop. This

loop also contains the regulatory amino acid residues T394 and D398. According to these results, the third residue which are found to be essential for interaction of DcuB with DcuSR, K353, is probably located in the membrane-spanning helix between Y340 and G373. Both junction sites, DcuBL333 and DcuBY340 mediated a PhoA/LacZ activity ratio greater than 1. Following the trend of activity ratios the DcuB C-terminus finally ends with an in-out transmembrane helix. The C-terminus of DcuB is either located within the membrane or at the periplasmic side of the membrane.

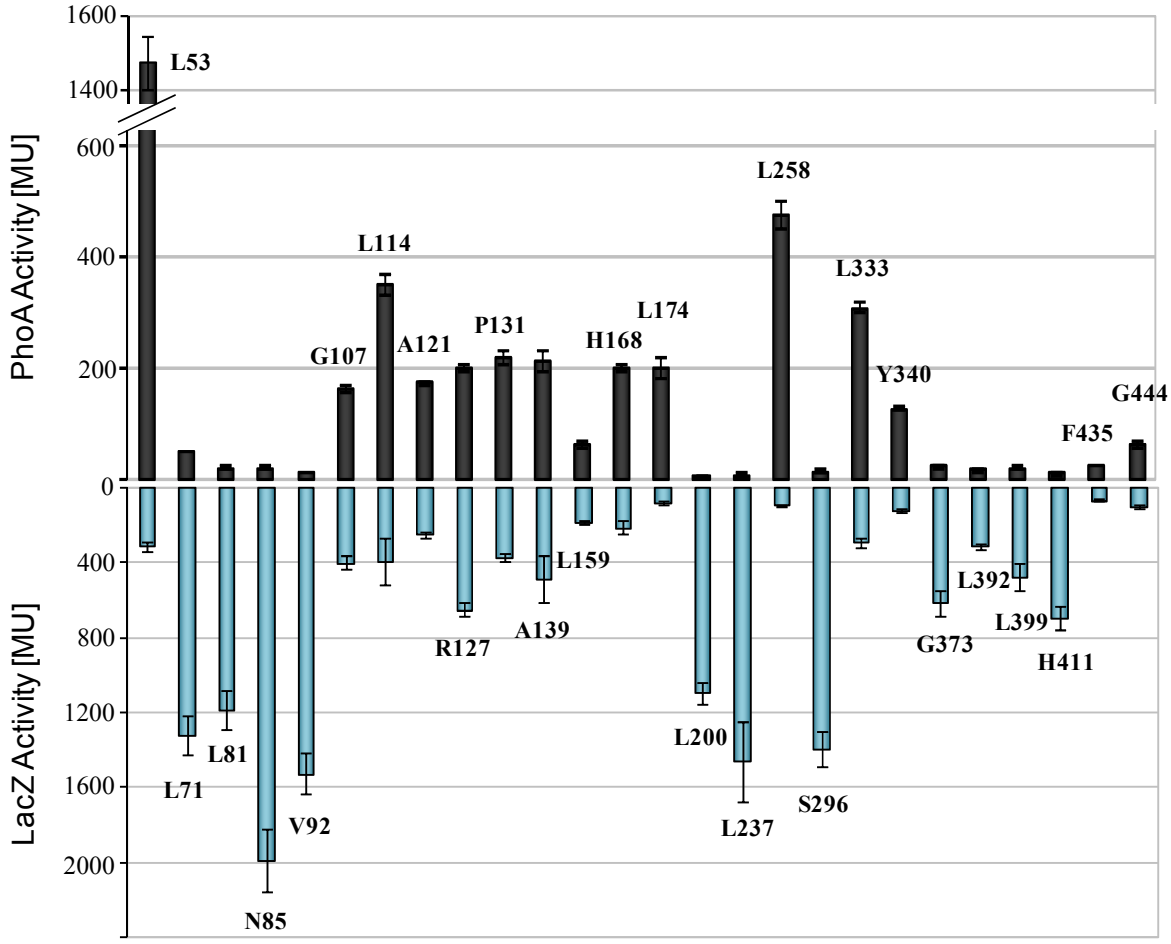

Figure R3: PhoA and LacZ activity of DcuB´-´PhoA and DcuB´-´LacZ fusion proteins. Plasmid-encoded and 3´-truncated *dcuB-phoA* and *dcuB-lacZ* fusions were expressed in *E. coli* CC181 under control of the P_{BAD} promoter. Cells were grown aerobically in LB broth with fumarate and induced with 0.2% arabinose in the exponential growth phase for 3 hours. Alkaline phosphatase and ß-galactosidase activity were determined by measuring the rate of hydrolysis of PNP and ONPG respectively. The amino acid residues indicate the DcuB junction sites with the reporter proteins.

DcuB fusions with the junction sites G107 to L159 showed an intermediate ratio of enzyme activities which did not allow attribution of a clear orientation of the residues. The results

imply that integration of the corresponding DcuB fusions occurred by chance. For further interpretation of the enzyme assays the localization of the surrounding loop was factored in. On the N-terminal side the area is confined by a cytoplasmic loop, on the C-terminal side by a periplasmic segment. As a consequence this part of DcuB has to comprise either three or just one transmembrane helices. Due to the size and hydrophobicity of the region the three helix solution is more probable and, a membrane-integrated localization of the concerned junction sites eventually would be an explanation for the inconclusive/ambigious PhoA/LacZ activity ratio.

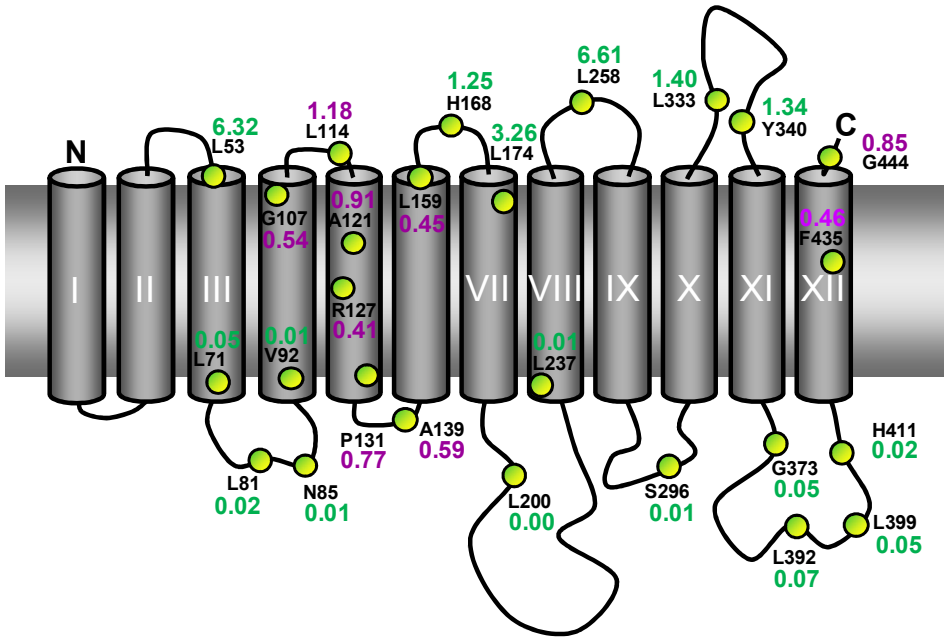

Figure R4: Topology model of DcuB based on PhoA and LacZ fusion studies. Positions of DcuB junction sites are marked by green circles and labeled with the according amino acid residues. The normalized PhoA/LacZ ratio of enzyme activities of alkaline phosphates and ß-galactosidase fused to the respective DcuB part are shown in green (clear result) and purple (no clear allocation).

Figure R4 shows a model of DcuB topology combining the results of both PhoA/LacZ fusion experiments and computational transmembrane helix prediction. The presence of eight transmembrane helices (II, III, VII-XII), a C-terminus facing the periplasm and two large cytoplasmic loops (TMHVII-TMHVIII and TMHXI-TMHXII) could be verified with high confidence. The region of DcuB with uncertain topology is marked by a PhoA/LacZ ratio shown in purple whereas unambiguous results are presented in green. Helix II was not determined by protein fusions but the composition and hydrophobicity of the corresponding amino acid sequence highly indicate a membrane-spanning segment. Presence of helix I is suggested since an even number of transmembrane helices is more common among bacteria

than an odd number and, in addition, this first helix was identified for the related carrier DcuA.

Expression studies with fusions of LacZ and PhoA to DcuA

Bacteria expressing DcuA-LacZ and DcuA-PhoA fusions were tested in the same way as described for DcuB. The PhoA/LacZ activity ratio of each junction site was calculated and used for determination of DcuA topology (Tab. R2). For interpretation of the data, a PhoA/LacZ activity ratio of > 3.0 was seen as a clear indicator for periplasmic localization whereas cytoplasmic localization resulted in PhoA/LacZ ratios below 0.3. Since the maximal measured activities of DcuA-PhoA (598 MU) and DcuA-LacZ (1690 MU) results in a ratio of 1/3 after normalization while normalized DcuB-PhoA/DcuB-LacZ activity ratio is approximately 1, the thresholds for interpretation of the results differ by the factor 3.

Table R2: Data obtained from DcuA-PhoA and -LacZ activity studies. Absolute enzyme activities of the reporter fusion (in Miller Units) and the PhoA/LacZ ratio of absolute and normalized activities were presented. The indicated orientation of the DcuA junction site is declared: P, periplasmic; C, cytoplasmic, M, membrane-integrated. Orientations predicted with high confidence are highlighted in bold.

DcuA junction site	**LacZ** activity [MU]	**PhoA** activity [MU]	**PhoA/LacZ** ratio	**orientation**	**normalized PhoA/LacZ**
V49	1226 ± 73	598 ± 16	0.49	P	1.38
R82	1690 ± 149	166 ± 4	0.10	**C**	0.28
S107	114 ± 16	158 ± 26	1.39	**P**	3.92
G123	229 ± 11	261 ± 11	1.14	**P**	3.22
V156	128 ± 10	56 ± 3	0.44	M	1.24
V171	53 ± 5	26 ± 2	0.49	M	1.39
L194	426 ± 51	36 ± 2	0.08	**C**	0.24
L229	477 ± 22	9 ± 1	0.02	**C**	0.05
A261	30 ± 1	211 ± 11	7.03	**P**	19.88
T289	873 ± 62	31 ± 2	0.04	**C**	0.10
V325	83 ± 20	297 ± 34	3.58	**P**	10.11
A353	786 ± 121	37 ± 6	0.05	**C**	0.13
S364	571 ± 48	52 ± 7	0.09	**C**	0.26
L387	169 ± 16	296 ± 17	1.75	**P**	4.95
R400	304 ± 19	270 ± 8	0.89	P	2.51
L416	218 ± 9	234 ± 6	1.07	**P**	3.03
L433	93 ± 7	375 ± 14	4.03	**P**	11.40

The C-terminal junction sites of DcuA including the amino acid residues L387 to L433 caused a high activity ratio (>3) of the corresponding fusion proteins (Tab. R2, Fig. R5) and

therefore are located in the periplasm. Fusion of DcuAS364 and DcuAA353 came along with a strong decreased PhoA/LacZ activity ratio (>0.3) indicating a cytoplasmic localization of the junction sites. The soluble loops containing residue V325, A261 or residues G122 and S107 are situated in the periplasm, whereas the junction sites DcuAT289, L229, L194 and R82 clearly show a cytoplasmic orientation. Fusions of PhoA and LacZ to the DcuA junction sites V171, V156 and V49 resulted in a PhoA/LacZ activity ratio of about 1.4 preventing reliable mapping of the residues.

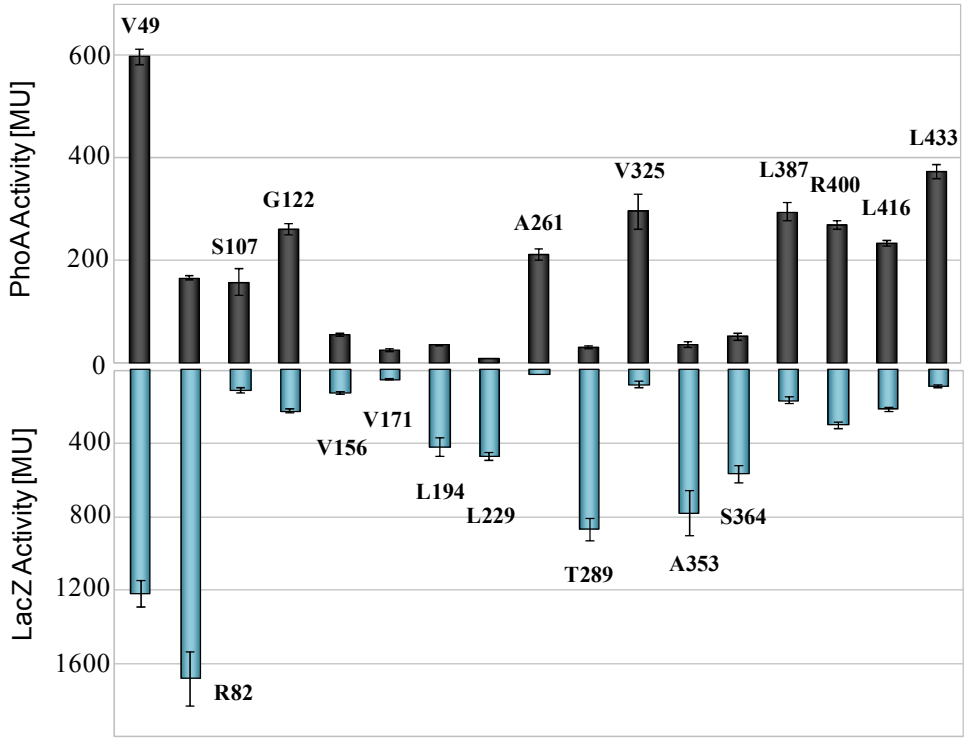

Figure R5: PhoA and LacZ activity of DcuA´-´PhoA and DcuA´-´LacZ fusion proteins. The diagram shows the enzyme activities of plasmid-encoded and 3´-truncated *dcuB´-´phoA* and *dcuB´-´lacZ* fusions after expression in *E. coli* CC181 under control of the P_{BAD} promoter. Bars were labeled with the amino acid residue forming the junction site of C-terminal truncated DcuA with the reporter proteins. Cells were cultivated aerobically in LB broth with fumarate. For protein expression the exponentially growing cultures were induced with 0.2% arabinose. Enzyme activities were determined after another 3 hours of aerobic incubation.

The results of PhoA and LacZ fusion protein studies of the DcuB-related carrier DcuA mostly support the topology model of DcuA postulated by Golby *et al.* (1998) which is presented in Figure R6. In contrast to DcuB, DcuA is predicted to comprise 10 transmembrane helices with a very short N-terminus und a large C-terminus (about 45 amino acid residues) both facing the periplasm. Similar to DcuB, DcuA contains a large cytoplasmic loop in the middle of the protein.

Despite the high sequence identity, topology of DcuA and DcuB clearly differs in some points. DcuA has a large soluble C-terminal domain, whereas the C-terminus of DcuB ends with a membrane-spanning segment attaining the membrane surface on the periplasmic side at most. Comparison of the enzyme activity ratios of the corresponding junction sites DcuAR400 and DcuBH411, or DcuAL387 and DcuBL399 (see Fig. R1) demonstrates that these residues are located on contrary sites of the membrane. The corresponding residues DcuAV325 and DcuBL333/Y340 are localized in the periplasm followed by DcuAT289 and DcuBS296 both situated in a cytoplasmic loop. Moving on in N-terminal direction another small periplasmic reagion in both carriers (DcuAA261, DcuBL258) is followed by a large cytoplasmic loop (DcuAL194/L229, DcuBL200/L237) containing the majority of positively charged residues. In DcuA this cytoplasmic part is predicted by Golby *et al.* (1998) to be even larger, including the residues V156 and V171. The according DcuA fusion proteins show very low enzyme activities, independent of the type of fused reporter protein. Based on the reporter protein activities, no clear orientation can be related to the residues. The corresponding part of DcuB (L174, H168) is located in a periplasmic loop followed by a membrane-spanning segment (L159). The cytoplasmic localization of DcuAR82 complies with the corresponding residue DcuBN85.

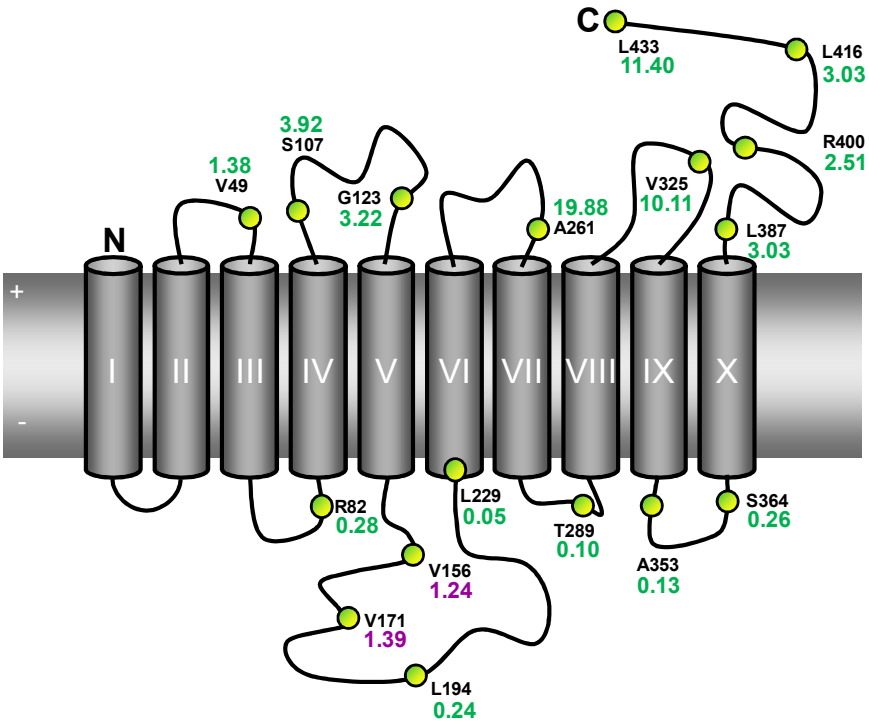

Figure R6: Topology model of DcuA according to Golby *et al.* (1998). The normalized ration of alkaline phosphatase to ß-galactosidase activities based on plasmid-encoded expression of DcuA-PhoA and DcuA-LacZ hybrid proteins in *E. coli* CC181 is shown in numbers. DcuA junction sites are marked by green circles. PhoA/LacZ activity ratios that do not exactly fit the model are shown in purple, ratios that are in accordance with the model are printed in green.

4.1.2 DcuB-BlaM expression studies

The topology of the anaerobic C_4-dicarboxylate carrier DcuA was determined experimentally by using *bla* as a reporter gene (Golby *et al.*, 1998). The *bla* gene encodes the bacterial ß-lactamase, a periplasmic protein that mediates resistance to ß-lactam antibiotics like penicillin or ampicillin. The resistence is based on hydrolyses of the ß-lactam ring, deactivating the molecule's antibacterial properties. ß-lactamase is initially synthesized as a preprotein with an N-terminal signal peptide. The ability of the plasmid-encoded BlaM fusions to protect individual cells against ampicillin correlates with the cellular orientation of the ß-lactamase part (Broome-Smith & Spratt, 1986).

DcuA topology was analysed with in-frame fusions of truncated *dcuA* fragments and the *blaM* gene coding for the mature portion of the ß-lactamase. Expression of the constructs led to a series of C-terminally truncated forms of DcuA fused to a ß-lactamase protein that lacks the N-terminal signal peptide. Without signal peptide the localisation of the reporter protein is mediated by the orientation of the corresponding DcuA C-terminus. Although the ß-lactamase is still active in the cytoplasm, cells with cytoplasmic localized ß-lactamase lose their ability to grow on ampicillin. For this reason, blaM-dependent antibiotic-resistance can be used as a marker for protein orientation within the membrane.

To analyse DcuB topology, fusions of full-length *dcuA* and *dcuB* with the mature ß-lactamase gene were designed (Fig. R7). Furthermore, *blaM* fusions with 3´-truncated *dcuB* and a gene fusion of *dcuB* with the *bla* gene including its export signal were constructed. The signal sequence of ß-lactamase is proteolytically removed during the secretion (Koshland & Botstein, 1982), resulting in a DcuB protein separated from the periplasmic localized ß-lactamase. This DcuB-Bla_{Leader} protein was used as a positive control in which 100% of the ß-lactamase moiety is secreted. The DcuA-BlaM fusion protein served for establishing the test conditions. The periplasmic orientation of the DcuA C-terminus has been determined by the same method (Golby *et al.*, 1998) and shown to tolerate ampicillin concentrations up to 100 µM. In addition, ß-lactamase fusions with the aerobic succinate uptake carrier DctA were made. For the DctA carrier a cytoplasmic localization of both termini is predicted by common membrane protein topology servers (TMHMM, TOPPRED, OCTOPUS). The DctA-BlaM and the BlaM-DctA protein therefore should mediate a cytoplasmic localization of the BlaM part with no or very low ampicillin resistance. An overview of the tested ß-lactamase fusions is presented in Figure R7.

The plasmids with the ß-lactamase fusion were transformed into competent *E. coli* JM109 or C43DE3, and Kan^r transformants were selected. The constructs were verified by sequencing. The transformants were tested for growth on LB broth agar containing 100 µg/ml ampicillin and 100 µM arabinose or 1 mM IPTG by spotting a droplet of an overnight culture on the surface for testing activity of the ß-lactamase part of the fusion protein. Periplasmic, but also cytoplasmically localised ß-lactamase provides protection against ampicillin when the cell density is high. Due to antibiotic-dependant cell lyses, ß-lactamase is released to the medium where it starts to degrade the ampicillin. As a consequence neighboring cells are protected from lysis (Kadonaga & Knowles 1985). Therefore functionality of the BlaM moiety in fusion proteins was checked by inoculating the cells at high density onto agar containing ampicillin. The carriers except DcuA were tested for antiport or uptake of C_4-dicarboxylates by growth experiment under anaerobic (DcuB) or aerobic (DctA) conditions. All constructs with full-length carriers linked to the ß-lactamase protein showed transport activity and enabled growth on fumarate.

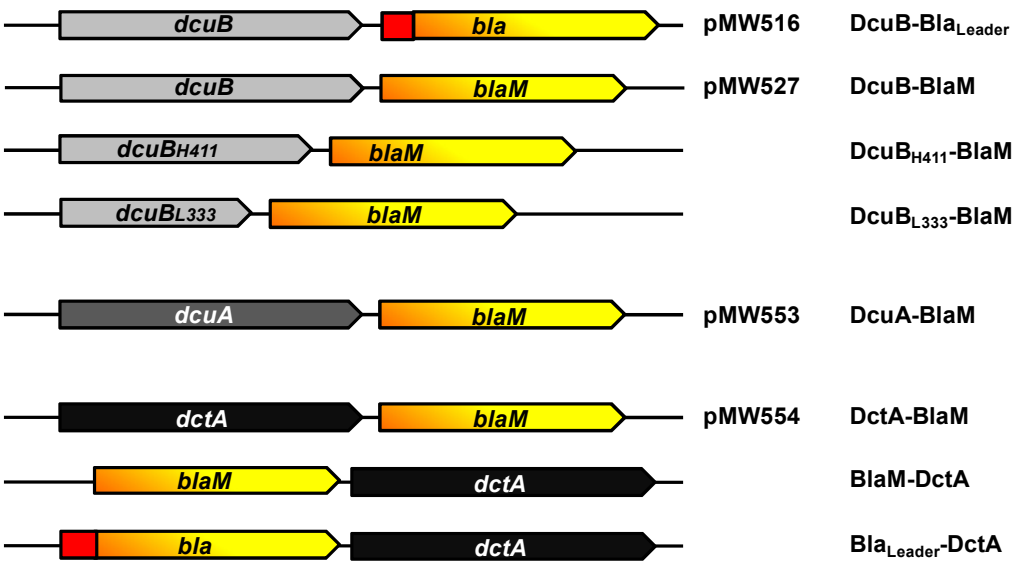

Figure R7: Schematic representation of gene fusions of *dcuA, dcuB* and *dctA* with *ß-lactamase.* All constructs were cloned into the arabinose-inducible expression vector pBAD18-Kan*(DcuA, DcuB) or the IPTG-inducible vector pET28a (DctA). C-terminal fusions of the ß-lactamase with (bla) or without (blaM) leaderpeptide were resulting in the plasmids pMW516, pMW527, truncated pMW527 derivatives, pMW553 and pMW554. Additional, two plasmids with *bla* and *blaM* N-terminal fused to full-length DctA were constructed. The coded fusion proteins are specified in the right column.

All constructs except the 5´end *bla-dctA* fusion coded for a ß-lactamase protein which is fully active (not shown). The ß-lactamase-containing pBAD18-Kan* and pET28a derivatives allowed cell growth on LB agar plates with at least 100 µg/ml ampicillin when inoculated at high density. The ß-lactamase part of fusion protein Bla_{Leader}-DctA showed a lower activity. C43 transformants expressing this protein tolerated only ampicillin concentrations up to 40 µg/ml. With the BlaM-DctA fusion protein no difference to the plasmid-free C43 strain could be observed. Both cell types only grow up to an ampicillin concentration of less than 5 µg/ml.

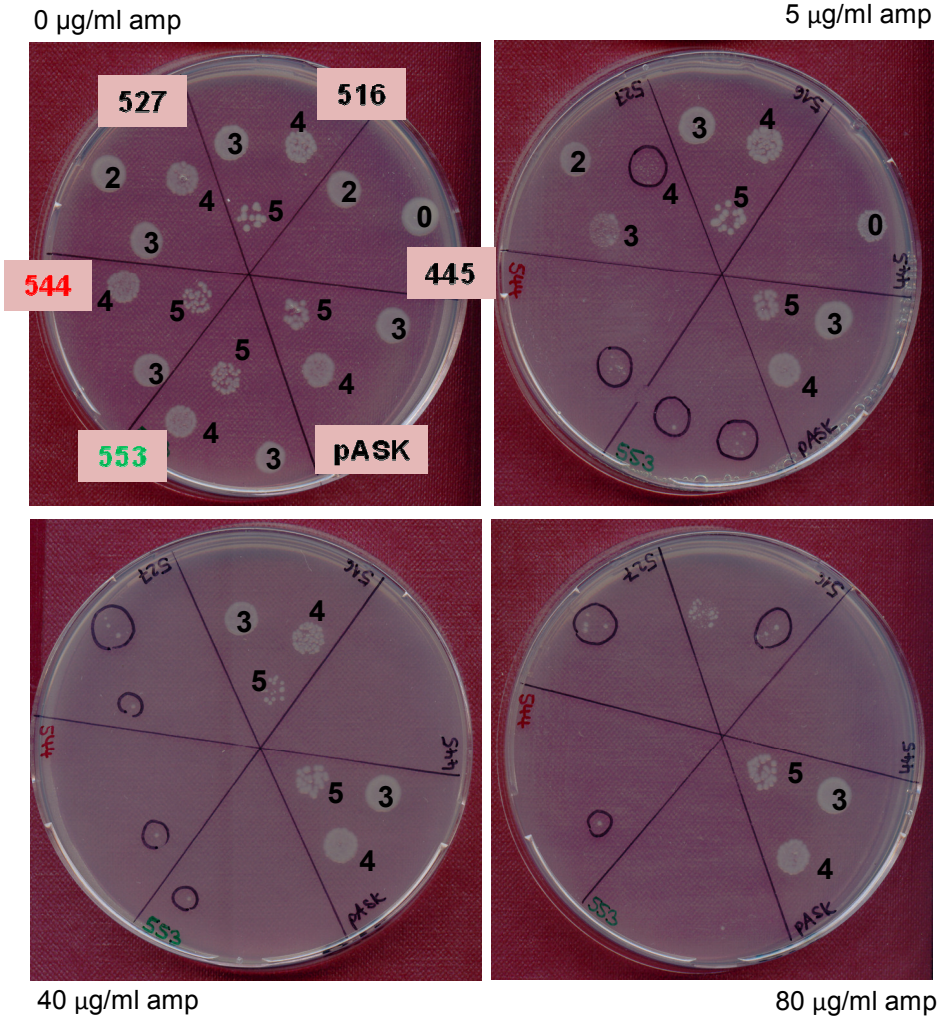

Figure R8: Spotting tests of *E. coli* strains with different plasmid-encoded ß-lactamase fusion protein on ampicillin-containing LB agar plates. All plates were inoculated with identical samples. The picture shows a selection of plates inoculated with cells at high, middle or low density. *E. coli* JM109 harbouring pMW516 (*dcuB-bla*$_{Leader}$), pMW527 (dcuB-blaM), pMW544 (also *dcuB-blaM*, but with extended linker), pMW553 (*dcuA-blaM*) or pMW445 (*dcuB*) was cultivated overnight in LB broth with 100µM kanamycin for plasmid selection. The cells were adjusted to an optical density of 3 and diluted 10^{-2} to 10^{-5}. The numbers 0-5 give the degree of dilution: 1 stands for undiluted cells, 2 for 10^{-2} and 5 is equal to the 10^{-5} dilution. Of each strain 4 µl of different dilutions were spotted on LB agar plates with ampicillin in a range of 0-80 µg/ml and 100 µM of the inducer arabinose. *E. coli* JM109 with vector pASK-IBA3^{+} containing an ampicillin resistance cassette for selection was used as a positive control.

To identify the MIC (Maximum Inhibitor Concentration) of single cells several dilutions of an overnight culture were made and a volume of 4 µl was spottet on LB agar plates containing ampicillin in a range of 1 to 80 µg/ml. A selection of plates inoculated with cell droplets of low density after overnight incubation is presented in Figure R8.

All tests demonstrated that none of the full-length DcuB-BlaM (pMW527) or truncated DcuB-BlaM fusion proteins (pMW527 H411, pMW527 G373, pMW527 L333, pMW527 H168 and pMW527 R127; data not shown) lead to an increased ampicillin resistance on the level of single cells. Similar to the ß-lactamase-free pMW445 (pBAD18-Kan* derivative for arabinose-induced expression of DcuB) diluted cells were not able to tolerate ampicillin concentrations above 5 µg/ml (including the 10^{-3} dilution!). Thereby no difference in growth was found by using 0 µM, 100 µM, 333 µM or 1 mM of the inducer arabinose.

An extension of the linker region between *dcuB* and *blaM* (encoded on pMW544) provided the same results. Furthermore transformants with plasmid pMW553 encoding DcuA-BlaM showed no growth on ampicillin-containing agar when inoculated at low density. Expression of ß-lactamase fusions with the aerobic succinate carrier DctA had no influence on growth of ampicillin-containing plates, either. But even if this last result was expected, all other issues demonstrate that the method is not working. Only the DcuB-Bla_{Leader} construct was suitable to protect cells against lysis up in the presence of about 50 µg/ml ampicillin. By comparison, cells carrying the expression vector pASK-IBA3^{+} (used as the origin of the *bla* gene) still form isolated colonies at concentrations of more than 100 µg/ml ampicillin. By Golby *et al.* (1998) MICs of 5-10 µg/ml ampicillin for cytoplasmic and of 20-120 µg/ml for periplasmically located BlaM parts were specified.

4.2 Accessibility studies by sulphydryl-labeling

The cysteine residues of DcuB can be replaced by serine residues without loss of function (Tab. R3; section 4.3 Fig. R17) similar to other secondary carriers of *E. coli* like the lactose permease (van Iwaarden et al., 1991), the melibiose permease (Weissborn et al., 1997) or the sodium/ proline transporter (Jung et al., 1998). Therefore active mutants of DcuB can be produced that carry single Cys residues at any position. The mutant forms of DcuB can then be used for accessibility studies by labeling of the Cys residues with thiol-specific reagents.

Detection of DcuB

For sulphydryl labeling experiments, immunodetection of the labeled protein with specific antibodies is required. There are no sensitive DcuB-specific antibodies available, therefore DcuB-PhoA encoded by pMW561 was used for specific detection of DcuB via the PhoA-tag. The C-terminal PhoA-tag can be detected in immunoblots by specific and highly sensitive antibodies. The alkaline phosphatase of *E. coli* is a hydrophilic protein of 471 amino acid residues. PhoA possesses 4 cysteine residues forming two disulfide bonds which are essential for the catalytic activity of the phosphatase (Sone et al., 1996), but not relevant for detection by anti-PhoA antibodies. The DcuB-PhoA fusion protein has an overall size of about 100 kDa and a mobility of a M_r ~85 kDa protein in SDS-PAGE and immunoblot.

Generation and denotation of plasmid coded DcuB-PhoA mutants

The cysteine residues of DcuB-PhoA were removed by site-directed mutagenesis resulting in plasmid pMW828 (Fig. R9; Fig. R10) for expression of a Cys-less protein variant $DcuB_{C12345S}$-$PhoA_{C1234S}$. As intermediate products, plasmid pMW826 coding for $DcuB_{C12345S}$-PhoA and the single cysteine derivatives pMW826 134 ($DcuB_{C12345S}$-$PhoA_{C134S}$) and pMW826 124 ($DcuB_{C12345S}$-$PhoA_{C124S}$) were obtained (Fig. R10).

*MGDRG*M1LF$_3$TIQLIIILIS13LFYGAR19KG21GIALGLLGGIGLVILVFVFHLQPGK46PPVDVMLVIIA
VVAASATLQASGGLDVMLQIAE79KLLRRNPK87YVS90IVAPFVTS98TLTILS104GTGHVVYT112
ILPIIY118DVAIKNN125IRPERPMAAS135SIG138AQMGIIAS146PVSVAVVS154LVAMLGNVT163
FDGR167HLEFL172D173LLAITIPSTLIGILAIGIFSWFRGKDLDKDE204EFQKFIS211VPENRE217
YVYGD222TATLLDKK230LPKSNWLAMWIFLGAIAVVALLGADSDLR259PS261FGGKPLSMVLV
IQMFMLLTGALIIILTKTNPASISKNE299VFRSGMIAIVAVYGIAWMAETMFGAHMSE328IQGVLGE
MVK338EYPWAYAIVLLLVS352KFVNS357QAAALAAIVPVALAIGVD375PAYIVASAPAS386YGY
YILPTYPSDLAAIQFDR406SGTTHIGR414FVINHSFILPGLIGVSVSS433VFGWIFAAMYG$_{444}$FL446
*VDLQESASDSYTQVASWTEPFPF*S$_{inker}$P$_{28}$VLENRAAQGDITAPGGARRLTGDQTAALRDSLSDKP
AKNIILLIGDGMGDSEITAARNYAEGAGGFFKGIDALPLTGQYTHYALNKKTGKPDYVTDSAASAT
AWSTGVKTYNGALGVDIHEKDHPTILEMAKAAGLATGNVSTAELQDATPAALVAHVTSRKS168Y
GPSATSEKS178PGNALEKGGKGSITEQLLNARADVTLGGGAKTFAETATAGEWQGKTLREQAQ
ARGYQLVSDAASLNSVTEANQQKPLLGLFADGNMPVRWLGPKATYHGNIDKPAVTS286TPNPQ
RNDSVPTLAQMTDKAIELLSKNEKGFFLQVEGASIDKQDHAANPS336GQIGETVDLDEAVQRAL
EFAKKEGNTLVIVTADHAHASQIVAPDTKAPGLTQALNTKDGAVMVMSYGNSEEDSQEHTGSQL
RIAAYGPHAANVVGLTDQTDLFYTMKAALGLK$_{471}$

Figure R9: Amino acid sequence of DcuB-PhoA encoded on plasmid pMW828. DcuB (F_3-G_{444}) is fused to the alkaline phosphatase PhoA (P_{28}- K_{471}) by a linker containing 26 amino acid residues. Amino acids of DcuB and PhoA are printed in bold letters; residues that do not belong to DcuB or PhoA either are written in italic. The cysteine residues were substituted by serine residues (purple). Amino acid residues of DcuB which were replaced by single cysteines for sulphydryl-labeling are shown in green. For creating of a DcuB mutant with a single cysteine at the N- and C-terminus of (M1C; L446C), the missing amino acid residues (L2; F445) were inserted simultaneously during site-directed mutagenesis. Relevant residues are numbered with their exact position within the proteins, DcuB and PhoA.

Mutants of $DcuB_{C12345S}$-$PhoA_{C1234S}$ containing each a single cysteine residue within the DcuB part were produced by site-directed mutagenesis (Fig. R9). The resulting pMW828 variants were denoted by the additional amino acid residue substitution, for example pMW828 M1C for the plasmid coding for $DcuB_{C12345S}$-$PhoA_{C1234S}$ M1C.

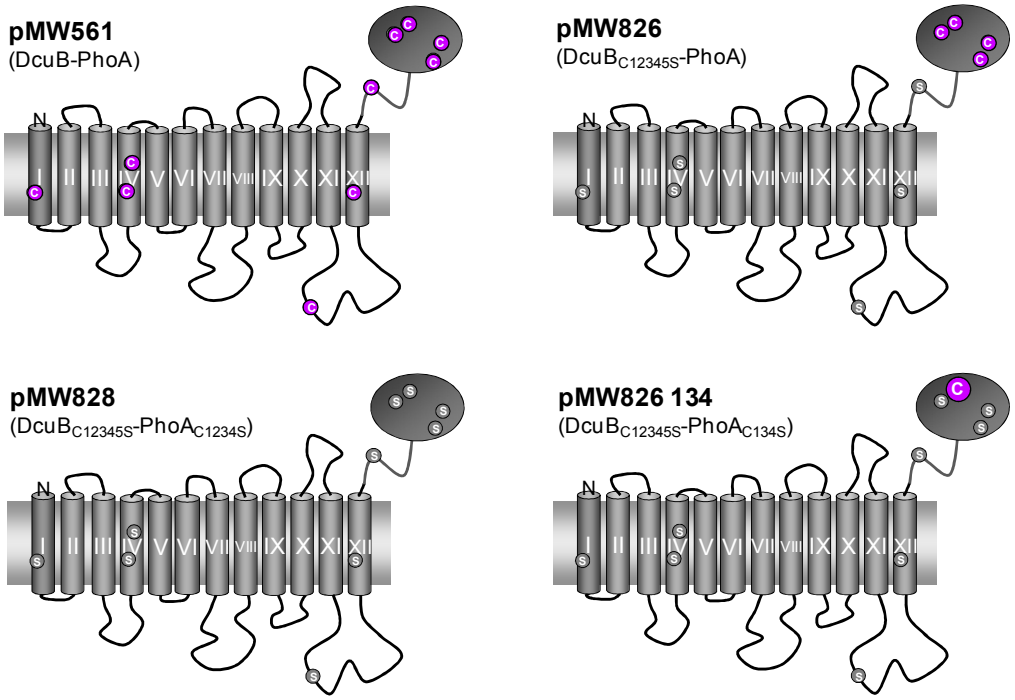

Figure R10: Denotation of plasmids encoding for various DcuB-PhoA mutants. The models show the positions of all physiological cysteines (purple) that were partly or completely substituted by serines (grey). Plasmid pMW561 codes for wild type DcuB fused to the mature PhoA comprising a total of ten cysteines: five were located within the DcuB part, four belong to PhoA and one cysteine is situated in the linker region. Plasmid pMW826 codes for a fusion protein in which the cysteines of DcuB and the linker region were replaced by serines. The four cysteines within the PhoA part remain. Additional substitutions of the cysteines 1, 3 and 4 of PhoA (C168S, C286S, C336S) led to plasmid pMW826 134. The fully cysteine-free variant of DcuB-PhoA is encoded on plasmid pMW828 which was used as a template for the positioning of single cystein residues within the DcuB part.

As a test for the functional insertion of the DcuB-PhoA fusion into the membrane, the constructs were checked for regulatory properties in *E. coli* IMW505 (*dcuA dcuB dcuC*) by a chromosomal *dcuB´-´lacZ* reporter gene fusion (Tab. R3). Although the regulatory activity of DcuB-PhoA six-fold mutants was reduced, the pMW828 derivatives restored the fumarate-dependent *dcuB´-´lacZ* expression in the *dcuB* mutant. The only exception was the mutant with E204C which was no longer active in regulation. A DcuB protein with the single amino acid substitution E204A on the other hand was fully active, indicating that the decreased activity is not based on a single amino acid exchange but on the high number of substitutions.

The DcuB-PhoA four-fold mutants coded on pMW828 C98, pMW828 C386 and pMW828 C433 show almost wild-type activity.

As mentioned in section 4.1.1, Fig. R2, the fusion with PhoA did not affect regulatory activity and transport of DcuB, but the expression levels did. While the six-fold DcuB mutant $DcuB_{C12345S}$-$PhoA_{C1234S}$ S261C showed only reduced activity when coded on the arabinose-inducable high-copy plasmid pBAD18-Kan*, the comparable mutant $DcuB_{C12345S}$ S261C was highly active when coded on pME6010 under the control of the *dcuB*-promotor. The ß-galactosidase activities of a series of DcuB single to six-fold mutants indicated a correct assembly of all single cysteine constructs of DcuB within the cytoplasmic membrane.

Table R3: Functional scan of DcuB mutants for affecting *dcuB´-´lacZ* expression in *E. coli* IMW505 (*dcuA dcuB dcuC*). Strain IMW505 carrying a chromosomal *dcuB´-´lacZ* reporter gene fusion was transformed with a series of *dcuB*-containing plasmids. Cells were grown anaerobically in eM9 medium supplemented with glycerol, DMSO and with or without fumarate. The expression of *dcuB´-´lacZ* in the absence and the presence of the effector fumarate was determined in exponentially growing cultures. DcuB variants encoded on the low-copy plasmid pME6010 are expressed under the control of their own promoter. Expression of *dcuB* mutants on pBAD18 (pBAD18-Kan*) depend on the arabinose-inducable P_{BAD} promoter. Strains expressing wild type DcuB alone or in a fusion with PhoA are shown in black bold print. Cysteine-free mutants of DcuB (five-fold mutants), which were used as a template for single cysteine replacements, are shown in green. Four-fold mutants are highlighted by grey colour. Strains that show no repression of *dcuB´-´lacZ* expression in the absence of effector are marked in purple.

Strain (relevant genotype)	**Plasmid origin**	Activity [MU] **without effector**	Activity [MU] **fumarate**
IMW505 (***dcuAΔdcuBdcuC***)		421 ± 29	484 ± 33
IMW505 pME6010	pME6010	686 ± 36	595 ± 27
IMW505 pMW228 (*dcuB*$^+$)	**pME6010**	**17 ± 1**	**405 ± 19**
IMW505 pMW737 (*dcuB*$_{Cys}^+$)	**pME6010**	**16 ± 2**	**414 ± 54**
dcuB-substitutions			
IMW505 pMW737 L2C	pME6010	24 ± 2	299 ± 21
IMW505 pMW737 G21C	pME6010	29 ± 2	392 ± 22
IMW505 pMW737 V49C	pME6010	37 ± 2	406 ± 40
IMW505 pMW737 S90C	pME6010	19 ± 2	403 ± 26
IMW505 pMW737 S211C	pME6010	18 ± 3	452 ± 25
IMW505 pMW737 S261C	pME6010	19 ± 3	411 ± 105
IMW505 pMW737 S240C	pME6010	338 ± 57	382 ± 21
IMW505 pMW737 L446C	pME6010	20 ± 1	456 ± 39
IMW505 pMW445 (*dcuB*$^+$)	**pBAD18**	**8 ± 2**	**255 ± 16**
IMW505 pMW635 (*dcuB*$_{Cys}^+$)	pBAD18	48 ± 22	166 ± 33

Strain (relevant genotype)	**Plasmid origin**	Activity [MU] **without effector**	Activity [MU] **fumarate**
IMW505 pMW561 (*dcuB-phoA*$^+$)	**pBAD18**	**9 ± 1**	**250 ± 16**
IMW505 pMW828 (*dcuB*$_{Cys}$-*phoA*$_{Cys}$$^+$)	**pBAD18**	**48 ± 10**	**225 ± 52**
dcuB-substitutions			
IMW505 pMW828 M1C	pBAD18	74 ± 15	195 ± 24
IMW505 pMW828 R19C	pBAD18	150 ± 57	238 ± 38
IMW505 pMW828 K46C	pBAD18	98 ± 25	267 ± 28
IMW505 pMW828 E79C	pBAD18	150 ± 21	282 ± 68
IMW505 pMW828 K87C	pBAD18	100 ± 22	286 ± 29
IMW505 pMW828 C98	**pBAD18**	**36 ± 7**	**239 ± 26**
IMW505 pMW828 T112C	pBAD18	69 ± 13	240 ± 49
IMW505 pMW828 Y118C	pBAD18	117 ± 24	236 ± 29
IMW505 pMW828 S135C	pBAD18	119 ± 12	260 ± 20
IMW505 pMW828 G138C	pBAD18	78 ± 29	196 ± 8
IMW505 pMW828 S146C	pBAD18	96 ± 12	203 ± 21
IMW505 pMW828 R167C	pBAD18	74 ± 10	192 ± 23
IMW505 pMW828 L172C	pBAD18	66 ± 18	222 ± 40
IMW505 pMW828 D173C	pBAD18	124 ± 13	253 ± 57
IMW505 pMW828 E204C	pBAD18	205 ± 60	163 ± 25
IMW505 pMW828 E217C	pBAD18	100 ± 31	245 ± 43
IMW505 pMW828 D222C	pBAD18	41 ± 23	232 ± 16
IMW505 pMW828 K230C	pBAD18	162 ± 52	225 ± 17
IMW505 pMW828 R259C	pBAD18	107 ± 11	240 ± 56
IMW505 pMW828 S261C	pBAD18	71 ± 18	237 ± 43
IMW505 pMW828 E299C	pBAD18	89 ± 14	257 ± 35
IMW505 pMW828 E328C	pBAD18	32 ± 3	255 ± 29
IMW505 pMW828 K338C	pBAD18	106 ± 87	235 ± 34
IMW505 pMW828 S352C	pBAD18	94 ± 13	276 ± 21
IMW505 pMW828 S357C	pBAD18	95 ± 27	200 ± 43
IMW505 pMW828 D375C	pBAD18	123 ± 24	237 ± 23
IMW505 pMW828 C386	**pBAD18**	**2 ± 1**	**253 ± 24**
IMW505 pMW828 R406C	pBAD18	133 ± 46	220 ± 33
IMW505 pMW828 R414C	pBAD18	143 ± 68	204 ± 17
IMW505 pMW828 C433	**pBAD18**	**19 ± 3**	**234 ± 23**

Strategy of sulphydryl-labeling

The accessibility of amino acid residues distributed across DcuB was investigated by testing the labeling of single introduced Cys residues with membrane-permeable and membrane-impermeable alkylating reagents. Due to high reactivity under mild conditions and high selectivity for cysteinyl thiols the maleimide derivatives NEM (N-ethylmaleimide), AMS (4-acetamido-4´-maleimidylstilbene-2,2´-disulfonic acid, disodium salt) and PEGmal (alpha-

Methoxy-omega-ethyl-maleimide polyethylene glycole) were used. Maleimide derivatives react with sulphydryl groups under formation of a thioether bond that is stable against reducing reagents like ß-mercaptoethanol and dithiothreitol.

AMS is an anion of ~540 Da with very low membrane penetration capatibility (Hagting *et al.,* 1997; Long *et al.,* 1998). In contrast, the small and hydrophobic NEM (~125 Da) is a membrane-permeable reagent and blocks Cys residues on both sides of the membrane and in membrane-spanning segments if water is available. The sulfhydryl group reacts as the thiolate form with the maleimide double bond. Deprotonation of the SH group to the thiolate requires a water molecule as a proton acceptor (Kimura-Someya *et al.*, 1998), therefore modification of water-isolated residues buried deep within the membrane is not possible. Since small molecules below ~600 Da can pass the outer membrane of *E. coli* (Henderson et al., 2004), pre-treatment by NEM and AMS can be applied to whole cells without the need for sphaeroplasts-preparation. The third alkylating reagent PEGmal is a bulky membrane-impermeable polymer with an average size of 5 kDa.

For a clear interpretation of the labeling results, four samples for each cysteine mutant were analyzed in parallel (Fig. R11). Cells of the first sample were pre-incubated with AMS (AMS pre-labeled or A sample), cells of the second sample with NEM (NEM pre-labeled or N sample). The reaction with AMS and NEM was terminated by 20-fold dilution with buffer followed immediately by centrifugation. The cell pellets were washed with buffer and resuspended in buffer containing 1% SDS to disrupt the membranes and to denature proteins. Then PEGmal was added to the denatured protein solution to label AMS/ NEM-unmodified Cys residues. Proteins of the third sample were without previous treatment with AMS or NEM incubated with PEGmal in the presence of SDS to achieve maximal PEGmal-alkylation (PEGmal or (-) sample). The fourth sample was a negative control containing solubilised but unlabeled protein (unlabeled or (=) sample). The final reaction of denaturated proteins with or without PEGmal was terminated by adding dithiothreitol. The protein samples were immediately mixed with SDS loading buffer, boiled in a water bath for 10 min and subjected to SDS-PAGE.

After SDS-PAGE and immunoblotting, PEGmal-labeled DcuB-PhoA was identified by a mobility-shift of the protein band. Blocking by AMS or NEM during the first incubation step resulted in DcuB-PhoA with the mobility of unmodified DcuB-PhoA and prevented PEGmal alkylation. PEGmal alkylation is supposed to increase the mass and to decrease the mobility of the protein significantly due to the high mass (5 kDa) of the label.

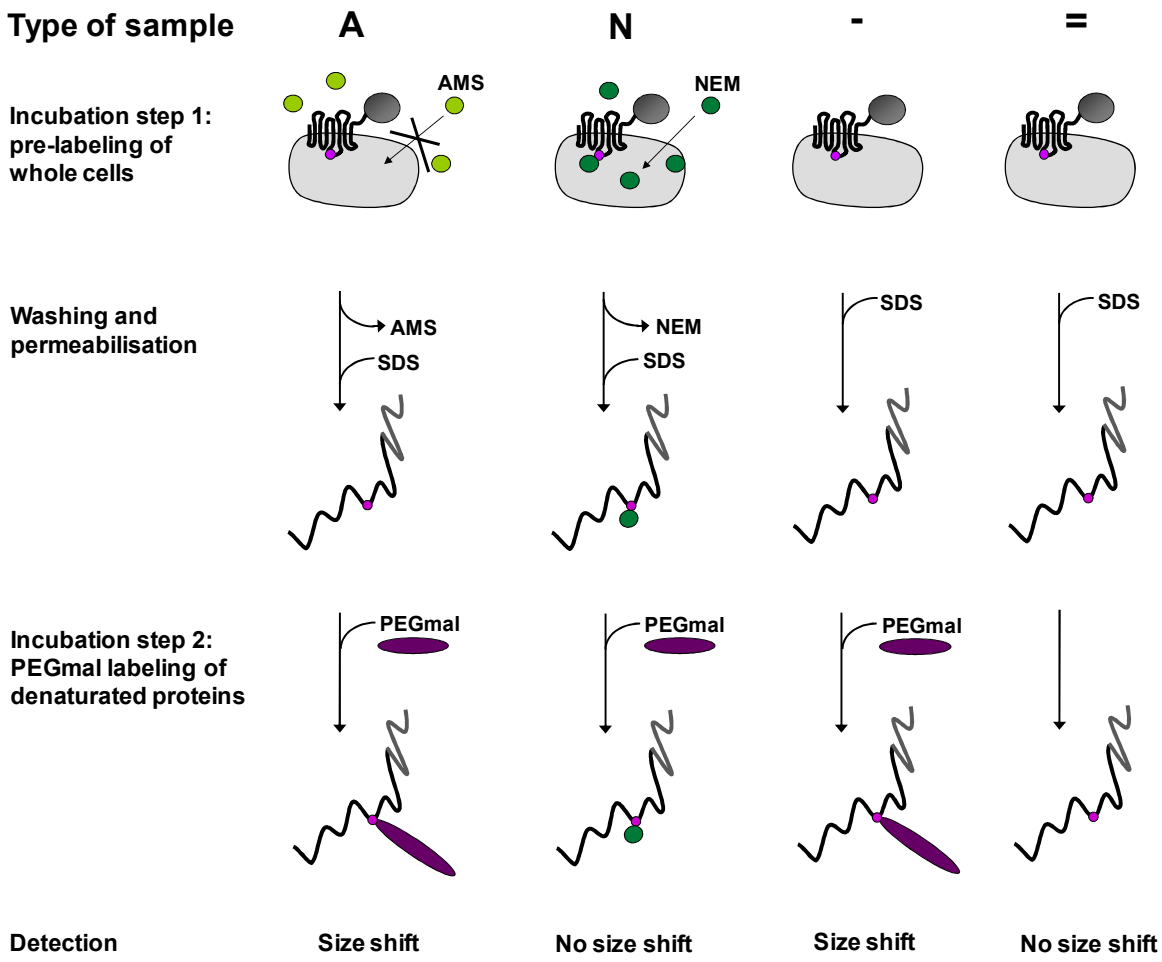

Figure R11: Strategy of sulphydryl-labeling using membrane-permeable and membrane-impermeable maleimide derivatives. Four different labeling procedures were applied on cells overproducing a single-cysteine mutant of DcuB-PhoA: **A, AMS pre-labeled sample.** Whole cells were pre-incubated with AMS. The excess AMS was removed by dilution and centrifugation steps and cells were permeabilized by SDS. The denaturated protein solution was finally incubated with PEGmal and analyzed by SDS-PAGE and immunoblotting. **N, NEM pre-labeled sample.** Identical approach as for the A sample, but with NEM used as blocking reagent in the first incubation step. **(-), PEGmal-labeled sample**. Incubation of denaturated proteins with PEGmal; no additional pre-labeling prior to PEGmal reaction. **(=), unlabeled sample,** containing denaturated unmodified proteins.

Controls

Labeling experiments were performed with *E. coli* strain C43DE3 overexpressing cytoplasmic SoxY (Fig. R12; Fig. R13) and a PhoA-DcuB Cys mutant. The Cys-less variant $DcuB_{C12345S}$-$PhoA_{C1234S}$ encoded by plasmid pMW828 served as a control for nonspecific labeling (Fig. R13A). Modification of a periplasmic cysteine-containing protein (PhoA) was tested with plasmids pMW826 134 (Fig. R13B) and pMW826 124 (data not shown). The experiments were analysed in parallel by SDS-PAGE and subsequent immunoblotting with anti-HA (detection of SoxY) and anti-PhoA (detection of DcuB-PhoA).

For checking the reactivity of the maleimides and the current state of the cells, plasmid pHASoxYZ for constitutive cytoplasmic expression of HA(hemeagglutinine)-tagged SoxY of *Paracoccus pantotrophus* was used. SoxY is a small hydrophilic protein (11 kDa) with a single exposed Cys-residue. Due to its cytoplasmic localization this residue was not accessible to membrane-impermeable AMS in intact cells, while membrane-permeable NEM could bind within minutes (Fig. R12). PEGmal incubation of AMS pre-treated cells resulted in a clear size-shift on the immunoblot from about 16 kDa to 28 kDa, indicating an effective reaction with PEGmal. Modification by PEGmal shifted the mobility of SoxY by approximately 10-15 kDa, in accordance with Lu & Deutsch, 2001. With NEM, as well as with AMS in the presence of SDS, a nearly total blocking of accessible residues was obtained. No additional protein band at 28 kDa was identified. Labeling with PEGmal on the other hand mostly resulted in an incomplete alkylation. In the exclusively PEGmal-treated and in the AMS pre-labeled fraction the band of unmodified protein was often still detectable.

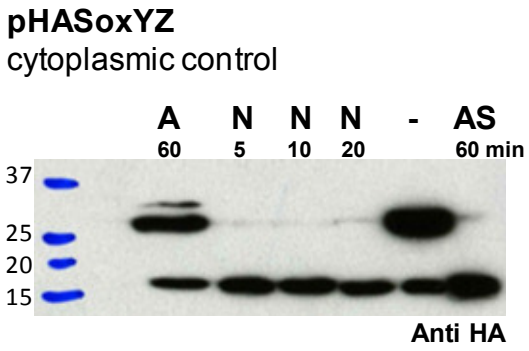

Figure R12: Sulphydryl labeling of cells overproducing the soluble protein HA-SoxY: AMS accessibility and time-course for modification by NEM. Whole cells were incubated with AMS (**A**), NEM (**N**) or AMS in the presence of SDS (**AS**) for various times (numbers above the figure indicate incubating-time in minutes) at room temperature. Excess prelabel reagent was removed (except for the AS sample), cells were solubilised and labeled with PEGmal for one hour. The minus (**-**) sample was directly labeled by PEGmal. The label reactions were interpreted by semi-dry western blotting of a 15% SDS polyacrylamide gel and detection of SoxY protein with anti-HA antibodies. Per lane 4 µg of total cell protein was applied.

The labeling results of cells overproducing $DcuB_{C12345S}$-$PhoA_{C1234S}$ and HA-SoxY indicate that PEGmal is highly specific for sulphydryl groups. No modification of the Cys-less DcuB-PhoA protein was observed. No second protein band in the only PEGmal-treated control (-) was identified on the immunoblot (Fig. R13A). After incubation with anti-HA the same sample shows a clear band of alkylated SoxY protein at 28 kDa, demonstrating the high reactivity of PEGmal in the presence of a sulphydryl group.

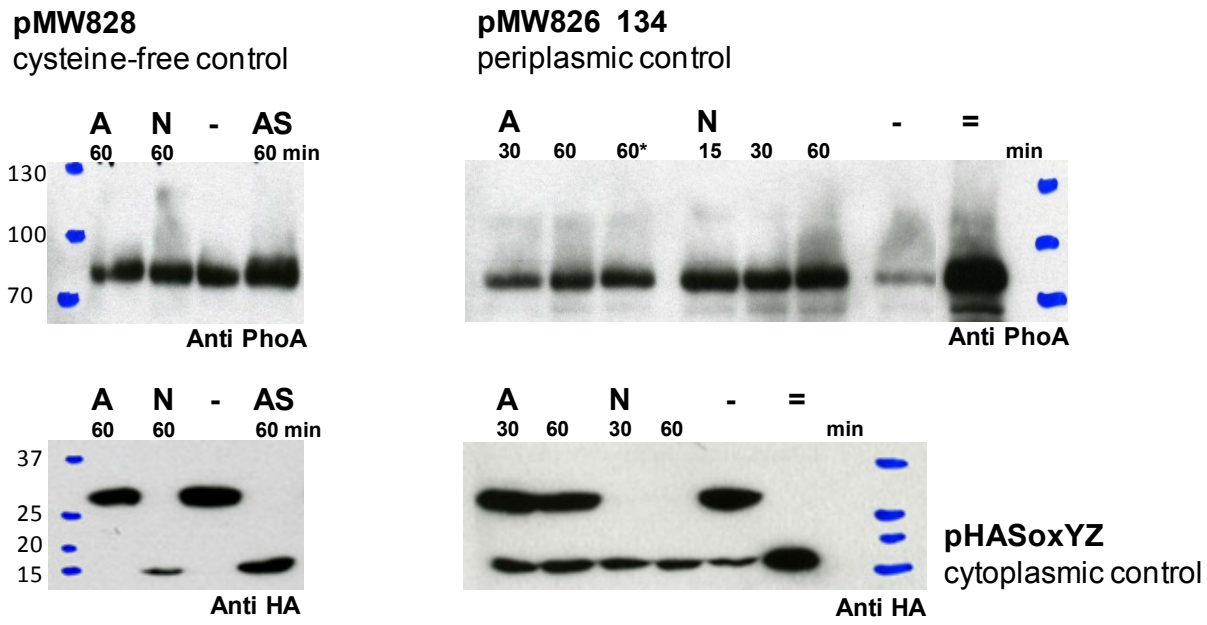

Figure R13: Sulphydryl labeling of *E. coli* C43DE3 pMW282 pHASoxYZ and C43DE3 pMW826 134 pHASoxYZ. Whole cells coexpressing cysteine-less DcuB-PhoA or $DcuB_{C12345S}$-$PhoA_{C134S}$ with the cytoplasmic protein SoxY were labeled with AMS (A) or NEM (N) in the absence of detergent. After prelabeling excessive label reagent was removed and cells were solubilised in SDS containing buffer and incubated with PEGmal for one hour. **A**, AMS prelabeled cells; **N**, NEM prelabeled cells; (-), no prelabel; (=), unlabeled sample; **AS**, cells prelabeled with AMS in the presence of SDS. Numbers give the time (min) of prelabeling at room temperature or 37°C (asterisk*). The labeling experiments were analyzed by 15% SDS-PAGE and immunoblotting with anti-PhoA and anti-HA antibodies. For detection with anti-HA 4µg of total cell protein was loaded per lane; SDS-PAGE for anti-PhoA detection was performed with 10µg per lane. **(A) Cysteine-specifity of PEGmal. (B) AMS accessibility to the periplasmic region.**

The periplasmic Cys residue of $DcuB_{C12345S}$-$PhoA_{C134S}$ (Fig. R13B) is highly accessible to AMS and NEM already in the absence of detergent. AMS and NEM pre-treated cells as well as the unlabeled sample (=) showed a single band at the position of unmodified protein. The PEGmal sample (-) of *E. coli* C43DE3 pMW826 134 pHASoxYZ showed a weak protein band at the position of unmodified protein and a weak and blurred band above as a consequence of PEGmal treatment. Although the same amount of protein is present (compare the identical sample incubated with anti-HA antibodies) no clear protein shift can be detected in the PEGmal sample after anti-PhoA incubation.

Modification of DcuB by PEGmal and to a lower extent by AMS and NEM often resulted in a decreased intensity of the corresponding protein band on the immunoblot. A reason for this observation could be a reduced blotting efficiency of the alkylated protein and, in the case of PEGmal, the heterogeneity in molecular size (Maegawa *et al.,* 2007). A decreased reactivity

with the anti-PhoA antibodies as a consequence of DcuB modification can also not be excluded. Although a quantitative detection of the labeled protein fractions was not possible, modification by PEGmal could be identified by a decreased amount of the band corresponding to the unmodified protein.

AMS accessible residues of DcuB

Nearly all positions within DcuB were accessible to the hydrophobic NEM already in the absence of detergent. Regarding the AMS accessibility, we can differ between two reactivity groups. In the following section residues of DcuB are presented which are fully or partly blocked by AMS. Due to the complex properties of protein with many transmembrane helices (low stability, reduced transfer efficiency, diverse running performance) the interpretation of the labeling experiments was mainly worked out by direct comparison of the four different protein fractions of a culture, which were all prepared at the same day under comparable conditions.

Periplasmic residues K46, R167 and S261 of DcuB (Fig. R14, shown in green) were well modifiable by AMS, resulting in a single strong protein band at the position of unmodified protein (~85 kDa) as shown for the unlabeled protein fraction (=) and the NEM pre-labeled sample. The lanes of PEGmal alkylated samples (-) on the other hand were characterized by a blurred shifted band (about 90-115 kDa) (K46C, S261C) while the intensity of the band at the size of unmodified protein was strongly reduced or even vanished (R167C).

The immunoblots of DcuB-PhoA mutants with single Cys substitutions at the supposed membrane-integral positions N125 and S357 as well as cytoplasmic positions S135, G138 and E217 also demonstrate complete alkylation by AMS. In all cases, the lanes containing AMS pre-labeled, NEM pre-labeled and unmodified protein showed a nearly identical pattern, whereas the PEGmal labeled fraction was distinguished by a band shift to higher sizes. The PEGmal labeled sample of DcuB N125C looked different. Two bands with the size of ~90 kDa and ~115 kDa could be identified. It can be speculated that these protein bands represent the successfully blotted DcuB-PhoA after PEGmal alkylation, and a degradation product of the sample. This is suggested by the observation, that the corresponding band was never found in unlabeled samples. The same clear pattern was also observed in the PEGmal labeled and AMS pre-labeled fractions of R19C, K87C and E299C (Fig. R16). An additional band

shifted in the opposite direction was observed in a few PEGmal labeled samples (S357C, D375C, C386, R414 and others), suggesting the formation of degradation products.

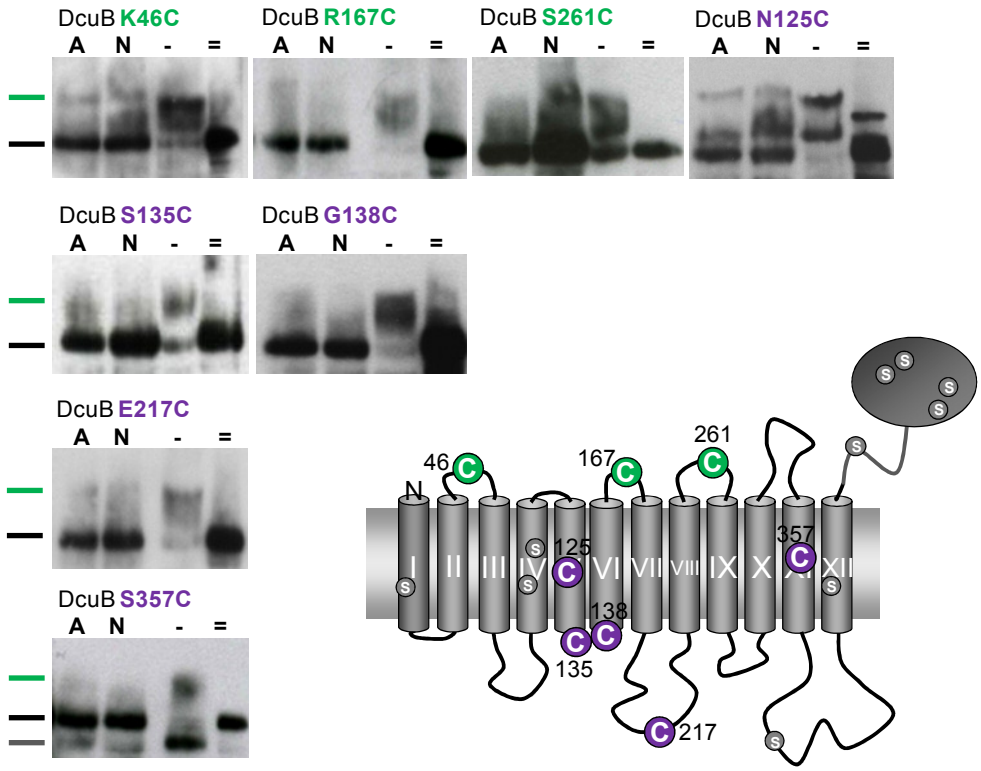

Figure R14: Slightly/Well AMS accessible residues of DcuB. **(A) Sulphydryl labeling of *E. coli* C43DE3** overproducing single cysteine variants of DcuB-PhoA and cytoplasmic SoxY was performed as follows. Whole cells were first incubated with AMS (**A**), NEM (**N**) or without any reagent, (-) and (=) sample. The cells were freed from excessive prelabel and solubilised by adding SDS. All protein solutions except (=) were labeled with PEGmal and analyzed by 15% SDS-PAGE (10µg of total cell protein per lane) and immunoblotting with anti-PhoA. The size of detected protein bands is marked on the left: green line, ~115 kDa; black line, ~85 kDa; grey line, ~70 kDa. **(B) The topology model of DcuB** illustrates the putative positions of the substituted amino acid residues within the protein. Residues that are located in the cytoplasm or within the membrane are shown in purple, periplasmic residues in green.

The DcuB-PhoA fusion protein in general exhibited low stability resulting in a number of protein fragments of different sizes smaller than 85 kDa. The main band of unmodified DcuB-PhoA at 85 kDa sometimes came along with a thin and clearly defined band at about 100 kDa (N125C, E204, L446 and others). This size corresponds to the real mass of DcuB-PhoA indicating that the main band could be a degradation product as well. However, this defined band was well specifiable and was not detected in the labeled protein fractions. The control samples with unmodified DcuB-PhoA often showed a much stronger protein band on the

immunoblot than the alkylated protein fractions underlining the declined transfer efficiency of modified DcuB-PhoA during western-blotting. The protein transfer was not improved by changing the blotting conditions (nitrocellulose membrane/PVDF membrane, Tris-glycine/Carbonatebuffer; semi-dry/wet-blot; different blotting times).

Other supposedly cytoplasmic residues of DcuB, like E204, S211, D222 and D357 (Fig. R15) were mostly accessible for AMS, showing only a weak blurred band at the size of PEGmal alkylated protein (90-115 kDa) while intensity of the band of unmodified DcuB-PhoA at ~85 kDa was nearly the same as in the NEM pre-labeled sample. In addition, the predicted membrane integral residue S146 seemed to be at least partly AMS accessible.

To prove that AMS accessibility of cytoplasmic or membrane-integrated Cys residues was not a consequence of cell lysis a second SDS-gel was ran simultaneously and checked by anti-HA antibodies. In all anti-HA immunoblots (compare Fig. R12 and R13), no difference between the AMS pre-labeled and the PEGmal labeled fraction was detectable, indicating that the cell integrity was not affected and that AMS was not able to pass the membrane (data not shown). In intact cells the cysteine residues of cytoplasmic proteins (as shown for SoxY in Fig. R12 and R13) did not react with membrane-impermeable AMS. Several cytoplasmically localized cysteins residues of DcuB were clearly accessible for the charged maleimide. This can be explained by assuming that AMS is able to get into the membrane-spanning transport channel of DcuB which is probably sealed by amino acid residues of cytoplasmic loops. Since reaction of maleimides with sulphydryl groups were catalyzed by water, the labeling results of DcuB N125C, S146C and D357C strongly suggest the existence of a water-filled transmembrane channel comprising the predicted hydrophilic helix V, helix VI and helix IX.

DcuB-PhoA variants with single Cys residues on the position of the periplasmic residues T163, K338 and L446 were modifiable by AMS as well. Also the N-terminus of DcuB-PhoA was shown to be partly AMS accessible, indicating that the N-terminus is located in or near the periplasm.

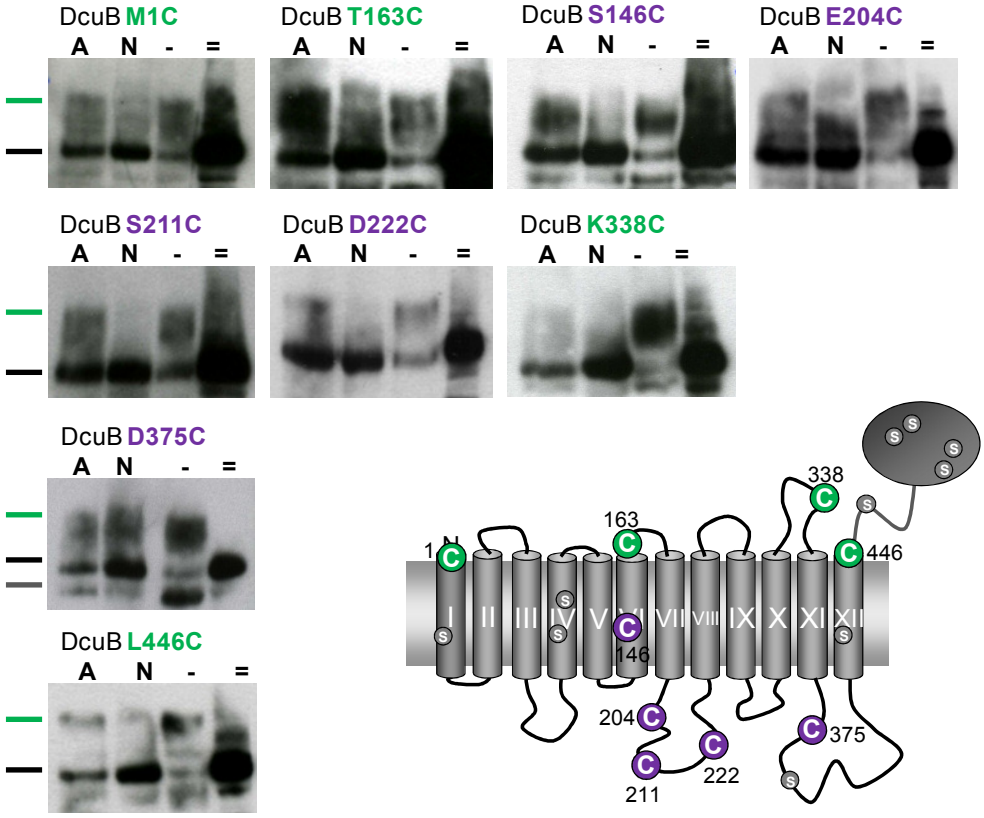

Figure R15: Partly/Mostly AMS accessible residues of DcuB. Whole cells coexpressing DcuB-PhoA containing a single periplasmic (green) or a non-periplasmic (purple) cysteine residue and the cytoplasmic protein SoxY were prelabeled by AMS (**A**) or NEM (**N**), washed, solubilised and incubated with PEGmal for one hour. Lanes marked by minus (**-**) contain non-prelabeled protein samples; lanes with equals sign (=) show protein bands of completely unlabeled samples. The size of detected protein bands is marked as follows: green line, ~115 kDa; black line, ~85 kDa; grey line, ~70 kDa. Sulphydryl labeling was analyzed by 15% SDS-PAGE and immunoblotting with anti-PhoA.

AMS non-accessible residues of DcuB

A series of putative cytoplasmic and membrane-integrated residues of DcuB was not blocked by AMS in the absence of SDS. The positions of DcuB residues C13, R19, G21, R79, K87, S90, Y118, K230, E299, C386, R414 and C433 (Fig. R16) were clearly not accessible to AMS, but could be modified by the membrane-permeable NEM. The physiological cysteine residue on position 98 as well as C104 (data not shown) and T112 were only partly accessible for NEM, indicating a position buried deep within the membrane or shielded by other residues.

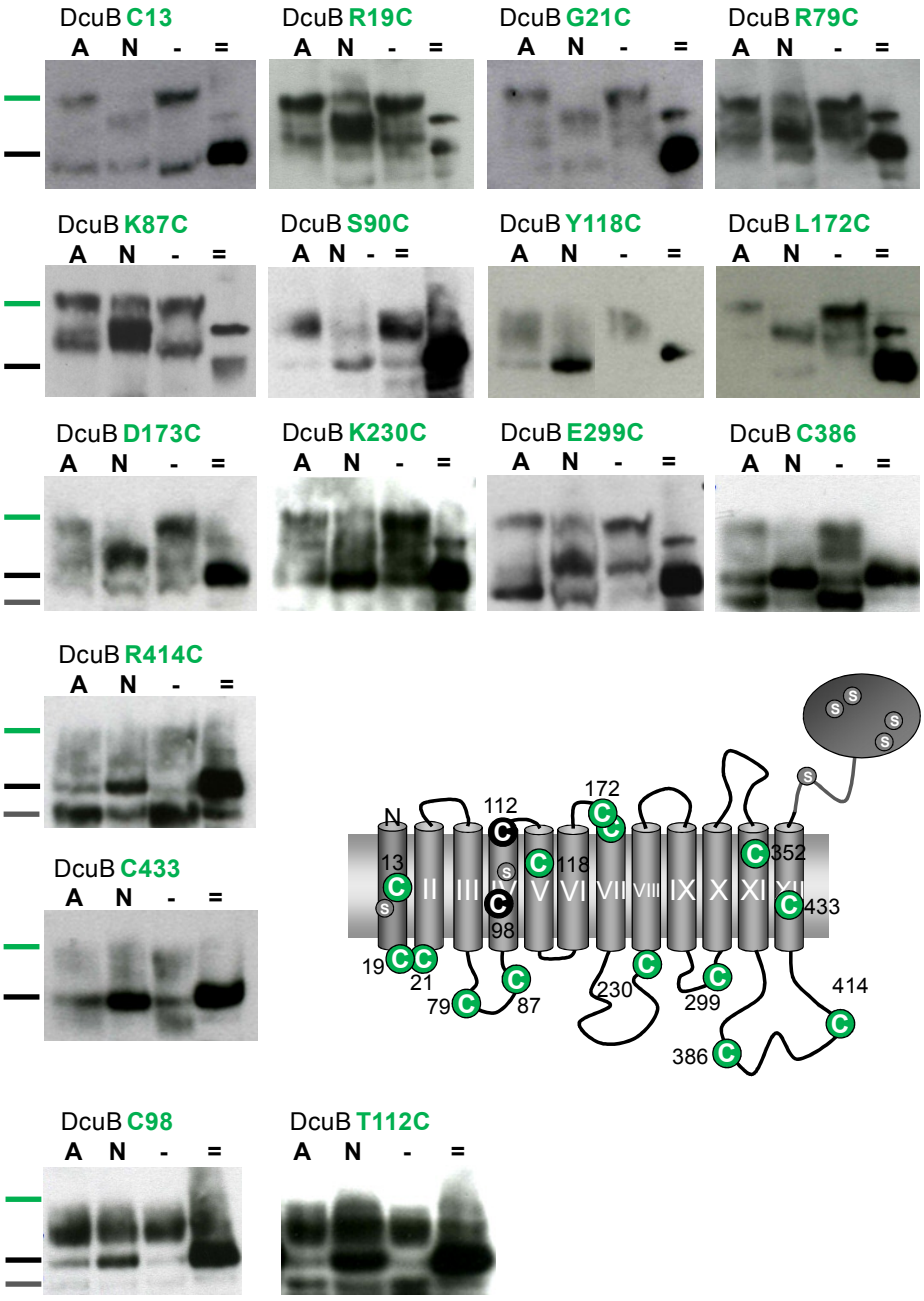

Figure R16: Amino acid residues of DcuB that are not accessible for the membrane-impermeable label reagent AMS. Whole cells coexpressing a single cysteine variant of DcuB-PhoA and the cytoplasmic protein SoxY were prelabeled with AMS (**A**) or NEM (**N**), washed, solubilised and incubated with PEGmal for one hour. The minus (**-**) samples were only labeled by PEGmal, the equals (=) samples were not labeled at all. The size of detected protein bands is marked as follows: green line, ~115 kDa; black line, ~85 kDa; grey line, ~70 kDa. The DcuB-PhoA fusion protein was detected by 15% SDS-PAGE followed by immunoblotting with anti-PhoA antibodies. The localization of the non-accessible cysteine of DcuB is presented in the model. Residues that were not accessible for NEM are shown in black.

4.3 The cysteine residues of DcuB

In transport assays, a sensitivity of the anaerobic C_4-dicarboxylate transport system to oxygen and other oxidizing substances like Nitrate and hexacyanoferrat(III) was observed (Engel *et al.*, 1992). The inhibition was reversed by incubation with reducing agents, suggesting a role of cysteine residues during posttranscriptional inactivation. Since DcuB is the most active carrier during anaerobic growth on C_4-dicarboxylates, the effect of oxygen and nitrate on the transport activity of DcuB was investigated by transport measurements. In addition, a Cys-less DcuB protein was generated and tested for uptake and regulatory properties as well as for oxygen- and nitrate-based inactivation.

All experiments were performed with the low-copy plasmid pMW228, that encodes *dcuB* with own promoter. By site-directed mutagenesis cysteine variants of the *dcuB* gene were created. DcuB possesses five cysteine residues, C13, C98, C104, C387 and C433, hereafter referred to as C1, C2, C3, C4 and C5. The cysteine residues were deleted step by step and replaced by a serine residue. In this way Cys single, double and finally the fivefold mutations of DcuB (DcuB-C12345S; pMW737) were obtained.

Anaerobic growth on glycerol plus fumarate was tested as an indicator for functional fumarate transport. The mutated *dcuB* genes were supplied on the low copy plasmid (Fig. R17). In strain IMW505 pMW228 the plasmid encoded *dcuB* mediates wild type-typical growth. The DcuB Cys single (DcuB-C1S, DcuB-C4S and DcuB-C5S), double (DcuB-C23S and DcuB-C45S) and triple muntants (DcuB-C123S) supported anaerobic growth with rates and yields very similar to DcuB. The quadruple mutant DcuB-C1235S showed growth as the wild type DcuB. The quadruple mutant C2345S and the fivefold mutant DcuB-C12345 (pMW737) were impaired in growth, but both strains achieved the same optical density as wild type DcuB after prolonged incubation. Thus the five-fold mutant is able to grow on glycerol plus fumarate and the impaired growth cannot be attributed to one particular residue. Overall, the experiments show that none of the cysteine residues is essential, but some of the multiple mutants render the strain less efficient for anaerobic growth on fumarate. Determination of *dcuB´-´lacZ* expression showed that all DcuB mutants maintained full regulatory activity.

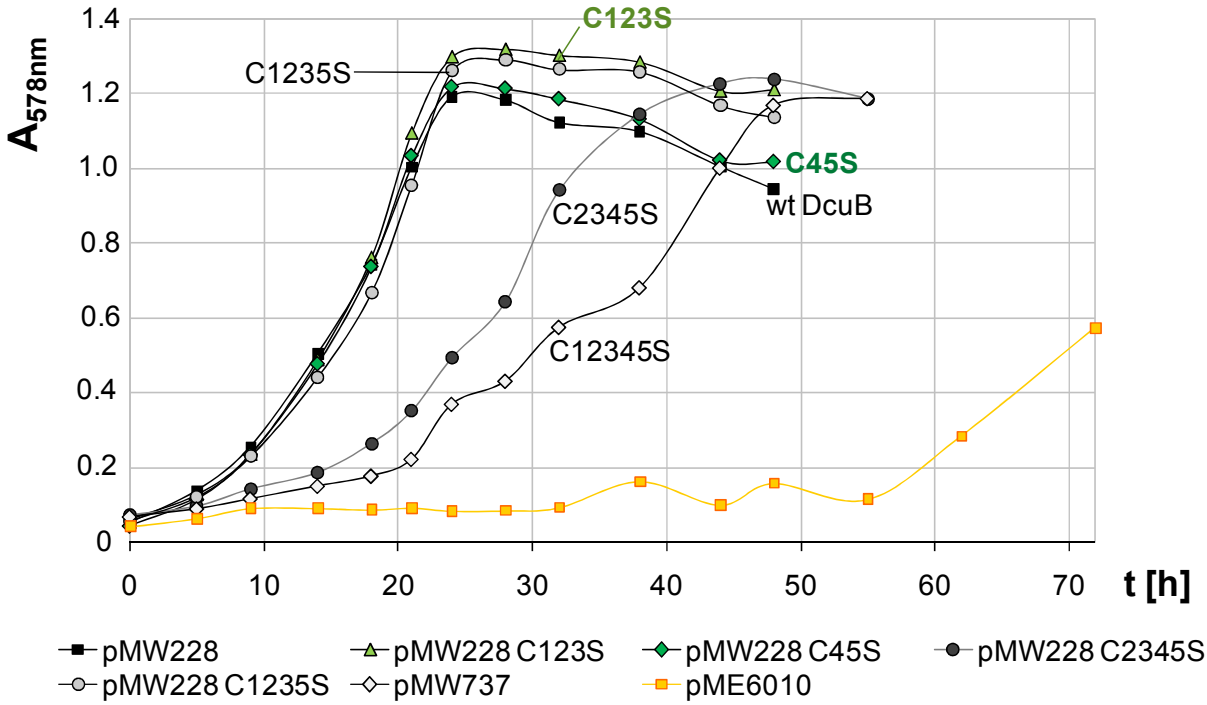

Figure R17: Anaerobic growth on fumarate mediated by DcuB cysteine-mutants. *E. coli* IMW505 (*dcuA dcuB dcuC*) containing the low-copy vector pME6010 and pME6010 derivatives encoding *dcuB* or *dcuB* cysteine-mutants was grown anaerobically in eM9 medium plus glycerol and fumarate. All DcuB proteins were expressed under the control of the *dcuB*-Promotor. The diagram shows the growth curves of *E. coli* IMW505 with plasmid pME6010 (plasmid without *dcuB*), plasmid pMW228 (*dcuB*) and plasmids encoding DcuB (C123S), DcuB (C45S), DcuB (C2345S), DcuB (C1235S) or DcuB (C12345S) (pMW737).

For transport measurements cells were grown under *dcuB*-inducing conditions in enriched M9 medium supplemented with glycerol, DMSO and fumarate. Exponentially growing bacteria were harvested and an anaerobic cell suspension was prepared which was incubated in the absence or presence of 100 mM sodium nitrate. Prior to the transport assays, cells were energized by adding glucose. The initial uptake-rate v_0 of ^{14}C-succinate was determined.

The strain with wild type DcuB showed an uptake rate of 9.2 U/g DW for ^{14}C-succinate compared to the *dcuB* deletion strain with 1.8 U/g DW. The strain with the DcuB mutants DcuB-C123S and DcuB-C45S showed an uptake rate of at least 8.5 and 7 U/g DW. Similar to the growth rates, the transport activities for most of the double and triple Cys mutants of DcuB were only slightly decreased. The quadruple mutant DcuB-C1235S showed an uptake rate of 9.2 U/g DW, equal to wild type DcuB. In the Cys-less mutant DcuB-C12345S and the second quadruple mutant DcuB-C2345S the transport activity decreased to approximately 4.7 U/g DW, representing still 51% of the wild type activity. Therefore replacing the Cys residues in DcuB by Ser residues has only a relatively small effect on transport activity.

The presence of nitrate in the incubation buffer resulted in a strong decrease of transport activity. In the presence of 100 mM sodium nitrate, uptake of succinate decreased to rates below 1.8 U/g DW for the strain with wild type DcuB and the DcuB-C123S, DcuB-C45S, DcuB-C2345S or DcuB-C12345S mutants (Fig. R18). Surprisingly, also the strain devoid of DcuB pMW6010 IMW505 and the strain with the Cys-less mutant DcuB C12345S showed a nitrate-effect and transport activity decreased to very low levels. Therefore the nitrate-effect appears to be independent of DcuB and of the Cys residues in DcuB. Incubation with 50 mM sodium nitrate had only a small effect on succinate uptake. It is concluded that the effect is caused by the salt concentration but not by oxidation via nitrate. When the anaerobic cell suspension was incubated with 100 mM magnesium sulfate or magnesium chloride or sodium chloride strong inhibition of transport was observed as well (Fig. R19). On the other hand, when a cell suspension was stirred vigorously in air, the transport activity was the same as for the anaerobic bacteria, or even higher. The results show that oxygen has no inhibitory effect. High salt concentrations on the other hand strongly inhibit succinate uptake in *E. coli.*

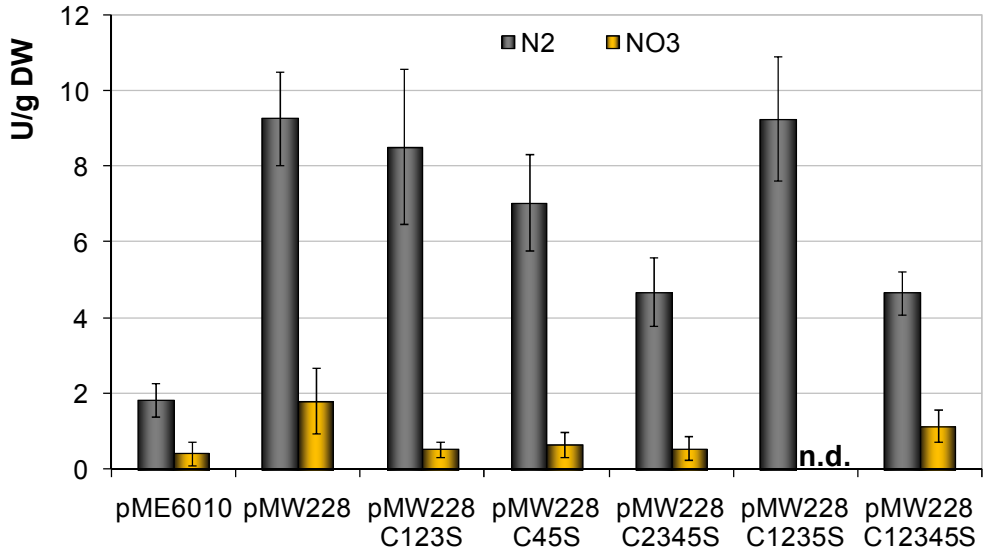

Figure R18: ^{14}C-succinate uptake-rate of DcuB cysteine mutants. Transport assays were performed with *E. coli* IMW505 (*dcuA dcuB dcuC*) complemented with plasmid-encoded *dcuB* and *dcuB* cysteine mutants after anaerobically growth in eM9 medium supplemented with glycerol, DMSO and fumarate. ^{14}C-succinate uptake was determined in exponentially growing cultures and, prior to the transport measurements, cells were incubated in the presence or absence of sodium nitrate in degassed infusion bottles. The *dcuB* genes were localized on the low-copy vector pME6010 and expressed under the control of the *dcuB* promotor. Transport assays of IMW505 with plasmid pME6010 (without *dcuB* gene), plasmid pMW228 coding for wild type DcuB and plasmids coding for DcuB-C123S, DcuB-C45S, DcuB-C2345S, DcuB-C1234S and DcuB-C12345S (pMW737) were analyzed. n.d., not determined.

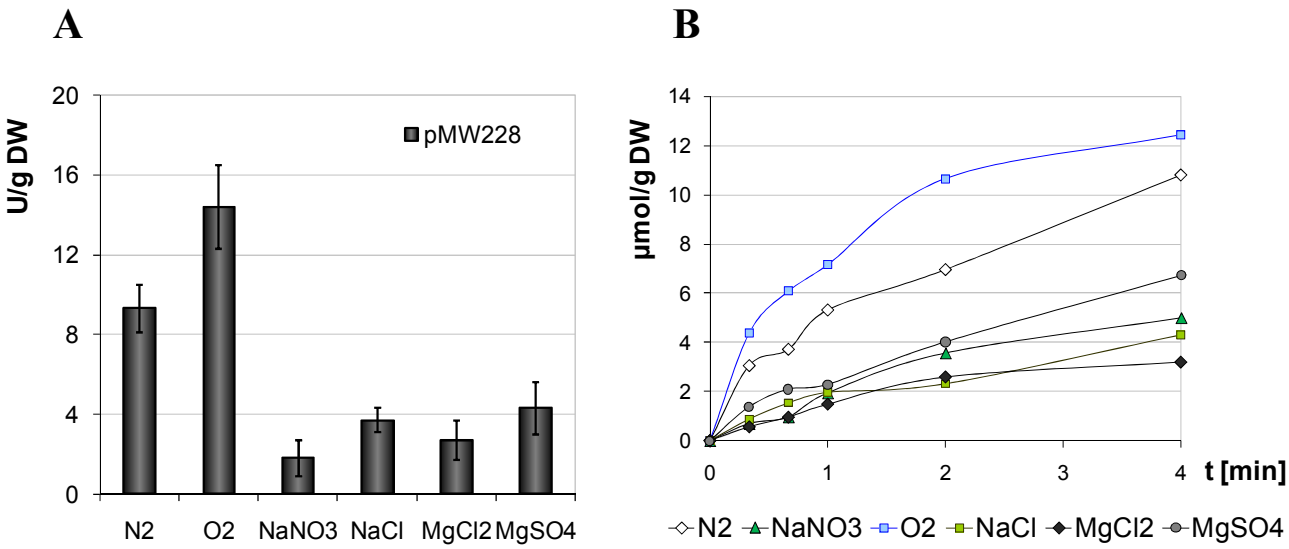

Figure R19: Salt-effect on C_4-dicarboxylate transport catalized by DcuB. The uptake of ^{14}C-succinate in *E. coli* IMW505 (*dcuA dcuB dcuC*) carrying plasmid-encoded wild type *dcuB* (pMW228) was measured. Cells were cultivated anaerobically in eM9 medium with glycerol, DMSO and fumarate to an optical density of about 0.8, corresponding to the exponential growth phase. Prior to the transport assays, cells were incubated for at least one hour anaerobically under nitrogen-atmosphere with 100mM sodium nitrate, sodium chloride, magnesium chloride, magnesium sulfate or without additional salt, respectively. One aliquot was stirred in air (O_2-sample). The diagrams show the initial uptake activity in Units per gram dry weight (**A**) and uptake of ^{14}C-succinate in µmol per gram dry weight against time (**B**)

4.4 Function of DcuB in transport and regulation

The fumarate/succinate antiporter DcuB is the most important carrier during growth by fumarate respiration. In *E. coli*, expression of *dcuB* is stimulated by the C_4-dicarboxylate-sensing two-component system DcuSR in the presence of C_4-dicarboxylates under anaerobic conditions (Zientz *et al.*, 1998). The carrier also affects the function of the DcuS-DcuR two-component system and acts as a second site for anaerobic C_4-dicarboxylate sensing: Deletion of the antiporter causes constitutive expression of the DcuSR-dependent genes in the absence of C_4-dicarboxylates. By random and site-directed mutagenesis several amino acid residues of DcuB were identified which are essential for transport or regulation (Fig. R20). Therefore DcuB is a bifunctional protein with independent sites for transport and regulation (Kleefeld *et al.,* 2009).

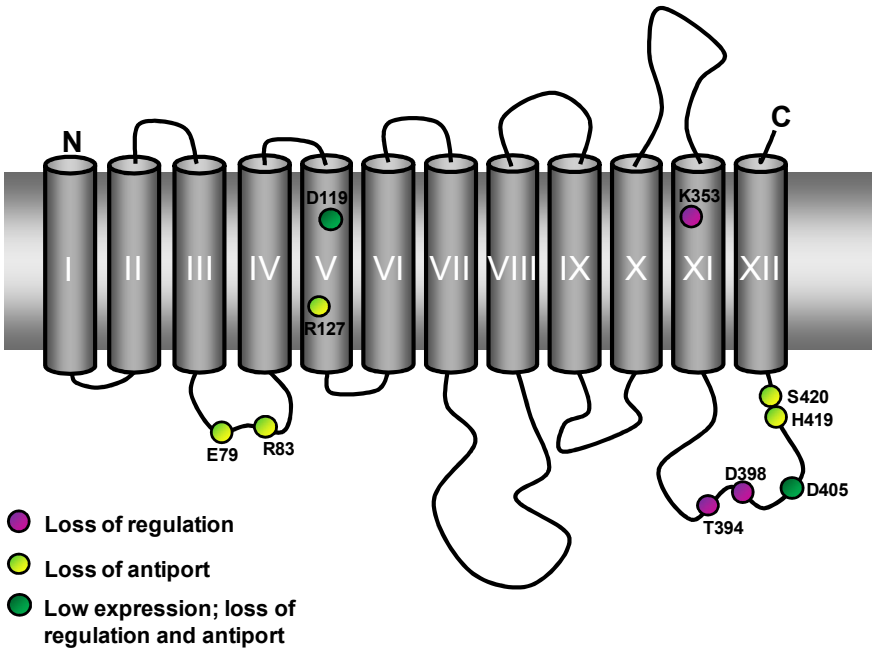

Figure R20: Essential amino acid residues of DcuB. The localisation of highly conserved residues which are essential for transport (light green) or sensory function (purple) is shown by using the topology model of DcuB based on DcuB-LacZ/ PhoA expression studies. Substitution of the amino acid residues D119 and D405 (dark green) led to a complete loss of DcuB function.

Regulatory mutants of DcuB

Three regulation relevant amino acid residues of DcuB are known: threonine 394, aspartate 398 and lysine 353 (Kleefeld *et al*., 2009). Substitution of DcuB T349 by isoleucine or alanine led to an effector-independent expression of *dcuB´-´lacZ* similar to *dcuB*-deletion strain (Tab. R4). The same effect was observed with DcuB D398N and DcuB K353A. The amino acid substitutions DcuB T394N/S and DcuB D398A/E had no effect on the expression controlled by the DcuSR two-component system.

Transport deficient mutants of DcuB

Substitution of the glutamate residue DcuB E79 by alanine (A), lysine (K) and glutamine (Q) resulted in strongly impaired growth on glycerol plus fumarate under anaerobic conditions and a loss of ^{14}C-succinate uptake (Tab. R5). The mutant DcuB E79D was not tested by now. Similar, DcuB R83A and DcuB K83Q showed a highly limited transport function. This loss of function was related to the loss of positive charge: DcuB R83K could fully complement DcuB function in a *dcuB* deficient strain. The charge of the aspartate residue R127 is also relevant for DcuB function; substitution by lysine had no effect, whereas exchange by alanine or glutamine caused a loss of transport function. *E. coli* IMW505 (*dcuA dcuB dcuC*) carrying

plasmid-encoded DcuB R127A was not able to grow on glycerol plus fumarate in the absence of oxygen. However, the succinate uptake of this mutant was comparable to the wild type, pointing to a loss of antiport. The histidine residue on position 419 and serine 420 were also important for at least antiport of C_4-dicarboxylates. Mutants DcuB H419A/F/Y no longer mediate anaerobic growth on glycerol and fumarate while still showing ^{14}C-succinate uptake-activity. The *dcuA dcuB dcuC*-deficient strain IMW505 with plasmid encoded DcuB S420C showed no growth on fumarate. Succinate-uptake activity of the strain was not measured by now.

In addition to the regulatory and transport deficient mutants, two amino acid residues of DcuB were identified whose replacement caused a complete loss of DcuB function in transport and regulation. Substitution of DcuB D119 by alanine or valine resulted in DcuB proteins which were not able to catalize transport of C_4-dicarboxylates and which showed no regulatory effect on DcuSR-dependant gene expression. No differences between DcuB and DcuB D119N activity were observed. Also a complete loss of DcuB function was found with DcuB D405A/V/N/E. It has to be verified if these fully-deficient DcuB mutants are generated in *E. coli* and if they were integrated within the inner membrane.

Table R4: Mutants of DcuB affecting expression of DcuSR-dependent genes while retaining transport function. Experiments were performed by A. Kleefeld and *B. Ackermann (Kleefeld *et al*., 2009) with *E. coli* IMW505 (*dcuA dcuB dcuC*) carrying plasmid-coded DcuB as indicated. Anaerobic growth was measured in eM9 medium with glycerol and fumarate. I, growth rate similar to strain with wild type *dcuB* (t_d = 3-5 h); III, no growth (t_d = 7-12 h). Transport activities (^{14}C-succinate uptake) were determined in anaerobic cell suspensions of exponentially grown cultures, ß-galactosidase activities in exponentially growing cultures without and with fumarate. Values comparable to the *dcuB*-delition strain are shown in bold letters.

Type of DcuB coded on pME6010	**Antiport** anaerobic Growth on glyc/fum	**Uptake** of ^{14}C-succinate [U/g DW]	**Regulation** expression of *dcuB´-´lacZ* [MU] **glycerol, DMSO**	**plus fumarate**
-	**III**	**0.9 ± 0.1**	**131 ± 31**	**125 ± 15**
DcuB wt	I	3.5 ± 0.4	12 ± 4	119 ± 10
*DcuB K383A	I	n.d.	**383 ± 133**	**281 ± 51**
DcuB T394I	I	3.9 ± 1.4	**262 ± 51**	**221 ± 38**
DcuB T394N	I	3.7 ± 0.9	33 ± 9	278 ± 16
DcuB T394S	I	3.9 ± 1.2	21 ± 6	282 ± 57
DcuB T394A	I	2.9 ± 0.8	87 ± 26	263 ± 49
DcuB D398N	I	4.0 ± 0.5	**372 ± 77**	**227 ± 45**
DcuB D398A	I	4.1 ± 0.6	17 ± 3	125 ± 6
DcuB D398E	I	2.1 ± 0.6	17 ± 1	104 ± 1

Table R5: Transport-deficient mutants of DcuB. Experiments were performed by B. Ackermann (Kleefeld *et al*., 2009) and *in this study. *E. coli* IMW505 (*dcuA dcuB dcuC*) with plasmid-coded DcuB was grown anaerobically in eM9 medium with glycerol and fumarate. I, growth rate similar to strain with wild type *dcuB* (t_d = 3-5 h); II, slowed and constricted growth (t_d = 5-6 h); III, no growth (t_d = 7-12 h). Uptake of ^{14}C-succinate and ß-galactosidase activities were determined as described in the legend to Tab. R4. Values comparable to the *dcuB*-delition strain are shown in bold letters.

Type of DcuB coded on pME6010	**Antiport** anaerobic Growth on glyc/fum	**Uptake** of ^{14}C-succinate [U/g DW]	**Regulation** expression of *dcuB´-´lacZ* [MU] **glycerol, DMSO**	**plus fumarate**
-	**III**	**0.9 ± 0.6**	**552 ± 82**	**550 ± 126**
DcuB wt	I	5.8 ± 2.3	20 ± 6	321 ± 61
DcuB E79A	**II**	**0.9 ± 0.5**	2 ± 1	415 ± 26
DcuB E79K	**III**	n.d.	n.d.	n.d.
DcuB E79Q	**III**	n.d.	n.d.	n.d.
DcuB K83A	**II**	**1.6 ± 0.5**	2 ± 1	409 ± 45
DcuB K83K	I	n.d.	n.d.	n.d.
DcuB K83Q	**II**	n.d.	n.d.	n.d.
DcuB D119A	**III**	**0.8 ± 0.5**	**168 ± 25**	**393 ± 35**
DcuB D119N	I	n.d.	n.d.	n.d.
DcuB D119V	**III**	n.d.	n.d.	n.d.
DcuB R127A	**III**	**5.7 ± 1.1**	**45 ± 5**	**418 ± 55**
DcuB R127K	I	n.d.	n.d.	n.d.
DcuB R127Q	**III**	n.d.	n.d.	n.d.
DcuB D405A	**III**	**1.5 ± 0.6**	**224 ± 77**	**295 ± 52**
DcuB D405N	**III**	n.d.	n.d.	n.d.
DcuB D405E	**III**	n.d.	n.d.	n.d.
DcuB D405V	**III**	n.d.	n.d.	n.d.
DcuB H419A	**II**	6.2 ± 2.4	56 ± 2	329 ± 47
DcuB H419F	**III**	n.d.	n.d.	n.d.
DcuB H419Y	**III**	n.d.	n.d.	n.d.
*DcuB S420C	**III**	n.d.	36 ± 9	324 ± 36

4.4.1 Expression of alternative DcuB carriers in *Escherichia coli*

The ability of fumarate respiration is widely distributed among bacteria and DcuB-like proteins exist in many *E. coli*-related organisms (Fig. R21). Although expression of *E. coli dcuB* depends on DcuSR, some *dcuB*-containing bacteria do not possess DcuSR-like proteins. With the following experiments we determined if alternative DcuB carriers are able to compensate DcuB deletion in *E. coli*.

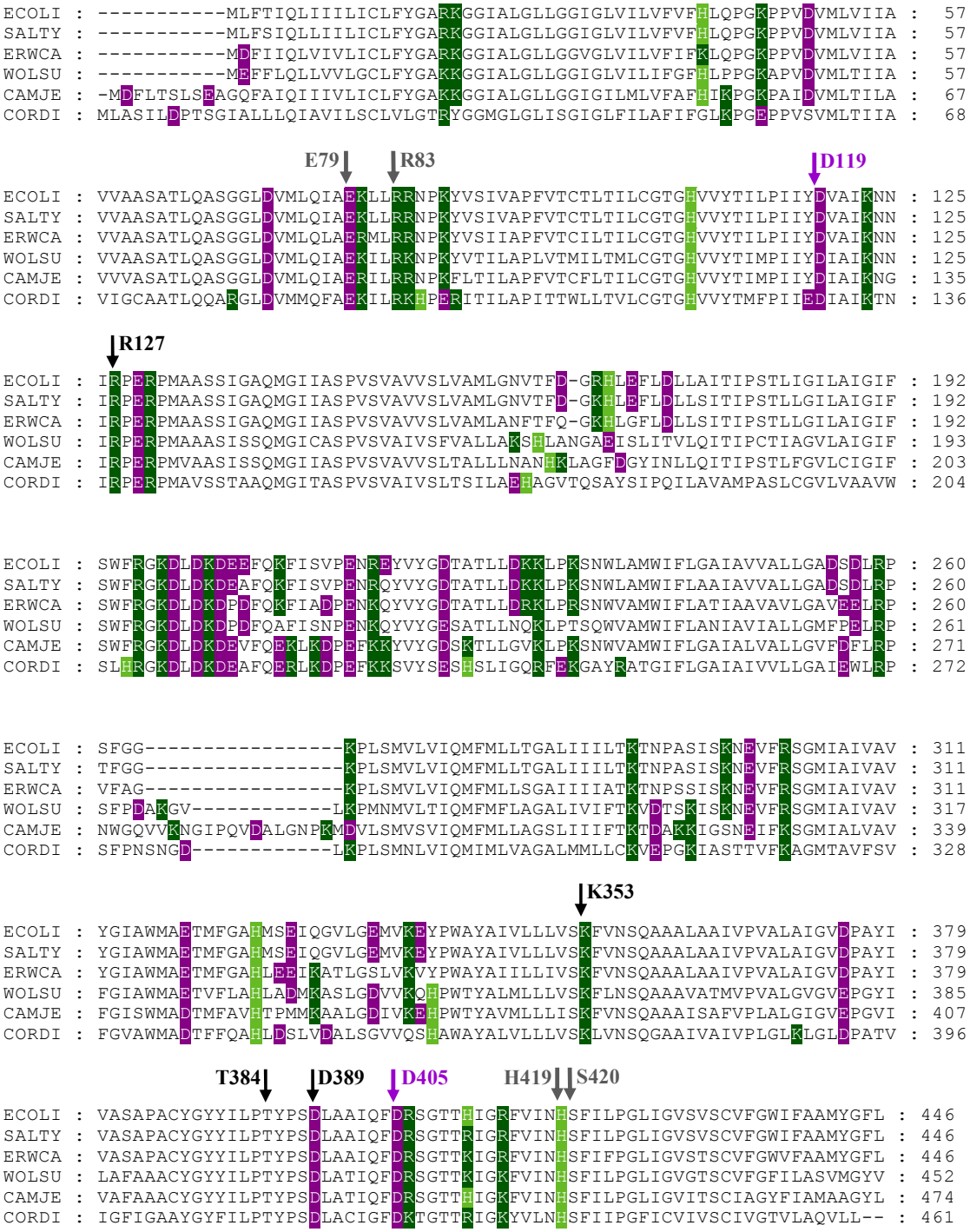

Figure R21: Sequence alignement of DcuB proteins of *Escherichia coli (Ecoli), Salmonella typhimurium (Salty), Erwinia carotovora (Erwca), Wolinella succinogenes (Wolsu), Campylobacter jejunii (Camje) and Corynebacterium diphtheria (Cordi)* Basic residues (Arg, Lys, His) are labeled by green, acidic residues (Asp, Glu) by purple backround. Highly conserved amino acid residues which are essential for either transport or regulatory function in *E. coli* are marked by arrows and numbered according to their position. Grey arrows highlight transport-relevant residues; black arrows show residues that are involved in sensing. Amino acid residues which lead to a complete loss of function if substituted are marked by purple arrows.

For the studies of DcuB function the *dcuB* genes of the γ-proteobacteria *E. coli, Salmonella typhimurium, Erwinia carotovora*, the ε-proteobacteria *Wolinella succinogenes* and *Campylobacter jejunii* and the gram positive *Corynebacterium diphtheria* were cloned into the arabinose-inducible vector pBAD18-Kan*. The resulting expression plasmids were used for transformation of the *dcuA dcuB dcuC*- deficient *E. coli* strain IMW505 and tested for functionality. All DcuB proteins show a sequence identity of at least 54% and the amino acid residues which are essential for DcuB function in transport and sensing in *E. coli* are conserved within all sequences (Fig. R21).

To verify transport activity of the alternative DcuB proteins, the plasmid-containing *E. coli* strains were cultivated anaerobically with glycerol as a carbon source and fumarate as sole electron acceptor. Growth indicates expression of a functional transporter, which catalizes fumarate/ succinate antiport. For optimal gene expression, growth experiments were performed with different concentrations of the inducer, in the range from 1 µM to 1000 µM arabinose. For induction of *dcuB* expression, 100 µM arabinose was found to give the best growth results.

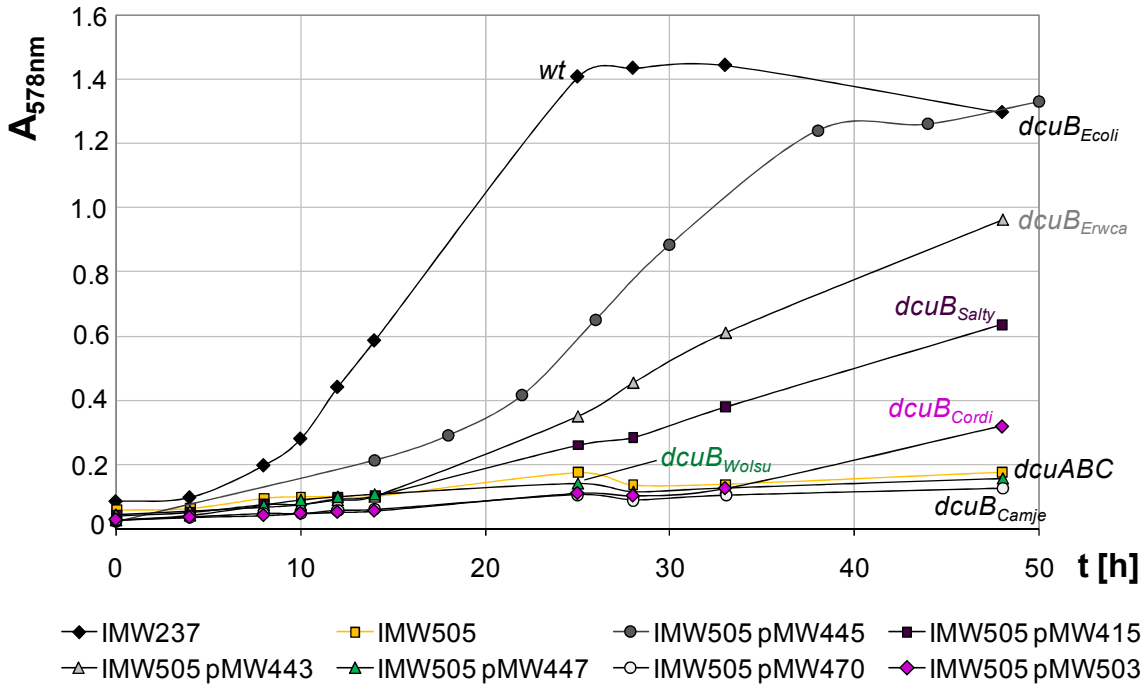

Figure R22: Anaerobic growth of E. coli IMW505 (*dcuA dcuB dcuC*) complemented with plasmid-encoded *dcuB* of related bacteria. The diagram shows growth of *E. coli* wildtype IMW237 and *dcuA dcuB dcuC*-negative strain IMW505 with and without plasmid-encoded DcuB from *Escherichia coli* (*Ecoli*, pMW445), *Salmonella typhimurium* (*Salty*, pMW415), *Erwinia Carotovora* (*Erwca*, pMW443), *Wolinella succinogenes* (*Wolsu*, pMW447), *Campylobacter jejunii* (*Camje*, pMW470) and *Corynebacterium diphtheria* (*Cordi*, pMW503). Strains were cultivated anaerobically in eM9 medium with glycerol as a carbon source and fumarate as sole electron acceptor.

E. coli IMW505 (*dcuA dcuB dcuC*) is not able to grow on fumarate under anaerobic conditions (Fig. R22). Due to the lack of the anaerobic C_4-dicarboxylate carriers DcuA, DcuB and DcuC, the uptake of fumarate is lost, and no fumarate respiration takes place. After 2 days of incubation, the cell density of IMW505 was below 0.2. In transformants carrying the plasmid-encoded *E. coli dcuB*, the ability to grow by fumarate respiration was largely restored. Strain IMW505 pMW445 with plasmid encoded $dcuB_{Ecoli}$ grew little slower than the wildtype strain IMW237 which possesses DcuA and DcuC in addition, but after 48 hours a comparable cell density was achieved. This means that the pBAD18-Kan* expression vector is appropriate to test DcuB function.

Unexpectedly DcuB protein of *Salmonella typhimurium* complemented anaerobic growth on fumarate only low despite the high identity (97%; Tab. R6) to $DcuB_{Ecoli}$ (Fig. R22). DcuB of *Erwinia carotovora* with 87% sequence identity supported growth on fumarate more successfully. $DcuB_{Salty}$ still had a positive effect on anaerobic growth on fumarate, but the growth was clearly slower than the growth with $DcuB_{Ecoli}$ and $DcuB_{Erwca}$-producing strains, corresponding to 40% of the level of $DcuB_{Ecoli}$. The strain with DcuB of *Wolinella* and *Campylobacter* showed no growth. On the other hand, DcuB protein of the gram-positive *Corynebacterium* (54% sequence identity to $DcuB_{Ecoli}$) stimulated growth of *E. coli*. After a long lag period of approximate 35 hours, the strain containing the corresponding gene on plasmid started to grow, in contrast to the negative control IMW505.

Table R6: Comparison of DcuB, DcuS and DcuR proteins of various bacteria. The sequence alignments of Dcu proteins of *E. coli, S. typhimurium (Salty), E. carotovora (Erwca), W. succinogenes (Wolsu), C. jejunii (Camje)* and *C. diphtheria (Cordi)* were analyzed for conserved and conservatively substituted amino acid residues. Substitutions with non-conserved residues, insertions or deletions were rated as mismatches. The identity and, for DcuB, the similarity to the corresponding proteins in *E. coli* is shown. (-), no homologous protein was identified.

Organism	**DcuB** identity [%]	**DcuB** similarity [%]	**DcuA** identity [%]	**DcuS** identity [%]	**DcuR** identity [%]
Ecoli	100	100	100	100	100
Salty	97	99	94	81	88
Erwca	87	94	64	56	55
Wolsu	71	85	61	-	-
Camje	69	80	53	-	-
Cordi	54	74	57	-	-

To investigate the regulatory function of the heterologous DcuB proteins in *E. coli*, ß-galactosidase reporter fusions were used. The test strain carries a chromosomal *dcuB´-´lacZ* reporter gene fusion as a marker for *dcuB* expression and is deficient of the *dcu* transporters. The cells were cultivated in enriched M9 medium supplemented with glycerol, DMSO, with and without the effector fumarate. The alternative electron acceptor DMSO is essential to allow growth of strains lacking a functional fumarate-uptake carrier. DMSO and the carbon source glycerol do not affect the expression of the DcuSR-dependent genes. The wildtype shows a clear fumarate-dependent expression of DcuB (Fig. R23). Expression of *dcuB´-´lacZ* increases about 6 times after growth on fumarate. In strain IMW505 lacking *dcuB* expression of *dcuB´-´lacZ* is maximal already in the absence of effector. A lack of DcuB protein accordingly leads to fumarate-independent expression of the DcuSR target genes. This "DcuB-effect" points to a repression of the DcuSR two component system by the carrier DcuB when no substrate for transport is available (Kleefeld *et al*., 2009). Hence, some kind of interaction, direct or indirect, between the carrier and the DcuSR system takes place at least in the absence of effector.

The fumarate-dependent expression of *dcuB´-´lacZ* in IMW505 was fully restored by plasmid-encoded DcuB of *E. coli* and by DcuB of *S. typhimurium* and *E. carotovora* (Fig. R23). Growth of IMW505 pMW445 ($dcuB_{Ecoli}$), IMW505 pMW415 ($dcuB_{Salty}$) and IMW505 pMW443 (*dcuB*Erwca) leads to a ten- to twenty-fold increased induction of *dcuB* expression in the presence of effector. The same induction was observed in the $DcuB_{Cordi}$-complemented strain IMW505 pMW503. Even though the DcuB protein of the gram-positive *Corynebacterium* shows a homology of just 54% to $DcuB_{Ecoli}$, it seems to control DcuSR function of *E. coli* efficiently. In contrast to *E. coli, S. typhimurium* and *E. carotovora*, do the ε-proteobacteria *W. succinogenes* and *C. jejunii* and *C. diphtheriae* contain no genes encoding proteins similar to *E. coli* DcuS or DcuR.

Expression of *dcuB´-´lacZ* in the $DcuB_{Camje}$-complemented strain IMW505 pMW470 showed regulatory capacities similar to the DcuB negative strain IMW505 (Fig. R23). Despite high sequence identity (69% identity, 80% similarity) no regulatory effect of $DcuB_{Camje}$ on DcuS of *E. coli* was observed. Therefore the DcuB protein of *C. jejunii* is not able to compensate the transport and regulatory function of DcuB in *E. coli*. DcuB of *Wolinella,* on the other hand, has an effect on *dcuB´-´lacZ* expression in *E. coli*. The inducibility of *dcuB* expression is restored in IMW505 pMW447, although the induction ratio of ß-galactosidase activity

between effector-containing and effector-less culture is lower than in the wildtype strain. The identity between DcuB$_{Wolsu}$ and DcuB$_{Ecoli}$ amounts to 71%.

These results indicate that the mere existence of essential amino acid residues in DcuB$_{Ecoli}$ is not sufficient for its transport activity and regulatory function in *E. coli*.

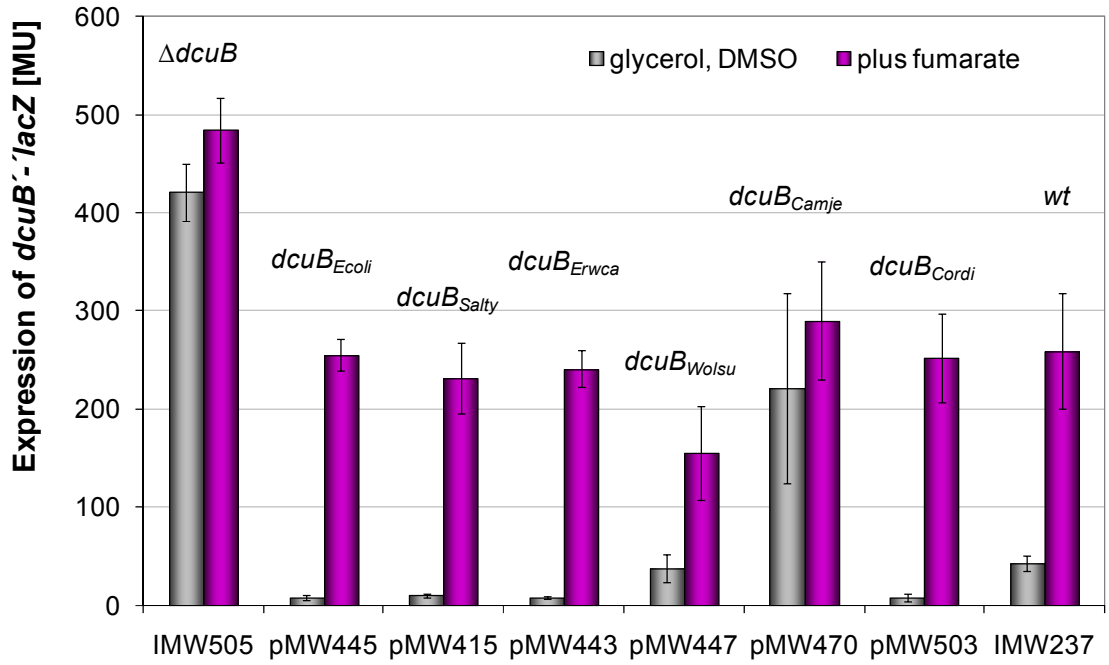

Figure R23: Effector-dependent expression of *dcuB´-´lacZ* in *E. coli* producing DcuB of various bacteria. Strain IMW505 (Δ*dcuB*) was complemented by plasmid-encoded DcuB proteins of *Escherichia coli* (Ecoli), *Salmonella typhimurium* (Salty), *Erwinia carotovora* (Erwca), *Wolinella succinogenes* (Wolsu), *Campylobacter jejunii* (Camje) and *Corynebacterium diphtheria* (Cordi). Cells were grown anaerobically in eM9 medium with glycerol, DMSO with or without fumarate. ß-galactosidase activity (shown in Miller Units) was determined by measuring the rate of ONPG hydrolysis in exponentially growing cultures.

4.4.2 Construction of a DcuA-DcuB hybrid protein

Expression of the Carrier DcuA is not controlled by the DcuSR two-component system and DcuA has no effect on *dcuB* expression (Kleefeld *et al*., 2009). DcuA is in the first place a general uptake-carrier for C_4-dicarboxylates, but in strains lacking the *dcuB* gene, DcuA can replace DcuB transport function. The *dcuA* gene is expressed constitutively in *E. coli*, but there are indications that DcuA is not active during aerobic growth (Engel *et al*., 1992). The mechanism of inactivation of DcuA by oxygen is not known. The sequence similarity between DcuA and DcuB is about 67%, the identity is 35% (Fig. R24).

By mutation the regulation-competent residue D384 of DcuB was introduced into the corresponding position L387 of DcuA. In addition the residues T386 and V388 of DcuA were substituted by the residue serine and leucine, respectively, to increase sequence identity to the regulatory site of DcuB. Two hybrid proteins comprising of the N-terminal part of DcuA and the C-terminus of DcuB were constructed as well.

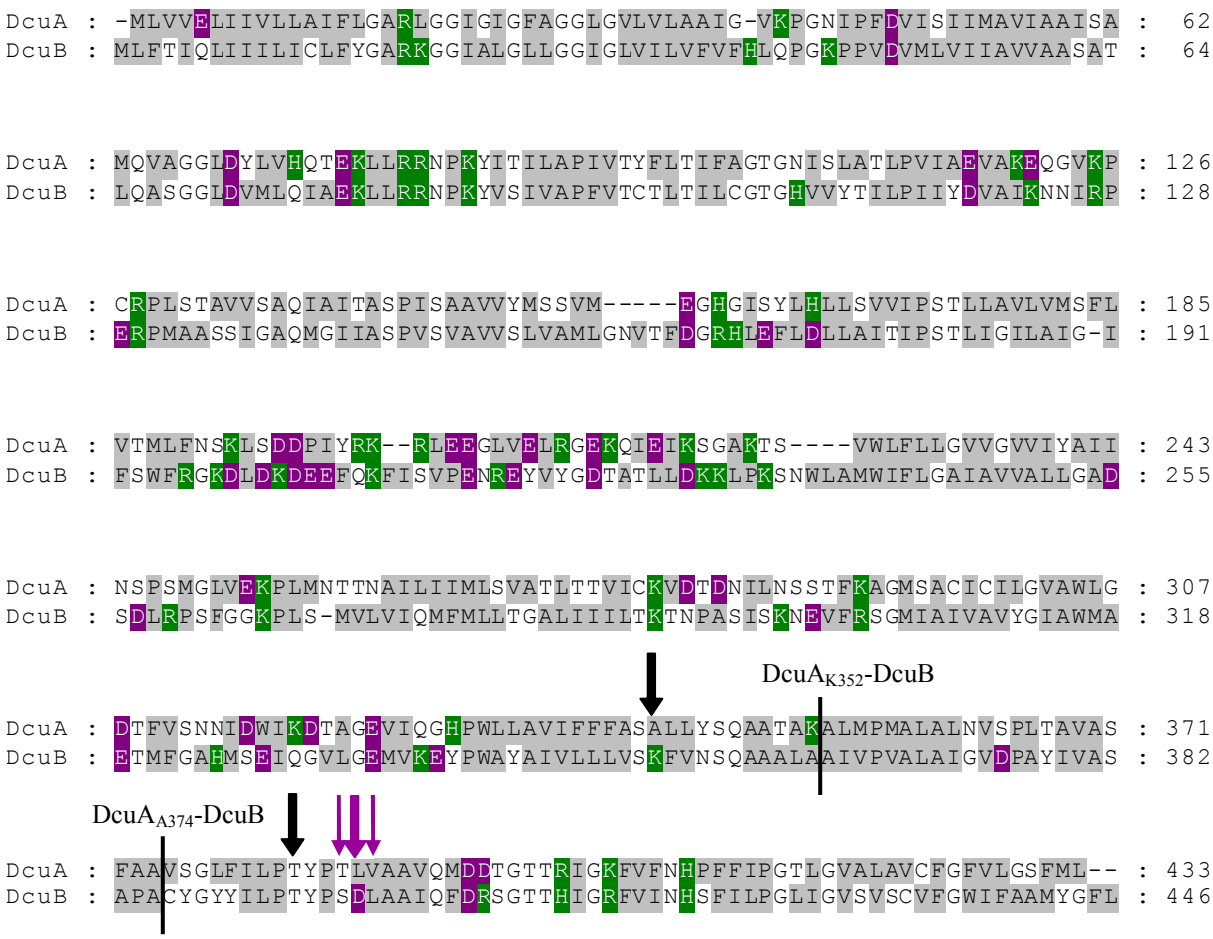

Figure R24: Sequence alignment of the DcuA and DcuB proteins of *E. coli*. Charged residues are coloured in green (positive) and purple (negative), hydrophobic residues are shown in grey. The regulatory relevant sites are marked by bold arrows; positions of amino acid substitutions in DcuA are highlighted by purple arrows. Vertical lines show the junction sites of the hybrids $DcuA_{A374}$-DcuB and $DcuA_{K352}$-DcuB.

The *dcuA* gene was amplified with its own promoter from genomic DNA of *E. coli* AN387 by PCR and cloned into expression vector pBAD18-Kan*. To adjust the amino acid sequence of DcuA to DcuB, the resulting plasmid pMW449 was modified by site-directed mutagenesis. With regard to the regulatory part of DcuB, substitutions of DcuA L387D, and in addition T386S and V388L were made, resulting in the plasmids pMW450 and pMW451. Also

originating from plasmid pMW449, two gene fusions of *dcuA* with *dcuB* were generated. The first construct codes for DcuA(M1-A374)-G-DcuB(Y387-L446)-YMHYE-His_6. The plasmid, listed as pMW629, hereafter is referred to as "$DcuA_{A374}$-DcuB". In a second gene fusion, a template for a fusion protein of DcuA up to K352, followed by a glycine, leucine and the C-terminus of $DcuB_{His}$ beginning with V366 was created. This plasmid pMW630 hereafter is termed as "$DcuA_{K352}$-DcuB". The DcuA derivatives were checked for anaerobic transport of fumarate by growth experiments and effect on DcuSR-dependent gene expression by ß-galactosidase assays. For all studies, the *dcuA*-containing plasmids were transformed into the *dcuA dcuB dcuC*-minus strain IMW505, which carries a chromosomal *dcuB´-´lacZ* reporter gene fusion.

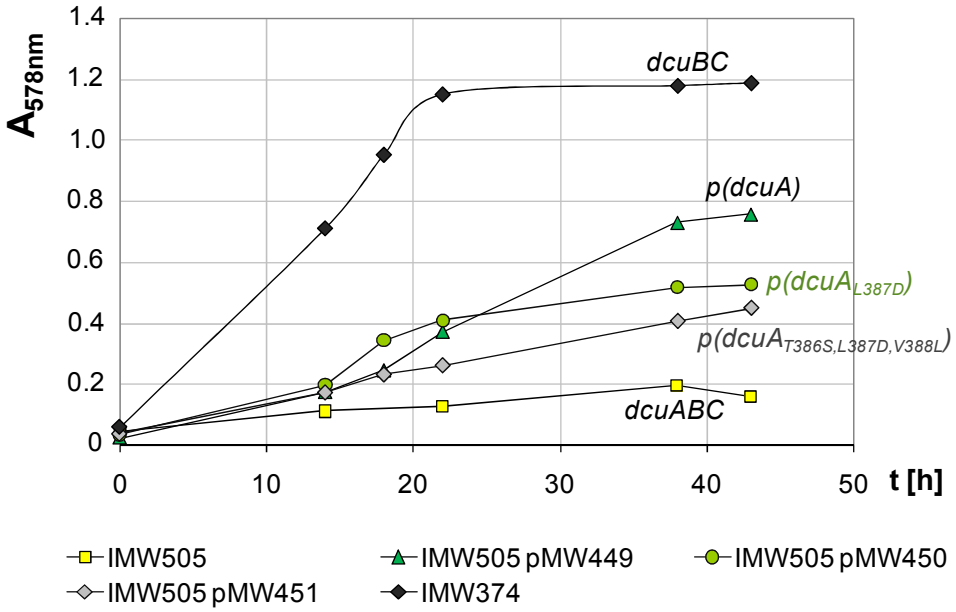

Figure R25: Growth of *E. coli* IMW505 *(dcuA dcuB dcuC)* by plasmid-encoded DcuA and DcuA mutants. *E. coli* IMW505 containing dcuA and mutated forms of dcuA with its own promotor on a plasmid were cultivated anaerobically in enriched M9 medium with glycerol and fumarate. Growth curves are shown for strain IMW505 encoding DcuA (pMW449), DcuA (L387D) (pMW450), DcuA (T386S L387D V388L) (pMW451) and no DcuA. In addition, growth of strain IMW374 (*dcuB dcuC*) with chromosomal encoded *dcuA* is presented.

To test various forms of DcuB for growth and regulatory capacity, the *dcuA dcuB dcuC*-negative strain IMW505 was used which was complemented by various alleles of *dcuA* on plasmid. Due to the lack of a C_4-dicarboxylate-uptake system the triple mutant IMW505 is not able to grow on fumarate plus glycerol under anaerobic conditions (Fig. R25). Supply of plasmid-encoded DcuA restored growth to levels of about 60% of chromosomally encoded

DcuA (IMW374). Substitution of residue L387 by aspartate affects growth on fumarate negatively. Plasmid-encoded DcuA (L387D) and DcuA (T386S, L387D, V388L) restored growth only to low levels, corresponding to 50% of the level of plasmid-encoded wildtype DcuA. Obviously, the capability for antiport is reduced by the leucine:aspartate amino acid exchange. However, both DcuA derivatives showed transport activity, which means that they were expressed and integrated within the cytoplasmic membrane correctly. In contrast to the DcuA point mutants, none of the DcuA-DcuB hybrids enabled growth on fumarate.

The regulatory properties the DcuA variants were screened by ß-galactosidase assays. After anaerobic growth in enriched M9 medium plus glycerol, DMSO with or without fumarate, expression of *dcuB´-´lacZ* was determined (Fig. R26).

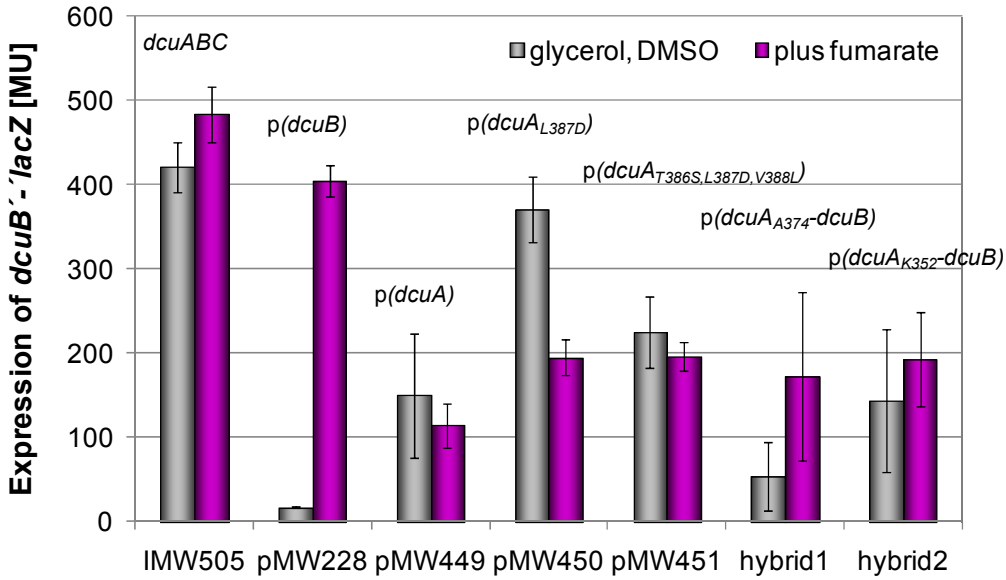

Figure R26: Influence of DcuA variants on *dcuB´-´lacZ* expression. *E. coli dcuA dcuB dcuC*-deficient strain IMW505 carrying plasmid-encoded DcuB (pMW228), DcuA (pMW449), DcuA L387D (pMW450), DcuA T386S L387D V388L (pMW451), $DcuA_{K352}$-DcuB or $DcuA_{A374}$-DcuB was grown anaerobically in eM9 medium with glycerol, DMSO with or without fumarate. Activity of ß-galactosidase was determined during the exponential growth phase.

The activities of *dcuB´-´lacZ* that are representative for the regulatory activity of the Dcu carriers are shown for *dcuA dcuB dcuC* mutant IMW505 complemented with different plasmid-encoded *dcu* genes. Without DcuB (IMW505), *E. coli* showed very high expression of *dcuB´-´lacZ* already in the absence of fumarate. The strain complemented by a plasmid coding for wild type DcuB under the control of its own promoter (pMW228) regained fumarate-dependent expression of *dcuB*. Plasmid-encoded DcuA (pMW449) did not abolish

the DcuB-effect of the DcuSR-regulated genes. The DcuA mutants DcuA (L387D) and DcuA (T386S L387D V388L) and the $DcuA_{K352}$-DcuB hybrid were not able to effect *dcuB´-´lacZ* expression. The $DcuA_{A374}$-DcuB hybrid protein led to a different pattern. Activity of ß-galactosidase after growth in the absence of effector was clearly lower than after induction by fumarate suggesting that the C-terminal part of DcuB is able to supply the regulatory function.

The ß-galactosidase assay clearly implies a regulatory effect of the $DcuA_{A374}$-DcuB hybrid protein on DcuSR function. However, strains that carry plasmid-encoded DcuA variants, in particular the DcuA-DcuB hybrid proteins showed only very poor growth and sometimes could not achieve an optical density higher than 0.4 (after three or four days of growth). The standard deviation of the determined ß-galactosidase activities was high.

4.5 The aerobic succinate carrier DctA of *Escherichia coli*

During aerobic growth of *E. coli* the dicarboxylate transport carrier DctA catalyses the uptake of succinate and other C_4-dicarboxylates in symport with 2-3 H^+ (Gutowski *et al.*, 1975). The C_4-dicarboxylates are oxidized in the citric acid cycle to CO_2 and the reducing equivalents are reoxidized in aerobic respiration. DctA is the most active carrier under aerobic conditions and *dctA* mutants show only poor growth on C_4-dicarboxylates. Similar to DcuB, expression of DctA depends on the DcuSR two-component system (Zientz *et al.*, 1998; Golby *et al*., 1999). Glucose repression effected by the cAMP-CRP complex leads to a strongly decreased expression of *dctA* and, typical for CRP-activated proteins, synthesis of DctA is maximal in the stationary growth phase (Davies *et al*., 1999). During anaerobic growth expression of *dctA* is repressed by ArcA. By growth experiments and expression studies the significance of DctA and DcuS for aerobic growth on C_4-dicarboxilates was studied in detail. Furthermore, direct interaction of DctA with the sensor histidine kinase DcuS was shown by *in vivo* FRET measurements.

4.5.1 Aerobic growth on C_4-dicarboxylates in *E. coli*

To study the significance of DctA and the influence of the DcuSR two component-system for aerobic growth on C_4-dicarboxylates *E. coli* strains IMW385 (*wt*), IMW386 (*dctA*) and IMW389 (*dcuS*) were cultivated in eM9 medium with different carbon sources in shaking Erlenmeyer flasks.

Uptake of the amino acid aspartate (Fig. R27F) in *E. coli* strongly depends on DctA too, but in contrast to growth on succinate, malate or fumarate the presence of a functional DcuSR two component-system seemed to be less important. Growth of *dcuS* mutant versus *dctA* mutant is about 2-4 fold increased with aspartate (compare to Tab. R7). A conclusion could be that aspartate- induced *dctA*-expression is regulated by an alternative system.

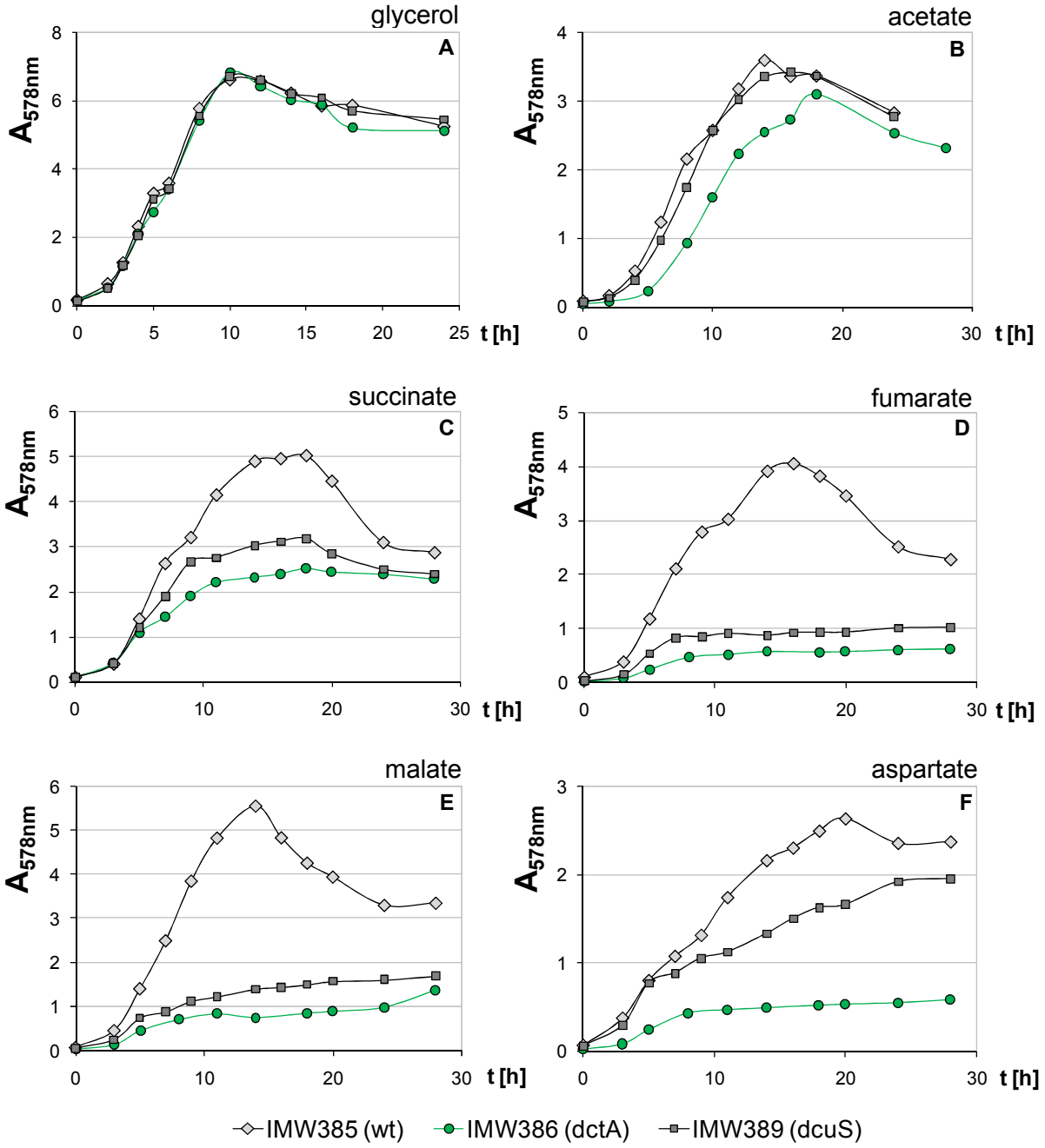

Figure R27: Aerobic growth of *E. coli* on several carbon sources. *E. coli* strains IMW385 (*wt*), IMW386 (*dctA*) and IMW389 (*dcuS*) were grown aerobically in pH-neutral eM9 medium with glycerol (A), acetate (B), succinate (C), fumarate (D), malate (E) or aspartate (F) as sole carbon source.

Wild type and mutants show nearly identical growth on glucose, pyruvate, gluconate (data not shown), glycerol (Fig. R27A) and acetate (Fig. R27B; Fig. R28A). With succinate as sole carbon source (Fig. R26 C) the *dctA* mutant IMW386 grew to 50%, the *dcuS* mutant IMW389 to 60% of the level of the wild type IMW385, indicating that *E. coli* possesses another aerobic carrier for succinate uptake in addition to DctA. Growth on fumarate (Fig. R27D) and malate (Fig. R27E) on the other hand was strongly limited (about 80-90%) in the *dctA* mutant, demonstrating that DctA is the main transporter for these substrates under aerobic conditions. The growth difference of IMW386 (*dctA*) on C_4-dicarboxylates was fully complemented by plasmid pMW457 containing the *dctA* gene with own promoter (data not shown). The growth curves indicate that expression of *dctA* basically depends on DcuSR: In the *dcuS* mutant growth on C_4-dicarboxylates is only slightly (factor 1.2-1.5) increased compared to the *dctA* mutant. Aerobic growth of the *dctA dcuS* double mutant on C_4-dicarboxylates was comparable with growth of the *dctA* mutant (Tab. R7).

4.5.2 Regulation of *dctA* expression by DcuSR

E. coli strains IMW385 (*wt*), IMW386 (*dctA*), IMW389 (*dcuS*) and IMW538 (*dctA dcuS*) carrying a chromosomal *dctA´-´lacZ* reporter gene fusion were cultivated under aerobic conditions with or without C_4-dicarboxylates. As an alternative carbon source glycerol or acetate were used, and the effect of C_4-dicarboxylates on *dctA* expression in the presence and absence of the additional carbon source was tested (Tab R7). ß-Galactosidase activities were assayed in several repeats and from duplicate or triplicate cultures grown to the postexponential growth phase (14h). To identify the different growth phases, the optical density of all cultures was continuously followed during growth (Fig. R28).

Compared to growth on glycerol expression of *dctA* in the wild type is induced by a factor of 4 to 6 in the presence of fumarate, succinate (Fig. R29) or malate and by the factor 10 with aspartate (Tab. R7). Mutation of *dctA* resulted in an increased *dctA* expression in the absence but also in the presence of C_4-dicarboxylates. In the *dctA* mutant *dctA* expression by C_4-dicarboxylates is induced about threefold in the presence of glycerol and four to six-fold in the absence of glycerol (Tab. R7). In strain IMW386 (*dctA*), carrying the *dctA*-containing high-copy plasmid pMW457, expression of *dctA´-´lacZ* with glycerol and acetate is equivalent to the wild type (data not shown). However, after growth on fumarate, succinate or malate expression is decreased, resulting in a loss of inducibility by C_4-dicarboxylates (data not shown). The inhibitory influence of the DctA carrier on *dctA*-expression in *E. coli* is enhanced by plasmid-encoded DctA.

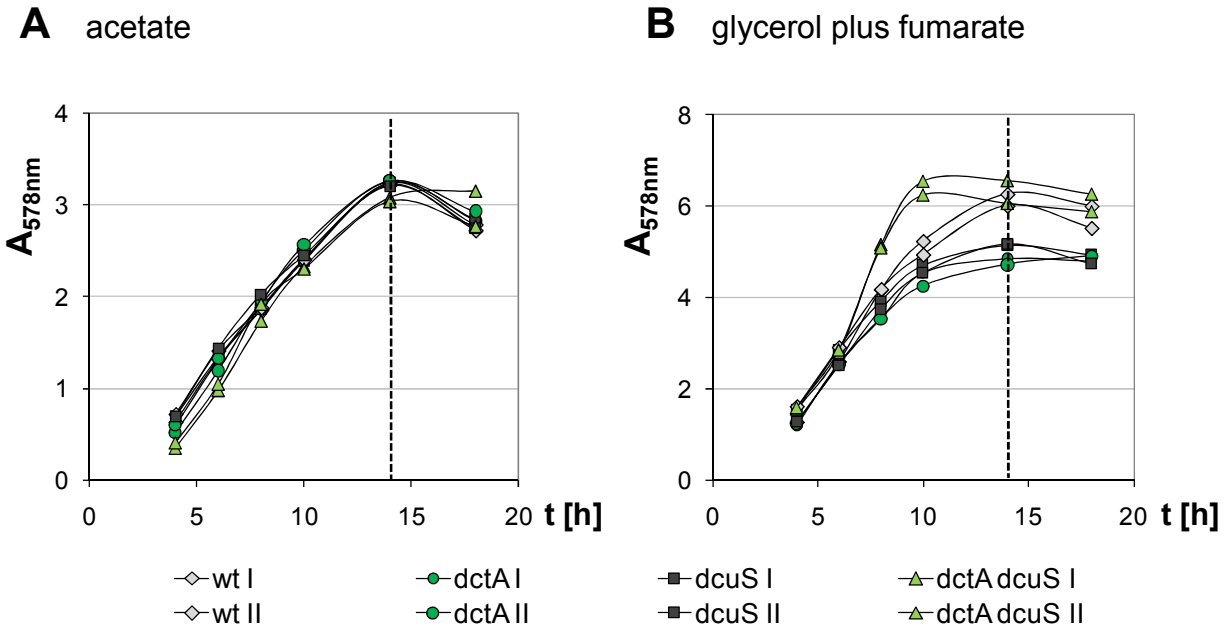

Figure R28: Example of growth-monitoring for *dctA* expression studies. During aerobic cultivation of *E. coli* for ß-galactosidase assays the optical density of all cultures was continuesly observed. Figure (**A**) shows aerobic growth of *E. coli* wild type, *dctA* mutant, *dcuS* mutant and *dctA dcuS* doublemutant in eM9 medium with acetate, figure (**B**) with glycerol plus fumarate.

Expression of *dctA´-´lacZ* in the *dcuS* mutant and the *dcuS dctA* double mutant was just slightly increased by C_4-dicarboxylates in the presence of glycerol (Tab. R7; Fig. R30), indicating that DctA synthesis strongly depends on the DcuSR two-component system. After growth on succinate, fumarate or aspartate in the absence of glycerol *dctA* expression clearly increased in the *dcuS* and *dctA dcuS* mutant, an effect also found in the *dctA* mutant. On the other hand, no inhibitory effect of glycerol on fumarate or succinate-induced *dctA*-expression was observed in the wild type. Therefore, the glycerol-effect potentially is caused by the limited growth of the *dctA dcuS* and *dcuS* mutants on C_4-dicarboxylates as sole carbon source and, as a consequence, the modified growth conditions in wild type and mutants.

Henceforth, ß-galactosidase activities were determined in cells aerobically cultivated on glycerol or acetate with or without succinate or fumarate to establish comparable growth conditions. CRP-activated DctA synthesis is strongly repressed by glucose. For this reason glucose, related substrates like gluconate or the degradation product pyruvate were not suitable as alternative carbon source in *dctA´-´lacZ* expression studies.

Table R7: Expression of *dctA´-´lacZ* in *E. coli* wild type, *dctA* mutant, *dcuS* mutant and *dctA dcuS* mutant after aerobic growth in eM9 medium supplemented with different carbon sources. The expression of a chromosomal encoded *dctA´-´lacZ* reporter gene fusion was measured in *E. coli* IMW385 (*wt*), IMW386 (*dctA*), IMW389 (*dcuS*) and IMW538 (*dctAdcuS*). Under each growth condition, at least two independent cultures of each strain were grown to the postexponential or early stationary phase) and the ß-galactosidase activities were determined in quadruplicate. The average value of identical cultures after 14 h is shown.

Strain (relevant genotype)	Carbon source	ß-Gal Activity [Miller Units]	Optical density A_{578nm}
IMW385	glycerol	4 ± 0	5.69
(***wt***)	glyc/succ	25 ± 5	7.73
	glyc/fum	21 ± 0	6.08
	acetate	11 ± 1	2.89
	ac/succ	19 ± 1	4.07
	ac/fum	18 ± 1	4.78
	succinate	17 ± 1	3.31
	fumarate	25 ± 4	3.40
	aspartate	52 ± 4	1.89
IMW386	glycerol	20 ± 1	5.48
(***dctA***)	glyc/succ	72 ± 13	7.01
	glyc/fum	56 ± 22	4.81
	acetate	84 ± 39	2.98
	ac/succ	42 ± 11	2.76
	ac/fum	90 ± 41	2.40
	succinate	126 ± 4	1.94
	fumarate	88 ± 28	0.48
	aspartate	107 ± 19	0.45
IMW389	glycerol	3 ± 0	5.54
(***dcuS***)	glyc/succ	5 ± 0	7.38
	glyc/fum	4 ± 0	5.13
	acetate	10 ± 1	2.93
	ac/succ	5 ± 0	3.45
	ac/fum	7 ± 1	3.20
	succinate	11 ± 1	2.56
	fumarate	14 ± 8	0.77
	aspartate	17 ± 3	1.00
IMW538	glycerol	3 ± 0	6.30
(***dctA dcuS***)	glyc/succ	5 ± 1	5.23
	glyc/fum	3 ± 0	5.06
	acetate	12 ± 1	3.05
	ac/succ	n.d.	n.d.
	ac/fum	12 ± 1	2.09
	succinate	13 ± 1	2.06
	fumarate	8 ± 1	0.50

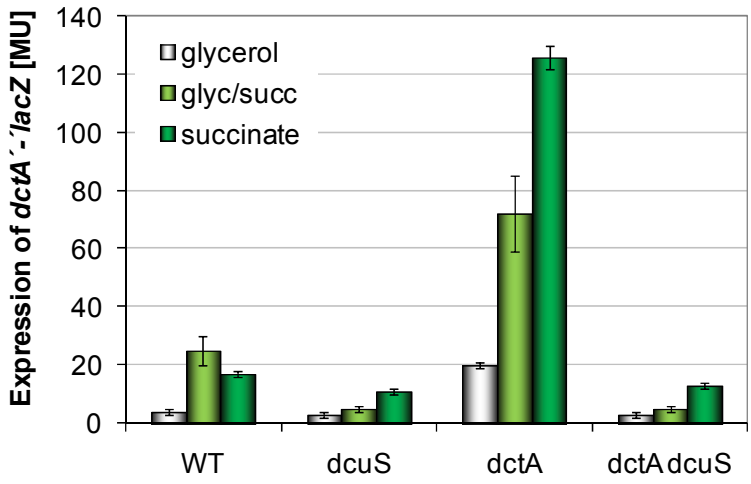

Figure R29: Induction of *dctA´-´lacZ*: Effect of succinate and effect of DcuS and DctA. The expression of chromosomal *dctA´-´lacZ* in *E. coli* wild type, *dctA* mutant, *dcuS* mutant and *dctA dcuS* mutant was determined after 14 hours of aerobically growth in eM9 medium with glycerol, glycerol plus succinate, or succinate.

In Figure R30 the effect of *dcuS* mutation is presented in detail. The expression level of *dctA* in wild type, *dcuS* mutant and *dcuS dctA* mutant is comparable in the absence of effector, but the presence of C_4-dicarboxylates no longer has an influence on *dctA´-´lacZ* expression when DcuS is missing. Therefore the induction of the *dctA* gene by C_4-dicarboxylates exclusively depends on DcuSR. Additional deletion of the *dctA* gene has no effect, indicating that the inhibitory effect of DctA on *dctA´-´lacZ* expression is also mediated by DcuSR.

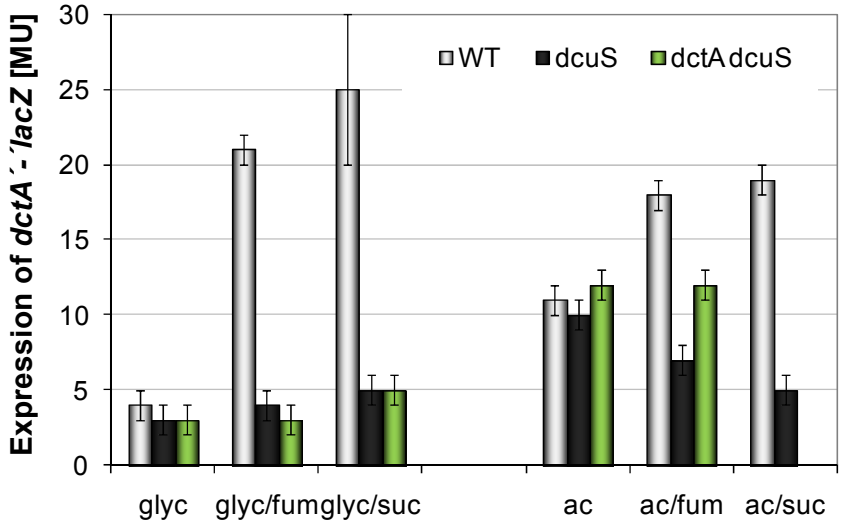

Figure R30: Effect of *dcuS*-deletion on expression of *dctA´-´lacZ* in *E. coli.* Strains IMW385 (*wt*), IMW389 (*dcuS*) and IMW538 (*dctA dcuS*), carrying a chromosomal *dctA´-´lacZ* reporter gene fusion, were grown aerobically in eM9 medium supplemented with glycerol or acetate with or without effector. ß-galactosidase activity was measured in cells entering the stationary phase of growth.

Acetate affects the expression of *dctA´-´lacZ* in the wild type, the *dcuS* mutant and the *dcuS dctA* double mutant (Fig. R30; Fig. R31) and in particular the *dctA* mutant (Fig. R31). In wild type and *dcuS* mutants growth on acetate led to a twofold increased expression of *dctA* compared to cultures grown on glycerol. The induction by succinate and fumarate decreased in the wild type by a factor of 1.7. Expression of *dctA´-´lacZ* in the *dcuS* and *dcuS dctA* mutant was not stimulated by C_4-dicarboxylates after growth on acetate.

In the *dctA* mutant an about fourfold increased *dctA* expression is caused by acetate compared to glycerol (Fig. R31). Although acetate is no substrate of the DcuSR system (Zientz *et al*. 1998) and is not transported by DctA (Davies *et al*., 1999) the acetate-effect on *dctA*-expression is duplicated in the absence of functional DctA.

Compared to cells grown on glycerol, acetate shows a clear inhibitory effect on fumarate or succinate-induced *dctA* expression in wild type and *dctA* mutant. DctA mutation actually results in constitutive expression of *dctA´-´lacZ* with respect to the absence or presence of C_4-dicarboxylates (Fig. R31).

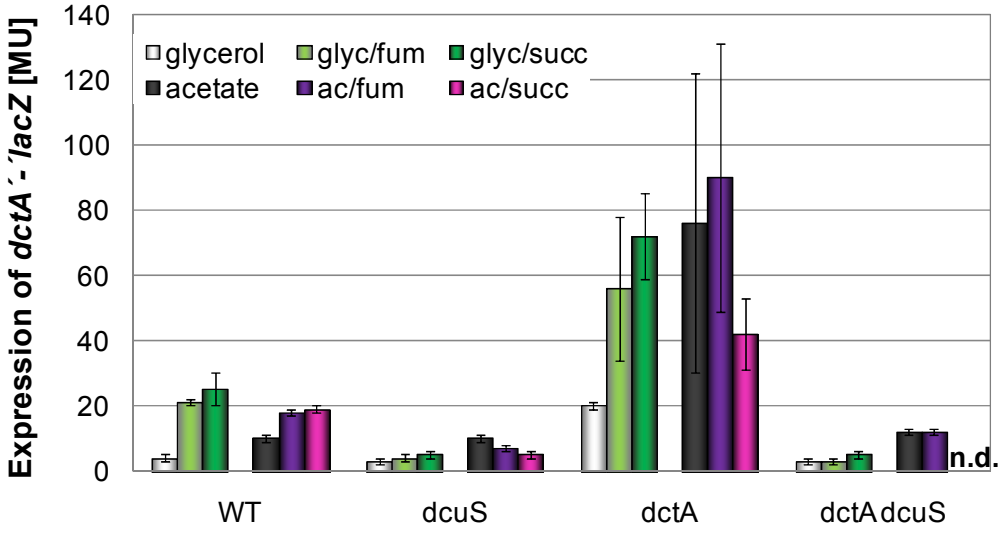

Figure R31: Effect of acetate on expression of *dctA´-´lacZ* in *E. coli* wild type, *dctA* mutant, *dcuS* mutant and *dctA dcuS* double mutant. Cells were grown aerobically in eM9 medium with glycerol, glycerol plus fumarate, glycerol plus succinate or under the same conditions with acetate instead of glycerol. ß-galactosidase activity of chromosomal coded *dctA´-´lacZ* reporter gene fusion was determined after 14 hours of cultivation, corresponding to the postexponential phase of growth.

4.6 Interaction studies of DctA and DcuS by *in vivo* FRET measurements

The expression of *dctA* is activated by the DcuSR two-component system under aerobic conditions in the presence of C_4-dicarboxylates. Deletion of *dctA* stimulates the expression of *dctA´-´lacZ* (Davies *et al*., 1999; this work), similar to deletion of the anaerobic antiporter DcuB. Since C_4-dicarboxylate-induced expression of *dctA* mainly depends on a functional DcuSR system (compare to section 4.5.2), it is very likely that DctA inhibits the DcuSR-mediated signal transduction. A potential site for repression by the carrier DctA is the membrane-bound sensor histidene kinase DcuS. Direct interaction of DctA with DcuS was tested by Fluorescence resonance energy transfer (FRET) *in vivo*.

FRET stands for Fluorescence Resonance Energy Transfer and describes the nonradiative energy transfer from a fluorescent donor molecule in its excited state to fluorescent acceptor molecule. The process of energy transfer takes place by a dipole-dipole coupling mechanism. The efficiency of FRET depends on the ratio of donor to acceptor, the distance between the fluorophores and the specific Förster distance of the donor-acceptor pair. The Förster distance is defined as the distance between donor and acceptor at which 50% of the excitation energy of the donor is transferred to the acceptor and it is based on physical values/variables like the relative dipole-dipole orientation of donor and acceptor and the extent of spectral overlap of donor emission and acceptor absorption spectrum. The method of FRET is suitable for studies on protein-protein interactions (Truong & Ikura, 2001): interacting proteins have to be in close proximity.

FRET pair CFP/YFP

To study protein-protein interactions *in vivo*, derivatives of the green fluorescent protein GFP are often fused genetically to the proteins of interest. Plasmids, encoding fusions of DcuS with the enhanced cyan fluorescent protein, ECFP, and the enhanced yellow fluorescent protein, EYFP were already successfully used to detect dimerisation of the sensor histidine kinase (Scheu, 2009).

The absorption maximum of the donor fluorophore CFP is at 433nm, maximum excitation of the acceptor YFP takes place at 513nm (Fig. R32A). The donor CFP shows two emission maxima, one at 475nm (main peak) and the other at 501nm. Excitation of the acceptor YFP leads to an emission spectrum with a maximum at 527nm. The emission spectrum of CFP overlaps with the absorption spectrum of YFP in the range from about 450nm to 540nm. The Förster distance of the FRET pair CFP/YFP is 4.92nm (Patterson *et al*., 2000).

Excitation at 433nm causes maximum emission of the donor CFP (Fig. R32B) while the acceptor shows only negligible emission. When both fluorophores are in close contact in one sample, a combined spectrum resulting from the addition of donor emission and acceptor emission is observed (grey dotted line). Close proximity of the FRET pair leads to energy transfer from CFP to YFP resulting in an emission spectrum with decreased CFP emission but increased YFP emission (black line).

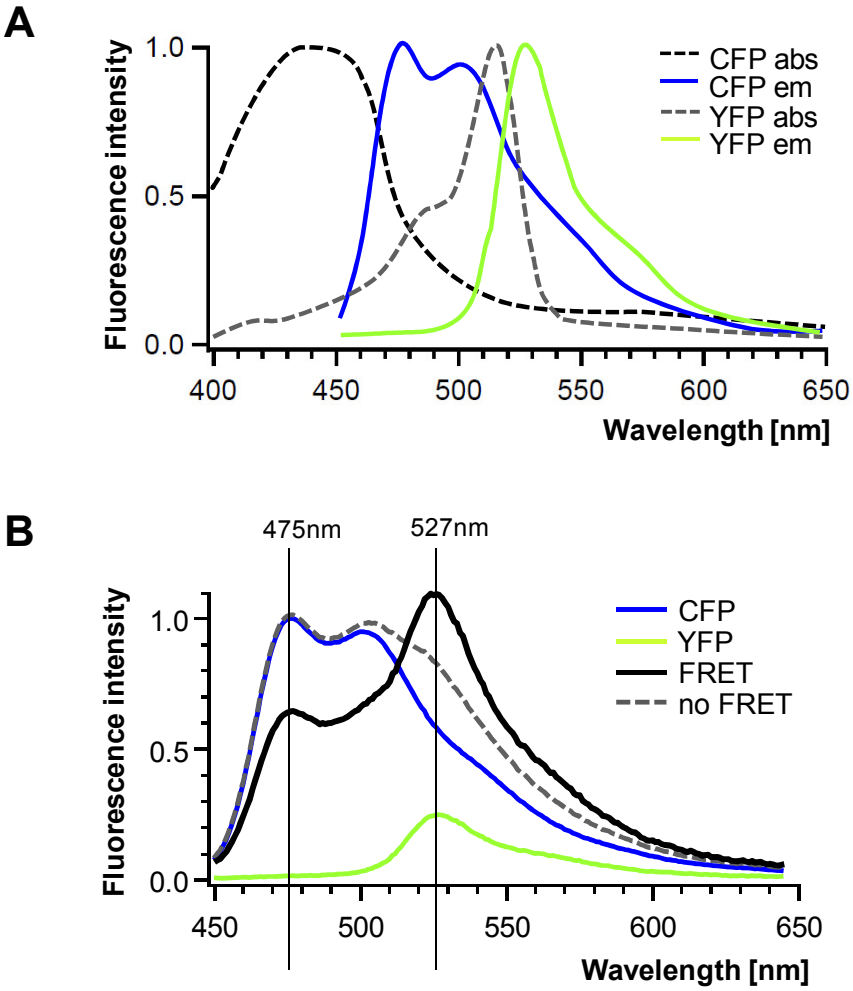

Figure R32: Principles of Fluorescence Resonance Energy Transfer as exhibited by the donor-acceptor pair CFP/YFP. (A) Normalised absorption and emission spectra of the fluorophores CFP and YFP (Liao, 2008). Excitation of CFP occurred at 433nm, YFP was excited at 488nm. abs, absorption; em, emission. **(B) Emission spectra of single CFP and YFP and effect of FRET on the overall emission spectrum after excitation at 433nm.** FRET, emission spectra of a donor/acceptor mixture showing Fluorescence Resonance Energy Transfer; no FRET, resulting emission spectrum after excitation at 433nm when no energy transfer via FRET takes place.

The GFP variants have to be folded properly to allow the formation of the p-hydroxybenzylidene-imidazolidinone chromophore which is generated by the protein´s own Ser-Tyr-Gly sequence. The three amino acid residues on positions 65-67 undergo a non-enzymatic cyclization mechanism followed by O_2-catalised oxidation of the tyrosine to dehydrotyrosine. As a consequence the cells have to be cultivated under aerobic conditions. In addition a cytoplasmic localisation of the GFP variants is required for a correct folding and formation of the fluorophore (Feilmeier *et al.*, 2000; Drew *et al*., 2001).

4.6.1 Qualitative FRET measurements and determination of FRET efficiencies

For *in vivo* FRET measurements a series of DctA-GFP fusions were genetically constructed as described in Materials and Methods. The plasmid encoded fusion proteins were checked for DctA activity by growth experiments (compare to section 4.6.2, Fig. R37) and for fluorescence of the GFP part. For growth experiments *dctA* (pMW505), *dctA-cfp, dctA-yfp, cfp-dctA* or *yfp-dctA* encoded on plasmid pET28a were expressed under the control of the IPTG-inducible T7 promotor in *E. coli* MDO800 (*dctA*) under aerobic conditions in eM9 medium plus fumarate. The plasmid encoded DctA fusions fully restored growth on fumarate in the *dctA* mutant (data not shown) indicating that all constructs coded for functional DctA. For fluorescence measurements and FRET experiments the gene fusions were subcloned into pBAD18-Kan* (*cfp* fusions) and pBAD30 (*yfp*-fusions). The DctA-GFP fusion proteins all showed fluorescence mediated by the coupled fluorophores. The highest amount of fluorescence was detected with the DctA-YFP protein (pMW526). Therefore the *dctA-yfp* was coexpressed with *dcuS-cfp* (pMW408) (Fig. R33F) and *cfp-dcuS* (pMW389) to prove direct interaction between DctA and DcuS.

Controls

To define the limits of the method several control setups were generated and tested under the given experimental conditions. The maximal accessible FRET efficiency was determined by using a CFP-YFP fusion protein (Fig. R33C). In this construct, coded on plasmid pMW766, the CFP protein is covalently coupled to YFP by a flexible linker of 9 amino acid residues making sure that the proteins show maximal energy transfer.

To determine the extent on nonspecific FRET caused by random contacts between the donor and acceptor fluorophores, plasmids containing single CFP (pMW762) and YFP (pMW765) were coexpressed in *E. coli* (Fig. R33B). A mixture of cells expressing single CFP with cells

expressing YFP (Fig. R33A) served as a marker for wrong positive results since no FRET is possible in this sample.

In addition, a truncated variant of the aspartate sensor Tar of *E. coli* was used as a negative control. Tar is a membrane-integrated protein with periplasmic sensory domain for signal recognition which controls chemotaxis in response to aspartate. In its functional state Tar shows a polar localisation in *E. coli*, but the C-terminal truncated Tar_{1-331} is no longer active and homogenously is distributed in the cell membrane (Kentner *et al.*, 2006). For FRET measurements Tar_{1-331}-CFP (pMW801) was coexpressed with DcuS-YFP (pMW407) and DctA-YFP (pMW526) (Fig. R33D; E).

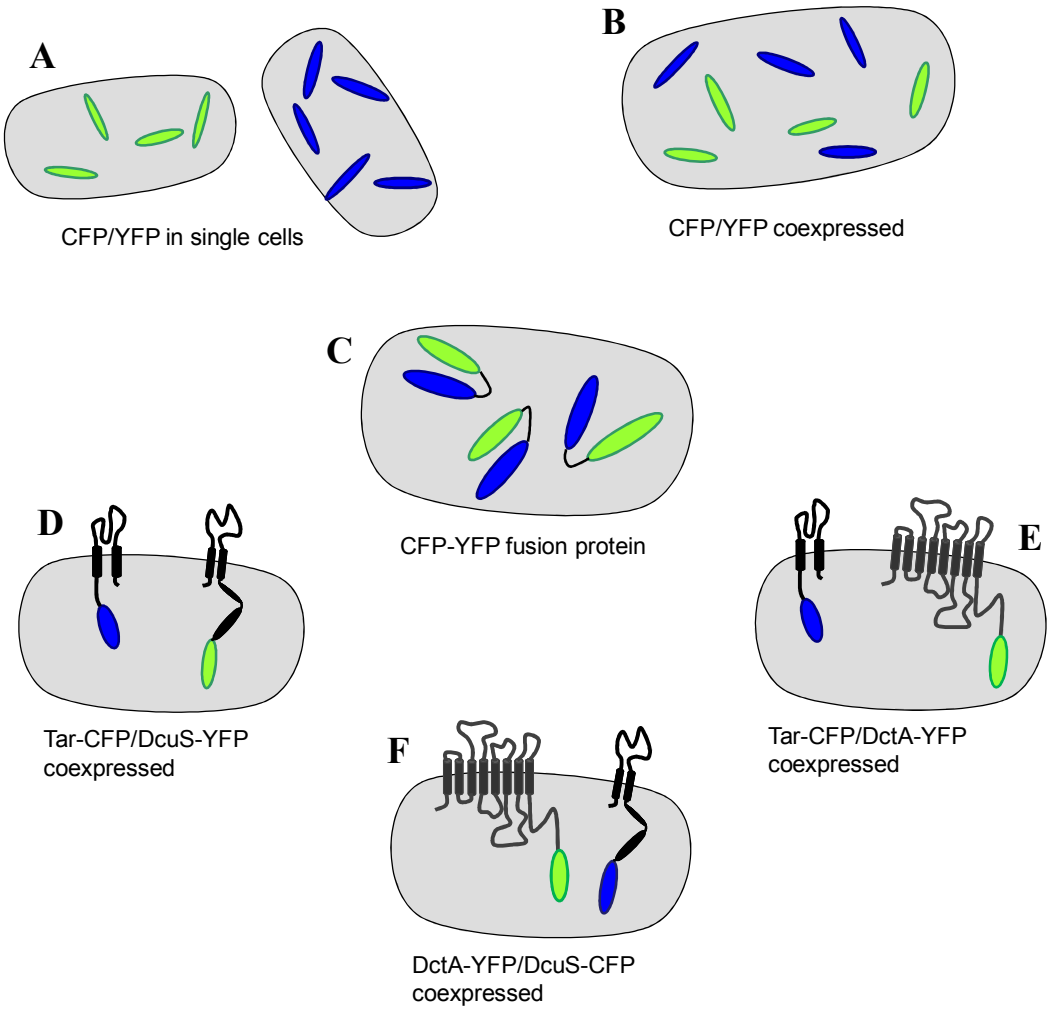

Figure R33: Experimental setup for *in vivo* FRET measurements. A, mixture of cells expressing single CFP or YFP; **B,** CFP and YFP coexpressed in one cell; **C,** Cells expressing a protein fusion of CFP with YFP; **D,** truncated Tar_{331}-CFP coexpressed with functional DcuS-YFP; **E,** truncated Tar_{331}-CFP coexpressed with functional DctA-YFP; **F,** coexpression of fully active fusion proteins DctA-YFP and DcuS-CFP.

FRET measurements

Due to strong background signals by the bacterial auto-fluorescence, Rayleigh scattering (cell particles) and Raman scattering (buffer) the spectra had to be corrected by background substraction. For this reason reference spectra of the buffer and of *E. coli* JM109 grown under identical conditions were recorded for each test series. From the corrected emission spectra of donor, acceptor and mixture of both donor fraction (f_D; ratio between CFP and total flourophore number) and FRET efficiency (E) was calculated according to Gordon *et al.*, 1998 (Liao, 2008). For an accurate determination of the FRET efficiency, the donor fraction should be about 0.5, which means that the amounts of donor and acceptor molecules are nearly equal. Therefore only the FRET efficiencies of samples with a f_D = 0.4-0.6 were used for interpretation of the experiments. The results are presented in Fig. R34.

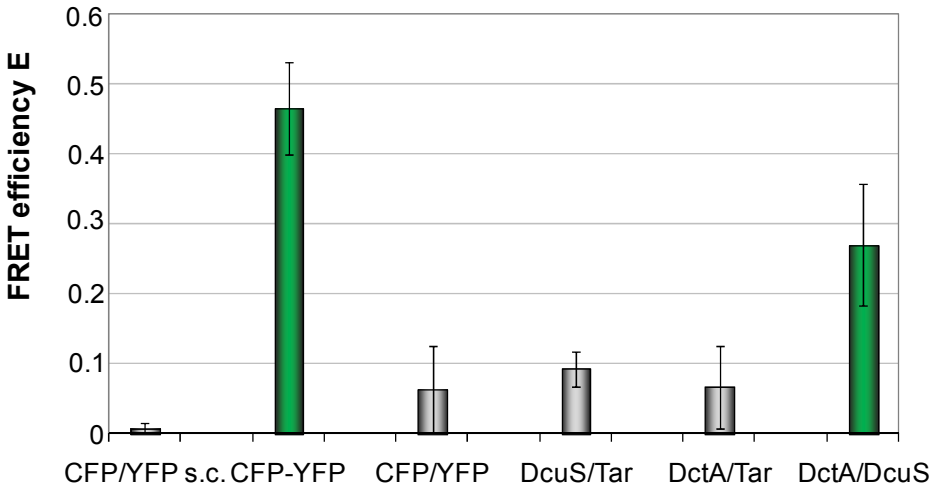

Figure R34: FRET efficiency E of *E. coli* JM105 expressing several fluorescent proteins or combinations of fluorescent proteins. CFP/YFP s.c. shows FRET efficiency obtained by a mixture of cells expressing only CFP with cells expressing only YFP. The CFP-YFP fusion represents the maximal accessible FRET efficiency. It is followed by the FRET efficiencies of single CFP and YFP coexpressed in one cell**,** DcuS-YFP coexpressed with Tar_{331}-CFP, DctA-YFP coexpressed with Tar_{331}-CFP and DctA-YFP coexpressed with DcuS-CFP.

The positive control, cells containing CFP-YFP fusion proteins, showed an average donor fraction of 0.49 ± 0.01 and a total FRET efficiency of 0.47 ± 0.07 (100% relative FRET efficiency). As a marker for an efficient background substraction and adequate calculation a mixture of CFP and YFP in different cells was used. The relative FRET efficiency of this sample was 0.008 ± 0.007 (2%) indicating that no artificial FRET efficiency was detected. Coexpression of *cfp* and *yfp* in one cell led to a relative FRET efficiency of 14% (E = 0.064 ± 0.062; f_D = 0.47 ± 0.04). This value for nonspecific energy transfer is confirmed by the

negative control with membrane-embedded Tar_{1-331}-CFP and DctA-YFP (E = 0.067 ± 0.059; fD = 0.49 ± 0.04). Cells coexpressing *tar*$_{1-331}$*-cfp* and *dcuS-yfp* showed a slightly higher FRET efficiencies of 0.093 ± 0.025 (about 20% relative FRET efficiency, corresponding to a mixture of Tar_{1-331}-YFP/ DcuS-CFP measured by Scheu, 2009) which can be defined as a threshold for nonspecific FRET. Samples containing DcuS-CFP and DctA-YFP fusion proteins in one cell resulted in a high relative FRET efficiency of about 60% (E = 0.27 ± 0.087; fd = 0.43 ± 0.07) indicating direct interaction of DctA with DcuS.

In cells with DctA-YFP and CFP-DcuS fusion protein (N-terminal fusion) no FRET was observed (data not shown), demonstrating that the exact position of the fluorophores has a strong influence on the FRET efficiency.

4.6.2 Screening of DctA mutants by FRET

By using the method of intermolecular in vivo FRET, regulatory mutants of DctA should be identified. As for DcuB, single amino acid residues of DctA are supposed to cause the inhibitory effect of DctA on *dctA* expression. Since DctA affects DcuSR-dependant expression by direct interaction with the sensor protein DcuS, substitution of relevant residues should result in a loss of interaction and therefore in a loss of FRET between the GFP-linked proteins (compare to section 4.6.1).

A sequence alignment of the carriers DctA and DcuB is presented in Figure R35. DctA and DcuB of *E. coli* show a sequence similarity of only 33% (7% identity) underlining the structural differences of the proteins. For DctA a topology with 8 transmembrane helices and cytoplasmic termini is predicted, whereas DcuB comprises 12 membrane-spanning segments and periplasmically oriented termini (Fig. R36). Nevertheless, both proteins interact or potentially interact with the sensor kinase DcuS which implies a similar regulatory site within the proteins.

The regulatory amino acid residues of $DcuB_{Ecoli}$, K353, T384 and D389 are highly conserved in DcuB proteins of related bacteria. In DcuB the regulatory site is located at the C-terminus with the essential residues situated within the penultimate helix and the final cytoplasmic loop. Considering the chemical nature of these residues (polare, charged), the neighbouring residues and the predicted localization within the protein, eight amino acid residues of DctA were selected (Fig. R35; R36) for mutagenesis: T296, D303, S340, K341, D376, S380, E381 and R383. No corresponding residues to S380 and E381 were identified in DctA of *Pseudomonas aeroginosa*, but this organism does not possess a DcuSR system anyway. The

point mutants of DctA were generated in plasmid pMW526 (*dctA-yfp*). By site-directed mutagenesis the single amino acid residues were exchanged against an alanine.

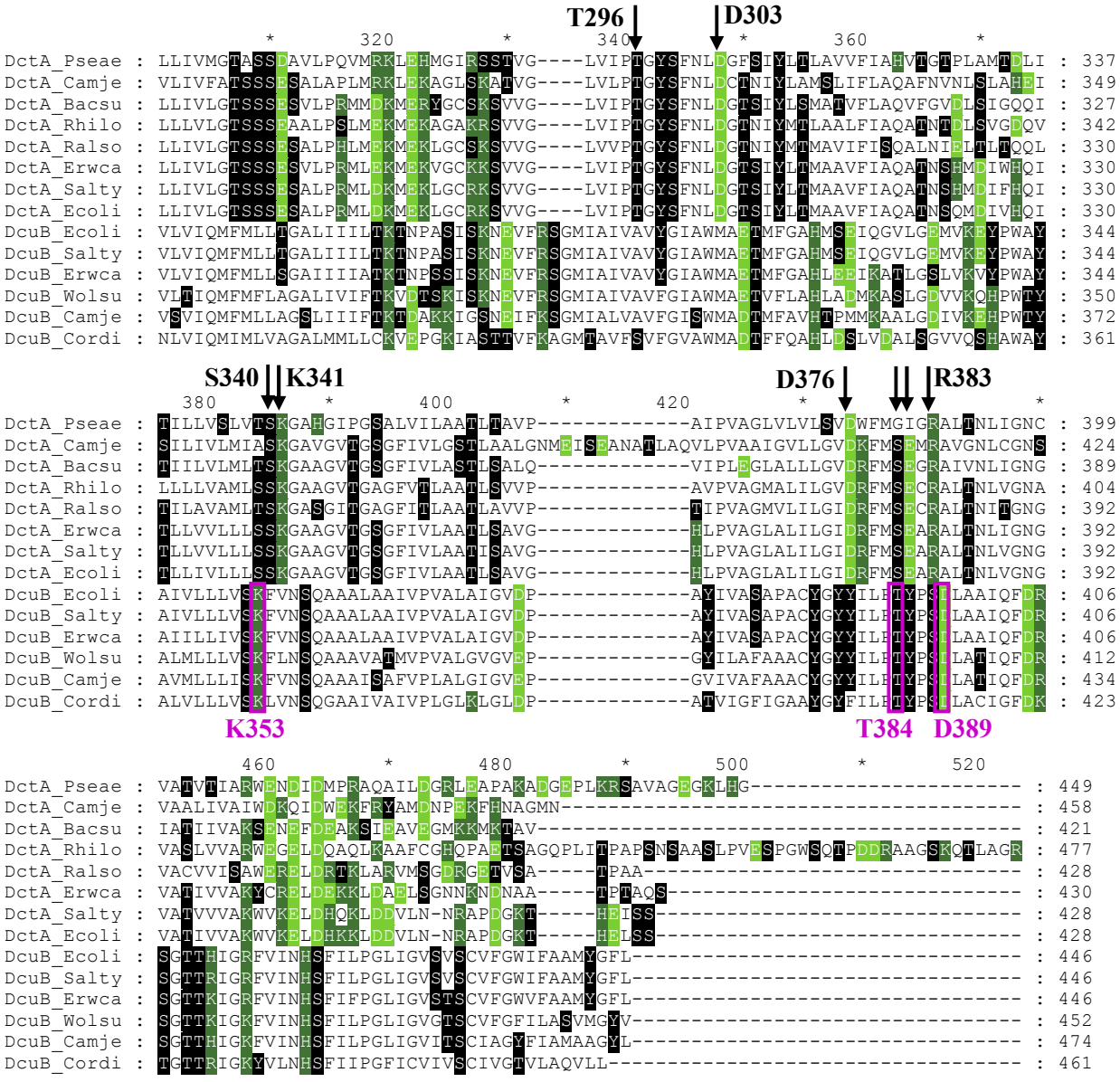

Figure R35: Multiple sequence alignment of the C-terminal part of DctA and DcuB proteins of various bacteria. Charged residues are coloured in green; basic residues (Arg, Lys, His) are marked by dark green, acidic residues (Asp, Glu) by light green backround. Amino acid residues with hydroxyl groups are highlighted by black backround. Highly conserved amino acid residues of DcuB which are essential for regulatory function in *E. coli* are surrounded by a purple box with the residue and its position in $DcuB_{Ecoli}$ below. Arrows show highly conserved hydrophilic residues of DctA, which were exchanged against alanine in $DctA_{Ecoli}$ by site-directed mutagenesis. The protein sequences of *Pseudomonas aeroginosa (Pseae), Campylobacter jejunii (Camje), Bacillus succinogenes (Bacsu), Rhizobium loti (Rhilo), Ralstonia solanacearum (Ralso), Erwinia carotovora (Erwca), Salmonella typhimurium (Salty), E. coli (Ecoli), Wolinella succinogenes (Wolsu)* and *Corynebacterium diphtheria (Cordi)* are presented.

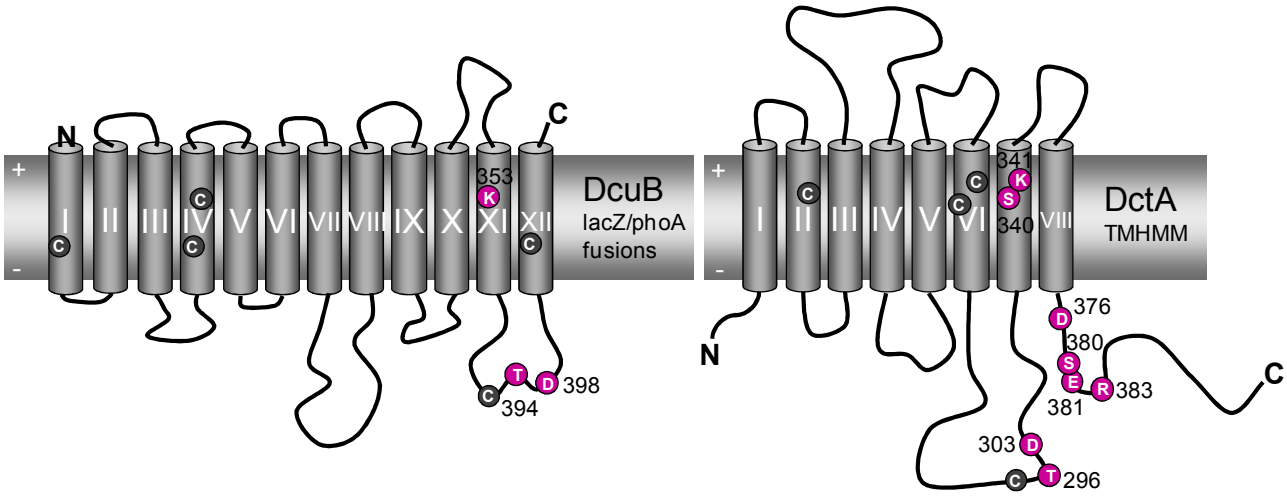

Figure R36: Topology models of the C_4-dicarboxylate carriers DcuB and DctA of *E. coli*. The Model of DcuB is based on the results of DcuB-PhoA and –LacZ expression studies; DctA topology is shown as predicted by the TMHMM server. The positions of regulatory amino acid residues of DcuB (K353, T394, D398) are marked in purple, putative corresponding residues of DctA. Cysteins are depicted in grey.

The regulatory amino acid residues of $DcuB_{Ecoli}$, K353, T384 and D389 are highly conserved in DcuB proteins of related bacteria. In DcuB the regulatory site is located at the C-terminus with the essential residues situated within the penultimate helix and the final cytoplasmic loop. Considering the chemical nature of these residues (polare, charged), the neighbouring residues and the predicted localization within the protein, eight amino acid residues of DctA were selected (Fig. R35; R36) for mutagenesis: T296, D303, S340, K341, D376, S380, E381 and R383. No corresponding residues to S380 and E381 were identified in DctA of *Pseudomonas aeroginosa*, but this organism does not possess a DcuSR system anyway. The point mutants of DctA were generated in plasmid pMW526 (*dctA-yfp*). By site-directed mutagenesis the single amino acid residues were exchanged against an alanine.

The construct were tested for transport activity by growth experiments. *E. coli* MDO800 (*dctA*) was complemented by the plasmid encoded DctA-YFP variants and cultivated under aerobic conditions with fumarate as sole carbon and energy source. The DctA point mutants were all fully active allowing wild type comparable growth of the *dctA* deficient mutant MDO800 (Fig. R37).

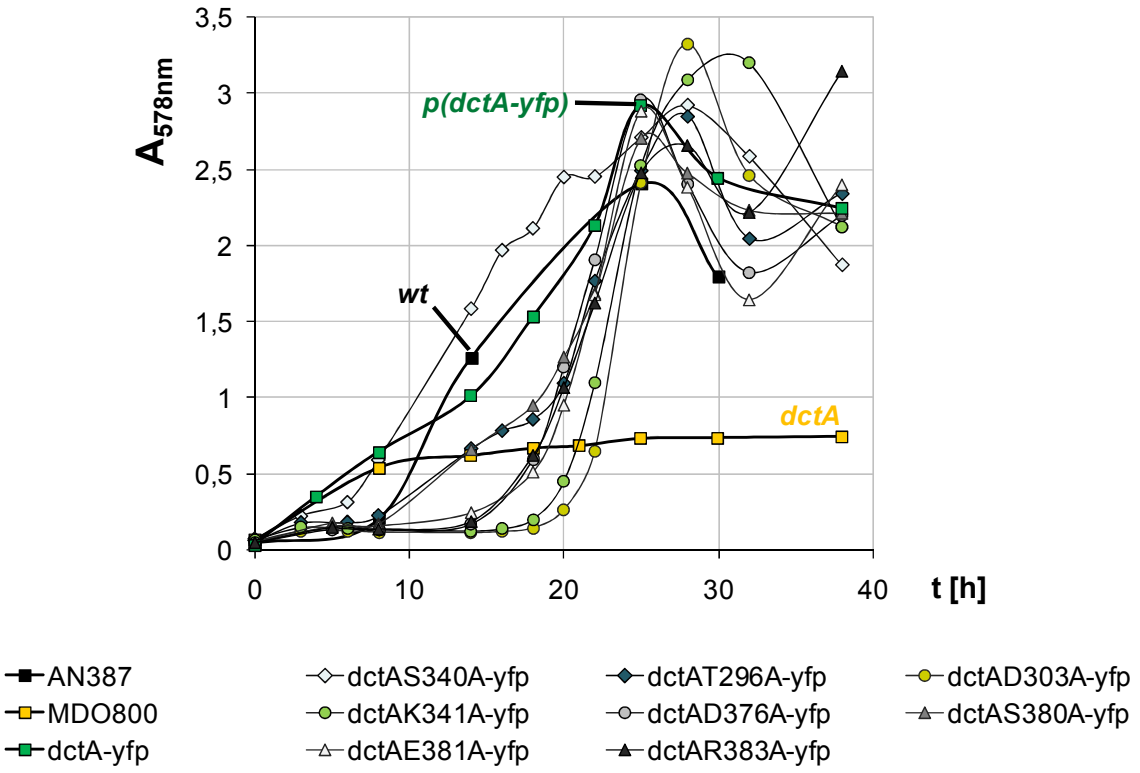

Figure R37: Aerobic growth on fumarate caused by DctA-YFP mutants. *E. coli* wild type AN387 and *dctA* mutant MDO800 complemented with plasmid encoded DctA-YFP (pMW527) or a DctA-YFP mutant carrying a single amino acid substitution within the DctA part were grown aerobically in eM9 medium with fumarate.

Coexpression of the DctA-YFP mutants with DcuS-CFP led to FRET efficiencies comparable to the FRET efficiency of unmodified DctA/ DcuS. The DctA mutants D296A, S340A, K341A, D303A, D376A, S380I and R383A provided FRET efficiencies of 0.12 to 0.15. With wild type DctA, FRET measurements at the same days led to an average FRET efficiency of 0.17. Therefore FRET measurements show no decreased interaction of DctA and DcuS as concluded from the similar FRET efficiencies. The mixture DctA(E381A)-YFP/DcuS only shows a FRET efficiency of about 0.08, but the donor fraction in all samples was clearly below 0.4.

The wild type-like FRET efficiencies obtained from cells producing DcuS-CFP and a DctA-YFP mutant and indicate that either none of the mutations has a regulatory effect, or that the substitution only affects the signal transduction not the oligomerisation.

4.7 *In vivo* Fluorescence measurements with DcuB fused to GFP variants

For interaction studies between DcuB and the membrane-integrated sensor histidine kinase DcuS *in vivo* FRET measurements were performed as described in section 4.6.

In-frame fusions of *dcuB* with *cfp* and *yfp* were constructed on the vector pBAD18-Kan*. The *ecfp* and *eyfp* genes were cloned behind or in front of the *dcuB* gene to obtain three different protein fusions: DcuB with C-terminal CFP (pMW466; DcuB-CFP), DcuB with N-terminal CFP (pMW493; CFP-DcuB) and DcuB with N-terminal YFP (pMW494; YFP-DcuB). The functionality of DcuB in the fusion proteins was checked by using the chromosomal *dcuB´-´lacZ* reporter gene fusion in *dcuB*-deletion strain IMW505. As shown in Figure R38, both N-terminal fused GFP derivatives deprive DcuB of normal regulatory function and are not suitable for functional studies. Fusion of the CFP protein to the C-terminus of DcuB retains the regulatory capacity of DcuB. There is no difference in *dcuB´-´lacZ* expression of DcuB-CFP and DcuB complemented IMW505. DcuB-CFP accordingly is a good candidate for FRET experiments with DcuS-YFP or YFP-DcuS. Unfortunately, however, the DcuB-CFP fusion showed no fluorescence, indicating that no functional CFP protein was formed which could be due to unfold protein or periplasmic localisation of CFP.

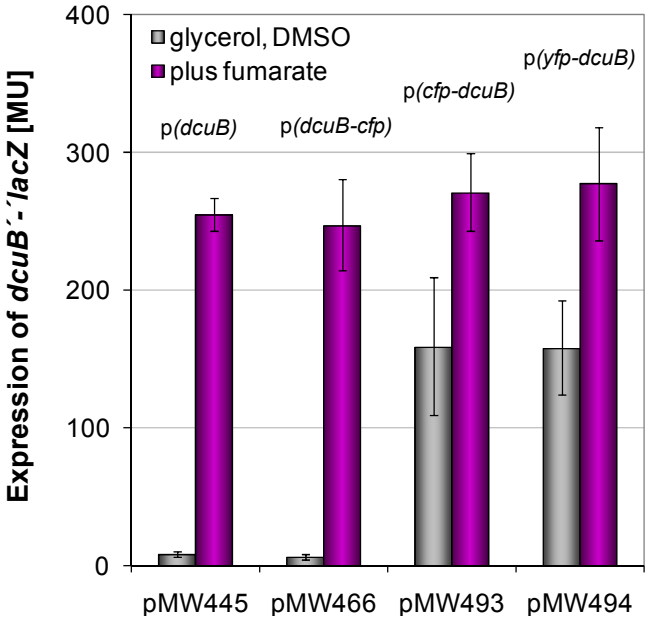

Figure R38: Effect of DcuB-GFP fusions on *dcuB´-´lacZ* expression. The *dcuB* gene, *dcuB-cfp* and *cfp/yfp-dcuB* are encoded on pBAD18-Kan*. Transformants of the *dcuA dcuB dcuC*-negative strain IMW505 were cultivated anaerobically in eM9 medium plus glycerol and DMSO, with and without the effector fumarate.

5. Discussion

5.1 Topology of DcuB

The number and orientation of transmembrane-spanning segments of the anaerobic fumarate/succinate antiporter DcuB were determined by DcuB-PhoA and DcuB-LacZ reporter fusions and cysteine labeling experiments. The topology studies indicate that DcuB consists of 12 membrane-integrated α-helices with both termini located at the periplasmic side of the membrane. For the membrane-spanning helices III and VII to XII, the orientation was clearly shown by PhoA and LacZ fusions. Helices IV to VI probably form hair-pin structures and do not completely span the membrane. This is concluded from an unclear PhoA/LacZ activity ratio and reduced enzyme activities for DcuB junction sites located in this region.

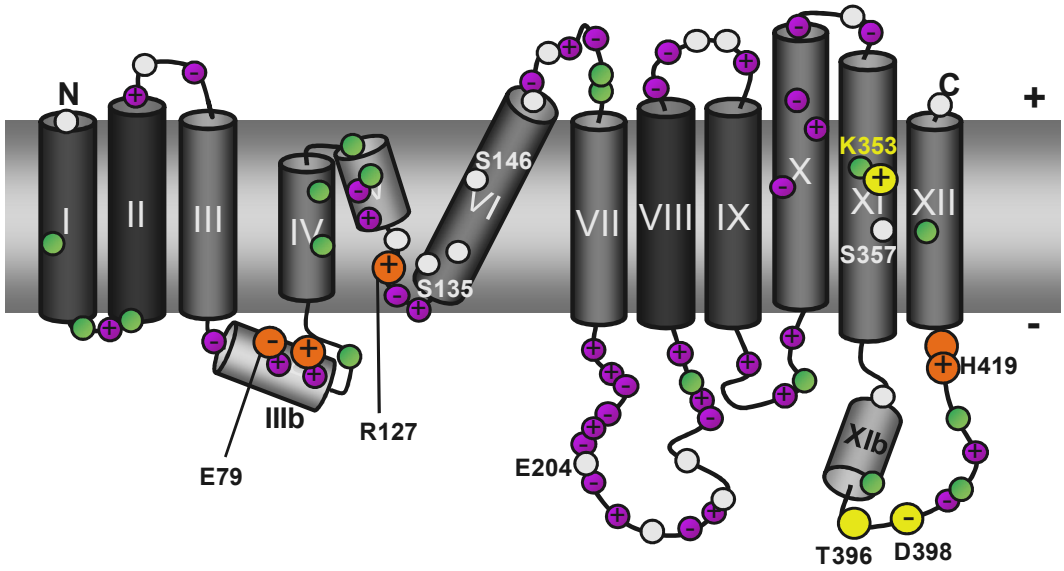

Figure D1: Topology model of DcuB based on PhoA/LacZ reporter fusions, hydropathy plot of the amino acid sequence and secondary structure prediction. Charged amino acid residues are presented in purple. White circles represent AMS accessible sites of the carrier, green circles positions which do not react with the membrane-impermeable sulphydryl reagent AMS in whole cells. Transport and regulatory relevant sites of the carrier were labeled by orange and yellow circles, respectively. The staining of the helices is adjusted to the hydrophobicity of the involved amino acid residues: The darker the color of the helices the more hydropobic the amino acid residues composition.

Provided that the hydrocarbon tail of a phosphatidylcholine bilayer is about 27 Å plus 5 Å for the phospholipid head groups (White *et al.*, 2001), a minimum number of 18 α-helically arranged amino acid residues is required to span the hydrophobic domain of the bilayer, with a few additional residues to tide over the phospholipid groups. For helices IV and V a maximum of only 12 to 15 residues is predicted by the PSIPRED server, whereas helix VI is

supposed to include a total of 29 amino acid residues with a short disruption (Fig. D2). Furthermore helices X and XI (harbouring the regulatory amino acid residue K353) are predicted to be very long with about 30 amino acid residues. In contrast, the α-helical structures of the membrane-spanning segments I and II are predicted to comprise of less than 18 residues. Helices III, VII, VIII, IX and XII are supposed to have a common length of about 20 amino acid residues. In addition to membrane-localised or membrane-spanning helices, three cytosolic α-helices were identified by computational analysis: one situated in the loop III-IV, a short one (not shown in Fig. D1) in the large loop VII-VIII and another within the last soluble segment between helices XI and XII. This last cytoplasmic loop is characterized by 3 β-sheets and a high number of essential amino acid residues required for transport and regulatory function of DcuB.

Labeling experiments with a series of single-cysteine mutants of DcuB demonstrated that most of the tested periplasmic positions are accessible for the thiol reagent AMS. AMS is a rod-like flat molecule with a dimension of about 7 Å in width and 18 Å in length (calculated by Chem3DUltra, AM1 model, www.cambridgesoft.com). Due to its negative charge, AMS is not able to pass the membrane and therefore cannot react with thiol groups of cytoplasmic proteins in intact cells (compare to section 4.3). However, several amino acid residues that are clearly shown to be located in the cytoplasm (E204, E217, S211, D222 in loop VII-VIII and D375 in loop XI-XII) or within the membrane (N125, S135, G138, S146 and S357) were at least partly labeled by AMS. The orientation of loop VII-VIII was clearly confirmed by PhoA/LacZ reporter fusions. Additionally this higly hydrophilic area contains the majority of positive charged amino acid residues and has to be cytoplasmic in accordance to the positive-inside rule (von Heijne, 1986). For D375 a position within the final cytoplasmic loop XI-XII was shown by reporter fusions as well. Since the reaction of maleimides with sulphydryl groups is catalyzed by water, AMS-accessibility of membrane-integrated residues strongly suggest the existence of a water-filled transmembrane channel. With regard to the accessibility studies it is likely that the long helix VI is located with diagonal arrangement in the membrane, adjoining directly to an aqueous channel open to the periplasmic side. Providing an α-helical structure, the AMS accessible amino acid residues S135, G138 and S146 are all located on one side of helix VI.

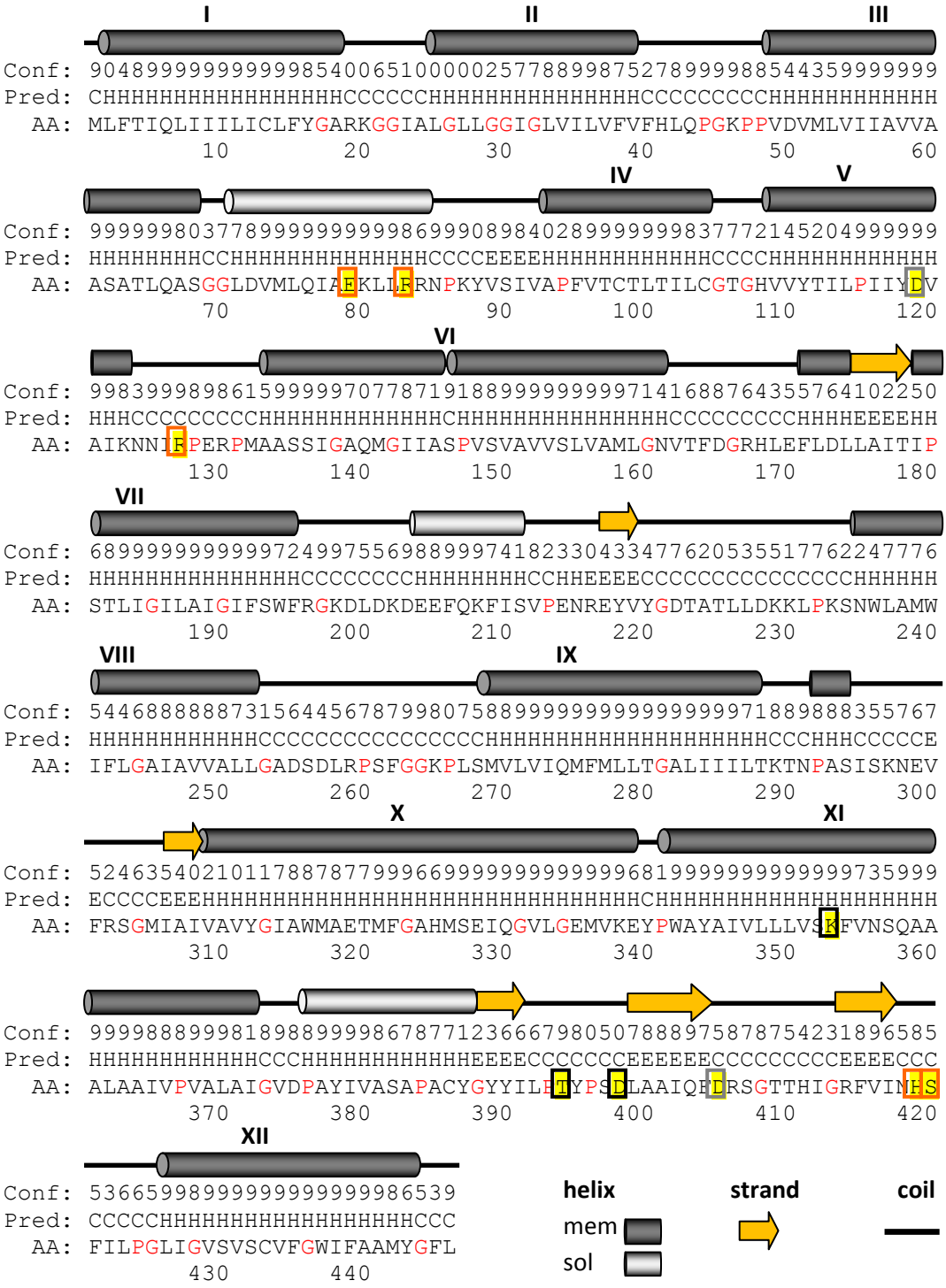

Figure D2: Prediction of secondary structure of DcuB by PSIPRED (PSIPRED V2.6 by D. Jones) Conf, Confidence (0=low, 9=high); Pred, Predicted secondary structure (H=helix, E=strand, C=coil); AA, amino acid sequence of DcuB. Membrane-integrated helices (dark grey barrels) are numbered in accordance to the DcuB topology model shown in Fig. D1 and D3. Essential amino acid residues of DcuB are highlighted in yellow and surrounded by coloured rectangles: orange, transport relevant sites; black, regulatory relevant site; grey, relevant for transport and regulatory function. Proline and glycine residues are shown in red.

Membrane-integrated cysteins were already shown to be accessible for bulky thiol reagents when located in a water-filled channel. For the multidrug ABC transporter LmrA of *Lactococcus lactis* a reaction of single cysteine residues in a predicted transmembrane helix (TM) with fluorescein-5-maleimide was observed (Poelarends & Konigs, 2002). The periodicity of fluorescein maleimide accessibility indicated the existence of a deep aqueous cavity which is faced by one side of the membrane-spanning alpha-helix. Residues that were not labeled by the membrane-impermeable thiol reagent are assumed to be exposed to the lipid environment. A similar accessibility was identified for residues that are located within TM II of the Na^+/proline transporter PutP (Pirch *et al.*, 2003).

The fluoresceine-derivative Oregon Green Maleimide was used to study the solvent exposure of TM XII of the osmoprotectant transporter ProP (Liu *et al.*, 2007). ProP is a member of the major facilitator superfamily (MFS) and catalizes ΔpH and ΔΨ dependent symport of proline (or other osmoprotectants) with H^+.

The distance between cysteinyl thiol group and peptide backbone is about 8-10 Å (Fu & Maloney, 1998). Therefore membrane-impermeable bulky maleimide derivatives generally can react with cysteines substitutions of the outer 5-6 amino acid residues of a TM. The presence of a deep aqueous cavity otherwise allows reaction of AMS with residues in the middle of the membrane, and possibly also with cytoplasmic amino acid residues. This assumption could provide an explanation for reaction of the cytoplasmic residues E204, E217, S211, D222 and D375. Since AMS was not able to pass the membrane, the results indicate an involvement of soluble parts of DcuB in facing the transport channel. In contrast to somer other transporters of known structure (LacY, GlpT, EmrD) the transport channel of DcuB seems to be widely open to the periplasm.

TM VI, the membranous loop between helices V and VI, TM XI and probably helices X (due to the number of charged amino acid residues) and XII (adjacent transport-relevant sites H419 and S420) are supposed to contribute to the transport channel. In addition a part of the large cytoplasmic loop VII/VIII and the soluble α-helix XIb seem to face the cytoplasmic part of the hydrophilic pore. The more hydrophobic helices I, II, VIII and XI are putatively embedded in the bilayer without solvent exposure, confining the channel-lining helices from the surrounding membrane.

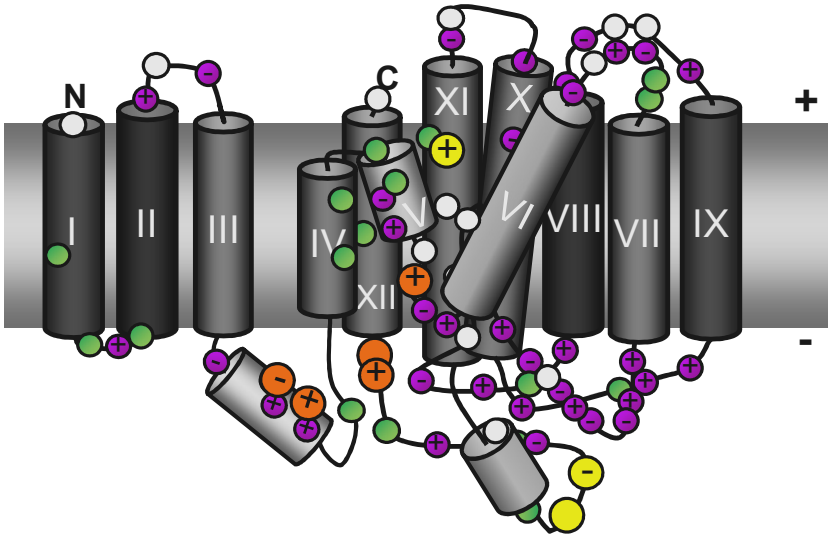

Figure D3: Potential arrangement of the channel-forming segments of DcuB within the membrane. Helices V, VI, X, XI and XII form a hydrophilic pore which almost passes through the phospholipide bilayer. The cytoplasmic part of the channel is faced by charged amino acid residues of loop V-VI and loop VII-VIII. Helices III, IV and VII as well as the higly hydrophobic helices I, II, VIII and IX are supposed to separate the central cavity from the lipid environment (for a clearer illustration these surrounding helices were placed on the side). The cytoplasmic α-helical structures may participate in closing the pore to the cytosol. At least two transport-relevant sites (E79, R83) were identified in the hydrophilic helix IIIb, indicating an interaction with transported substrate or with the transport channel. For the beginning of helix XIb, AMS-accessibility in whole cells was identified. Purple circles, charged amino acid residues; white circles, AMS accessible; green circles, not AMS accessible; orange circles, transport sites; yellow circles, regulatory sites.

The topology of the carrier DcuA clearly differs from the topology of DcuB. In particular the C-terminal part of the related proteins shows a strong structural discrepancy (Fig. D4A; B). While the C-terminus of DcuB is characterized by a large cytoplasmic loop finally resulting in a terminating in-out helix, DcuA possesses a large soluble terminus located in the periplasm. Since the correct fold of a protein is essential for function, these differences could be the reason for the lack of regulatory features of DcuA. Single amino acid substitutions in DcuA were not sufficient to create a regulatory DcuA variant, supporting the view that not only the amino acid sequence but the total structure of a carrier defines its nature. Interestingly, the $DcuA_{A374}$(TMX)-DcuB(loopXI/XII) hybrid protein, composed of the N-terminal part of DcuA and the C-terminal helical segment of DcuB, was shown to affect DcuSR-dependent expression. These findings support the conclusion, that similarity between proteins is not only based on the sequence similarity but also on the structure.

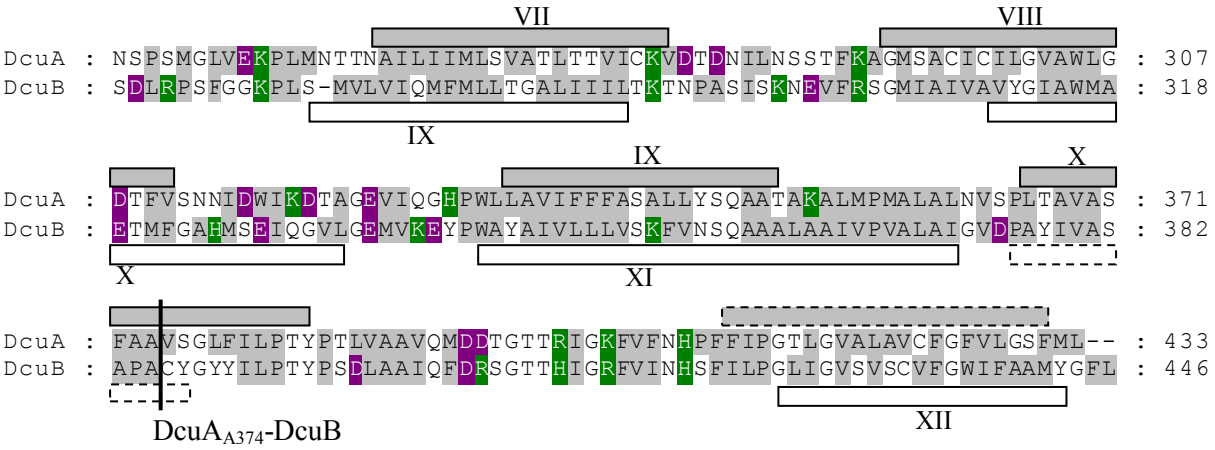

Figure D4A: Sequence alignment of the C-terminals of DcuA and DcuB. The positions of predicted transmembrane helices (black lined bars) and soluble helical structures (dotted lines) at the C-terminus of DcuA (grey bars; Golby *et al.*, 1998) and DcuB (white bars) are shown. Hydrophobic, acidic and basic amino acid residues are highlighted in grey, purple and green. The junction site of the DcuA$_{A374}$-DcuB hybrid protein is marked by the black line in the sequence alignment and by a star in the according topology models of DcuA and DcuB.

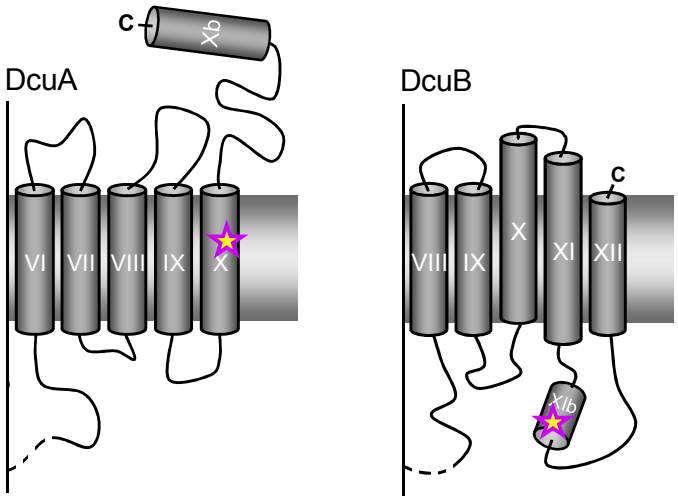

Figure D4B: C-terminal topology of DcuA (by Golby *et al.*, 1998) and DcuB. The positions of TM VII, VIII and IX of DcuA are in accordance with TM IX, X and XI of DcuB. Helix X of DcuA corresponds to the cytoplasmic helical structure in loop XI-XII of DcuB while the last helix of DcuB complies with the terminal periplasmic helix of DcuA.

Analogy to transport proteins of known structure

The Protein Data bank contains only few structures of transmembrane carriers with ten or more helices. The candidates most similar to DcuB are members of the major facilitator superfamily (MFS), or belong to other families of secondary transporters and antiporters.

Hydropathy sequence analysis and reporter fusion experiments indicate that most MFS proteins have 12 transmembrane helices and are organized in two six-helix halves with the N- and C-termini located in the cytosol (Pao *et al.*, 1998). Although MFS proteins show similar transmembrane topology, only weak sequence similarity was observed (Maiden *et al.*, 1987).

Well studied proteins of the MFS are Ox1T, the oxalate/formate antiporter of Oxalobacter formigenes, and the transporters GlpT, LacY and EmrD of *E. coli*.

X-ray structures of LacY were obtained for the conformationally constrained C154G mutant (Abramson *et al*., 2003) as well as from wild-type LacY (Guan *et al*., 200/). Both crystal structures showed the same global fold of two six-helix bundles organized with twofold pseudosymmetry. The six-helix bundles are connected by a long loop and complement each other to a heart-shaped structure with a large interior hydrophilic cavity that isopen to the cytoplasmic side (Fig. D4). In contrast to the findings for DcuB, the periplasmic side of LacY was shown to be tightly closed.

In its largest dimensions, LacY was about 60 Å in height and 60 Å in width. Normal to the membrane, the monomer was shown to be oval-shaped with dimensions of 30 by 60 Å. The hydrophilic cavity opens to the cytoplasm with dimensions of 25 by 15 Å. It is faced by a total of eight helices: TM I, II, IV, and V that belong to the N-terminal domain and helices VII, VIII, X, and XI of the C-terminal domain. The remaining helices III, VI, IX, and XII were found to be largely embedded in the phospholipid bilayer (Fig. D4). The binding site of the lactose homologue β-D-galactopyranosyl-1-thio-β-D-galactopyranoside within the hydrophilic cavity was detected at a similar distance from both sides of the membrane involving residues of helices I, IV, V, VII and IX (Abramson *et al*., 2003).

Based on thermodynamic considerations and kinetic studies (Jencks, 1980; West, 1997) an alternating access mechanism for secondary carriers was developed, which is supposed to be characterized by an inward-facing (Ci) and an outward-facing (Co) conformation. For LacY the inward-facing conformation is assumed to represent the lowest free-energy state in the membrane (Guan *et al*., 2007). Substrate-binding is supposed to cause rotation between the N- and C-terminal domains around the axis parallel to the membrane (Abramson *et al*., 2003) resulting in opening of the transport channel to the periplasmic side. This hypothesis is sustained by the finding that the eight channel-forming helices are disturbed by kinks and bends. Each of these helices harbors proline and glycine residues commonly found in irregular helices which are assumed to provide structural flexibility required for conformational changes. Helices VI, IX, and XII, which are not part of the hydrophilic cavity, are unperturbed. For DcuB disrupted (TM VI), proline or glycine-rich (TM II, VI, VII, X) and irregular short α-helical structures (helices IV, V) are predicted in a similar way.

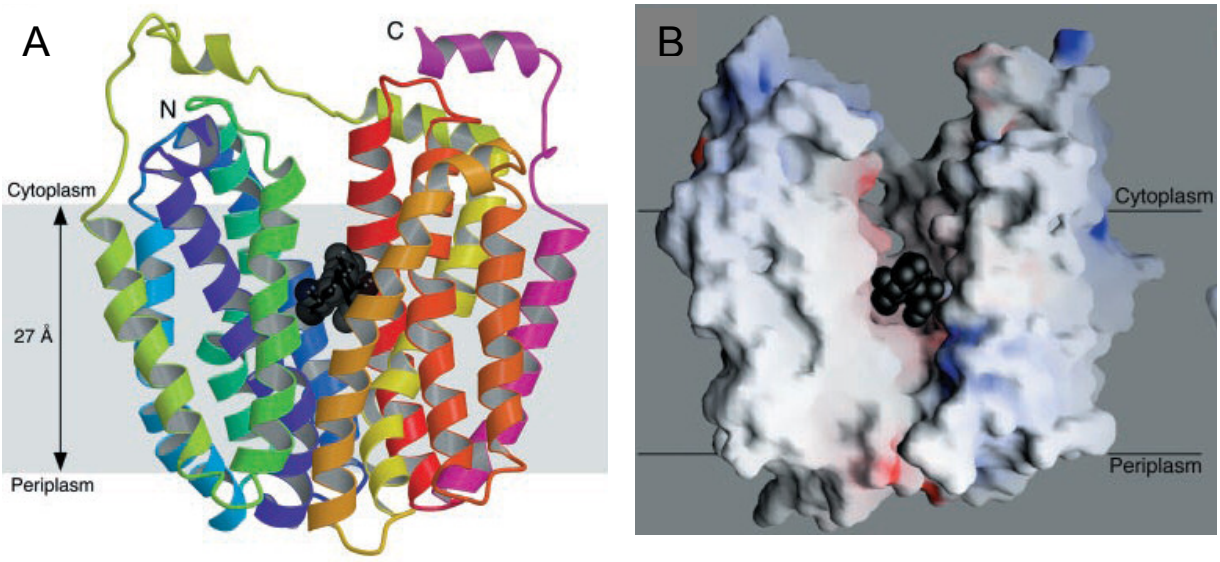

Figure D4: Crystall structure of LacY C154G mutant with the lactose analogon TDG. (**A**) Ribbon representation of LacY viewed parallel to the membrane. The 12 transmembrane helices are colored from the N-terminus in purple to the C-terminus in pink; TDG, β-D-galactopyranosyl-1-thio-β-D-galactopyranoside, is represented by black spheres. (**B**) View to the membrane- internal hydrophilic cavity of LacY. The polar surfaces are colored blue (positively charged) and red (negatively charged). The black spheres denote TDG. For clarity, helices V and VIII have been removed (Picture taken from Abramson *et al*., 2003).

The structure of the glycerol-3-phosphate transporter GlpT of *E. coli* was determined by x-ray crystallography (Huang *et al*. 2003), revealing a LacY-related global fold. GlpT is composed of a funnel-shaped outer part and a cylindrical inner part. The inner part measures 10 by 8 Å with several amino acid side chains protruding into the channel. The pore is about 30 Å in depth and, in the crystallized form, opens from the middle of the membrane to the cytoplasm. The whole molecule measures about 35 by 60 Å at the cytoplasmic side narrowing to 35 by 45 Å at the periplasmic side. As determined for LacY, the height of GlpT is about 60 Å (Huang *et al*. 2003). Since GlpT is assumed to function as a monomer, the central pore at the interface of the N- and C-terminal domains is supposed to forms the substrate-translocation pathway. Similar to LacY, the putative translocation channel is lined by eight (four peripheral and four central) helices.

A well characterized example for a membrane-integrated antiporter is the $Na^{+/}H^{+}$ antiporter NhaA of *E. coli*. NhaA posesses 12 transmembrane segments with its N- and C-termini exposed to the cytoplasm (Hunte *et al*., 2005). Experimental studies have shown that NhaA functions as a dimer in the native membrane (Williams *et al*., 1999; Gerchman *et al*., 2001; Hilger *et al*., 2005) although the monomer was found to be fully active. In contrast to the members of the MFS, a cross-section of the antiporter normal to the membrane showed the

presence of a cytoplasmic and a periplasmic funnel, separated by a hydrophobic barrier (Hunte *et al*., 2005, Padan *et al*., 2009).

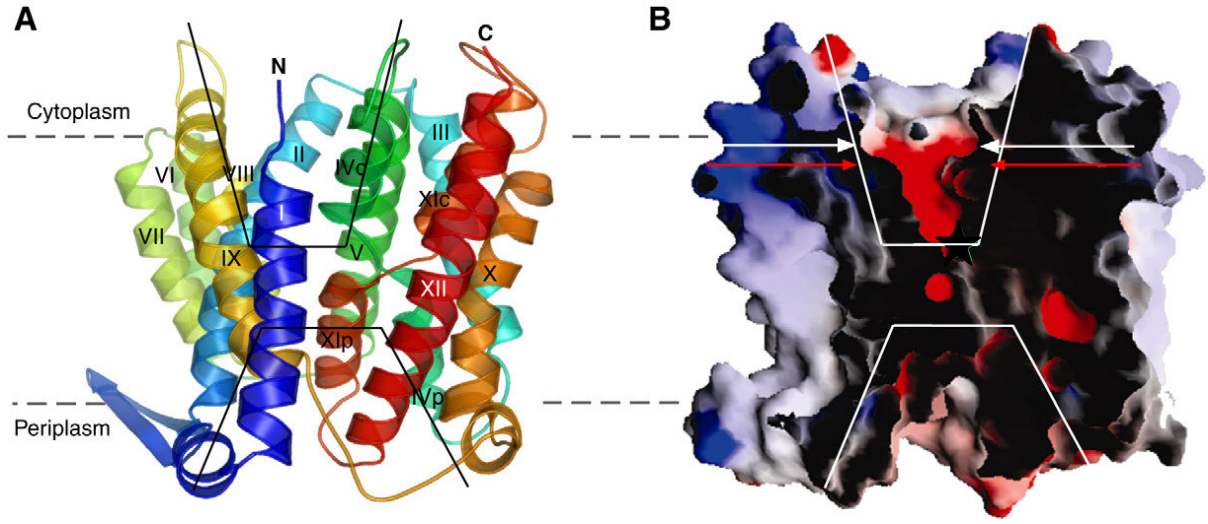

Figure D5: Structure of the Na^+/H^+ antiporter NhaA. (**A**) Ribbon representation of the crystal structure of NhaA, viewed parallel to the membrane. Funnels are marked by continuous black lines. (**B**) Cross-section through the antiporter, normal to the membrane, with the front part removed. The cytoplasmic and periplasmic funnels are marked by white lines (Picture taken from Hunte *et al*., 2005).

NhaA shows an intra-molecular inverted topology of several helices, including a pair of discontinuous helices interrupted by an extended chain (Hunte *et al.,* 2005; Screpanti & Hunte, 2007). The X-ray structures revealed that the extended chain, the partially charged helical termini and the polar or charged residues in close proximity provide the structural basis for the ion-binding site (Padan *et al*., 2009).

Similar structures that are supposed to confer flexibility for conformational changes were also identified for other ion transporters like different kinds of ATPases (Olesen *et al*., 2007; Takahashi *et al*., 2007; Morth *et al*., 2007; Pedersen *et al*., 2007) and other secondary transporters like the Sodium Galactose Transporter SGlT of *Vibrio parahaemolyticus* (Faham *et al*., 2008), the Leucine transporter $LeuT_{Aa}$ of *Aquifex aeolicus* (Yamashita *et al*., 2005) and Glt_{Ph} of *Pyrococcus horikoshii* (Yernool *et al*., 2004). The crystal structure of the DctA-related glutamate transporter homologue Glt_{Ph} revealed a trimeric aggregation pattern of the protein. Sodium-dependent glutamate transporters are members of an integral membrane transporter family including some eukaryotic glutamate and neutral amino acid transporters and a large number of bacterial amino acid and C_4-dicarboxylate transporters (Slotboom *et al.* 1999). In contrast to their diverged amino acid sequences, the hydropathy profiles of the

members of the family are extremely well conserved suggesting a comparable global structure (Slotboom *et al.*, 1999).

Due to a higher expression level and improved crystallization properties, a multiple point mutant of Glt_{Ph}, $Glt_{Ph}H7$, was used for structural studies by Yernool *et al*. (2004). However, data obtained from an isomorphous Glt_{Ph} crystal indicate no significant differences between wild type protein and mutant. The $Glt_{Ph}H7$ trimer was found to be about 65 Å in height, bowl-shaped and showed a three-fold NCS (non-crystallographic symmetry) with the axis perpendicular to the membrane. It formed a solvent-filled extracellular pore of about 50 Å in diameter and 30 Å in depth. The surface of the deep cavity was identified to be highly hydrophilic, allowing substrates and ions to reach the midpoint of the membrane bilayer where the substrate-binding sites are located.

The protomers of $Glt_{Ph}7H$ comprise of eight primarily a-helical transmembrane segments (TM) and two helical hairpins (HP) and are shaped like pointed wedges (Fig. D6). The wide ends of three protomers define the periplasmic rim of the basin while the converging tips configure the cytoplasmic bottom of the basin. The C-terminal half of each protein (helix 7, helix 8, HP1 and HP2) was identified to be surrounded by the N-terminal helices which mediate the intersubunit contacts in the trimer (Fig. D6B).

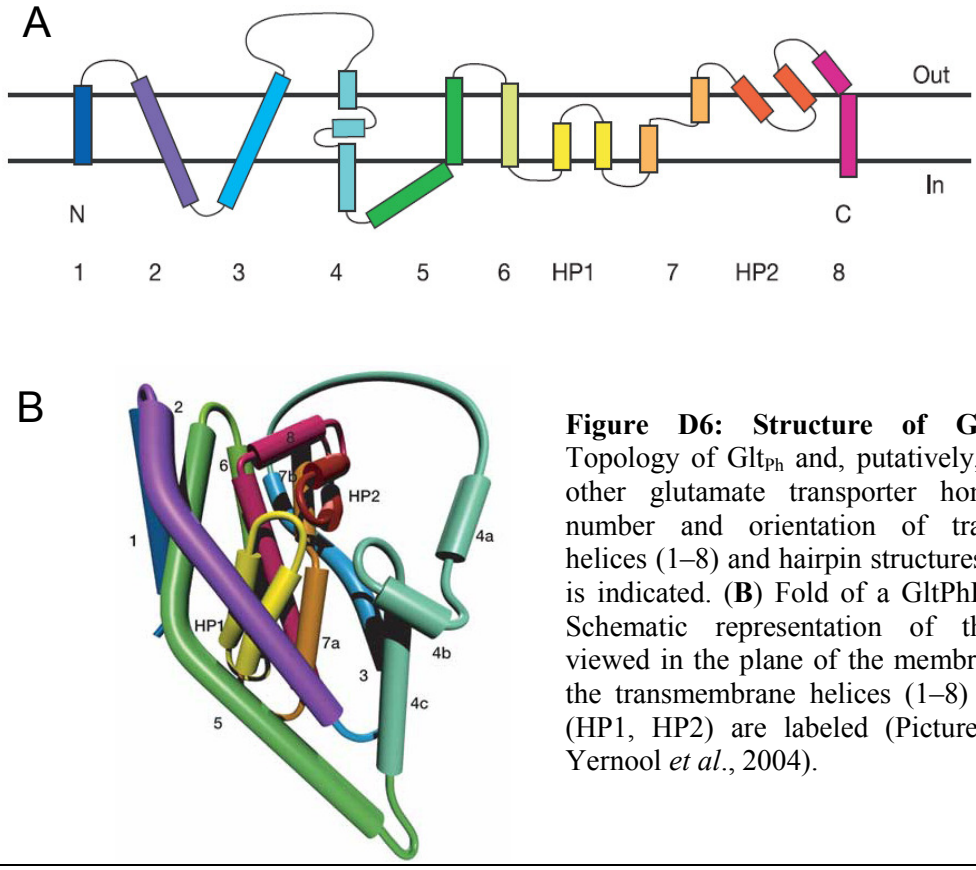

Figure D6: Structure of $Glt_{Ph}H7$. (A) Topology of Glt_{Ph} and, putatively, topology of other glutamate transporter homologs. The number and orientation of transmembrane helices (1–8) and hairpin structures (HP1, HP2) is indicated. **(B)** Fold of a GltPhH7 protomer. Schematic representation of the protomer viewed in the plane of the membrane in which the transmembrane helices (1–8) and hairpins (HP1, HP2) are labeled (Picture taken from Yernool *et al*., 2004).

In eukaryotic and prokaryotic glutamate and neutral amino acid transporters the C-terminal residues are involved in substrate binding, substrate transport and ion-coupling (Kanner & Borre, 2002; Slotboom *et al*., 2001). With regard to the isolated transport sites it is suggested that each Glt_{Ph}7H monomer has an independent substrate-translocation pathway.

As shown for LacY and NhaA, Glt_{Ph}7H is composed of a number of unexpected elements of secondary structure. Helices 2, 3 and 5 are up to 49 residues in length and strongly tilted from the membrane normal. Helix 7 interrupted by an extended chain as described for helix XI of NhaA. The membrane-integrated parts of hairpin structure HP1 and helix 8 are highly hydrophilic and therefore not predictable by common topology server. Helix 4 finally is composed of three elements presenting an unusual corkscrew-like, helix-turn-helix-turn-helix motif. Some of these elements, like very long or short helices, putatively interrupted and kinked helices might also exist in DcuB.

Since DctA of *E. coli* and Glt_{Ph} belong to the same family of transport proteins, it is possible that DctA shows a Glt_{Ph}-like structure. The sequence identity of both proteins is only 26%, but the hydropathy profile within the family of glutamate is conserved and it is assumed that the members share a similar global structure. (Slotboom *et al.*, 1999). A trimeric oligomerisation state as shown for Glt_{PH} was also determined for the human glutamate transporter EAAT2 and the GltP of *E. coli* (Gendreau *et al*., 2004) which is at least 37% identical to DctA. The topology of DctA was not investigated experimentally, but by transmembrane helix predictions (TMHMM server). In particular the C-terminal half of the predicted topology of DctA differs strongly from the topology determined for Glt_{Ph} (Fig. D7). However, this is no evidence for a divergent structure, since the computational predictions for Glt_{Ph} do not fit the determined structure as well. As expected, the highly hydrophilic helices were not predicted by common topology servers.

Determination of the DctA topology analogues to DcuB would be important to confirm a Glt_{Ph}-like structure of the succinate transporter. Furthermore the oligomerisation states of DctA and DcuB should be identified, for example by chemical cross-linking and in the case of DctA by additional FRET measurements. To obtain more information about transport and regulatory function of DctA, the active sites of DctA should be identified by growth experiments, transport measurements and *dctA´-´lacZ* expression studies with DctA point mutants.

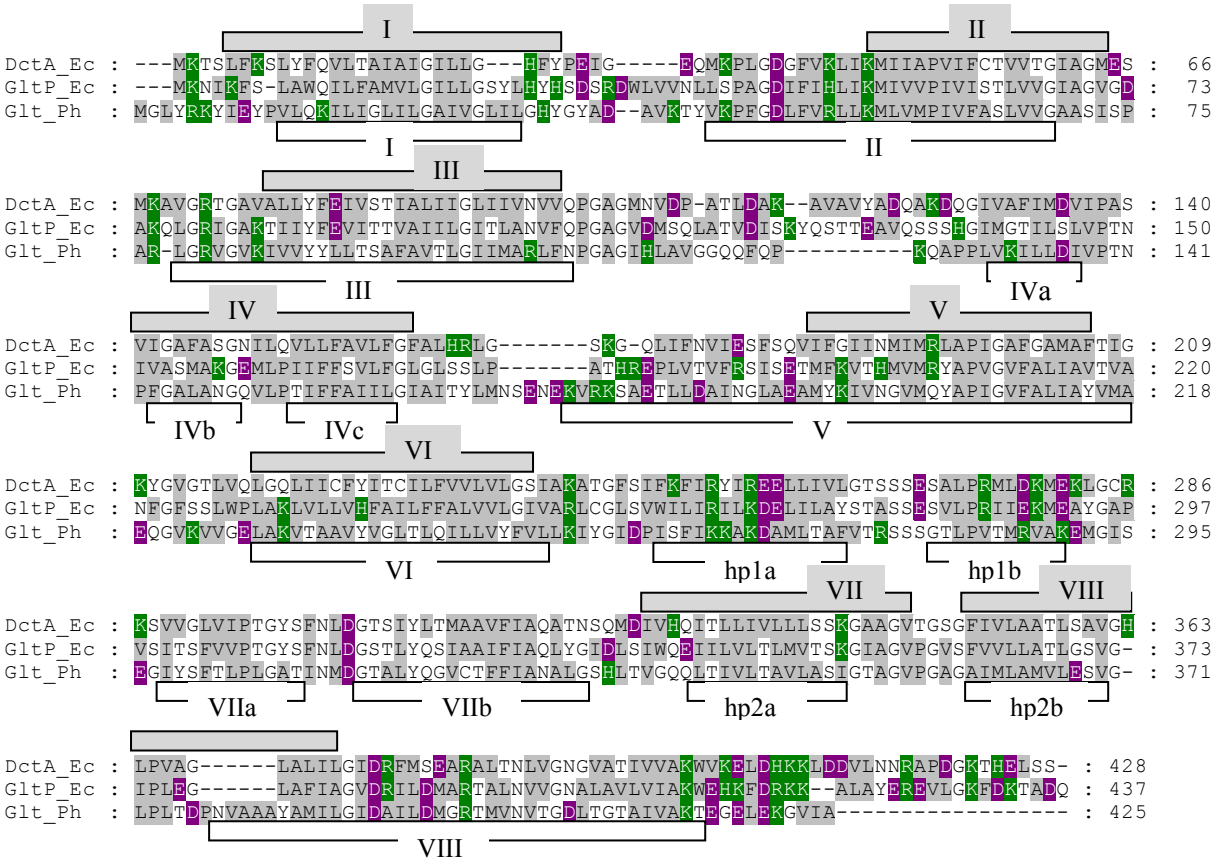

Figure D7: Sequence alignment of bacterial members of the glutamate transporter family. TMHMM-predicted transmembrane helices of the succinate carrier DctA of *E. coli* (DctA_Ec) are represented by grey bars above the sequences; membranous segments of the glutamate transporters Glt of *Pyrococcus horikoshii* (Glt Ph) are indicated on the bottom of each line. In addition, the sequence of GltP of *E. coli* (GltP_Ec) is shown. The identities are 37% for DctA_Ec and GltP_Ec, 33% for GltP_Ec and GltPh and 26% for DctA_Ec and GltPh. Hydrophobic amino acid residues are highlighted in grey, acidic residues in purple and basic residues in green. hp, hairpin.

The examples of membrane carriers with solved structure demonstrate, that hydrophobic, regular α-helices oriented normal to the membrane bilayer do exist, but are not the rule as expected originally. Helices of varying compositions from polar and apolar amino acid residues and variable size cross the membrane in the different angles. The helices can be kinked, bended or interrupted by coiled segments. Helices have been identified, which lie on the surface of the bilayer or span only part of the membrane, turning back and forming re-entrant loops or hairpins. The membrane-embedded structures do not even have to be α-helical. All these characteristics of multitransmembrane proteins hinder the computational topology prediction since the programs mainly analyze the preference of amino acid residues to be located within the membrane, at the interface, or in a loop inside or outside the membrane. Most prediction programs are working very well for isolated peptides, but reach

their limitations for proteins of more complex structures. Potential interactions between single helices that benefit the integration of more hydrophilic elements are not predictable by now. The first topology prediction program that is able to model re-entrant regions is OCTOPUS by Viklund & Elofsson (2008).

5.2 Model for sensing of C_4-dicarboxylates in *E. coli*

In *E. coli* C_4-dicarboxylate metabolism is regulated by the two-component system DcuSR. Under anaerobic conditions and in the presence of functional DcuB, the sensor kinase DcuS activates expression of the anaerobic target genes *dcuB, fumB* and *frdABCD* in the presence of C_4-dicarboxylates (Fig. D8). Is the succinate/fumarate antiporter deleted or inactivated, the expression of the target genes becomes independent of effector (Fig. D8C), indicating a permanent "on"-state of DcuS. DcuB and, in a similar manner, the aerobic succinate carrier DctA act as regulatory cosensors of the DcuSR system. In the absence of C_4-dicarboxylates DcuB is supposed to block the gene activation by direct interaction with DcuS (Kleefeld *et al.*, 2009). Therefore DcuB or DctA are required for an inactivation of DcuSR when no effector is available.

Close proximity or interaction of DctA and the sensor kinase DcuS was proven by FRET-based interaction studies. We can conclude that at least in the absence of effector transporter and sensor get in touch with each other. It is assumed that the transporter inhibits signal transduction by direct interaction with DcuS. The regulatory relevant amino acid residue K353 of DcuB is located within or close to the putative substrate translocation channel. The absence of substrate may be sensed by this residue leading to a conformational change of the protein, in particular of the adjacent cytoplasmic loop. The large loop harbors another regulatory site of DcuB which supposedly interacts with DcuS. It is suggested that the cytoplasmic PAS domain (PAS_C) of DcuS shows an intrinsical plasticity and plays an important role in signal transduction (Etzkorn *et al.*, 2008). The cytoplasmic PAS domain presumably contains the relevant site for interaction with DcuB and DctA.

Several point mutations within the periplasmic binding domain of DcuS were identified that inactivate DcuS and cause permanent repression of *dcuB`-`lacZ* expression independent of effector and independent of DcuB (Kleefeld *et al*., 2009). Effector-binding is supposed to induce a conformational change in DcuS resulting in activation of the sensor kinase (Kneuper *et al*., 2010). A functional DcuSR system therefore depends on the presence of two factors: effector-binding and presence of a cosensing transport protein. It is likely that the inactive

state of DcuS requires protein-protein interaction with DcuB or DctA. For activation of the sensor, on the other hand, an intact substrate-binding site is essential.

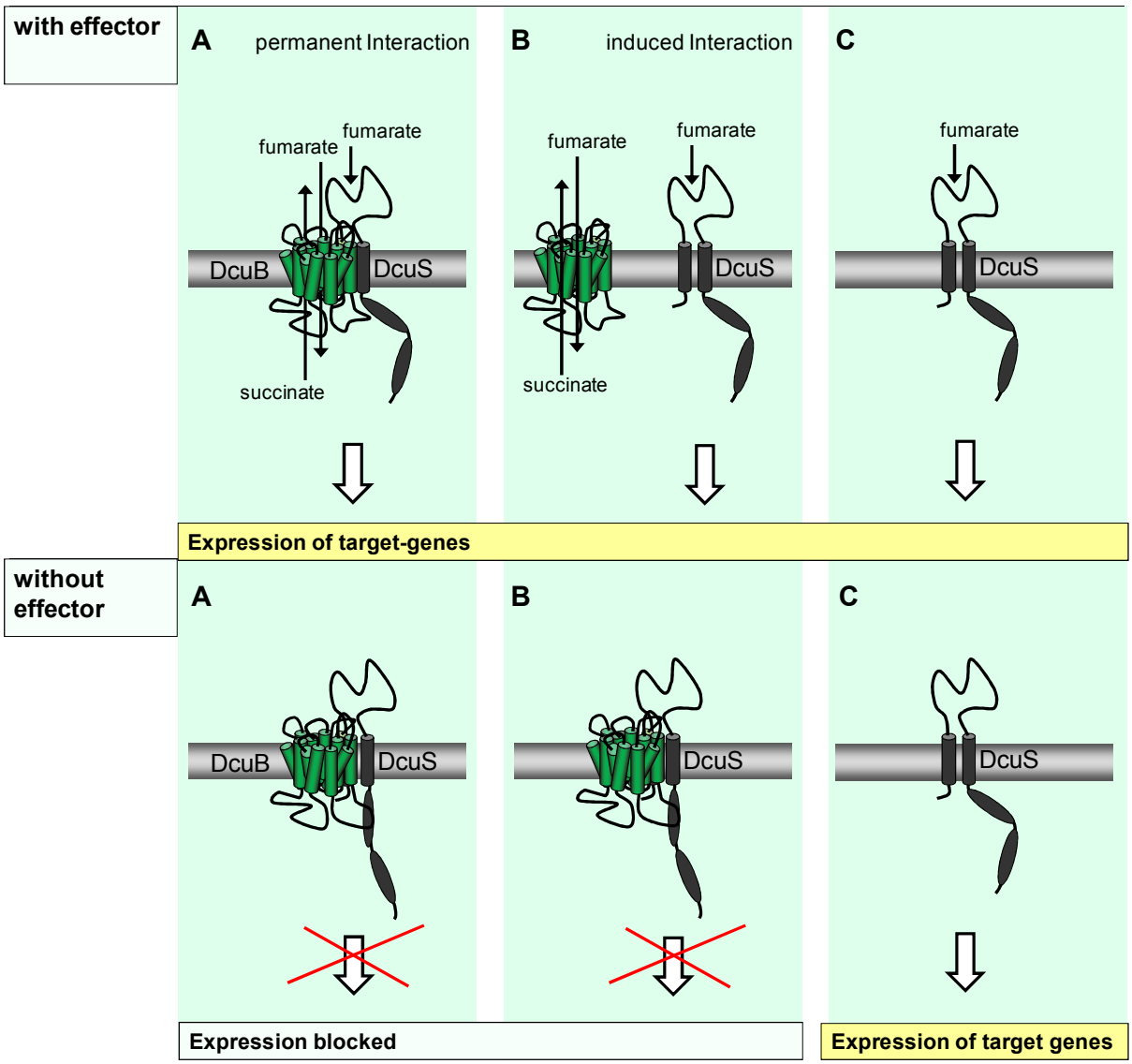

Figure D8: Models for regulation of DcuSR dependent gene expression by DcuB. In the presence of C_4-dicarboxylates ("with effector") transport is catalized by the anaerobic fumarate/succinate antiporter DcuB while expression of the target genes is stimulated by the two-component system DcuSR. If no effector is available for transport ("without effector"), the expression of the DcuSR target genes is prevented by interaction between DcuB and the membrane-integrated sensor kinase DcuS. Direct interaction between DcuB and DcuS could be continuously with DcuB-induced repression of signal transduction in the absence of effector (**A**) or effector-dependent (**B**). A lack of functional DcuB protein was found to cause an effector-independent expression of the target genes (**C**).

Two alternative models of C_4-dicarboxylate sensing by DcuS and DcuB/DctA as a cosensor can be proposed (Fig. D8A and B). The first model postulates a permanent interaction of transporter and sensor, whereas the second model suggests a negative effector-induced

interaction. Signal transduction by DcuS in response to C_4-dicarboxylates requires an intact substrate-binding site of DcuS, the presence of effector and the presence of regulatory DcuB/DctA. As long as fumarate is available, the substrate-binding sites of DcuS and DcuB/DctA are occupied and the effector-induced signal transfer through the membrane causes expression of the target genes. It is possible, that the signal-transferring state of DcuS is supported or stabilized by DcuS/DcuB (Fig. D8A). In the absence of effector, the respective carrier is supposed to interact directly with DcuS repressing the conformational change, autophosphorylation or phosphorylation of the response regulator. In the absence of DcuB, DcuS is in a permanent "on"-state (Fig. D8C), but only if the periplasmic binding site is intact. The lack of DcuB propably leads to a destabilization of the protein structure and therefore to a constant signal transduction of functional DcuS.

Regarding the *dctA´-´lacZ* expression studies, a permanent interaction or at least permanent contact between carrier and sensor is more likely than an effector-dependent interaction. In the *dctA*-deletion mutant a generally increased *dctA* expression was observed, indicating a slight repression of DcuSR in the absence and in the presence of effector.

The concentration of sensor proteins is generally low compared to the amount of transport proteins. Therefore only a small fraction of transporters might be in direct touch with the two-component system. Studies with plasmid-encoded DcuB are in accordance with this conclusion. Complementation of regulation was achieved with low-copy and high-copy plasmids and after strong and weak induction, or even in the non-induced state. In contrast, complementation of anaerobic C_4-dicarboxylate transport and growth required a higher content of DcuB protein. Only expression plasmids that are gradually inducible or allow expression under the control of the *dcuB*-promotor were suitable to mediate growth by fumarate respiration. Therefore, an overexpression or recombinant expression of the fumarate/succinate antiporter for anaerobic growth was successful only under specific conditions. Low DcuB concentrations obviously led to insufficient transport capacities; high DcuB concentrations caused cell death, presumably due to membrane damage. Based on these observations it is concluded that only a small portion of DcuB interacts with DcuSR, while the majority functions as antiporter.

DcuB and DctA strongly influence the expression of DcuSR target genes, but on the other hand, synthesis of both carriers completely depends on gene activation by DcuR. Even though *dctA* expression increases only two to four-fould in the presence of C_4-dicarboxylates, the *dcuS* mutant is not able to grow aerobically on fumarate as a carbon and energy source. By

growth experiments nearly no difference for growth on C_4-dicarboxylates between *dctA* mutant, *dcuS* mutant and *dctA dcuS* double mutant was detectable.

For half-maximal expression of the anaerobic DcuSR target genes, C_4-dicarboxylate concentrations up to 3 mM are required (Kneuper *et al*., 2005), which corresponds to an apparent K_m value for the sensor kinase. The studies on substrate affinity and specifity were performed with the intact DcuSR system that is in a DcuB-positive background. Therefore the values presented presumably represent the response of the DcuB-DcuSR system with the contribution of effector binding to the binding sites of DcuS and DcuB. The apparent K_m values for the isolated transporters (about 10 µM for DctA and 100 µM for DcuB) were determined by transport measurements (Six *et al*., 1994; Engel *et al*., 1994). Since the presence of effector is not required for expression of the DcuSR-dependent genes in a *dcuB*-negative background, signal transduction is not only caused by substrate binding at the periplasmic PAS domain (PAS_P) of DcuS. The sensor kinase possesses two sites for signal-input: PAS_P and the cytoplasmic PAS_C domain. Experiments with transport active, but regulatory-restricted DcuB mutants also cause continuous signal transduction by DcuS similar to the *dcuB* mutant. These findings could mean that the regulatory site of DcuB is required to stabilize DcuS in the "off"-state as long as no effector is available. A loss of interaction between carrier and sensor may lead to a disorder in the DcuS-PAS_C structure and therefore activation of the response regulator. It is not excluded that the carriers have partly adopted the periplasmic sensing function of DcuS (mediated by PAS_P), similar as suggested for the lysine permease LysP and the membrane-integrated transcription factor CadC (Tesch *et al*., 2008). For the C_4-dicarboxylate sensor DctB of *Rhizobium meliloti* interaction with the transporter DctA is supposed to improve the substrate specifity of the two-component system DctBD (Yurgel *et al*., 2000).

5.3 Database research for bacterial DcuB, DcuSR and DctA homologues

Screening of bacterial genomes for the presence of *dcuSR, dcuB* and *dctA* genes (Tab. D1) indicates that the combination of DcuSR and the transporters DcuB and DctA is a characteristic of γ-proteobacteria, in particular of the enteric bacteria. All examined enteric bacteria contain DcuB, DctA, DcuS and DcuR homologues. There was only one exception: the opportunistic pathogen *Providencia stuartii* that is commonly found in soil, water and sewage. The facultative anaerobic bacterium does not possess a DcuSR-like two-component system, but genes coding for DcuB and DctA-like proteins with an identity of 86 and 60% to

the respective proteins of *E coli*. The highly conserved DcuB proteins of *Salmonella typhimurium* (97% identity) and *Erwinia carotovora* (87% identity) were shown here to complement DcuB function in E. coli. Both DcuB homologues could mediate anaerobic growth on fumarate to a *dcuA dcuB dcuC* mutant of *E. coli* and showed a clear regulatory effect on *dcuB*`-`*lacZ* expression. These results indicate an interaction of the foreign proteins with the *E. coli* DcuSR system. Since *S. typhimurium* and *E. carotovora* both have a DcuSR system similar to *E. coli* a cosensory function of the DcuB proteins can be supposed in these organisms as well.

Within the γ-proteobacteria the strictly respiratory bacterium *Pseudomonas aeroginosa* (DctA homologue with 48% identity to $DctA_{Ecoli}$) and the facultative anaerobic pathogen *Vibrio cholera* (DcuB homologue with 46% identity to $DcuB_{Ecoli}$) contain DctA or DcuB homologues, but no DcuSR-like two-component system.

The ε-proteobacteria *Wolinella succinogenes*, *Campylobacter jejunii* and the β-proteobacterium *Rhodoferax ferrireducans* contain proteins that are homolog to the transporters DcuB and DctA of *E. coli,* but no DcuSR system. Expression of the carriers therefore depends on a different system for C_4-dicarboxylate sensing, or takes place constitutively. Interestingly, the DcuB protein of *W. succinogenes* (71% identity) was found to be regulatory active in *E. coli*, while DcuB of *C. jejunii* (69% identity) showed no repressing effect on DcuSR-dependent expression. The DctA proteins of *W. succinogenes* and *C. jejunii* are less conserved; they show only a sequence identity of 43-44% to DctA of *E. coli*. In contrast, the DcuB and DctA homologues of the facultative anaerobic bacterium *R. ferrireducans* both exhibit a high identity (73 and 71%) to the respective proteins of *E. coli*. *R. ferrireducans* was shown to grow with a wide range of substrates, including glucose, fructose, sucrose, xylulose, acetate and lactate by transferring the metabolic generated electrons to iron (III) or other minerals rather than to oxygen.

For another β-proteobacterium, *Ralstonia solanacearum,* only a DctA homologue was identified. This soil bacterium is a microaerophil plant pathogen and related to the heterogeneous family of pseudomonades.

The DctBD two-component system of *Rhizobium meliloti* activates expression of *dctA* in response to C_4-dicarboxylates. In a similar way as assumed for $DcuB_{Ecoli}$ and $DctA_{Ecoli}$, rhizobial DctA controls its own expression (Reid & Poole, 1998). The aerobic α-proteobacterium forms an endosymbiotic nitrogen fixing association by colonizing plant cells

within root nodules. While the DctA proteins of *R. meliloti* and *E. coli* show a high identity (60%), the corresponding C_4-dicarboxylate sensing systems DcuSR and DctBD only show an sequence identity of less than 14%.

Table D1: Distribution of DcuB, DcuS, DcuR and DctA homologs in bacteria. The identity of the putative carriers, the sensor kinases and the response regulators is given in % to the proteins of *E. coli*. The listed bacteria belong to the class of γ-Proteobacteria, orders Enterobacteriales (*E. coli to* Y. *ruckeri*), Vibrionales (*V. cholera*) or Pseudomonadales (*P. aeroginosa*), ε-Proteobacteria (Campylobacterales *W. succinogenes* and *C. jejunii*), β-Proteobacteria (Burkholderiales *R. solanacearum* and *R. ferrireducens*), α-Proteobacteria (*R. meliloti*) and to the gram-positive bacteria (*C. diphtheriae*, *B. anthracis, B. subtilis*). Organisms whose DcuB proteins were tested in *E. coli* are highlighted in bold letters. -, not detected in database.

Organism	**DcuB** identity [%]	**DcuS** identity [%]	**DcuR** identity [%]	**DctA** identity [%]
Escherichia coli	**100**	**100**	**100**	**100**
Shigella flexneri	100	99	99	99
Salmonella typhimurium	**97**	**81**	**88**	**94**
Citrobacter sp.	96	84	89	94
Klebsiella pneumoniae	94	57	66	93
Dickeya zeae	89	56	55	88
Serratia proteamaculans	89	53	53	85
Pectobacterium carotovorum	88	57	56	87
Erwinia carotovora	**87**	**56**	**55**	**86**
Providencia stuartii	86	-	-	60
Yersinia ruckeri	56	57	54	86
Vibrio cholerae	46	-	-	-
Pseudomonas aeruginosa	-	-	-	48
Wolinella succinogenes	**71**	**-**	**-**	**43**
Campylobacter jejunii	**69**	**-**	**-**	**44**
Ralstonia solanacearum	-	-	-	59
Rhodoferax ferrireducens	73	-	-	71
Rhizobium meliloti	-	14 (DctB)	8 (DctD)	60
Corynebacterium diphtheriae	**54**	**-**	**-**	**-**
Bacillus anthracis	43	39	43	54
Bacillus subtilis	- 12 (CitN) 13 (MaeN)	27 (DctS) 26 (CitS) 35 (MalK)	34 (DctR) 27 (CitT) 44 (MalR)	52

Corynebacterium diphtheriae possesses a DcuB-homologue with 54% sequence identity to $DcuB_{Ecoli}$ and surprisingly showed a regulatory effect on DcuSR of *E. coli*. It can be assumed that $DcuB_{C.diphtheriae}$ is not expressed under anaerobic conditions in *C. diphtheriae* since the gram-positive pathogen is growing exclusively under aerobic conditions. With regard to the topology studies it is supposed that the transport protein of *C. diphtheriae* is folded in a $DcuB_{Ecoli}$-like manner, whereas the DcuB protein of *C. jejunii* shows an alternative structure. Since the relevant residues are still conserved within the sequences of $DcuB_{C.jejunii}$ another arrangement within the membrane (perhaps similar as found for $DcuA_{Ecoli}$) could be an explanation for the loss of regulatory properties.

For the facultative anaerobic bacterium *Bacillus anthracis* all homologues of proteins required in *E. coli* for C_4-dicarboxylate-sensing could be identified. The sequence identity is 54% for the DctA homologue, 43% for the DcuB homologue and 39% for the DcuS-like protein. *Bacillus subtilis* on the other hand only provides a DctA homologue with 52% identity to $DctA_{Ecoli}$. The C_4-dicarboxylate-sensing two-component system DctSR of *B. subtilis* shows low sequence identity to DcuSR of *E. coli* while the MalKR system controlling the maltose metabolism is more similar to DcuSR (identity of 34% and 44%, respectively). *B. anthracis* does not possess the MalKR, the CitST or the DctSR system for C_4-dicarboxylate-sensing, the identified "sensory box histidin kinase" only shows a sequence identity of 33% to $DctS_{B.subtilis}$, 28% to $CitS_{B.subtilis}$ and 44% to $MalK_{B.subtilis}$. In contrast to *B. anthracis* no DcuB homologue was found in *B. subtilis,* indicating that the two-component system of *B. anthracis* is a homologue of $DcuSR_{Ecoli}$.

6. References

Abramson, J., Smirnova, I., Kasho, V., Verner, G., Kaback, H.R. & Iwata, S. (2003)
Structure and mechanism of the lactose permease of *Escherichia coli*.
Science. 301(5633): 610-5

Antoine, R., Huvent, I., Chemlal, K., Deray, I., Raze, D., Locht, C. & Jacob-Dubuisson, F. (2005)
The periplasmic binding protein of a tripartite tricarboxylate transporter is involved in signal transduction.
J. Mol. Biol. 351: 799–809

Bairoch, A. & Apweiler, R. (2000)
The SWISS-PROT protein sequence database and its supplement in TrEMBL in 2000.
Nucleid Acids Res. 28: 45-48

Baker, K.E., Ditullio, K.P., Neuhard, J., Kelln, R.A. (1996)
Utilization of orotate as a pyrimidine source by *Salmonella typhimurium* and *Escherichia coli* requires the dicarboxylate transport protein encoded by *dctA*.
J. Bacteriol. 178(24): 7099-105

Bauer, J. (Diplomarbeit, 2006)
Der anaerobe Fumarat/Succinat-Antiporter DcuB aus Proteobakterien: Funktion in Transport und Regulation
Johannes Gutenberg-Universität, Mainz

Bogdanov, M., Zhang, W., Xie, J. & Dowhan, W. (2005)
Transmembrane protein topology mapping by the substituted cysteine accessibility method (SCAM(TM)): application to lipid-specific membrane protein topogenesis.
Methods. 36(2): 148-71

Brickman, E., Beckwith, J. (1975)
Analysis of the regulation of *Escherichia coli* alkaline phosphatase synthesis using deletions and phi80 transducing phages.
J. Mol. Biol. 96(2): 307-16

Broome-Smith, J.K. & Spratt, B.G. (1986)
A vector for the construction of translational fusions to TEM ß-lactamase and the analysis of protein export signals and membrane protein topology.
Gene. 49: 341-349

Bryson, K., McGuffin, L.J., Marsden, R.L., Ward, J.J., Sodhi, J.S. & Jones, D.T. (2005)
Protein structure prediction servers at University College London.
Nucleic Acids Res. 33 (Web Server Issue), W36-38

Calamia, J. & Manoil, C. (1990)
Lac permease of *Escherichia coli*: topology and sequence elements promoting membrane insertion.
Proc. Natl. Acad. Sci. U. S. A. 87(13): 4937-41

Cheung, J. & Hendrickson, W. A. (2008)
Crystal Structures of C_4-Dicarboxylate Ligand Complexes with Sensor Domains of Histidine Kinases DcuS and DctB.
J. Biol. Chem. 283: 30256-30265

Cox, G.B., Webb, D. & Rosenberg, H. (1989)
Specific amino acid residues in both the PstB and PstC proteins are required for phosphate transport by the *Escherichia coli* Pst system.
J. Bacteriol. 171: 1531-1534

Culham, D.E., Hillar, A., Henderson, J., Ly, A., Vernikovska, Y.I., Racher, K.I., Boggs, J.M. & Wood, J.M. (2003)
Creation of a fully functional cysteine-less variant of osmosensor and proton-osmoprotectant symporter ProP from *Escherichia coli* and its application to assess the transporter's membrane orientation.
Biochemistry. 42(40): 11815-23

Davies, S., Golby, P., Omrani, D., Broad, S.A., Harrington, V.L., Guest, J. R., Kelly, D.J. & Andrews, S. C. (1999).
Inactivation and regulation of the aerobic C_4-dicarboxylate transport (*dctA*) gene of *Escherichia coli.*
J. Bacteriol. 181: 5624–5635

Deguchi, Y., Yamato, I. & Anraku, Y. (1989)
Molecular cloning of *gltS* and *gltP*, which encode glutamate carriers of *Escherichia coli B*.
J. Bacteriol. 171(3): 1314-9

Dower, W. J., Miller, J. F., and Ragsdale, C. W. (1988)
High efficiency transformation of *E. coli* by high voltage electroporation.
Nucleic. Acids. Res. 16: 6127-6145

Drew. D.E., von Heijne, G., Nordlund, P. & de Gier, J.W. (2001)
Green fluorescent protein as an indicator to monitor membrane protein overexpression in *Escherichi coli*.
FEBS Lett. 507: 220-224

Engel, P, Krämer, R. & Unden, G. **(**1992)
Anaerobic fumarate transport in *Escherichia coli* by an fnr-dependent dicarboxylate uptake system which is different from aerobic dicarboxylate uptake.
J. Bacteriol. 174: 5533–5539

Engel, P, Krämer, R. & Unden, G. (1994)
Transport of C_4-dicarboxylates by anaerobically grown *Escherichia coli*: energetics and mechanism of exchange, uptake and efflux.
Eur. J. Biochem. 222: 605–614

Etzkorn, M., Kneuper, H., Dünnwald, P., Vijayan, V., Krämer, J., Griesinger, C., Becker, S., Unden, G. & Baldus, M. (2008)
Plasticity of the PAS domain and a potential role for signal transduction in the histidine kinase DcuS.
Nat. Struct. Mol. Biol. 15: 1031-1039

Faham, S., Watanabe, A., Besserer, G.M., Cascio, D., Specht, A., Hirayama, B.A., Wright, E.M. & Abramson, J. (2008)
The crystal structure of a sodium galactose transporter reveals mechanistic insights into Na^+/sugar symport.
Science. 321(5890): 810-4

Farinha, M.A. & Kropinski, A.M. (1990)
High efficiency electroporation of *Pseudomonas aeruginosa* using frozen cell suspensions.
FEMS Microbiol. Lett. 58(2): 221-225

Feilmeier, B.J., Iseminger, G., Schroeder, D., Webber, H. & Phillips, G.J. (2000)
Green fluorescent protein functions as a reporter for protein localization in *Escherichia coli*.
J. Bacteriol. 182(14): 4068-76

Fu, D. & Maloney, P.C. (1998)
Structure-function relationships in OxlT, the oxalate/formate transporter of *Oxalobacter formigenes*. Topological features of transmembrane helix 11 as visualized by site-directed fluorescent labeling.
J. Biol. Chem. 273(28): 17962-7

Gendreau, S., Voswinkel, S., Torres-Salazar, D., Lang, N., Heidtmann, H., Detro-Dassen, S., Schmalzing, G., Hidalgo, P. & Fahlke, C. (2004)
A trimeric quaternary structure is conserved in bacterial and human glutamate transporters.
J. Biol. Chem. 279(38): 39505-12

Gerchman, Y., Rimon, A., Venturi, M. & Padan, E. (2001)
Oligomerization of NhaA, the Na^+/H^+ antiporter of *Escherichia coli* in the membrane and its functional and structural consequences.
Biochemistry. 40(11): 3403-12

Golby, P., Kelly, D.J., Guest, J. R. & Andrews, S. C. **(**1998)
Topological analysis of DcuA, an anaerobic C_4-dicarboxylate transporter of *Escherichia coli.*
J. Bacteriol. 180: 4821–4827

Golby, P., Kelly, D.J., Guest, J. R. & Andrews, S. C. (1998)
Transcriptional regulation and organization of the *dcuA* and *dcuB* genes, encoding homologous anaerobic C_4-dicarboxylate transporters in *Escherichia coli.*
J. Bacteriol. 180: 6586–6596

Golby, P., Davies, S., Kelly, D.J., Guest, J. R. & Andrews, S. C. (1999)
Identification and characterisation of a two-component sensor-kinase and response-regulator system (DcuS-DcuR) controlling gene expression in response to C_4-dicarboxylates in *Escherichia coli.*
J. Bacteriol. 181**:** 1238-1248

Gordon, G. W., Berry, G., Liang, X. H., Levine, B. & Herman, B. (1998)
Quantitative fluorescence resonance energy transfer measurements using fluorescence microscopy.
Biophys. J. 74(5): 2702-2713

Guan, L., Mirza, O., Verner, G., Iwata, S. & Kaback, H.R. (2007)
Structural determination of wild-type lactose permease.
Proc Natl Acad Sci U S A. 104(39): 15294-8

Gutowski, S.J. & Rosenberg, H. (1975)
Succinate uptake and related proton movements in *Escherichia coli* K12.
Biochem. J. 152: 647–654

Guzman, L.-M., Belin, D., Carson M.J. & Beckwith J. (1995)
Tight Regulation, Modulation and High-Level Expression by Vectors Containing the Arabinose P_{BAD} Promotor.
J. Bacteriol. 177: 4121-4130

Hagting, A., Kunji, E.R., Leenhouts, K.J., Poolman, B. & Konings, W.N. (1994)
The Di-and Tripeptide Protein of Lactococcus lactis.
J. Biol. Chem. 269: 11391-11399

Hazelbauer, G.L. (1975)
Maltose chemoreceotor of *Escherichia coli*.
J. Bacteriol. 122: 206-214

Heeb, S., Itoh, Y., Nishijyo, T., Schnider, U., Keel, C., Wade, J., Walsh, U., O'Gara, F. & Haas, D. (2000)
Small, stable shuttle vectors based on the minimal pVS1 replicon for use in gram-negative, plant-associated bacteria.
Mol. Plant Microbe Interact. 13: 232-237

Heijne von, G. (1986)
The distribution of positively charged residues in bacterial inner membrane proteins correlates with the transmembrane topology.
EMBO J. 5: 3021-3027

Henderson, N.S., So S.S., Martin, C., Kulkarni, R. & Thanassi, D.G. (2004)
Topology of the outer membrane usher PapC determined by site-directed fluorescence labeling.
J. Biol. Chem. 279(51): 53747-54

Hilger, D., Jung, H., Padan, E., Wegener, C., Vogel, K.P., Steinhoff, H.J. & Jeschke G. (2005)
Assessing oligomerization of membrane proteins by four-pulse DEER: pH-dependent dimerization of NhaA Na+/H+ antiporter of *E. coli*.
Biophys. J. 89(2): 1328-38

Huang, Y., Lemieux, M.J., Song, J., Auer, M. & Wang, D.N. (2003)
Structure and mechanism of the glycerol-3-phosphate transporter from *Escherichia coli*.
Science. 301(5633): 616-20

Hunte, C., Screpanti, E., Venturi, M., Rimon, A., Padan, E., Michel, H. (2005)
Structure of a Na^+/H^+ antiporter and insights into mechanism of action and regulation by pH.
Nature. 435(7046): 1197-202

Island, M.D. & Kadner, R.J. (1993)
Interplay between the membrane-associated UhpB and UhpC regulatory proteins.
J. Bacteriol. 175:5028-5034

Iuchi, S. & Lin, E. C. C. (1988)
arcA (*dye*), a global regulatory gene in *Escherichia coli* mediating repression of enzymes in aerobic pathways.
Proc Natl Acad Sci USA 85:1888-1892

Iuchi, S., Cameron, D.C. & Lin, E.C.C. (1989)
A second global regulatory gene (*arcB*) mediating repression of enzymes in aerobic pathways of *Escherichia coli*.
J. Bacteriol. 171: 868-873

Iwaarden van, P.R., Pastore, J.C., Konings, W.N. & Kaback, H.R. (1991)
Construction of a functional lactose permease devoid of cysteine residues.
Biochemistry. 30(40): 9595–9600

Janausch, I.G., Kim, O.B. & Unden, G. (2001)
DctA- and Dcu-independent transport of succinate in *Escherichia coli*: contribution of diffusion and of alternative carriers.
Arch. Microbiol. 176(3): 224-30

Janausch, I.G., Zientz, E., Tran, Q.H., Kröger, A. & Unden, G. (2002)
C_4-dicarboxylate carriers and sensors in bacteria.
Biochim. Biophys. Acta 1553: 39–56

Janausch, I.G, Garcia-Moreno, I., Lehnen, D., Zeuner Y. & Unden, G. (2004)
Phosphorylation and DNA-binding of the response regulator DcuR of the fumarate two-component system DcuSR.
Microbiology. 150: 877–883

Jones, D.T., Taylor, W.R. & Thornton, J.M. (1994)
A model recognition approach to the prediction of all-helical membrane protein structure and topology.
Biochemistry. 33: 3038–3049

Jung, H., Tebbe, S., Schmid, R. & Jung, K. (1998)
Unidirectional reconstitution and characterization of purified Na^+/proline transporter of *Escherichia coli*.
Biochemistry. 37: 11083-11088

Jung, H., Ruebenhagen, R., Tebbe, S., Leifker, K., Tholema, N., Quick, M. & Schmid, R. (1998)
Topology of the Na^+/proline transporter of *Escherichia coli*.
J. Biol. Chem. 273: 26400-26407

Kadonaga, J.T., Knowles, J.R. (1985)
A simple and efficient method for chemical mutagenesis of DNA.
Nucleic Acids Res. 13(5): 1733-45

Kanner, B.I. & Borre, L. (2002)
The dual-function glutamate transporters: structure and molecular characterisation of the substrate-binding sites.
Biochim. Biophys. Acta. 1555(1-3): 92-5

Kay, W.W. & Kornberg, H.L. (1971)
The uptake of C_4-dicarboxylic acids by *Escherichia coli*.
Eur. J. Biochem. 18(2): 274-81

Kentner, D., Thiem, S., Hildenbeutel, M. & Sourjik, V. (2006)
Determinants of chemoreceptor cluster formation in *Escherichia coli*.
Mol. Microbiol. 61: 407-417

Kim, O. (Dissertation 2006)
Carrier und Regulatoren des Tartrat- und C_4-Dicarboxylatstofwechsels von *Escherichia coli.*
Johannes Gutenberg-Universität, Mainz

Kimura-Someya, T., Iwaki, S. & Yamaguchi, A. (1998)
Site-directed chemical modification of cysteine-scanning mutants as to transmembrane segment II and its flanking regions of the Tn10-encoded metal-tetracycline/H^+ antiporter reveals a transmembrane water-filled channel.
J. Biol. Chem.. 273(49): 32806-11

Kleefeld, A. (Diplomarbeit 2002)
Der Einfluss der C_4-Dicarboxylat-Carrier DcuB und DctA auf die DcuSR-abhängige Genregulation in *Escherichia coli*.
Johannes Gutenberg-Universität, Mainz

Kleefeld, A. (Dissertation 2006)
Der Carrier DcuB als zweiter Sensor des Zweikomponentensystems DcuSR in *Escherichia coli*.
Johannes Gutenberg-Universität, Mainz

Kleefeld, A., Ackermann, B., Bauer, J. Krämer, J. & Unden, G. (2009)
The fumarate/succinate antiporter DcuB of *Escherichia coli* is a bifunctional protein with sites for regulation of DcuS-dependent gene expression.
J. Biol. Chem. 284:265-275

Kneuper, H., Janausch, I.G., Vijayan, V, Zweckstetter, M., Bock, V., Griesinger C. & Unden, G. (2005)
The Nature of the Stimulus and the Fumarate Binding Site of the Fumarate Sensor DcuS of *Escherichia coli*.
J. Biol. Chem. 280: 20596-20603

Kneuper, H., Scheu, P., Etzkorn, M., Sevvana, M., Dünnwald, P., Becker, S., Baldus, M., Griesinger, C. & Unden, G. (2010)
Sensing ligands by periplasmic sensing histidine kinases with sensory PAS domains.
Book chapter. Editor: S. Spiro (in press)

Koshland, D. & Botstein, D. (1982)
Evidence for posttranslational translocation of beta-lactamase across the bacterial inner membrane.
Cell 30 (3): 893-902

Krämer, J., Fischer, J., Zientz, E., Vijayan, V., Griesinger, C., Lupas, A. & Unden, G. (2007)
Citrate sensing by the C_4-dicarboxylate/citrate sensor kinase DcuS of *Escherichia coli*: binding site and conversion of DcuS to a C_4-dicarboxylate- or citrate-specific sensor.
J. Bacteriol. 189(11): 4290-4298

Laemmli, U.K. (1970).
Cleavage of structural proteins during the assembly of the head of bacteriophage T4.
Nature. 227: 680-685

Lakowicz, J. R. (2006)
Principles of Fluorescence Spectroscopy.
3rd Plenum, New York, 2006

Liao, Y.-F. (Dissertation 2008)
Oligomerization and Protein-Protein Interactions of the Sensory Histidine Kinase DcuS in *Escherichia coli*.
Johannes Gutenberg-Universität, Mainz

Liu, F., Culham, D.E., Vernikovska, Y.I., Keates, R.A., Boggs, J.M. & Wood, J.M. (2007)
Structure and function of transmembrane segment XII in osmosensor and osmoprotectant transporter ProP of *Escherichia coli*.
Biochemistry. 46(19): 5647-55

Long, J.C., Wang, S. & Vik, S.B. (1998)
Membrane topology of subunit a of the F1F0 ATP synthase as determined by labeling of unique cysteine residues.
J. Biol. Chem. 273(26): 16235-40

Lu, J. & Deutsch, C. (2001)
Pegylation: a method for assessing topological accessibilities in Kv1.3.
Biochemistry. 40(44): 13288-301

Maegawa, S., Koide, K., Ito, K., Akiyama, Y. (2007)
The intramembrane active site of GlpG, an E. coli rhomboid protease, is accessible to water and hydrolyses an extramembrane peptide bond of substrates.
Mol. Microbiol. 64(2): 435-47

Maiden, M.C., Davis, E.O., Baldwin, S.A., Moore, D.C. & Henderson, P.J. (1987)
Mammalian and bacterial sugar transport proteins are homologous.
Nature. 325(6105): 641-3

Mascher, T., Helmann, J.D. & Unden, G. (2006)
Stimulus perception in bacterial signal transducing histidine kinases.
Microbiol. Mol. Biol. Rev. 70: 910-938

Manoil, C., Boyd, D. & Beckwith, J. (1988)
Molecular genetic analysis of membrane protein topology.
Trends Genet. 4: 223–226

Michaelis, S., Guarente, L. & Beckwith, J. (1983)
In vitro construction and characterization of *phoA-lacZ* gene fusions in *Escherichia coli.*
J. Bacteriol. 154(1): 356-65

Miller, J.H. (1992)
A short course in bacterial genetics.
Cold Spring Harbour Laboratory Press New York.

Miroux, B. & Walker, J.E. (1996)
Overproduction of Proteins in *Escherichia coli*: mutant hosts that allow syntheses of some membrane proteins and globular proteins at high levels.
J. Mol. Biol. 260: 289-298

Morth, J. P., Pedersen, B. P., Toustrup-Jensen, M. S., Sorensen, T. L., Petersen, J., Andersen, J. P., Vilsen, B. & Nissen, P. (2007)
Crystal structure of the sodium-potassium pump.
Nature. 450: 1043-1049

Mullis, K. B., Farone, F. A., Schar, S., Saiki, R., Horn, G. & Ehrlich, H. (1986)
Specific amplification of DNA *in vitro*: the polymerase chain reaction.
Cold Spring Harbor Symp. Quant. Biol. 51:263-273

Novick, R.P. (1987)
Plasmid Incompatibility.
Microbiol. Rev. 51: 381-395

Olesen, C., Picard, M., Winther, A. M., Gyrup, C., Morth, J. P., Oxvig, C., Moller, J.V. & Nissen, P. (2007)
The structural basis of calcium transport by the calcium pump.
Nature. 450: 1036-1042

Pappalardo, L. Janausch, I.G., Vijayan, V., Zientz, E., Junker, J., Peti, W., Zweckstetter, M., Unden, G. & Griesinger C. (2003)
The NMR structure of the sensory domain of the membranous two-component fumaratesensor (histidine protein kinase) DcuS of *Escherichia coli*.
J. Biol. Chem. 278: 39185-8

Padan, E., Kozachkov, L., Herz, K. & Rimon, A. (2009)
NhaA crystal structure: functional-structural insights.
J. Exp. Biol. 212(11): 1593-603

Pao, S.S., Paulsen, I.T. & Saier, M.H. Jr. (1998)
Major facilitator superfamily.
Microbiol. Mol. Biol. Rev. 62(1): 1-34

Patterson, G. H., Piston, D. W. & Barisas, B. G. (2000)
Forster distances between green fluorescent protein pairs.
Anal. Biochem. 284: 438-440

Pedersen, B. P., Buch-Pedersen, M. J., Morth, J. P., Palmgren, M. G. & Nissen, P. (2007)
Crystal structure of the plasma membrane proton pump.
Nature. 450: 1111-1114

Pirch, T., Landmeier, S. & Jung, H. (2003)
Transmembrane domain II of the Na+/proline transporter PutP of *Escherichia coli* forms part of a conformationally flexible, cytoplasmic exposed aqueous cavity within the membrane.
J. Biol. Chem. 278(44): 42942-9

Poelarends, G.J. & Konings, W.N. (2002)
The transmembrane domains of the ABC multidrug transporter LmrA form a cytoplasmic exposed, aqueous chamber within the membrane.
J. Biol. Chem. 277(45): 42891-8

Popkin, P.S. & Maas, W.K. (1980)
Escherichia coli regulatory mutation affecting lysine transport and lysine decarboxylase.
J. Bacteriol. 141: 485-492

Pos, K.M., Dimroth P. & Bott M. (1998)
The *Escherichia coli* citrate carrier CitT: a member of a novel eubacterial transporter family related to the 2-oxoglutarate/malate translocator from spinach chloroplasts.
J. Bacteriol. 180: 4160–4165

Reid, C.J. & Poole, P.S. (1998)
Roles of DctA and DctB in Signal Detection by the Dicarboxylic Acid Transport System of *Rhizobium leguminosarum*.
J Bacteriol 180: 2660-2669.

Sambrook, J. & Russel, D.W. (2001)
Molecular cloning: A Laboratory Manual (Third Edition), Volume 3
Cold Spring Harbor Laboratory Press, New York

Scheu, P. (Diplomarbeit 2005)
Der Fumaratsensor DcuS von *Escherichia coli*.
Johannes Gutenberg-Universität, Mainz

Scheu, P. (Dissertation 2009)
Oligomerisation, localisation and interaction of the sensor histidine kinases *DcuS* and CitA in *Escherichia coli*.
Johannes Gutenberg-Universität, Mainz

Scheu, P., Sdorra, S., Liao, Y.-F., Wegner, M., Basché, T., Unden, G. & Erker, W. (2008)
Polar accumulation of the metabolic sensory histidine kinases DcuS and CitA in *Escherichia coli*.
Microbiology 154: 2463-2472

Schwöppe, C., Winkler, H.H. & Neuhaus, H.E. (2003)
Connection of transport and sensing by UhpC, the sensor for external glucose-6-phosphate in *Escherichia coli*.
Eur. J. Biochem. 270: 1450-1457

Screpanti, E. & Hunte, C. (2007)
Discontinuous membrane helices in transport proteins and their correlation with function.
J Struct Biol. 159(2): 261-7

Shaw, D.J. & Guest, J.R. (1982)
Nucleotide sequence of the *fnr* gene and primary structure of the Fnr protein of *Escherichia coli*.
Nucl. Acids Res. 10: 6119-6230

Silhavy, T.J., Berman, M.L. & Enquist, L.W. (1984)
Experiments with Gene Fusions.
Cold Spring Harbor Laboratory Press New York.

Six, S., Andrews, S.C., Unden G. & Guest, J.R. **(**1994)
Escherichia coli possesses two homologous anaerobic C4-dicarboxylate membrane transporters (DcuA and DcuB) distinct from the aerobic dicarboxylate transport system (Dct).
J. Bacteriol. 176: 6470–6478

Slotboom, D.J., Konings, W.N., Lolkema, J.S. (1999)
Structural features of the glutamate transporter family.
Microbiol. Mol. Biol. Rev. 63(2): 293-307

Slotboom, D.J., Konings, W.N., Lolkema, J.S. (2001)
Cysteine-scanning mutagenesis reveals a highly amphipathic, pore-lining membrane-spanning helix in the glutamate transporter GltT.
J. Biol. Chem. 276(14): 10775-81

Slotboom, D.J., Konings, W.N., Lolkema, J.S. (2001)
The structure of glutamate transporters shows channel-like features.
FEBS Lett. 492(3): 183-6

Sone, M., Kishigami, S., Yoshihisa, T. & Ito, K. (1997)
Roles of Disulfide Bonds in Bacterial Alkaline Phosphatase.
J. Biol. Chem. 272: 6174-6178.

Stewart, V. (1993)
Nitrate regulation of anaerobic respiratory gene expression in *Escherichia coli*.
Mol. Microbiol. 9: 425-434

Stewart, V. & Darwin, A.J. (1995)
Expression of the narX, narL, narP, and narQ genes of *Escherichia coli* K-12: regulation of the regulators.
J. Bacteriol. 177(13): 3865-3869

Studier, F.W. & Moffatt, B.A. (1986)
Use of bacteriophage T7 RNA polymerase to direct selective high-level expression of cloned genes.
J Mol Biol 189: 113-130

Takahashi, M., Kondou, Y. & Toyoshima, C. (2007)
Interdomain communicationin calcium pump as revealed in the crystal structures with transmembrane inhibitors.
Proc. Natl. Acad. Sci. USA 104: 5800-5805

Taylor, B.L. & Zhulin, I.B. (1999)
PAS domains: internal sensorsof oxygen, redox potential and light.
Microbiol. Mol. Biol. Rev. 63: 479-506

Tetsch, L., Koller, C., Haneburger, I. & Jung, K. (2008)
The membrane-integrated transcriptional activator CadC of *Escherichia coli* senses lysine indirectly via the interaction with the lysine permease LysP.
Mol. Microbiol. 67: 570-583

Towbin, H., Staehelin, T. and Gordon, J. (1979)
Electrophoretic transfer of proteins from polyacrylamide gels to nitrocellulose sheets: procedure and some applications.
Proc. Natl. Acad. Sci. USA 76: 4350-4354

Truong, K. and Ikura, M. (2001)
The use of FRET imaging microscopy to detect protein–protein interactions and protein conformational changes *in vivo*.
Struc. Biol. 11: 573-578

Ullmann, R., Gross, R., Simon, J., Unden, G. & Kröger, A. (2000)
Transport of C_4-dicarboxylates in Wolinella succinogenes.
J. Bacteriol. 182: 5757-5764

Unden, G. & Kleefeld, A. (2004)
C_4-Dicarboxylate degradation in aerobic and anaerobic growth.
Module 3.4.5; R. Curtiss III (Editor in Chief), EcoSal - *Escherichia coli* and *Salmonella*: Cellular and Molecular Biology.
(Online) http://www.ecosal.org. ASM Press, Washington, D.C.

Viklund, H., Elofsson, A. (2008)
OCTOPUS: improving topology prediction by two-track ANN-based preference scores and an extended topological grammar.
Bioinformatics. 24(15): 1662-8

Wallace, B.J. & Young, I.G. (1977)
Role of quinines in electron transport to oxygen and nitrate in *Escherichia coli*
Biochim. Biophys. Acta. 233: 109-122

Wanner, B. L. (1996)
Phosphorus assimilation and control of the phosphate regulon.
Escherichia coli and Salmonella: *Cellular and Molecular Biology*, Ed. 2, edited by F. C. Neidhardt. Washington, DC: ASM Press, pp. 1357–1381

West, A. H. & Stock, A. M. (2001)
Histidine kinases and response regulator proteins in two-component signaling systems.
T. Biochem. Scien. 26 No.6

Weissborn, A. C., Botfield, M. C., Kuroda, M., Tsuchiya, T. & Wilson, T. H. (1997)
The construction of a cysteine-less melibiose carrier from *Escherichia coli*.
Biochim. Biophys. Acta 1329**:** 237–244

White, S.H., Ladokhin, A.S., Jayasinghe, S. & Hristova, K. (2001)
How membranes shape protein structure.
J. Biol. Chem. 276(35): 32395-8

Williams, K.A., Geldmacher-Kaufer, U., Padan, E., Schuldiner, S. & Kühlbrandt, W. (1999)
Projection structure of NhaA, a secondary transporter from *Escherichia coli*, at 4.0 Å resolution.
EMBO J. 18(13): 3558-63

Yamashita A, Singh SK, Kawate T, Jin Y, Gouaux E. (2005)
Crystal structure of a bacterial homologue of Na^+/Cl^--dependent neurotransmitter transporters.
Nature. 437(7056): 215-23

Yanisch-Perron, C., Vieira, J. & Messing, J. (1985)
Improved M13 phage cloning vectors and host strains: nucleotide sequences of the M13mpl8 and pUC19 vectors.
Gene. 33: 103-119

Yernool, D., Boudker, O., Jin, Y. & Gouaux, E. (2004)
Structure of a glutamate transporter homologue from *Pyrococcus horikoshii*.
Nature. 431(7010): 811-8

Yurgel, S., Mortimer, M.W., Rogers, K.N. & Kahn, M.L. (2000)
New substrates for the dicarboxylate transport system of *Sinorhizobium meliloti*.
J. Bacteriol. 182: 4216–4221

Zientz, E., Six, S. & Unden, G. (1996)
Identification of a third secondary carrier (DcuC) for anaerobic C_4-dicarboxylate transport in *Escherichia coli*: role of the three Dcu carriers in uptake and exchange.
J. Bacteriol. 178: 7241–7247

Zientz, E., Bongaerts, J. & Unden, G. (1998)
Fumarate regulation of gene expression in Escherichia coli by the DcuSR (*dcuSR* genes) two-component regulatory system.
J. Bacteriol. 180:5421–5425

Zientz, E., Janausch, I.G., Six, S. & Unden, G. **(**1999)
Function of DcuC as the C_4-dicarboxylate carrier during glucose fermentation by *Escherichia coli.*
J. Bacteriol. 181: 3716–3720

7. Publications

Publications in reviewed Journals:

Bauer, J., Fritsche, M., Palmer, T., Unden, G.
Topology of the anaerobic Fumarate/Succinate Antiporter DcuB of *Escherichia coli.*
Manuscript in preparation

Bauer, J., Witan, J., Liao, Y.-F., Scheu, P., Basché, T., Unden, G., Erker, W.
The C_4-dicarboxylate carrier DctA of *Escherichia coli* interacts with the sensor kinase DcuS.
Manuscript in preparation

Scheu, P., Liao, Y.-F., Bauer, J., Kneuper, H., Basché, T., Unden, G., Erker, W.
Oligomeric sensor kinase DcuS in the membrane of *Escherichia coli* and proteoliposomes: Chemical Crosslinking and FRET Spectroscopy.
Submitted

Kleefeld, A., Ackermann, B., Bauer, J. Krämer, J. and Unden, G. (2009).
The fumarate/succinate antiporter DcuB of *Escherichia coli* is a bifunctional protein with sites for regulation of DcuS-dependent gene expression.
J. Biol. Chem. 284:265-275

Posters:

Plasmid-Symposium Göttingen 10/2008
DcuB of *Escherichia coli* acts as antiporter and sensor for C_4-dicarboxylates: Function and topology
Julia Bauer, B. Ackermann, A. Kleefeld and Gottfried Unden
Institut für Mikrobiologie und Weinforschung, Johannes Gutenberg-Universität, Mainz, Germany

VAAM Frankfurt 3/2008
The fumarate/succinate antiporter DcuB as a site for C_4-dicarboxylate sensing by the DcuSR two-component system
Julia Bauer, B. Ackermann, A. Kleefeld and Gottfried Unden
Institut für Mikrobiologie und Weinforschung, Johannes Gutenberg-Universität, Mainz, Germany

Talk:

VAAM Bochum 3/2009
Control of the DcuSR two-component system of *Escherichia coli* by interaction with the transporter proteins DctA and DcuB
Julia Bauer[1], Wolfgang Erker[2], Yun-Feng Liao[2], Thomas Basché[2], Gottfried Unden[1]
[1]*Institut für Mikrobiologie und Weinforschung, Johannes Gutenberg-Universität, Mainz, Germany*
[2]*Institut für Physikalische Chemie, Johannes Gutenberg-Universität, Mainz, Germany*

Table A1: Oligonucleotides for gene amplification (MWG Biotech; Ebersberg; HPSF-purified)

Primer	Sequenz (5´-3´)	Tm [°C]	Restriction site
alternative dcuB			
SalI-Camje	GGA GTT AAA **GTC** GAC TTT TTA ACA AGC C	62.2	SalI
Camje-Pst1	CCT GCT AAA AA**C TGC AG**A AGA TAA CCT G	63.7	PstI
EcoRI-Cordi-for	GTG GCA TGA ATT **C**GA AAG GCT TCT GC	64.8	EcoRI
Rev-Cordi-XhoI	CAC TTC TAC TCT **CG**A GAA GTA CTT GGG	65.0	XhoI
dcuB			
cterm-dcuB-PvuII	GCT TCA GCA CC**A** GCT **G**GC TAC GG	67.8	PvuII
cterm-dcuB-XbaI	GTC CAC TAT T**CT** AGA ACG TGG AC	60.6	XbaI
ctermdcuBPvuII2	GCT GGC G**CA GCT G**GT TCC GGT CGC	73.0	PvuII
dcuB-BglII-for	GGT AAA GAT CTG GAT AAA GAC G	56.5	BglII
Strep-XhoI-rev	GGC TGA AA**C TCG AG**T CTC ATC CGC	66.1	XhoI
dcuBhis-XhoI-rev	GAG GC**C TCG** AGG GGT TAT GC	63.5	XhoI
dcuA			
dcuA_for	ACG TGA A**T**T CGT TCT GGA ACG CG	62.4	EcoRI
dcuA_rev	CAC CTC **TCT** AGA ACA GAT GGA ACC	62.7	XbaI
EcoRI-dcuA-for	CAA GGA AGG CT**G AAT TC**C TAG TTG TAG	63.4	EcoRI
XhoI-dcuA-rev	CGA TTG ATC AC**T CGA G**CA TGA AGC	62.7	XhoI
dctA			
dctA-BamHI-for	CTA AAG GA**T CC**C CTA TGA AAA CC	58.9	BamHI
dctA-XhoI-rev	GTG GTG CTC GAG A□T AAG AGG	59.4	XhoI
gfp			
PstI-CFP	CCA CC**C TGC AG**A GCA AGG	60.5	PstI
CFP-HindIII	CCA GAC AAG **CTT** GTA ATG GTA GC	60.6	HindIII
SacII-gfp	GTA CCG GTC **CGC GG**C ATG GTG AGC	71.3	SacII
gfp-EcoRI	GGA ATT CTA G_G TCG CGG CCG CT**A** TAC TTG	69.5	EcoRI
for-gfp-NcoI	GGT CGC CAC CAT GGT GAG C	63.1	NcoI
rev-BamHI-gfp	GGA ATT CTA GAG TCG **GAT** CCG CT**A** TAC TTG	66.8	BamHI
for-gfp-XhoI	GGT CGA CTC T**C**G AGG ATC C	61.0	XhoI
HindIII-gfp-rev	CAC CAG ACA AGA AG**C TT**G TAA TGG	61.0	HindIII
BamHI-gfp-for	CTC TAG AG**G GAT** CCC GGG TAC C	65.8	BamHI
tar			
Tar_NcoI-for	GGA GTG TGC CAT GGG TAT G	58.8	NcoI
Tar_NcoI-rev	GCT CAC CAT **GG**C ACC TCC GG	65.5	NcoI
bla fusions			
for-PstI-bla	TTG AAA A**CT GC**A GAG TAT GAG TAT TC	58.5	PstI
HindIII-bla-rev	CGA GAC A**AG CT**T AAT TCC TAC C	58.4	HindIII
XhoI-blaM-for	CTT CCT GTT **CTC GAG** CAC CCA G	64.0	XhoI
NcoI-blalead-for	AAG GAA GA**C CAT GG**G TAT TCA AC	58.9	NcoI
NcoI-blaM-for	CTT CCT G**CC ATG G**CT CAC CCA G	65.8	NcoI
BamHI-bla-rev	CAT CAT TAA TTC **GGA TCC** ATG CTT AAT C	60.7	BamHI
lacZ-/phoA fusions			
lacpho2-PstI-for	CGT CAC GG**C** TGC AGG AAA GCG	65.7	PstI
lacZ2-rev	CTC ATG TTT GAC AGC TTA TCA TCG	59.3	-
phoA2-HindIII-rev	GCC ATT AAG **CT**T GGT TGC TAA CAG C	63.0	HindIII
dcuB fragments			
pBAD-dcuBXbaIfor	GTA CCC GGG GAT CCT CTA G	61.0	XbaI
dcuBL53-PstI-re	CGC AAT GAT **CTG** CAG CAT GAC ATC	62.7	PstI
dcuBL71-PstI-re	GCA GCA TGA C**CT GC**A GAC CGC C	67.7	PstI
dcuBL81-PstI-re	CGG CG**C TGC AG**C TTC TCG G	65.3	PstI
dcuBN85-PstI-re	GAG ACA TA**C TGC AG**G TTG CGG	61.8	PstI

dcuBV92-PstI-re	GGT CAC AAA CTG CAG GAC AAT TGA G	63.0	PstI
dcuBG107-PstI-re	GGT GTA AAC CTG CAG ACC CGT ACC	66.1	PstI
dcuBL114-PstI-re	GAT GAT CTG CAG AAT GGT G	54.5	PstI
dcuBA121-PstI-re	GGA TGT TGT TCT GCA GGG CGA CG	66.0	PstI
dcuBR127-PstI-re	CAT CGG ACG CTG CAG ACG GAT G	65.8	PstI
dcuBP131-PstI-re	GAA CTT GCC TGC AGC GGA CGT TCC	67.8	PstI
dcuBA139-PstI-re	CGA TAA TCC CCT GCA GTG CAC C	64.0	PstI
dcuBL159-PstI-re	GTG ACA TTC TGC AGC ATC GCA ACC	64.4	PstI
dcuBH168-PstI-re	GAG GAA CTG CAG ATG GCG ACC	63.7	PstI
dcuBL174-PstI-re	GGT GAT TGC CTG CAG ATC G	58.8	PstI
dcuBL200-PstI-re	CGT CTT TCT GCA GAT CTT TAC CG	60.6	PstI
dcuBL237-PstI-re	CCA CAT CTG CAG CCA GTT GC	61.4	PstI
dcuBL258-PstI-re	GAT GGC TGC AGG TCC GAA TCA G	64.0	PstI
dcuBS296-PstI-re	GGA AGA CTT CCT GCA GTG AGA TAG ACG C	68.0	PstI
dcuBL333-PstI-re	CAC CAT TTC CTG CAG TAC GCC	61.8	PstI
dcuBY340-PstI-re	CAT AGG CCT GCA GAT ACT CTT TCA C	63.0	PstI
dcuBG373-PstI-re	GTA TGC CGG CTG CAG GCC GAT CG	69.6	PstI
dcuBL392-PstI-re	CGG ATA AGT CTG CAG GAT GTA	57.9	PstI
dcuBL399-PstI-re	CTG AAT CGC CTG CAG ATC GCT CG	66.0	PstI
dcuBH411-PstI-re	GAC GAA GCG CTG CAG GTG GGT GGT GC	72.7	PstI
dcuBF435-PstI-re	GGC GAA GAT CTG CAG GAA GAC GCA CG	69.5	PstI
dcuA fragments			
dcuAV49-XhoI-re	CCA TGA TAA TCT CGA GGA CAT CGA ACG	65.0	XhoI
dcuAR82-XhoI-re	GAT GTA TTT CTC GAG ACG GCG CAG C	66.3	XhoI
dcuAS107-XhoI-re	CAG TGT CTC GAG AGA GAT GTT GC	62.4	XhoI
dcuAG122-XhoI-re	GGC AAG GCT CGA GGC CTT GTT CC	67.8	XhoI
dcuAV156-XhoI-re	CCA TGA CCC TCG AGC ACG GAA G	65.8	XhoI
dcuAV171-XhoI-re	GGG TGG ACT CGA GGA CCA CGG	67.6	XhoI
dcuAL194-XhoI-re	CGG ATC GTC CTC GAG TTT GGA G	64.0	XhoI
dcuAL229-XhoI-re	CCA GCA GCT CGA GCC AGA CGG AC	69.6	XhoI
dcuAA261-XhoI-re	CAT GAT GAT CTC GAG TGC GTT GG	62.4	XhoI
dcuAT289-XhoI-re	CAT ACC TGC CTC GAG GGT GCT GG	67.8	XhoI
dcuAV325-XhoI-re	GAT GAC CCT CGA GCA CTT CAC CAG	66.1	XhoI
dcuAA353-XhoI-re	CAT CGG CTC GAG TGC TTT TGC G	64.0	XhoI
dcuAS364-XhoI-re	CAG CGG TCT CGA GTG AAA CGT TCA G	66.3	XhoI
dcuAL387-XhoI-re	CCG CAG CCT CGA GCG TCG GG	69.6	XhoI
dcuAR400-XhoI-re	CGA ATT TCT CGA GAC GGG TAG TAC	62.7	XhoI
dcuAL416-XhoI-re	GGC AAC CTC GAG AGT ACC CGG	65.7	XhoI

Table A2: Oligonucleotides for mutagenesis (MWG Biotech; Ebersberg; HPSF-purified)

Primer	Sequenz (5´-3´)	Tm [°C]	Restriction site
Woli-dcuBmut-for	CGT CAG CGA CAT TGC AAG CAT CAG GCG G	71.0	-HindIII
Woli-dcuBmut-rev	CCG CCT GAT GCT TGC AAT GTC GCT GAC G	71.0	-HindIII
Cordi-mut-for	GGT CTT AAG CTC GGT CTG GAT CCT GC	68.0	-HindIII
Cordi-mut-rev	GCA GGA TCC AGA CCG AGC TTA AGA CC	68.0	-HindIII
dcuBMutfor	CAT CGG CGA CCT TGC AAG CAT CGG GCG G	82.0	-HindIII
dcuBMutfor	CCG CCC GAT GCT TGC AAG GTC GCC GAT G	82.0	-HindIII
dcuB-SacIImutfor	CAG CTG GTT CCG TGG TAA AGA TCT GG	66.4	-SacII
dcuB-SacIImutrev	CCA GAT CTT TAC CAC GGA ACC AGC TG	66.4	-SacII
pBAD18-EcoRIfor	GGC TAG CGA ATC CGA GCT CGG TAC C	69.5	-EcoRI

pBAD18-EcoRIrev	GGT ACC GAG CTC GGA TTC GCT AGC C	69.5	-EcoRI
pMW505HindIIIfor	CGA AAG GAA GCT TAG TTG GCT GCT GC	66.4	HindIII
pMW505HindIIIrev	GCA GCA GCC AAC TAA GCT TCC TTT CG	66.4	HindIII
pEGFP-XbaImutfor	GCC GCG ACT CTA GGA TTC CAA CTG AGC GC	72.3	-XbaI
pEGFP-XbaImutrev	GCG CTC AGT TGG AAT CCT AGA GTC GCG GC	72.3	-XbaI
pMW280mut-for	GGT TCT TAT ATA TGC ACT ACG AGC ACC ACC	66.8	-Stop, -XhoI
pMW280mut-rev	GGT GGT GCT CGT AGT GCA TAT ATA AGA ACC	66.8	-Stop, -XhoI
dcuA-PvuIImut-fo	GCT TCT TTC GCA GCT GTG TCT GGT CTG	68.0	PvuII
dcuA-PvuIImut-re	CAG ACC AGA CAC AGC TGC GAA AGA AGC	68.0	PvuII
dcuAPvuIImut2-fo	GGC TGC AAC CGC AAA ACA GCT GAT GCC GAT GGC	74.5	PvuII
dcuAPvuIImut2-re	GCC ATC GGC ATC AGC TGT TTT GCG GTT GCA GCC	74.5	PvuII
blalead-PstI-for	GCC TTC CTG TTT TTC TGC AGC CAG AAA CGC TGG	72.0	PstI
blalead-PstI-rev	CCA GCG TTT CTG GCT GCA GAA AAA CAG GAA GGC	72.0	PstI
pMW527-EcoRI-for	GGG CTA GCG AAT ACG AGC TCG GTA CCC G	72.4	-EcoRI
pMW527-EcoRI-rev	CGG GTA CCG AGC TCG TAT TCG CTA GCC C	72.4	-EcoRI
pMW527-XhoI-for	CAA CGG GAA ACG TCT TGT TCG AGG CCG CG	72.3	-XhoI
pMW527-XhoI-rev	CGC GGC CTC GAA CAA GAC GTT TCC CGT TG	72.3	-XhoI
pMW445-StopF-for	CGC CGC GAT GTA CGG GTT CTT AGA GGT CGA CC	74.6	-XhoI, F445
pMW445-StopF-rev	GGT CGA CCT CTA AGA ACC CGT ACA TCG CGG CG	74.6	-XhoI, F445

Table A3: Oligonucleotides for amino acid substitution (MWG Biotech; Ebersberg; HPSF-purified and Sigma Aldrich)

Primer	Sequenz (5´-3´)	Tm [°C]	AA exchange
dcuA mutants			
dcuAmut-for	CCG ACC TAC CCG ACG GAC GTT GCT GCG GTA CAG ATG G	>75	L386D
dcuAmut-rev	CCA TCT GTA CCG CAG CAA CGT CCG TCG GGT AGG TCG G	>75	L386D
pMW450mutfor	CCG ACC TAC CCG TCG GAC CTG GCT GCG GTA CAG ATG G	82.8	T385S, V387L
pMW450mutrev	CCA TCT GTA CCG CAG CCA GGT CCG ACG GGT AGG TCG G	82.8	T385S, V387L
dcuB mutants			
dcuB-Cys1mut-for	CAT AAT ACT GAT ATC TCT GTT TTA TGG TGC	61.3	C13S
dcuB-Cys1mut-rev	GCA CCA TAA AAC AGA GAT ATC AGT ATT ATG	61.3	C13S
dcuB-Cys2mut-for	GTG ACC TCT ACA CTG ACC ATT CTT TCC GGT ACG	70.7	C98S, C104S
dcuB-Cys2mut-rev	CGT ACC GGA AAG AAT GGT CAG TGT AGA GGTCAC	70.7	C98S, C104S
dcuB-Cys4mut-for	GCA CCG GCT TCC TAC GGT TAT TAC ATC C	68.0	C387S
dcuB-Cys4mut-rev	GGA TAT AAT AAC CGT AGG AAG CCG GTG C	68.0	C387S
dcuB-Cys5mut-for	GGT GTG AGC GTA TAG TCC GTC TTC GGC TGG	73.6	C433S
dcuB-Cys5mut-rev	CCA GCC GAA GAC GGA CGA TAC GCT CAC ACC	73.6	C433S
dcuB-C1-for	CAT AAT ACT GAT ATG TCT GTT TTA TGG TGC C	62.9	S13C
dcuB-C1-rev	GGC ACC ATA AAA CAG ACA TAT CAG TAT TAT	62.9	S13C

	G		
dcuB-C2-for	CGT TTG TGA CCT GTA CAC TGA CCA TTC	65.0	S98C
dcuB-C2-rev	GAA TGG TCA GTG TAC AGG TCA CAA ACG	65.0	S98C
dcuB-C3-for	GAC CAT TCT TTG CGG TAC GGG TCA TGT G	68.0	S104C
dcuB-C3-rev	CAC ATG ACC CGT ACC GCA AAG AAT GGT C	68.0	S104C
dcuB-C4-for	CAG CAC CGG CTT GCT ACG GTT ATT ACA TCC	69.5	S387C
dcuB-C4-rev	GGA TGT AAT AAC CGT AGC AAG CCG GTG CTG	69.5	S387C
dcuB-C5-for	GTG AGC GTA TCG TGC GTC TTC GGC TGG	71.0	S433C
dcuB-C5-rev	CCA GCC GAA GAC GCA CGA TAC GCT CAC	71.0	S433C
M1C-dcuB-phoA-fo	GGA GAC CGC GGT TGC CTA TTC ACT ATC CAA CTT ATC	71.7	M1C
M1C-dcuB-phoA-re	GAT AAG TTG GAT AGT GAA TAG GCA ACC GCG GTC TCC	71.7	M1C
dcuB-L2C-for	CGA GGG TTC ACA CAT GTG TTT TAC TAT CCA AC	66.9	L2C
dcuB-L2C-rev	GTT GGA TAG TAA AAC ACA TGT GTG AAC CCT CG	66.9	L2C
dcuB-R19C-for	CTG TTT TAT GGT GCC TGT AAG GGT GGT ATC GCG C	79.6	R19C
dcuB-R19C-rev	GCG CGA TAC CAC CCT TAC AGG CAC CAT AAA ACA G	79.6	R19C
dcuB-G21C-for	GCC AGA AAG TGT GGT ATC GCG CTG GG	69.5	G21C
dcuB-G21C-rev	CCC AGC GCG ATA CCA CAC TTT CTG GC	69.5	G21C
dcuB-K46C-for	CCT TCA GCC AGG TTG TCC ACC AGT TGA TGT C	79.0	K46C
dcuB-K46C-rev	GAC ATC AAC TGG TGG ACA ACC TGG CTG AAG G	79.0	K46C
dcuB-V49C-for	GGT AAA CCA CCA TGT GAT GTC ATG CTG G	66.6	V49C
dcuB-V49C-rev	CCA GCA TGA CAT CAC ATG GTG GTT TAC C	66.6	V49C
dcuB-E79C-for	GCT GCA AAT TGC CTG CAA GCT GCT GCG CCG	87.1	E79C
dcuB-E79C-rev	CGG CGC AGC AGC TTG CAG GCA ATT TGC AGC	87.1	E79C
dcuB-K87C-for	GCC GCA ACC CGT GTT ATG TCT CAA TGG TCG C	81.4	K87C
dcuB-K87C-rev	GCG ACA ATT GAG ACA TAA CAC GGG TGG CGG C	81.4	K87C
dcuB-S90C-for	CCG AAA TAT GTC TGT ATT GTC GCG CCG	66.5	S90C
dcuB-S90C-rev	CGG CGC GAC AAT ACA GAC ATA TTT CGG	66.5	S90C
dcuB-T112C-for	CAT GTG GTT TAC TGC ATT CTG CCG ATC	65.0	T112C
dcuB-T112C-rev	GAT CGG CAG AAT GCA GTA AAC CAC ATG	65.0	T112C
dcuB-Y118C-for	GCC GAT CAT CTG CGA CGT CGC CAT TAA G	69.5	Y118C
dcuB-Y118C-rev	CTT AAT GGC GAC GTC GCA GAT GAT CGG C	69.5	Y118C
dcuB-N125C-for	GCC ATT AAG AAC TGC ATC CGT CCG GAA CGT CC	81.5	N125C
dcuB-N125C-rev	GGA CGT TCC GGA CGG ATG CAG TTC TTA ATG GC	81.5	N125C
dcuB-S135C-for	CGT CCG ATG GCG GCA TGT TCT ATC GGT G	71.0	S135C
dcuB-S135C-rev	CAC CGA TAG AAC ATG CCG CCA TCG GAC G	71.0	S135C
dcuB-G138C-for	GGC AAG TTC TAT CTG TGC ACA GAT GGG	72.8	G138C
dcuB-G138C-rev	CCC ATC TGT GCA CAG ATA GAA CTT GCC	72.8	G138C
dcuB-S146C-for	GGG ATT ATC GCC TGT CCG GTG TCG G	69.5	S146C
dcuB-S146C-rev	CCG ACA CCG GAC AGG CGA TAA TCC C	69.5	S146C
dcuB-S154C-for	GGT TGC GGT CGT GTG TCT GGT TGC GAT GC	72.3	S154C
dcuB-S154C-rev	GCA TCG CAA CCA GAC ACA CGA CCG CAA CC	72.3	S154C
dcuB-T163C-for	GCT GGG TAA TGT CTG CTT TGA TGG TCC C	68.0	T163C
dcuB-T163C-rev	GGG ACC ATC AAA GCA GAC ATT ACC CAG C	68.0	T163C
dcuB-R167C-for	GTC ACC TTT GAT GGT TGC CAT CTT GAG TTC C	76.4	R167C
dcuB-R167C-rev	GGA ACT CAA GAT GGC AAC CAT CAA AGG TGA C	76.4	R167C
dcuB-L172C-for	CCA TCT TGA GTT CTG CGA TCT GCT GGC	68.0	L172C
dcuB-L172C-rev	GCC AGC AGA TCG CAG AAC TCA AGA TGG	68.0	L172C

dcuB-D173C-for	CAT CTT GAG TTC CTC **TGT** CTG CTG GCA ATC ACC	78.6	D173C
dcuB-D173C-rev	GGT GAT TGC CAG CAG **ACA** GAG GAA CTC AAG ATG	78.6	D173C
dcuB-E204C-for	GAT CTG GAT AAA GAC **TGT** GAG TTC CAG AAA TTC ATC	72.6	E204C
dcuB-E204C-rev	GAT GAA TTT CTG GAA CTC **ACA** GTC TTT ATC CAG ATC	72.6	E204C
dcuB-S211C-for	CCA GAA ATT CAT CT**G C**GT ACC GGA AAA CCG	68.1	S211C
dcuB-S211C-rev	CGG TTT TCC GGT AC**G C**AG ATG AAT TTC TGG	68.1	S211C
dcuB-E217C-for	GTA CCG GAA AAC CGT **TGT** TAT GTT TAC GGT GAT ACC	75.5	E217C
dcuB-E217C-rev	GTT ATC ACC GTA AAC ATA **ACA** ACG GTT TTC CGG TAC	75.5	E217C
dcuB-D222C-for	GAG TAT GTT TAC GGT **TGT** ACC GCG ACG CGG C	77.7	D222C
dcuB-D222C-rev	GCA GCG TCG CGG T**AC A**AC CGT AAA CAT ACT C	77.7	D222C
dcuB-K230C-for	CGC TGC TGG ATA AA**T GT**C TGC CGA AAA GCA AC	79.5	K230C
dcuB-K230C-rev	GTT GCT TTT CGG CAG **ACA** TTT ATC CAG CAG CG	79.5	K230C
dcuB-R259C-for	GAT TCG GAC CTG **T**GT CCA TCC TTC GGC G	80.9	R259C
dcuB-R259C-rev	CGC CGA AGG ATG G**AC A**CA GGT CCG AAT C	80.9	R259C
dcuB-S261C-for	CCT GCG TCC AT**G C**TT CGG CGG CAA ACC	72.6	S261C
dcuB-S261C-rev	GGT TTG CCG CCG AA**G C**AT GGA CGC AGG	72.6	S261C
dcuB-E299C-for	CGT CTA TCT CAA AAA AC**T GT**G TCT TCC GTT CCG G	77.2	E299C
dcuB-E299C-rev	CCG GAA CGG AAG AC**A CA**G TTT TTT GAG ATA GAC G	77.2	E299C
dcuB-E328C-for	GCG CAT ATG TCT **TGT** ATT CAG GGC GTA CTG G	76.4	E328C
dcuB-E328C-rev	CCA GTA CGC CCT GAA T**AC A**AG ACA TAT GCG C	76.4	E328C
dcuB-K338C-for	GGT GAA ATG GTG **TGT** GAG TAT CCG TGG G	75.5	K338C
dcuB-K338C-rev	CCC ACG GAT ACT C**AC A**CA CCA TTT CAC C	75.5	K338C
dcuB-S352C-for	CTG CTG CTG GTT T**G**C AAG TTT GTA AAC TC	72.1	S352C
dcuB-S352C-rev	GAG TTT ACA AAC TTG **C**AA ACC AGC AGC AG	72.1	S352C
dcuB-S357C-for	CCA AGT TTG TAA ACT **GT**C AGG CTG CGG C	76.1	S357C
dcuB-S357C-rev	GCC GCA GCC TGA **C**AG TTT ACA AAC TTG G	76.1	S357C
dcuB-D375C-for	GCG ATC GGC GTT **TGT** CCG GCA TAC ATC GTG	84.4	D375C
dcuB-D375C-rev	CAC GAT GTA TGC CGG **ACA** AAC GCC GAT CGC	84.4	D375C
dcuB-R406C-for	CGA TTC AGT TTG AC**T** GTT CCG GCA CCA CCC AC	82.3	R406C
dcuB-R406C-rev	GTG GGT GGT GCC GGA **ACA** GTC AAA ATG AAT CG	82.3	R406C
dcuB-R414C-for	CAC CCA CAT CGG T**TG C**TT CGT CAT CAA CC	80.0	R414C
dcuB-R414C-rev	GGT TGA TGA CGA A**GC A**AC CGA TGT GGG TG	80.0	R414C
dcuB-S420C-for	GCT TCG TCA TCA ACC AC**T GC**T TTA TTC TGC CG	69.5	S420C
dcuB-S420C-rev	CGG CAG AAT AAA **GCA** GTG GTT GAT GAC GAA GC	69.5	S420C
dcuB-L446C-for	GTA CGG GTT CT**G T**TA AAT GCA CCT CGA GC	68.1	L446C
dcuB-L446C-rev	GCT CGA GGT GCA TTT A**AC A**GA ACC CGT AC	68.1	L446C
L446C-phoA-for	GCG ATG TAC GGG **T**TC **TGC** GTC GAC CTG CAG G	74.8	L446C
L446C-phoA-rev	CCT GCA GGT CGA C**GC A**GA **A**CC CGT ACA TCG C	74.8	L446C
phoA			
C-linkerPhoA-for	CCC GTT T**C C**CC TGT TCT GGA AAA CCG G	69.5	C linker S
C-linkerPhoA-rev	CCG GTT TTC CAG AAC AGG **GGA** AAA CGG G	69.5	C linker S

PhoA-C1S-for	CCT CGC GCA AAT **C**CT ACG GTC CGA GC	71.1	C168S
PhoA-C1S-rev	GCT CGG ACC GTA G**G**A TTT GCG CGA GG	71.1	C168S
PhoA-C2S-for	GCG ACC AGT GAA AAA T**C**T CCG GGT AAC GC	69.5	C178S
PhoA-C2S-rev	GCG TTA CCC GGA **G**AT TTT TCA CTG GTC GC	69.5	C178S
PhoA-C3S-for	CCG CAG TCA CCT **C**TA CGC CTA ATC CGC	71.0	C286S
PhoA-C3S-rev	GCG GAT TAG GCG TA**G** AGG TGA CTG CGG	71.0	C286S
PhoA-C4S-for	GCT GCG AAT CCT T**C**T GGG CAA ATT GGC G	69.5	C336S
PhoA-C4S-rev	CGC CAA TTT GCC CA**G** AAG GAT TCG CAG C	69.5	C336S
dctA mutants			
dctA-T296A-for	GGC TGG TCA TCC CG**G** CAG GCT ACT CG	72.7	T296A
dctA-T296A-rev	CGA GTA GCC TG**C** CGG GAT GAC CAG CC	72.7	T296A
dctA-D303A-for	GGC TAC TCG TTT AAC CTT G**C**T GGC ACA TCG	69.5	D303A
dctA-D303A-rev	CGA TGT GCC A**G**C AAG GTT AAA CGA GTA GCC	69.5	D303A
dctA-S340A-for	GCT GCT TTC T**GC** TAA AGG GGC GGC AGG G	72.4	S340A
dctA-S340A-rev	CCC TGC CGC CCC TTT AG**C** AGA AAG CAG C	72.4	S340A
dctA-K341A-for	GCT GCT TTC TTC T**GC** AGG GGC GGC AGG G	73.9	K341A
dctA-K341A-rev	CCC TGC CGC CCC T**GC** AGA AGA AAG CAG C	73.9	K341A
dctA-D376A-for	CCT CGG TAT C**G**C CCG CTT TAT GTC AGA AGC	70.9	D376A
dctA-D376A-rev	GCT TCT GAC ATA AAG CGG **G**CG ATA CCG AGG	70.9	D376A
dctA-S380A-for	CGA CCG CTT TAT G**GC** AGA AGC TCG TGC GC	72.3	S380A
dctA-S380A-rev	GCG CAC GAG CTT CTG **C**CA TAA AGC GGT CG	72.3	S380A
dctA-E381A-for	CGA CCG CTT TAT GTC AG**C** AGC TCG TGC GC	72.3	E381A
dctA-E381A-rev	GCG CAC GAG CT**G** CTG ACA TAA AGC GGT CG	72.3	E381A
dctA-R383A-for	GCT TTA TGT CAG AAG CT**G C**TG CGC TGA CTA ACC	70.7	R383A
dctA-R383A-rev	GGT TAG TCA GCG CA**G C**AG CTT CTG ACA TAA AGC	70.7	R383A